

AN
EXPERIMENTAL STUDY
OF
FRICTION
BETWEEN
WET AND DRY HUMAN SKIN
AND
NONWOVEN FABRICS

A DISSERTATION SUBMITTED TO
UNIVERSITY COLLEGE LONDON
FOR THE DEGREE OF
DOCTOR OF PHILOSOPHY (PH.D)

SABRINA SIMONNE FALLOON

*Continence and Skin Technology Group
Department of Medical Physics and Biomedical Engineering
University College London*

Copyright © 2014 Sabrina Falloon

Permission is granted to copy, distribute and/or modify all original material in this document under the terms of the GNU Free Documentation License, Version 1.3 or any later version published by the Free Software Foundation; with no Invariant Sections, no Front-Cover Texts, and no Back-Cover Texts. A copy of the license is available at <http://www.gnu.org/licenses/fdl.html>.

All non-original material included in this work is acknowledged in the text at point of use. Individuals or organisations distributing this document should seek permission from the copyright holders of all such material prior to distribution.

Sabrina Falloon has asserted her moral right to be identified as the author of this work.

This thesis has been set in Cambria using $X_{\text{q}}\text{L}^{\text{T}}\text{E}_{\text{X}}$ with the author's `ssfthesis` class, which is in turn derived from David Cottenden's `djcthesis` $X_{\text{q}}\text{L}^{\text{T}}\text{E}_{\text{X}}$ class.



Continence & Skin Technology Group



Declaration

I, Sabrina Falloon, confirm that the work presented in this thesis is my own. Where information has been derived from other sources, I confirm that this has been indicated in the thesis.

Sabrina Simonne Falloon
December 19, 2014

Abstract

Many people who have urinary incontinence manage it with the use of absorbent hygiene products, such as pads. Long-term use of these products can lead to abrasion by friction between the topsheet (a nonwoven fabric) and the skin, and is exacerbated when the skin is wet. However, the nature and mechanisms of friction between skin and nonwovens are poorly understood, hindering progress to improve products. Most work on skin friction to date has involved the use of skin surrogates or real skin in the dry state only. Moreover, only a narrow range of different nonwoven fabrics have been investigated. The work described in this thesis aimed to improve understanding of friction between nonwoven fabrics and human skin, and was divided into four main blocks.

In the first, friction was measured between a skin *surrogate* (Lorica Soft) and 13 different nonwoven fabrics, varying in structure, fibre material and manufacturing techniques. Amontons' law was closely obeyed for all nonwovens (that is, coefficients of friction were independent of normal force) and the data were used to select a representative subset of five nonwovens for subsequent work.

In the second block of work, an *in vivo* study of friction was conducted between the subset of (five) nonwovens and the dry volar forearm skin of 19 female volunteers (aged 20-95 years). It was found that Amontons' law also held for all of these measurements, despite the general viscoelastic nature of human skin, the range of skin types (from smooth and firm to wrinkled and flaccid) and the difference in ages. The coefficient of friction for a given fabric varied considerably between participants (an increase of up to 101% of the lowest coefficient value), but the fabrics were generally ranked in the same order for all volunteers.

The third block of work involved the measurement of wet friction between the subset of five nonwovens and volar forearm skin of five of the study participants. In general, the coefficient of friction increased with skin wetness/hydration by up to a factor of thirteen until the skin was damp/moist. The relationship for very wet skin (with surface water) – thought to be lubricated – was unclear and varied between participants and between nonwovens. However, further work would be required to locate and quantify the excess water in and on the skin, in order to more accurately evaluate the contribution of water to friction.

Finally, in the fourth block of work, the fibre footprints of nonwovens against a surrogate skin surface (glass microscope slide) were examined, providing insight into how friction is mediated by the interface. Total fibre contact length was always extremely low (typically $0.3\text{-}1.6\text{ mm} \cdot \text{mm}^{-2}$) and increased linearly with the log of pressure, usually due to an increase in the number of contacts and sometimes because of an increase in the lengths of *existing* fibre contacts.

Acknowledgements

Firstly and most obviously, I would like to thank my supervisors, Prof Alan Cottenden and Prof Jem Hebden, for their continued support, advice and guidance throughout this project. Prof Alan Cottenden (primary supervisor) has been particularly understanding and was always around to answer any niggling questions or give me a nudge in the right direction! I really appreciate the amount of time, effort and consideration he put in with me despite having several other students in his group! I thank Dr Anna Nihlstrand, my primary supervisor at SCA, who has also been wonderful, sharing useful tips and giving me plenty of feedback on my experimental work whenever she could. I am grateful to Per Bergström, who, with Anna, has continually contributed to our meetings with plenty of advice and suggestions, and to Maria Fernkvist, Dr Shabira Abbas and Marie-Louise Lagerstedt Eidrup, who have also taken an active interest in this work. I also gratefully acknowledge SCA Hygiene Products AB and the Engineering and Physical Sciences Research Council for funding my work.

When exploring other routes and methods for measuring fibre footprints, Prof Peter Rich and Dr Amandine Marechal (Department of Structural and Molecular Biology, UCL) were kind enough to allow me to use their FTIR equipment and to provide multiple tutorials on its use! This collaboration was owed to Dr Adrien Desjardins (Department of Medical Physics and Bioengineering, UCL), who spotted the opportunity and introduced us. I must also thank Santiago Garcia for quickly and efficiently producing various components for the FTIR rig needed to carry out this exploratory work. With regards to measuring skin wetness, a very big thank you goes to Dr Perry Xiao (Faculty of Engineering, Science and the Built Environment, London South Bank University) for the loan of his fingerprint sensor equipment, and his PhD student, Wei Pan, for his consistent help and advice in the face of my million questions and trouble with equipment/software!

I am grateful to Dr Lena Ciric (Department of Civil, Environmental and Geomatic Engineering, UCL) for allowing and organising my use of the environmentally controlled room for the final part of my study when we were uprooted from our base in Archway! Dr Anne-Lise Jourdan (Department of Geography, UCL) kindly allowed me to use the micro-balance in her lab, without which, the analysis of some of my fibre footprint data would have been rather limited! In specific work-related matters, finally, I thank Lotta Jonsson and Alan Wilson (Breast Clinic, Whittington Hospital) for their tremendous efforts in helping me to obtain samples of skin for a research study on excised skin, despite their busy schedules. Although the study could not be completed, I am nonetheless grateful for their help! I must also thank all of the participants in both of my research studies – you shall remain anonymous but you know who you are.

There are several people who had no official role directly linking to my project, but have nonetheless been fantastic supports. Many thanks go to Dr David Cottenden, from whose work mine continues and

who has been a wealth of knowledge regarding not only the experimental and technical aspects of my work, but also little things relating to LaTeX and computer problems! I would like to show my gratitude to Margaret Macaulay, who has been very patient and a tremendous help with the ethics application (and amendments), as well as all the other preparation for the volar forearm study. Both David and Margaret have gone above and beyond to spend time doing things that were not actually their jobs! John Adams (IT for SLMS, UCL) has also been a great help – always ready to attend whenever my computer was playing up and saving me a lot of time trying to work out the impossible!

I thank Dr Vasileios Asimakopoulos for his help and collaboration on the joint part of our research study and his entertaining comments that made for a rather interesting experience at the nursing home. Tal Hart has also provided an endless supply of (often) comical remarks, which certainly helped to lighten the mood on stressful days, even if there were occasions when it did not have the desired effect! Of course, I owe a big thank you to Mihaela Şoric, with whom I have spent the entire duration of my PhD and who has been a good friend, an amazing support and has done wonders for my sanity!!! With a combination of her good advice, hilarious stories and general positive attitude, she has helped me to push forward through tough times. Cristina Bogatu has also helped me in more ways than she knows – thank you! I very much appreciate the endless flow of positive energy from all of my friends over the past few years, especially Sayrah Javed, Chammi Wickramaratna, Inez Gani and María Bonillo Vidal!

Last but not least, I thank my parents (Norman and Mina), sisters (Lisa and Dani) and the rest of my family for being an infinite source of emotional support and encouragement when, on days when things were not going so well, they put everything back into perspective! I am also grateful to my grand uncle Fernie and aunt Linda for showing their support and helping me with some funding along the way. A special thanks goes to my grandmother (Irmtraud Ekemode) who was a tremendous inspiration and a constant source of motivation. Despite her passing in the final year of this project, I have continued to feel her unwavering belief in me, which has helped me to maintain a positive outlook on just about everything! To everyone I love, I hope I do you all proud! Finally, I dedicate this thesis to my grandparents, Irmtraud Ekemode and Rupert Roy Falloon, both of whom have passed but still played a huge part in my journey up to this point.

Glossary

Amontons' laws of friction Friction force (F) is directly proportional to the applied normal force (L) ($F = \mu \cdot L$) and the coefficient of friction (μ) is independent of nominal contact area.

Asperity A peak or projection on a surface, which reaches higher than the average height of the surface and contributes to its surface roughness. This is where true contact initially occurs.

Compliance The ability of a material or body to deform under stress; low compliance implies high modulus and vice versa.

Coverstock The top sheet of an absorbent hygiene product (such as an incontinence pad). This component remains in contact with the skin and is usually a nonwoven.

Decitex The standard international unit of the linear density of fibres that make up a fabric, measured in grams per 10km.

Dynamic or kinetic friction (force) The frictional force that resists sliding at the interface of two surfaces that are in relative motion.

Elastic deformation Temporary/reversible deformation of a material without energy dissipation.

Necking Lateral deformation (narrowing) of a strip of nonwoven fabric, between two points of contact with other bodies, in response to tensile stress.

Nonwoven A fabric composed of one long continuous fibre or many shorter fibres of any material, using any web-forming and/or bonding process except for weaving or knitting.

Pinning This is effectively localised stick-slip as fibres pinned to a point are suddenly released before pinning themselves again to another region. It means that there is weak viscoelastic deformation and that slip at individual points of contact occurs at a much greater speed than the mean sliding speed, resulting in a large dissipation of energy and, therefore, a higher friction force.

Plastic deformation Permanent/irreversible deformation of a material or body.

Ploughing A mechanism of friction involving the plastic deformation of interacting surfaces due to the creation of grooves on one surface by asperities on the other.

Rucking The formation of folds in the skin, usually caused by the application of a shear stress.

Static friction (force) The frictional force that resists the initiation of sliding between the surfaces of two stationary objects.

Stick-slip The phenomenon of sliding between two surfaces, interspersed with pauses, where the difference between static and dynamic friction forces is large, and the relative velocity of the interacting surfaces is usually much faster than the mean.

Transepidermal water loss The passive flux of water out of the body through the dermal and epidermal layers of the skin. It is natural and constant and is measured in mass (grams) per unit area of skin (square metres) per unit time (hour). *Abbreviation: TEWL.*

Tribology The study of friction, wear and lubrication (or relative motion between surfaces in contact).

Viscoelastic deformation A time-dependent material deformation, in which the rate of deformation determines the stress required. Deformation is not normally permanent.

Voigt and Reuss models Simplified models of (isotropic) composite materials under constant strain (Voigt) or constant stress (Reuss), which can be used to approximate their elastic properties.

Water vapour flux density The flux density of water measured on the surface of the skin, from TEWL and any other source (including water applied by occlusion). The units, as for TEWL, are grams per square metre per hour ($\text{g}\cdot\text{m}^{-2}\cdot\text{h}^{-1}$). *Abbreviation: WVFD.*

Abbreviations and common symbols

The following abbreviations and symbols are used relatively frequently throughout this thesis and have been grouped according to their usage. Most were defined when they were first mentioned in the text, but this list serves as a quick reference for their inclusion beyond that point.

Materials

LS	Lorica Soft (the skin surrogate)
Dtex	Decitex (a measure of linear density)
MD	Machine direction
PP	Polypropylene
PET	Polyethylene terephthalate
PE	Polyethylene
S/C bico	Sheath/core bicomponent

Friction

CoF, μ	Coefficient of friction
μ_s	Coefficient of static friction
μ_d	Coefficient of dynamic friction
F_{\max}	Maximum tensometer force
\varnothing	Diameter
ECR	Environmentally Controlled Room
RH	Relative humidity
S-S	Stick-slip

Skin hydration

TEWL	Transepidermal water loss
WVFD	Water vapour flux density
FPS	Fingerprint sensor
GS	Greyscale
BL	Baseline

Fibre footprints

TIFF	T agged I mage F ile F ormat
EPS	E ncapsulated P ost S cript
BASH	B ourne A gain S hell

Contents

1	INTRODUCTION	1
2	LITERATURE REVIEW	3
2.1	Incontinence	3
2.1.1	Definition	3
2.1.2	Prevalence	4
2.1.3	Management	5
2.1.4	Problems associated with incontinence product use	5
2.2	Skin	6
2.2.1	Anatomy and physiology	6
2.2.1.1	Epidermis	6
2.2.1.2	Dermis	8
2.2.1.3	Hypodermis	8
2.2.1.4	Other structures	8
2.2.1.5	Stratum corneum	9
2.2.2	Transepidermal water loss	11
2.2.3	Skin trauma	12
2.2.4	Skin Biomechanics	13
2.2.4.1	<i>In vivo</i> tests on dermis	13
2.2.4.2	Instrumentation and methods	14
2.2.4.3	<i>In vitro</i> tests on dermis	16
2.2.4.4	The effect of age on mechanical properties of the skin	18
2.3	Biotribology: Friction	18
2.3.1	Friction mechanisms and lubrication	19
2.3.1.1	Adhesion	20
2.3.1.2	Plastic deformation	22
2.3.1.3	Other mechanisms	23
2.3.2	Friction with skin	24
2.3.3	Stick-slip	39
2.4	Nonwoven Fabrics	39
2.4.1	Manufacturing: formation of webs	40
2.4.2	Manufacturing: Bonding	42
2.4.3	Mechanical properties	43

2.5	Skin surrogates	44
2.6	Summary	49
2.7	Aims & objectives	49
2.7.1	Friction between a skin surrogate and nonwoven fabrics	50
2.7.2	Friction between excised skin and nonwoven fabrics	50
2.7.3	Friction between volar forearm skin and nonwoven fabrics in dry (normal) conditions	50
2.7.4	Friction between volar forearm skin and nonwoven fabrics in wet conditions . .	51
2.7.5	Interfacial contact (fibre footprint)	51
3	FRICITION MEASUREMENTS ON SKIN SURROGATE	52
3.1	Materials	53
3.1.1	Skin surrogate	53
3.1.2	Nonwoven coverstock fabrics	53
3.2	Comparison of a wider range of nonwoven fabrics: Selection of a subset	55
3.2.1	Methodology	55
3.2.2	Results	60
3.2.3	Discussion	66
3.3	Skin surrogate in a curved configuration	69
3.3.1	Materials and methods	70
3.3.2	Results and conclusions	71
4	FRICITION MEASUREMENTS ON DRY VOLAR FOREARM	74
4.1	Materials and method development	75
4.1.1	Selection of nonwoven fabrics and other variables	75
4.1.1.1	Methodology	75
4.1.1.2	Results and conclusions	76
4.2	The effect of inter-strip area density variation on friction	82
4.2.1	Methodology	82
4.2.2	Results and conclusions	84
4.3	Volar forearm study	85
4.3.1	Ethical considerations, identification of subjects and consent	85
4.3.2	Methodology	86
4.3.3	Results	90
4.3.4	Discussion	96
4.3.4.1	Lorica Soft compared with dry (normal) volar forearm skin friction data	100
5	FRICITION MEASUREMENTS ON WET VOLAR FOREARM	101
6	FIBRE FOOTPRINTS OF NONWOVENS AGAINST A SUBSTRATE	102
6.1	Materials & Methods	103
6.1.1	Equipment calibration and fibre diameter measurement	103
6.1.2	Investigating the effect of applied pressure on fibre footprint	104
6.1.2.1	Micrograph collection	104
6.1.2.2	Alterations to the method	105
6.1.2.3	Image processing	106

6.1.3	Investigating the effect of local area density on fibre footprint	109
6.2	Results	111
6.2.1	Investigating the effect of applied pressure on fibre footprint	111
6.2.2	Investigating the effect of local area density on fibre footprint	116
6.3	Discussion	117
6.3.1	Investigating the effect of applied pressure on fibre footprint	117
6.3.2	Investigating the effect of local area density on fibre footprint	120
6.3.3	Relationship between fibre footprints and friction data	122
6.3.4	Improvements for future analysis	123
7	CONCLUSIONS	126
7.1	Summary of conclusions	126
7.1.1	Friction between nonwoven fabrics and Lorica Soft	126
7.1.2	Friction between nonwoven fabrics and volar forearm skin in dry conditions	126
7.1.3	Friction between nonwoven fabrics and volar forearm skin in wet conditions	127
7.1.4	Fibre footprints of nonwoven fabrics against a glass slide	127
7.2	Evaluation of the project based on objectives achieved	128
7.2.1	Friction between a skin surrogate and nonwoven fabrics	128
7.2.2	Friction between volar forearm skin and nonwoven fabrics in dry (normal) conditions	128
7.2.3	Friction between volar forearm skin and nonwoven fabrics in wet conditions	128
7.2.4	Interfacial contact (fibre footprint)	129
7.3	Future work	129
A	NONWOVEN FABRICS: A COMPREHENSIVE TABLE OF MATERIAL PROPERTIES AND MANUFACTURING PROCESSES	131
B	RESEARCH ETHICS COMMITTEE APPLICATION: VOLAR FOREARM FRICTION STUDY PROTOCOL	133
C	ORDER OF LOAD APPLICATION: VOLAR FOREARM FRICTION	159
D	A FULL SET OF DRY FRICTION DATA: MAXIMUM TENSOMETER FORCE VS APPLIED LOAD	160
E	A FULL SET OF WET FRICTION DATA: MEASURING FRICTION AS A FUNCTION OF SKIN WETNESS (GREYSCALE)	170
F	PROCESSING OF FIBRE FOOTPRINT IMAGES	171
F.1	Enhancing raw micrographs	171
F.2	Extracting the numerical data	171
G	FRICTION MEASUREMENTS ON EXCISED HUMAN SKIN	173
G.1	Friction measurements	173
G.1.1	Materials	173
G.1.2	Methodology development	174
G.1.2.1	Experimental procedure	174
G.1.2.2	Preliminary results	175
G.1.3	Developed methodology	178

G.1.3.1	Experimental procedure	178
G.1.3.2	Results	179
G.1.3.3	Discussion	181
G.2	Compression tests	181
G.2.1	Materials & methods	182
G.2.2	Results	183
H	RESEARCH ETHICS COMMITTEE APPLICATION: EXCISED SKIN FRICTION STUDY PROTOCOL	185

“Die Augen sind größer als der Bauch! (The eyes are bigger than the belly!)”
— Irmtraud Ekemode, 1941-2013

CHAPTER 1

INTRODUCTION

“The essence of science: ask an impertinent question, and you are on your way to a pertinent answer.”

— Jacob Bronowski, 1908-1974

URINARY INCONTINENCE (UI), the involuntary loss of urine, is very common. Approximately five million people in the UK are known to be incontinent of urine, and the prevalence is anticipated to increase further as the older proportion of the population grows [1]. There is a large range of causes of UI, some of which can be eliminated to cure the condition. Where this is not possible, some symptoms may be alleviated using physiotherapy, medication or surgery. However, in many cases, the aforementioned treatments are either inappropriate or ineffective when implemented alone and it is necessary to manage the condition with products such as incontinence pads and diapers.

Absorbent products are currently the most commonly used for management of UI, but many pad users suffer skin damage or irritation in the diaper area following long-term use of these products [2]. This is referred to as Incontinence Associated Dermatitis (IAD) [2], of which there are two major contributors: friction and urine. In order to understand the mechanisms by which the skin damage occurs, it is necessary to first consider the mechanical and chemical components separately.

In previous studies by students of the Continence and Skin Technology Group of University College London, friction has been the component of interest. Wong [3] examined friction between volar forearm skin and nonwoven fabrics in the presence and absence of moisture. Cottenden [4] investigated friction between nonwoven fabrics and a skin surrogate, where adhesion was identified as the most likely main friction mechanism, and measured the fibre footprint at the interface. The principal aim of *this* project was to improve the understanding of frictional interaction between nonwoven fabrics and human skin, focusing on the impact of skin hydration and age, and the various nonwoven properties and manufacturing processes. It builds on work carried out to date and it is anticipated that this will eventually lead to the improvement of nonwoven materials so that they are more “skin-friendly”.

In this thesis, there are seven chapters, four of which describe experimental work carried out during this project. After this chapter comes a review of the literature (chapter 2) on friction between skin and various materials, and other related work. Chapter 2 ends with a comprehensive explanation of the aims and objectives of the work presented in this thesis. Subsequent chapters (3-6) describe the experimental work – which has been split into four main strands – and their overall outcome (chapter 7).

Chapter 3 contains work on nonwoven-skin surrogate friction, a continuation of work carried out by Cottenden [4], using a wider range of nonwoven fabrics with different material properties.

Chapter 4 describes the first part of a study on friction between volar forearm skin *in vivo* and nonwoven fabrics. This involved measurements on the normal/dry skin of 19 female volunteers (aged 20-95 years), the methodology for which was based on that used by Wong [3].

Chapter 5 focuses on the second part of the same study, which involved wetting the skin and nonwoven and measuring friction as a function of skin wetness, as the skin dried out.

Chapter 6 describes the investigation of nonwoven fibre footprints against glass microscope slides, using the same techniques as Cottenden [4]. The effects of applied pressure and area density on total fibre contact length were compared.

In order to maintain a coherent structure, the details (methods, results, discussions) of each of these strands are discussed in their individual chapters, but a brief general discussion of all results and conclusions is found in chapter 6. Here, findings from one strand of work may help to interpret those of another that could not be explained alone. A summary of conclusions and suggestions for future work are detailed in the final chapter (7).

CHAPTER 2

LITERATURE REVIEW

“All progress is precarious, and the solution of one problem brings us face to face with another problem.”

— Martin Luther King, Jr., 1929–1968

In order to improve the understanding of friction between human skin and nonwoven fabrics, it is important to first have some understanding of the anatomy and physiology of the skin, some of its mechanical properties and how it interacts with various other materials in friction. Knowledge of the manufacturing processes and properties of nonwoven fabrics, as well as general friction mechanisms, also contributes to the comprehension of their behaviour when in contact with the skin. This chapter covers all of these, with particular focus on the existing literature on skin friction, which highlights the most relevant work carried out to date that has led to the advancement of various products and technologies that come into contact with the skin. It ends with a summary of what is already known about skin, nonwovens and friction, followed by the aims and objectives of this project.

2.1 *Incontinence*

Incontinence has long been a taboo topic of conversation and used to be considered a shameful condition, not to be discussed openly in public or even in private, if possible. More recently, people have become more aware of its prevalence and the available treatment options, while progressive research has enabled the enhancement of such treatments and provided new alternatives.

2.1.1 *Definition*

The term urinary incontinence (UI) refers to the involuntary leakage of urine from the bladder [5, 6]. There are different types of UI, defined by their symptoms – see below. Stress and urgency incontinence are the most common types, estimated to account for about 90% of cases [7].

Stress incontinence is the term that describes UI occurring due to weakening of the pelvic floor muscles, resulting in leakage of urine when there is raised abdominal pressure (e.g. when coughing, sneezing, laughing, jumping or weight-lifting) [7, 8]. The pelvic floor often becomes damaged during labour, causing stress incontinence post partum.

Urgency incontinence is the type of UI relating to the sufferer feeling a strong desire to void immediately before or during an uncontrollable release of urine [7]. It is commonly found in people who have had a spinal cord injury or detrusor-sphincter-dyssynergia, or have a congenital disease such as spina

bifida; it is often paired with faecal incontinence in such cases [8, 9]. Lower urinary tract infection is another cause.

Mixed UI is a combination of the two types described above.

Overflow incontinence is typically not considered a type of incontinence as it mostly involves chronic retention of the urine in the bladder. However, the fact that people who have this condition cannot fully empty their bladder, means that they frequently void small volumes of urine [10]. It is mostly associated with an obstruction of the urethra, caused by conditions such as benign prostate hyperplasia (in men).

2.1.2 Prevalence

In the UK, an estimated 3-6 million [7], and in the “developed world” over 50 million people are known to be incontinent of urine [11], however, it has been suggested that there is a considerable number more who suffer with urinary continence, too ashamed to tell anyone. The use of pads for *women* is more common than any other management device or treatment in at least four countries in Europe (UK, Spain, France and Germany), although the figures are trivial compared to the total number of women suffering from urinary incontinence in these countries [12]. Figure 2.1 shows the estimated prevalence of different types of UI worldwide for 2008 and future years.

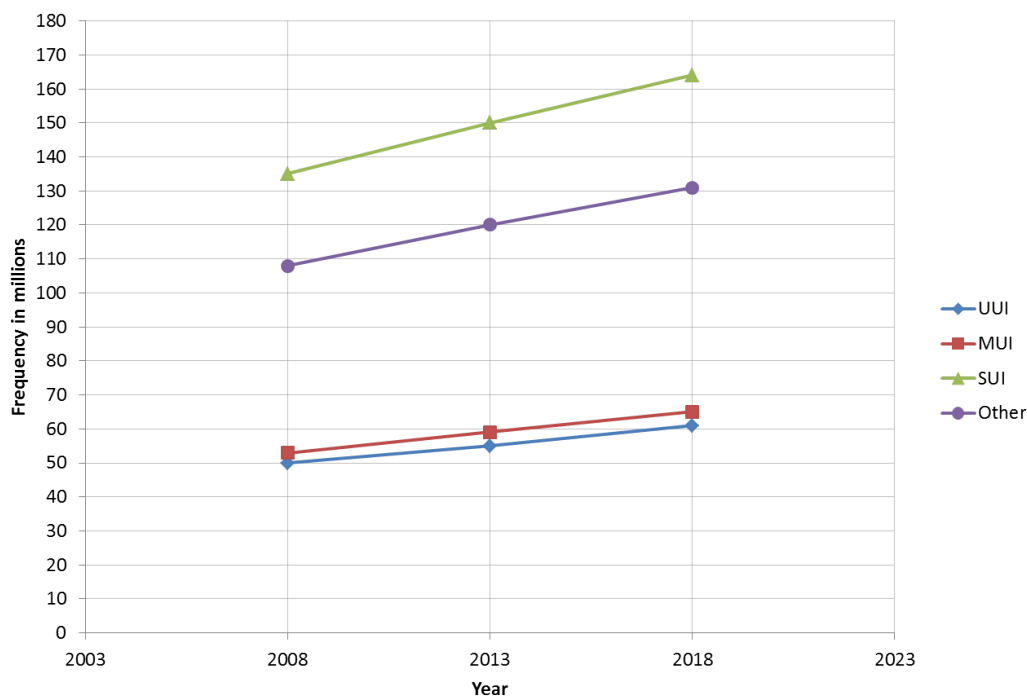


Figure 2.1: Total number of people worldwide estimated to have urinary incontinence in 2008, 2013 and 2018 (based on [13]); UUI = urgency urinary incontinence, MUI = mixed urinary incontinence and SUI = stress urinary incontinence

2.1.3 Management

Depending on the type and severity of the incontinence and the condition of a person's health, it can be cured, treated or managed. In an ideal situation, *all* cases of incontinence would be cured (urinary *and* faecal), but this is not possible, so other "solutions" are sought for those who cannot be cured. Some types of incontinence can be treated with medication and/or surgery, for example, the insertion of a sling to support the bladder when the pelvic floor is damaged, or the implantation of a device to stimulate the sacral nerves for those with urgency incontinence. Other, non-surgical treatment includes bladder training, exercising weak pelvic floor muscles and dietary changes. Nonetheless, as long as the incontinence remains, it also needs to be managed. There is a plethora of obstruction, drainage, containment and absorbent products available to manage incontinence, the distribution of which depends on available funding, resources, healthcare policies, needs of the user and user/carer preference. Some examples of existing *absorbent* product types were described by Cottenden *et al.* [2] and have been summarised below.

Inserts, sometimes referred to as liners or shields, are placed in underwear and are used for light urinary and faecal incontinence. Disposable inserts often have an adhesive strip and/or colour indicator to guide the user with replacement frequency. They are sometimes elasticated longitudinally to prevent lateral leakage.

Diapers are also 'all-in-ones' or briefs. They commonly have elasticated waist and leg regions, and self-adhesive tabs (for disposable products) or velcro tabs (for washable ones). Some diapers come with built-in 'wetness' indicators and standing gathers. These are used by people with moderate to very heavy urinary and/or faecal incontinence.

Pull-ups are normal-looking pants with an absorbent material incorporated into the design, either at the crotch or throughout the pant. The design varies to cater for a range of levels of incontinence (light-heavy).

Underpads: Different-sized rectangles of absorbent material, known as underpads, are placed on beds and chairs. Washables sometimes have high-friction backing or wings to secure it to the surface. They can act as back-ups for pads if they are low in absorbency, or can provide sole protection if they are highly absorbent.

2.1.4 Problems associated with incontinence product use

With such a variety of devices for the management of incontinence, there still exist some problems associated with their use. Examples include risk of infection with catheters, and leakage and skin damage with absorbent products. Although the benefits often outweigh the risks, the impact on social and health aspects persists and does not always abate. For UI, the aim of absorbent products is to absorb and contain the urine, while keeping the skin dry. If the pad leaks – due to insufficient capacity or low absorption rate – it would defeat the purpose of its use. Moreover, it has the potential to compromise the integrity of the skin when worn for long periods of time, on a long-term basis. It is further exacerbated by the presence of urine in contact with the skin and can lead to other health problems or worsen existing ones.

Incontinence-associated (or perineal) dermatitis (IAD) occurs when the skin comes into contact with urine and/or faeces for prolonged periods of time, resulting in localised inflammation of the skin [14]. This can occur when the skin is occluded by absorbent or other containment products [15]. It has

also been associated with friction between the skin and topsheet of a pad and can be confused with other skin conditions when the cause is not clear [16]. In recent years, much work has been done to investigate the diagnosis and treatment of IAD, but less research has been conducted to properly analyse its onset and mechanisms that stimulate it. The contribution of friction is currently unclear as most of the focus has been placed on the impact of moisture on perineal skin alone, possibly because it would be unethical to deliberately induce friction between the topsheet of a pad and a person's skin until damage actually occurs. According to Getliffe *et al.* [17], "comfort when wet" or "keeping skin dry" is ranked in the top five most important features of absorbent products by women with light UI for both day and night. These factors are also important to many others, so the influence that pad design may have on IAD is worth investigating.

2.2 Skin

2.2.1 Anatomy and physiology

The skin is the largest organ of the human body, typically covering an area of around 2 m² on a fully grown adult and varying in thickness across the body [18]. Its main functions are to inhibit the loss of water and other vital substances in the body, and to protect the body from unwanted and harmful substances and environmental factors (see table 2.1). The skin consists of three layers, each of which has a particular purpose. These are the *epidermis* (superficial), the *dermis* and the *hypodermis* (deep), and are described in detail in anatomy and physiology books by Weller and Hunter [18], and Saladin [19].

Table 2.1: Functions of various skin components (an adapted reprint from Weller *et al.* [18] Copyright © 2008 Richard Weller, John Hunter, John Savin, Mark Dahl, with permission from John Wiley and Sons)

Function	Structure/cell involved
Protection against:	
chemicals, particles	Horny layer
ultraviolet radiation	Melanocytes
antigens, haptens	Langerhans cells
microbes	Langerhans cells
Preservation of a balanced internal environment	Horny layer
Prevents loss of water, electrolytes and macromolecules	Horny layer
Shock absorber (strong, yet elastic and compliant)	Dermis and subcutaneous fat
Temperature regulation	Blood vessels, endocrine sweat glands
Insulation	Subcutaneous fat
Sensation	Specialised nerve endings
Lubrication	Sebaceous glands

2.2.1.1 Epidermis

A collection of graduated strata make up the epidermis; every layer is dense with cells. Cells from the deepest (*basal*) layer travel upwards toward the surface as the outermost cells are removed and new ones are generated. This top layer is called the *stratum corneum* and consists of flattened dead cells. Depending on the thickness of the skin, there are four or five sub-layers to the epidermis, namely, from deep to superficial, the *stratum basale* (SB), *stratum spinosum* (SS), *stratum granulosum* (SG), *stratum lucidum* (SL) and the *stratum corneum* (SC).

Stratum basale: The SB (or basal layer) contains keratinocytes and stem cells, usually cuboidal in shape. When the stem cells divide, replacement keratinocytes are produced.

Stratum spinosum: In the SS, mitosis gradually stops, leaving cells filled with increasing amounts of keratin filaments, which gives them a flattened form where the SS meets the SG. When the skin is thin or an average thickness, this is the thickest layer; otherwise the SC is recognised as thickest.

Stratum granulosum: Several layers of flattened keratinocytes filled with coarse *keratohyalin granules* make up the SG, as well as relatively few dendritic cells. This layer is partly responsible for producing some impermeability to water by means of a lipid concoction secreted from *membrane-coating vesicles*. These vesicles are produced by the cells after apoptosis begins and the cytoskeleton becomes a mass of keratin when it bonds with matter discharged by the granules. All cells above this layer tend to die quickly due to its poor permeability to water, which in turn impedes the transport of nutrients.

Stratum lucidum: It is for the above reason that nuclei and organelles are absent from the cytoplasm of SL cells. The layer is consequently translucent and only visible in thicker skin.

Stratum corneum: Thirty layers of dead keratinocytes constitute the SC. The layer produces an almost completely waterproof surface with relatively high elastic moduli (indentation – 600kPa at 25% RH; tension – $0.04\text{-}10 \times 10^6\text{kPa}$ at 25% RH or $6\text{-}10 \times 10^4\text{kPa}$ at 98% RH) well-suited to its position as most superficial stratum [20].

The epidermis and dermis have processes that interconnect at the layer interface: *epidermal ridges* from the basal layer of the epidermis and *dermal papillae* from the dermis [19]. (See figure 2.2.)

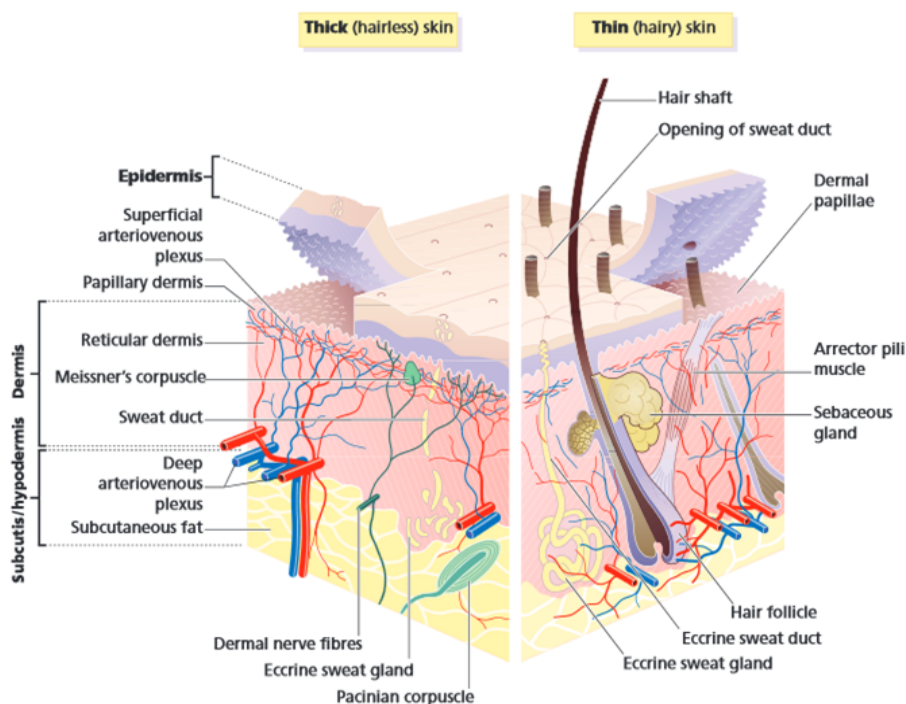


Figure 2.2: Diagram showing layers and components of human skin (reprinted from Weller *et al.* [18] Copyright ©2008 Richard Weller, John Hunter, John Savin, Mark Dahl, with permission from John Wiley and Sons)

2.2.1.2 Dermis

The dermis acts as a source of nutrition for the epidermis and also provides structural support. Bundles of fibres (mainly collagen) in a woven lattice that make up the dermis enable its structural role. Strength is provided by the collagen (approximately 70–80% of the dry weight) and elasticity by elastin (roughly 2%), both of which contribute to the skin's resistance to tears and permanent deformation when exposed to tensile forces.

Collagen fibres are able to withstand high tensile forces along their length due to their structure – narrower structures called fibrils, composed of triple helical structures known as microfibrils (collagen molecules), combine to form the collagen fibres. The triple helices are formed from three individual polypeptide chains, both ends of which are not helical. Fibres are “finer” in the papillary dermis than deep in the reticular dermis.

Hyaluronic acid, dermatan sulphate, heparan sulphate and chondroitin sulphate, together make up the dermal “amorphous ground substance”, which is responsible for many important roles of the dermis. Namely:

- damping of the skin by providing “bulk” to oppose impact forces
- nutrient transport facilitation – water molecules are cohesively bound for the transport of nutrients, waste products and hormones through this layer

The ground substance also lubricates all the fibres (collagen and elastin), enabling the dermis to move and deform quite easily/smoothly. Wrinkling and stretch marks (*striae*) in the skin can occur due to the rupture of collagen fibres (pregnancy, obesity, *etc.*) when the skin is distended excessively [19].

2.2.1.3 Hypodermis

The hypodermis, also known as the *subcutis*, contains a large amount of subcutaneous fat (or adipose tissue) which acts as an energy store and also provides insulation from the cold [18, 19]. There are also collagen fibres present in this layer [21]. It is well vascularised and therefore provides a nutrient supply to the dermis and good transport system for the extraction of harmful substances from the skin.

The interface between the dermis and hypodermis is not clearly defined, although the layers can roughly be identified by their composition. The adipose tissue is more highly concentrated in some areas of the body than others, such as the abdomen and thighs. It is typically thinner in men, young children and elderly people.

2.2.1.4 Other structures

Muscle: Muscles in the skin have reduced function compared with those of other animals. “Goose pimples” arise due to the reaction of smooth muscle in cold temperatures. Some facial expressions are controlled by some of the muscles in the dermis.

Blood vessels: Body temperature is maintained or adjusted by the network of blood vessels within the skin. In cold conditions, blood is retracted from superficial vessels to conserve heat, but normally, vessels in a plexus close to the dermis-hypodermis interface supply the sweat glands. Blood has no nutritional purpose in the superficial epidermis because most of the cells in this layer are dead.

Nerves: There is an abundant supply of nerve fibres in the skin, the majority of which are concentrated in the face and limbs. Of the free sensory nerves, only the minority extend as far as the epidermis; these are non-myelinated. However, these nerves do not typically penetrate the skin superficial to the dermis. Nerves of the autonomic system are responsible for regulation of the arrector pili muscles and sweat glands, as well as the blood vessels. Our ability to sense skin deformation in one form or another depends on the mechanoreceptors, and heat and pain on nociceptors. These contribute to the preservation of the skin's barrier activity.

Hair: Hair shafts are cylindrical in shape, consisting of a soft keratin centre (*medulla*), hard keratin in the *cortex* (intermediate layer), and the *cuticle* (outer layer), making the hair stiffer [22]. Each shaft is fixed in the skin by means of the hair root and is produced by the hair follicles, which are found as deep as the lower part of the dermis, often penetrating the hypodermis.

Exocrine glands: *Sebaceous glands* and *sweat glands* are the exocrine glands of the skin [22]. Secretory sebaceous gland cells rupture to release large amounts of lipids known as sebum. This coats the hair shaft to protect them from breakage; once dead, keratinised cells are susceptible to dehydration and rupture outside the body. Sebum also reduces bacterial growth.

2.2.1.5 *Stratum corneum*

The stratum corneum, also known as the *horny layer*, is the most superficial layer of the epidermis [18, 19]. It is of particular interest here because it is the layer of skin that comes into direct contact with the coverstocks of incontinence pads and similar products. It is where initial damage arises. The stratum corneum consists of *corneocytes* (flattened and dead keratinocytes) in an extracellular matrix with lipids [18] – see figure 2.3. Corneocytes are full of keratin filaments and are enclosed by a keratohyalin granule derivative, making each entire cell mechanically tough and resistant to chemicals. According to Forslind [23], it is feasible that the extracellular lipid bilayers are, in fact, supported by a 'mechanical scaffold' of corneocytes. It is also thought that the mechanical stability of corneocytes, parallel to the surface of the skin, is a result of keratin fibres within the corneocytes, mostly aligned in the same direction.

The top layer of corneocytes are removed by a process called *desquamation* (or exuviation), which usually occurs to displace external harmful matter from the surface of the skin [23]. New keratinocytes

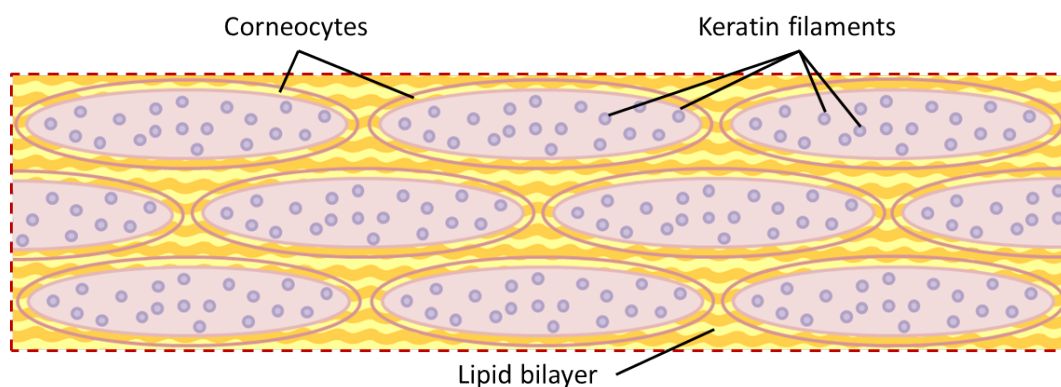


Figure 2.3: Corneocytes in extracellular matrix of lipids

are continuously being regenerated to replace those shed from the superficial epidermis [18, 19]. Mitosis occurs deep in the epidermis and new keratinocytes are forced upward (for 30-40 days). Trauma to the skin causes an increase in rate of regeneration of these cells. In fact, it is injured epidermal tissue that has the highest rate of all bodily tissues [19]. The time required for a cell from the deep epidermis to reach the surface increases with age, which may explain why old skin appears to be thinner than young skin.

When the stratum corneum swells, this happens almost entirely perpendicular to the surface of the skin, thereby reducing parallel deformation of intercellular matter as well as surface roughness. These may be desirable because lipids in the intercellular matter are required to minimise water transport through the skin and so must maintain their area parallel to the skin to remain effective. If it were possible for swelling to *increase* skin surface roughness, other mechanical properties of the skin would also be compromised. Although it is often perceived that the hydrophobic nature of lipids would cause water to travel only through the corneocytes, there are some cases where water can also pass *around* the cells. This is, specifically, when lipid bilayers are in their *liquid*-crystalline state (between a normal liquid and a solid crystal state, where molecules may have a common orientation but no fixed position) [23]. Nevertheless, most lipid bilayers are in a crystalline *gel* state and are therefore closely packed and essentially impermeable to water.

Although the stratum corneum (SC) is not completely impermeable to fluids, it acts as a good barrier on both sides – against endogenic fluids evaporating via routes other than sweat pores, and exogenic fluids attempting to enter the body. If essential fatty acids (such as cholesterol, ceramides and free fatty acids) are withdrawn from the epidermis, its effective permeability is increased, thereby compromising the skin's barrier function. Removing the stratum corneum altogether, over-hydrating, dehydrating, and applying detergents to the skin can all (individually) increase cutaneous permeability considerably [18].

Desquamation of corneocytes *passively* protects against infection, however, a range of *antimicrobial peptides* present in the skin provide an active defense against unwanted microorganisms. The rate of penetration of a material through the epidermis normally depends on local SC thickness and concentration gradient across this layer. It also depends on the substance itself; water permeates more easily than, for example, sodium and potassium ions, and other electrolytes. The SC also has low permeability to various non-ionising compounds such as urea and glucose. Although the properties of a solvent are, for the most part, responsible for the permeation of a solute, the temperature of the skin can increase penetration rate.

The surface topography of human skin on a microscale should, logically, depend on the most superficial layers of cells in the stratum corneum. It has been widely investigated, using a variety of mechanical and optical measurement techniques, *in vivo* and *in vitro*, leaving much to be desired by way of accuracy. However, a recently published study, by Kottner *et al.*, compared two optical techniques for examining the skin profile *in vivo* [24]. It was concluded that both methods (SELS – digitally processed camera imaging – and PRIMOS – measuring the deflection of projected lines on the skin) were consistent in their prediction of surface topography of the skin. While this was an interesting study, the imaging techniques would be inappropriate for use during friction measurements to monitor changes in the surface of the stratum corneum.

2.2.2 Transepidermal water loss

Much has been discussed here about the role of the stratum corneum (SC) as a barrier against water/fluid loss. However, there is a natural constant loss that takes place regardless, called *transepidermal water loss* (TEWL) [25]. TEWL inevitably occurs due to passive water flux through the dermal and epidermal layers (approx. 70% hydrated) toward the essentially dessiccated (approx. 10% hydrated) superficial layers of the SC [26]. Some water remains in the skin, while some evaporates from the surface, the ratio of which depends on the temperature and humidity of the surroundings.

It is important to note that TEWL does *not* include water lost in sweat. It is now commonly accepted that damage to the skin negatively affects its barrier function, thereby increasing TEWL [25]. This damage may occur due to trauma, excessive hydration, or any of the other aforementioned mechanisms (see §2.2.1.5). TEWL can be quantified by taking measurements, on untreated skin, of *water vapour flux density* (WVFD), which is defined as “the flux density of liquid water in grams per square meter per hour ($g \cdot m^{-2} \cdot h^{-1}$) measured on the skin surface that is not only contributed to by TEWL” [3].

It is not possible to directly measure TEWL practically because water loss through the skin is not visible, therefore it is unclear what proportion of the WVFD is attributed to TEWL. However, with the external application of excess water to the skin surface, the WVFD graph will show a peak, eventually followed by a plateau at equilibrium. The plateau indicates *baseline* TEWL, which is the TEWL in stable, environmental (temperature and humidity) and bodily conditions, when the person (on which measurements are being made) is relaxed – see figure 2.4. The peak represents the loss of excess water, the area beneath which is equivalent to skin surface water loss (total mass of excess water lost from the surface per square meter), when baseline TEWL has been subtracted [3].

Many evaporimetry devices (for measuring TEWL at the skin surface) have been used in a range of applications and some have been compared for reliability [3]. However, the general consensus is that, provided measurements are normalised, there is good agreement between instruments [25]. TEWL measurement techniques are grouped according to instrument design: open-chamber, closed-chamber and ventilated chamber methods. Some are used more than others, but no further detail will be included here as it is not particularly useful or relevant to any choice of evaporimetry device used in this work.

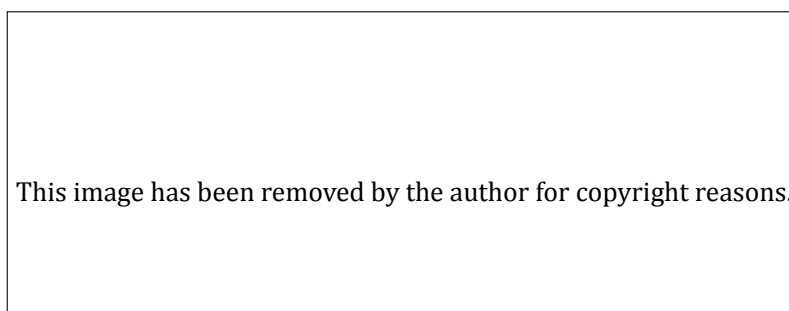


Figure 2.4: Example desorption curve (change in WVFD over time) – from [26]

While TEWL can be converted directly to an estimated value of the water content in the skin, such measurements are typically time-consuming and an instantaneous value cannot be obtained. Other instruments for quickly estimating the hydration of the skin include a fingerprint sensor and Corneometer [27, 28]; both are capacitive devices that provide a representative (arbitrary) value of skin hydration. The former works by measuring the capacitance of a region of skin and creating a visual plot of local readings and corresponding greyscale values (on the computer to which the device is attached); this measurement is repeated several times during the space of as little as one second. The mean greyscale of the output images is related to the skin hydration – the higher the value, the more water is present in the skin (with a maximum value of 255) [27]. Unfortunately, the depth of penetration is not known, so it is difficult to determine by how much the readings are influenced by water present deeper in the epidermis. The Corneometer consists of two probes (digital and analogue), containing gold electrodes, connected to a small recording device [28]. Any frequency shift in the oscillating system, associated with capacitance of the skin, is recorded and the value is considered to represent skin hydration. With the digital probe, a larger variation in values can be observed when the skin is dry – possibly because the capacitors are more sensitive in these conditions – but less so when there is an excess of liquid. Experiments have been conducted to investigate the measurement depth, and it was found that readings were still obtainable at 15 μm from the probe, although values were considerably lower.

2.2.3 Skin trauma

As previously mentioned, skin can undergo both chemical and mechanical damage due to a combination of urine (and faeces) and friction forces in the case of people with incontinence. It is important to understand why and how this can occur in order to be able to alleviate symptoms or to treat or prevent the trauma altogether. Much research has been carried out to investigate the impact of overhydration and friction of the skin on skin damage. This varies from studies on lesions that can arise from daily activities, such as shaving, rubbing leading to blister formation and the application of cosmetics, to skin trauma as a direct result of prolonged pad usage or immobility. Dowson described work done by others to investigate the formation of blisters [29]. Earlier research revealed that only some areas of skin on the body could form blisters, whereas other skin sites experienced abrasive damage to their thinner, less cohesive stratum corneum, which would – *presumably* – include skin of the perineum or groin. Comaish investigated this further and discovered that the relationship between friction force and number of cycles could be described mathematically [30]. Predictably, based on Comaish's findings, they were inversely proportional for forearm skin.

Bronneberg *et al.* [31] studied the impact of sustained loading on a biological skin surrogate *in vitro* to provide a better insight into the formation of pressure ulcers. They found that skin damage *did* occur after prolonged application of a normal stress, particularly a high stress, and that a marker produced by the tissue was a particularly good indicator of damage. Moreover, it is already accepted that shear stress between the skin layers contributes to the formation of pressure ulcers. Although they are not the same as IAD or other forms of perineal dermatitis, a link does exist between them, in that they develop under very similar circumstances. In 2004, Gray reported on the causes and management of perineal dermatitis with particular focus on IAD [15]. Mechanical damage due to friction could ensue following small movements of a pad against and/or forceful cleansing of the skin. Intraepidermal shear stresses and pressure would worsen the damage and both are associated with the manifestation of superficial ulceration. Preceding studies have emphasised the relevance of friction *in combination with* the hydration state of the skin to skin damage [32, 33] and such research has since continued.

2.2.4 Skin Biomechanics

In 1991 Marks [34] wrote a review of studies on the mechanical properties of the skin. Some of this has been summarised in this section and some more recent examples included. For the skin, more focus has been placed on its biochemistry than its physical properties and behaviour. This is possibly due to the complexity and impracticality of interpretation of data, as it is difficult to achieve meaningful data consistently. It is a challenge to identify certain behaviours and accurately attribute them to a particular feature of the skin because of the synergistic nature of its sub-structures.

As discussed previously in §2.2.1, the physical properties of skin vary considerably with age, gender and region of the body. Viscoelasticity adds to this variation, in that it reduces the possibility of producing a result without having allowed the skin to “recover”. Of course, environmental temperature and humidity affects several structures within the skin (blood vessels, sweat glands, hair and the SC), which, in turn, influences its physical behaviour. The skin displays anisotropic behaviour when loads are applied in any plane.

Over 20 years ago, it was apparent that there was a lack of consistency in testing and analysis of the skin’s physical and mechanical properties. There was, however, one exception: standards of mechanical testing for dermis *in vivo* set by a subcommittee of the International Society of Bioengineering & the Skin and published in 1982 [34]. The dermis has commonly been tested in the same way as many rubbers, despite its obviously very different structure. Experiments that produce stress-strain curves have been used to assess its viscoelasticity. Stress-relaxation has also been examined.

Curves from such measurements are essentially split into a linear and nonlinear region. The linear region is said to represent the elastic (Hookean) phase, within which applied load and extension are directly proportional, and the skin can be returned to its original dimensions once the load has been removed. In the nonlinear region that follows, the skin continues to extend, but plastic deformation occurs here. For this, the load must be kept constant, and the extension that takes place is known as “creep”, “viscous extension” or “viscous slip”. Further permanent deformation can occur, representing a third phase. However, in a paper by Agache *et al.* (2000), it was explained that the middle phase relates to *viscoelasticity* displayed by skin and represents *variable creep*, whereas in the last phase, creep is *constant*.

The extent and type of deformation depends on the point at which the load is removed and the number of times the loading is repeated within a given time period. This is something that should be considered when carrying out repeated friction measurements on volar forearm skin (see chapters 4 and 5). Marks [34] comments that collagen from the dermis tested by itself appears to produce a similar mechanical result to skin as a whole, suggesting that dermal collagen is the biggest contributor to the biomechanical properties. He also suggests that the increased epidermal thickness on palms of hands and soles of feet would change this.

2.2.4.1 *In vivo* tests on dermis

These tests are more useful and/or relevant than those *in vitro* / *ex vivo* but are typically problematic. Natural tension loss in skin after excision from the body also causes thickening of the dermis. The direction of the maximum resting skin tension in different areas of the body are indicated by Langer’s lines, as shown in figure 2.5, to which most dermal collagen and elastin fibres are parallel [35]. This is particularly interesting when considering friction measurements because it is likely that the response of the skin will be different depending on the orientation of applied shear load. However, for now the focus will continue to be on non-shear methods; friction will be covered later in the chapter (§2.3.2).

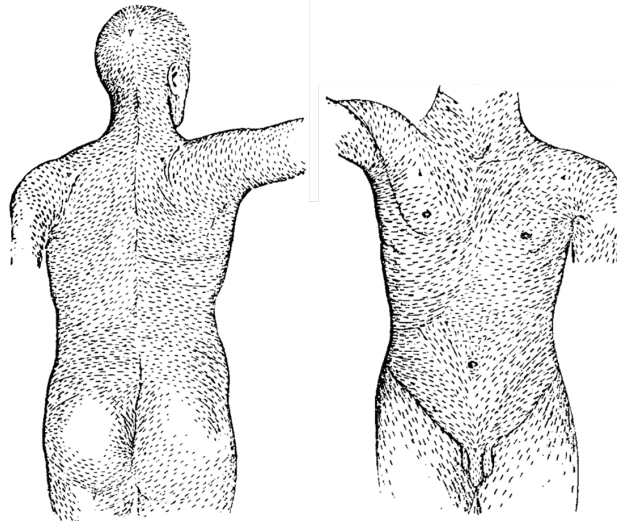


Figure 2.5: Diagram of Langer's lines on an adult female [36]. Reprinted from *British Journal of Plastic Surgery*, Vol. 31, Langer, On the anatomy and physiology of the skin: I. The cleavability of the cutis, pp. 3–8, Copyright 1978, with permission from Elsevier.

Marks [34] explained that the dimensions of the tested area of skin are important as they affect the property data obtained. Thickness is tricky to estimate *in vivo*, but variation would be limited provided the same site is used on every participant, who should also be the same gender and similar age. When working with skin *in vivo*, there is of course the added challenge of keeping the test site still for the measurements. Body movements, even those that are apparently small, can greatly alter the data recorded.

A range of calipers, as well as radiography and ultrasound have all been used to measure skin thickness. Such measurements are currently taken with a view to assess the effect of a particular drug on the skin, for example, whereas originally they were used for general studies on human health and lifestyle.

2.2.4.2 Instrumentation and methods

Marks [34] has reviewed several methods of assessing skin biomechanics and their instrumentation, which have been categorised as follows: tensile, torsional, indentation, normal traction types and wave propagation tests. Work done in three of these areas (tensile, indentation and traction) and related comments from Marks will be summarised before going on to discuss friction on skin.

Tensile testing is most commonly executed with “extensometers” and is described as uni- or bi-axial depending on the skin sample dimensions. For *in vitro* testing, when the parts of the skin gripped by the extensometer (tabs) are narrower than the region of interest (length between grips), then it is uni-axial; if they are wider than the length, bi-axial. As with any other human tissue tensile testing is notoriously difficult to do when it comes to gripping the sample and making measurements on the inter-grip section only. For this reason, skin around this site should be constrained for bi-axial tensile testing. *In vivo* tensile testing of the skin requires different devices to those available for *in vitro* measurements, such as that in figure 2.6.

Khatyr *et al.* [38] performed single-axis tensile tests on forearm skin *in vivo*. They designed and built their own mechanical testing machine (the “extensionmeter”), which can apply “monotonous” compressive and tensile loads. Khatyr and colleagues also claimed that it can be used to investigate

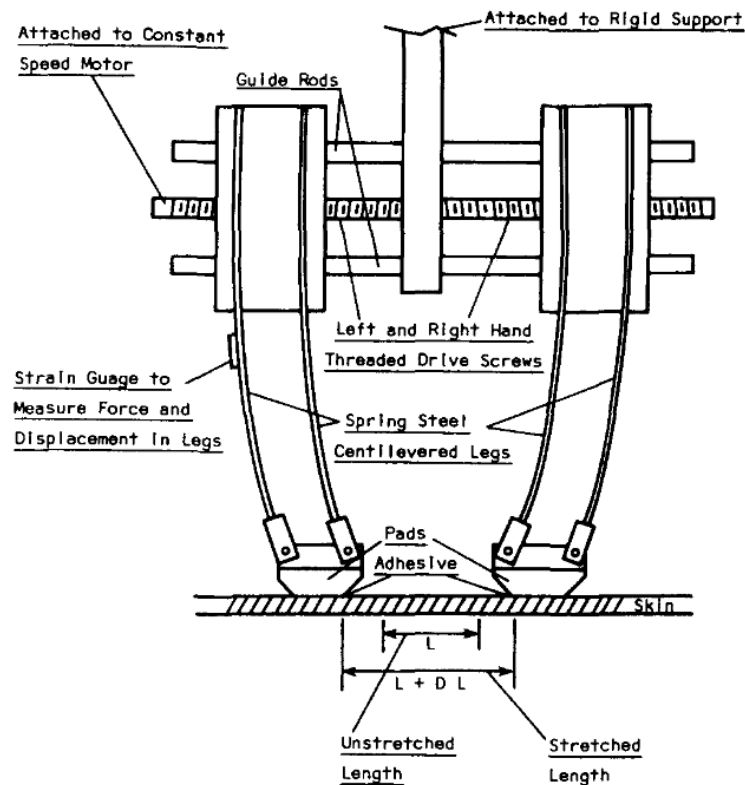


Figure 2.6: Example uniaxial extensometer for *in vivo* measurements of tension and compression on human skin; skin is adhered to pads and is displaced when mobile arms move; strain gauges measure force [37]. Reprinted with permission from *Review of Scientific Instruments*, Vol. 48, Thacker, J. G., Iachetta, F. A., Allaire, P. E., Edgerton, M. T., Rodeheaver, G. T., & Edlich, R. F. (1977) *In vivo* extensometer for measurement of the biomechanical properties of human skin, pp. 181–185. Copyright 1977, AIP Publishing LLC.

creep and relaxation effects on skin of the forearm. The team produced a computational model of the test to aid analysis of results obtained from the physical measurements. Jaws were attached to skin and pulled in different directions, while displacement and tensile force were measured.

Khatyr and colleagues attempted to improve the viscoelastic model produced by Agache *et al.* in 2000. This improvement aimed to tackle the false assumption that skin's creep behaviour is always permanent (i.e. it does not recover from compression) and could therefore be modelled using a shock absorber. Unfortunately, the results section is rather unclear. There does not appear to be any evidence for the findings stated by the authors, despite claims that their simple model worked and could be used by dermatologists.

The use of extensometers facilitates data interpretation, more so than other instrumentation. However, the distribution of stresses and strains on the skin is non-uniform due to attachment sites on the tensometer. Stresses are transmitted via the adhesive in the grips and the epidermis. Furthermore, the applied stresses are susceptible to changes in the mechanical properties of the adhesive: some display creep behaviour, which makes for a negative addition to the already-time-dependent nature of skin.

Indentation testing of skin typically involves the use of a small probe to compress the skin under a known load or at a known displacement rate. The probe end is usually spherical [39, 40, 41] or flat (cylindrical) [42, 43], but can be virtually any other shape, such as conical [44]. Most indentation stud-

ies have been carried out on the whole skin or dermis, but microindentometers (with probe diameters <1mm) have been used to measure the indentation properties of the stratum corneum specifically, as well as the whole skin [45, 46]. In past studies, load has been applied discretely using (dead) weights, and continuously, and in other cases, displacement rate was set while forces were measured. Unfortunately, such testing requires complex analysis by computational and mathematical modelling where the skin is modelled as an elastic half-space. No more detail on this will be provided here as it becomes more relevant to friction between skin and nonwovens later on in this chapter.

2.2.4.3 *In vitro* tests on dermis

Most of the skin used in these studies has been sourced from human cadavers and animals, with only some excised during surgery on a living person. The aim of some of these studies has been to relate certain physical features or components of the skin to its mechanical properties. Not all experimental work has been carried out using the skin specifically, but often using other anatomical structures, such as ligaments. The purpose of such a substitution would be to aid data interpretation for experiments implementing real skin. Although tissue from cadavers and animals may be adequate for the study of some mechanical properties given appropriate assumptions, there are, of course, benefits to using freshly excised human skin. One example of this would be the fact that it has not been chemically treated or frozen. Such modifications *may* impair its mechanical integrity, causing the skin to display uncharacteristic behaviour. On the other hand, even the use of fresh excised skin has limitations. A positive outcome of *in vitro* testing is the possibility of collecting large amounts of data from extensive cyclic loading and loading to failure. Many of the studies performed on animals are not relevant to the work described in this thesis, and for that reason, are not described in this section. While the primary experiments of interest are those measuring friction forces, it would also be useful to understand some of the other mechanical properties of skin.

In 1983, Dunn and Silver [47] carried out a range of tensile tests on skin from the thorax and abdomen of cadavers along with other tissues (e.g. thoracic aorta and dura mater). Microbial growth on the tissues was suppressed by treating all tissues with saline in a phosphate buffer. Each sample was tested within seven days of excision from the donor bodies (at autopsy) and those not used immediately were stored at 4°C. Dunn and Silver state that the length of storage period did not affect mechanical properties of the tissue, at least not up to seven days. Y-shaped pieces of skin were taken from male cadavers and T-shaped pieces from women, although the reason for this was not explained. A gauge length of 20mm was set for each sample. The authors refer to “wet specimens” being tested along the “Y” but do not explain what this means and how it relates to testing of the T-shaped pieces from women.

Dunn and Silver claim to use a similar technique to Sanjeevi [48] to study stress relaxation. The skin was extended by 10% at 10%.min⁻¹ before being relaxed at a constant strain rate, until stress reached equilibrium. This was repeated until the tissue began to fail. The authors examined the elastic and viscous aspects of these viscoelastic materials separately, hoping to be able to attribute individual features to mechanical behaviour. Their resulting stress-strain graphs for skin demonstrate that the proportion of elastic contribution is always higher than that of viscosity after ~45% strain. (See figure 2.7 for an example stress-strain curve from an independent set of measurements.) The idea to separate these mechanical components stems from the suggestion that each component may depend on specific structures within the skin.

It is important to note that the viscous contribution is lower in these tensile tests than those with a higher strain rate because some tissue relaxation takes place *during* loading as well as in the intervals

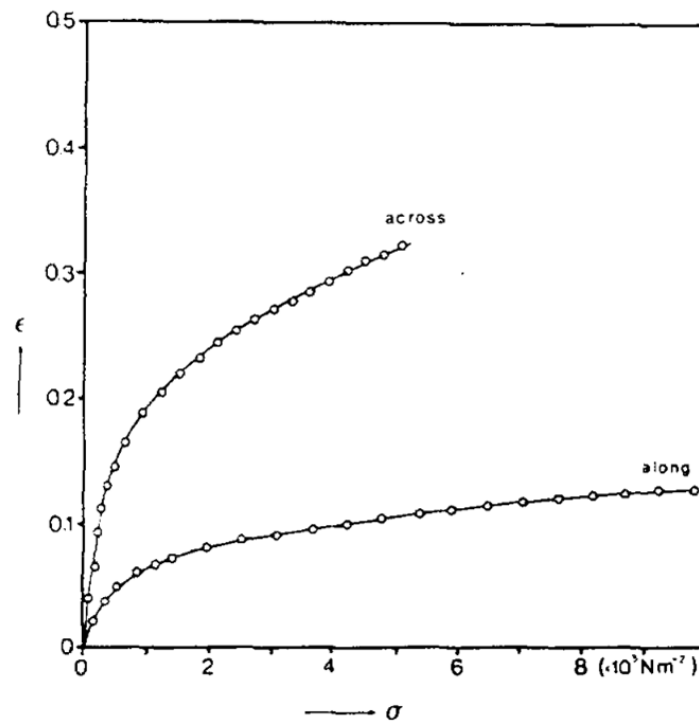


Figure 2.7: Example stress-strain curve from tension measurements on human skin; higher strain across the calf than along it; the x-axis is *stress* (σ) $\times 10 \text{ N} \cdot \text{m}^{-2}$ and the y-axis is *strain* (ϵ) [49]. Reprinted from *Journal of Biomechanics*, Vol. 19, Manschot and Brakkee, The measurement and modelling of the mechanical properties of human skin in vivo—II. The model, pp. 517–521, Copyright 1986, with permission from Elsevier.

between increasing load. At a higher rate, less relaxation occurs, therefore stress depends more on the viscous component. However, the elastic contribution does not change with strain rate. Dunn and Silver explain that collagen fibrils in skin, which are normally relatively random in orientation, can align themselves parallel to the applied force. Using this knowledge, they infer from their results that the realignment may require a substantial loss of viscous energy. It also appears that, provided tensile forces are applied uniaxially, they may be applied to a sample of skin in any direction without being affected by fibre orientation. As soon as the fibres are aligned, the skin begins to behave in a similar way to a tendon under tension.

Silver *et al.* [50] aimed to investigate if the elastic spring constant was identical for collagen molecules in both skin and tendon tissue. This was to be done through analysis of viscoelasticity of the skin *in vitro*. They also endeavoured to compute the same for elastin but did not state why. The data on skin was from the Dunn and Silver paper described above [47]. Various “decellularised collagenous substances” were mechanically tested and analysed: incremental tensile stress relaxation test, same parameters (strain rate, gauge length etc.) as the Dunn and Silver paper [47]. The method is rather unclearly presented, perhaps because the authors also describe other/previous work. The authors found that the skin had lower compressive moduli and elastic spring constant than the tendon.

2.2.4.4 The effect of age on mechanical properties of the skin

There are some obvious visible changes to skin that occur during the ageing process and it would be useful to have an understanding of how these physical changes relate to the mechanical properties. This is of particular interest for the work presented in this thesis due to the range of ages of incontinence-product users and the greater prevalence (growing population) of *elderly* incontinent people. Unfortunately, the range of anatomical features and mechanisms involved complicates the experimental assessment and quantitative analysis of data collected. Analysis is further complicated by the uniqueness of each person's skin, both genetically and environmentally. An example of the latter would be apparent premature ageing due to excessive exposure of the skin to ultraviolet light: such a person may have wrinkles earlier than expected due to a depletion of collagen in the skin, although the associated atrophy would not occur until old age [51].

In general, the epidermis becomes thinner with age and the transition region between the dermis and epidermis compresses. This makes older skin more susceptible to blistering by epidermal detachment [52]. Although the epidermis thins in bulk, the stratum corneum itself generally does not lose thickness, but it is regenerated at just over half the rate in the elderly. The implication of this is that tissue repair takes longer than it does for young people and this is accompanied by reduced barrier function of the stratum corneum. Much as the slowed production of collagen fibres increases the compliance of the skin, it is widely accepted that a loss of elasticity occurs with ageing due to a gradual loss of elastic fibres [53]. More recently, dermal fibroblasts were also shown to increase in stiffness with age [54]. This age-related change in elastic modulus was also found by several others [55, 56].

2.3 Biotribology: Friction

Tribology – a term first published in a report by H. P. Jost in 1966 – stems from “tribos”, a Greek word that means “rubbing”, and is technically defined as “the science of rubbing”, or perhaps more appropriately now, the study of friction, wear and lubrication [57, 58, 59]. *Biotribology* simply specifies that such interaction is between a *biological* substrate and another material. It is the primary focus of work that will be described in this thesis – particularly friction – and has been the basis for many research studies on the use of products and medical devices that come into direct contact with the human body. In this section, the principles of friction and some friction mechanisms will be discussed, followed by published work on measurements of friction between human skin and various materials. Before exploring the theory and commencing a review of the relevant literature, it is first necessary to define the key basic laws and two important terms used throughout this thesis that are fundamental to the understanding of frictional interaction in general.

Amontons' laws of friction state that friction force (F) is directly proportional to the applied normal force (L) ($F = \mu \cdot L$); and that the coefficient of friction (μ) is independent of nominal contact area.

Static friction (force) is the shear force required to *initiate* relative movement between surfaces in contact, where the initial velocity of displacement is equal to zero.

Kinetic or dynamic friction (force) is the force required to *maintain* relative movement between the contacting surfaces. Normally, static friction force is greater than kinetic friction force.

2.3.1 Friction mechanisms and lubrication

Although Amontons' law is ideal for simple cases of friction between two hard solid objects, it is not sufficient where there is, for example, adhesion (see §2.3.1.1) between surfaces because a range of friction forces can arise at a certain applied load rather than one finite force. This means that, if relative motion between contacting bodies depends on an additional force to that of friction, it is most likely because there is another mechanism involved. Such a mechanism would be detectable on a smaller scale than the dominating friction component, but would still contribute to the measured force. For example, a critical shear force must be reached before two surfaces can become un-"pinned" from their adhesive contact state [60]. Experimental data suggests that there is little difference between geometry at the contact site during static friction and that during kinetic friction, whether smooth or rough ("stick-slip" – see section 2.3.3). When two objects come into contact, deformation of one or both occurs as a consequence of externally applied normal loads and/or interfacial attractive forces. The following sections describe some of the mechanisms associated with friction; the first two are particularly relevant to friction between skin and various materials.

Lubrication of two interacting surfaces in friction can occur either in the presence or absence of a liquid. In the case of friction between human skin and other materials, the state of a lubricant is most likely to be liquid, so definitions of different types of lubrication given here will focus on that. Many forms of lubrication exist; the occurrence of each depends on a combination of factors. The main types are described below and compared on a Stribeck curve in figure 2.8.

Boundary lubrication: The lubricant is of molecular thickness on the surfaces of the interacting bodies [61]. When sliding is smooth, Amontons' law is obeyed (friction force \propto applied load); this is true for steel with various lubricating liquids [62]. Intermittent sliding results in a similar, but non-linear relationship and very low loads induce an increase in coefficient of friction as they decrease, even if the solid surfaces are not in contact. It is possible that two interactions are measured – each solid surface with the lubricant. A change in low sliding speeds has a negligible effect on mean coefficient of friction, whereas static and dynamic coefficients decrease slightly with increasing speed.

Fluid film lubrication: Interacting surfaces are completely separated by the lubricant. It is usually in the form of hydrodynamic (rotation or non-parallel sliding of one surface against another draws liquid/lubricant into a converging gap between them and keeps them apart; can be affected by elastic deformation of interacting bodies and thermal energy in the system) or hydrostatic (applying an external pressure to a lubricant between interacting surfaces) lubrication [61].

Mixed lubrication: A combination of both fluid film and boundary lubrication. It can be associated with intermittent motion.

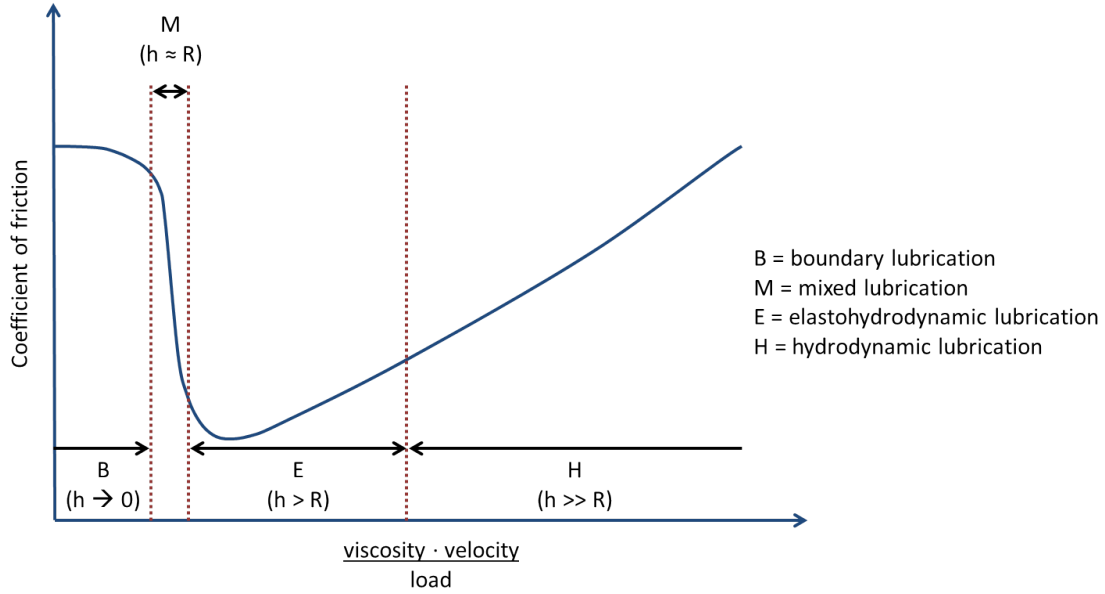


Figure 2.8: Stribeck curve (based on [61] and [63]); R = surface roughness

2.3.1.1 Adhesion

Hertz developed a model for compression between two elastic spheres *without* the presence of attractive forces. Here, when $F = 0$, $d = 0$ and $A = 0$, where F is external force, d is displacement (of one sphere relative to the others) and A is contact area [64]. With the inclusion of attractive forces, the Johnson-Kendall-Roberts and Derjaguin-Muller-Toprov theories were devised due to the more complex deformations that could not be described using Hertz's system. Berman and Israelachvili [64] explained that the former (JKR) is used for large bodies with a large surface energy, whereas the latter (DMT) is suited to small bodies with a high modulus and small surface energy.

The JKR theory is more applicable to skin-nonwoven fabric contact due to the potentially large amount of deformation of both materials on a macroscale. For this reason, the theory is discussed here in more detail. Although the skin and nonwoven fabrics are not spherical objects the example given is of two spheres in contact as a result of attractive forces at the interface, but no externally applied forces. When the increasing real contact area, under normal load, F , reaches a "mechanical equilibrium", the radius of this area, r , can be expressed as:

$$r^3 = \frac{R}{K} \left[F + 6\pi \cdot R\gamma + \sqrt{12\pi \cdot R\gamma \cdot F + (6\pi \cdot R\gamma)^2} \right], \quad (2.1)$$

where

$$R = \frac{R_1 \cdot R_2}{R_1 + R_2},$$

[R_1 and R_2 are the radii of the spheres], K is bulk elastic modulus and γ is surface energy.

Assuming $\gamma = 0$, the equation becomes the same as that given by Hertz's model. The adhesion force, F_s , also stems from the JKR theory; this is the force required to separate the adhered surfaces and can be calculated as shown below:

$$F_s = -3\pi \cdot R\gamma_s, \quad (2.2)$$

where γ_s is the surface energy [$\gamma_s = W/2$ where W is reversible work of adhesion].

When considering the above equations (2.1 and 2.2) [64], it can be seen that, theoretically, adhesion force (F_s) is independent of bulk elastic modulus (K) despite the effects of K on real contact area. This theory has indeed been validated in experimental work by Johnson *et al.* who measured contact diameters of optically smooth spheres – made from rubber and gelatine – under a range of normal loads and related the contact to surface energy [65].

Where there is adhesion between two surfaces, friction force and load are not directly proportional. With rough surfaces, the attractive forces must counteract the repulsion from high asperities on each surface that are compressed against each other, in order to have an increase in contact area (see figure 2.9). For this reason, adhesion is typically higher between easily-deformed viscoelastic surfaces, such as human skin perhaps, and the relationship between friction force and contact area is nonlinear here.

However, the area-load relationship *is* linear and Amontons' law *does* hold for Hertzian contact between rough surfaces. The linearity is lost when two *smooth* surfaces are in Hertzian contact (see figure 2.10). Contact between smooth surfaces with adhesion is not directly proportional to externally applied normal forces, and is potentially smaller than that between easily deformable rough surfaces.

In fact, it is the forces due to the adhesive effect that are proportional to contact area. This gives rise to the following equation describing smooth, adhesive friction, with no hydration or lubrication at the interface.

$$F = F_k = S_c A + \mu \cdot L, \quad (2.3)$$

where F_k is the friction force, S_c is a constant – critical shear stress (as described earlier on in this section), A is the contact area, μ is coefficient of friction and L is applied normal force.

Of course, when $L \gg S_c$, the equation can be written [64]:

$$F = \mu \cdot L, \quad (2.4)$$

(Amontons' law) and when applied load is small, it can be expressed

$$F = S_c A = S_c \pi \cdot r^2. \quad (2.5)$$

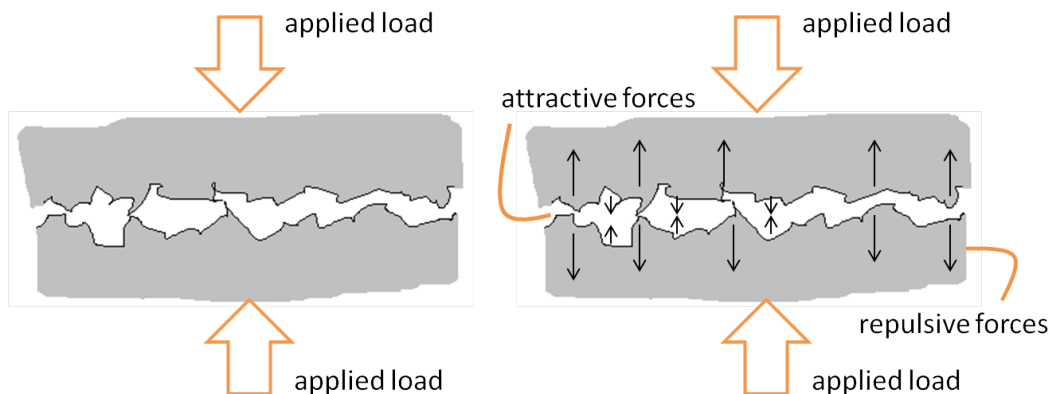


Figure 2.9: Diagram of Hertzian contact (left) and adhesive contact (right) between rough surfaces; note that the inclines of the asperities are much shallower in reality than this diagram suggests – they have been exaggerated for demonstration purposes only

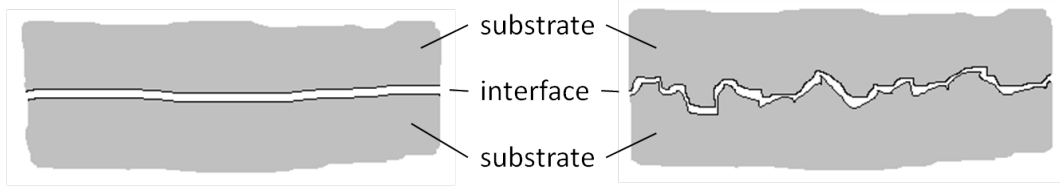


Figure 2.10: Diagram of smooth contact (left) and rough contact between soft surfaces (right); note that the inclines of the asperities are much shallower in reality than this diagram suggests – they have been exaggerated for demonstration purposes only

Substituting r from equation 2.1,

$$F = S_c \pi \left[\frac{R}{K} \left(L + 6\pi \cdot R\gamma + \sqrt{12\pi \cdot R\gamma \cdot L + (6\pi \cdot R\gamma)^2} \right) \right]^{2/3}. \quad (2.6)$$

The first equation (2.4) indicates a load-dominated contribution, and the second (2.5) suggests adhesion domination.

In general, lubrication of two interacting bodies (*in shear*) is more effectively achieved with liquids than with solids. Nevertheless, this depends very much on the ability of the fluid to remain between the surfaces with increasing externally applied pressure. If the liquid lubricant is forced out of the interfacial space, it cannot carry out its function; this in turn depends on the relative shapes of the surfaces and the possible routes for fluid to escape from the system.

When considering incontinence pads, the nonwoven-skin contact in the diaper area provides several routes for the passage of liquids:

- into the pad (absorbed by superabsorbent polymers and wood fluff pulp);
- into the skin (transepidermal uptake);
- through the interface gaps (leakage when pad absorption of urine is too slow or has reached capacity).

However, due to the flexibility and relatively low compressive moduli of the surfaces on a macroscale, it seems unlikely that urine (or any other fluid) would provide effective lubrication at this interface.

2.3.1.2 Plastic deformation

Bowden and Tabor reportedly created a model for friction by plastic deformation, resulting in an equation for coefficient of static friction as follows [66]:

$$\mu_s = \sigma_y / \sigma_h,$$

where σ_y is yield strength and σ_h is hardness (stress) of the softer of two materials in shear contact.

In this case, it is understood that friction between two solid bodies, in the absence of a lubricant, is characterised by plastic deformation of asperities on a microscale. It is also accepted that the real area of contact between such surfaces, A_{real} , is considerably smaller than the apparent contact area (i.e. most contact occurs between rough peaks). Therefore,

$$L = \sigma_h A_{real},$$

where L is net load, and

$$F_s = \sigma_y A_{\text{real}},$$

where F_s is net shear force.

Bowden and Tabor have indeed made it clear that their model is intended for metal-on-metal contact rather than any other materials.

However, two strong arguments that suggest that plastic deformation ought not to be considered a *dominant* mechanism of friction are:

1. Both the interacting solid surface and the lubricant (when present) contribute to the friction, in terms of their mechanical properties.
2. Theoretically, not all points of contact on a microscale should undergo plastic deformation, but in fact, a tiny proportion only.

All of the above describes contact between clean, dry, solid surfaces in the absence of any kind of lubricant. Some lubricants are deliberately introduced into contact systems, some are contaminants; either way, they can have a huge impact on the mechanisms by which the main contacting surfaces interact. Provided the lubricating or contaminating molecules adhered to the surfaces remain in the interfacial space, they can diminish plastic deformation of asperities on the surfaces and the subsequent wear.

Alternatively, one or two layers of these absorbed molecules can form if the lubricant molecules become trapped at the interface under high pressures experienced between asperities (microscale), resulting in solidification of the molecules. A typical consequence of this is boundary lubrication. Molecules of lubricant or contaminant are often some distance apart, meaning that most of their interactions are with the opposing surfaces of the main bodies. This means that when a shear force is applied, the surfaces are “locked” into position, until the force is high enough to overcome the energy barrier. There are, of course, more mechanisms that result in the dissipation of surface energy to surmount static friction but none of these appear to be relevant to nonwoven-skin interaction.

Whilst the above example refers to two solid interacting bodies, usually hard, it does bear some relevance, due to the natural ability of skin and nonwoven fabrics to easily collect dust and other contaminants. Cottenden showed that plastic deformation as a friction mechanism played a role with nonwoven fabrics [4], while others have demonstrated that it is irrelevant to skin [67, 68]. So far, mechanisms for friction between two solid surfaces have been described, but the principles that apply here, do not apply to friction between a solid and a fluid. The static friction force that would normally be higher than the kinetic friction force does not exist in the latter situation.

2.3.1.3 Other mechanisms

Many friction mechanisms exist, other than interfacial adhesion and plastic deformation, but they depend on the physical and mechanical properties of the interacting bodies. The two examples given below were considered, by Cottenden [4], as potential mechanisms for skin-nonwoven friction, as well as the two described in §2.3.1.1 and §2.3.1.2. However, following some experimental work, Cottenden disregarded viscoelastic deformation and pinning as mechanisms for this frictional interaction.

Viscoelastic deformation: This is very similar to plastic deformation, except that the effect of *this* mechanism is temporary as the deformation is reversible when loading is removed. It is different to elastic deformation in that it is affected by sliding velocity and there is some energy dissipation.

Pinning: This is effectively localised stick-slip (see §2.3.3) as fibres pinned to a point are suddenly released before pinning themselves again to another region. It means that there is weak viscoelastic deformation and that slip at individual points of contact occurs at a much greater speed than the mean sliding speed, resulting in a large dissipation of energy and, therefore, a higher friction force.

2.3.2 Friction with skin

A large amount of work pertaining to friction between skin and various materials has been carried out with a range of devices to which the material of interest is attached. The three main types of device are torque devices (usually disks), probes (sometimes also rotating) and force plates: disks and probes often apply a normal force to the skin site under investigation and measure the friction force; force plates remain in a fixed position and measure the normal load and friction force as the skin slides across it. Most research has focused on friction with hard (non-textile) substrates, relevant to the tribology of the skin with hard surfaces, whether consumer products or medical equipment. As only relatively few papers have been published on work directly related to that presented in this thesis, the broader range of investigations using hard substrates will be covered before converging on the most pertinent ones. The most recent studies conducted are described first. Others have been summarised in table 2.2 (placed towards the end of this section on pages 31-37).

Derler and Rotaru [69] investigated the stick-slip phenomenon in relation to friction between the skin of the index finger pad and smooth glass. Both the skin and glass were wet and all measurements were carried out on one participant only. Prior to friction measurements, the participant acclimatised for 10 min at $\approx 23^\circ\text{C}$ and 50% relative humidity. The skin and glass were both cleaned with ethanol and deionised water; the skin was soaked in and the glass covered by a film of deionised water. Over the course of 30 seconds, 5-15 individual friction runs were performed by the participant, sliding his finger across the glass, which was fixed to a tri-axial force plate that measured and calculated normal force and friction force (see figure 2.11). Displacement was always 40mm but applied load and speed were entirely dependent upon the volunteer.

The authors found that the coefficient of friction (CoF) for stick-slip was generally lower (by roughly $\frac{1}{3}$) than it was for normal friction, without stick-slip, as well as for “initial phase” friction. Low CoF in the absence of stick-slip (or during “stationary sliding”) was attributed to lubrication at the interface

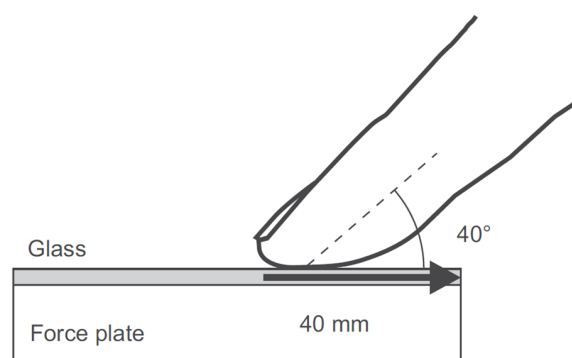


Figure 2.11: Diagram of finger sliding across a tri-axial force plate [69]. Reprinted from *Wear*, Vol. 301, Derler and Rotaru, Stick-slip phenomena in the friction of human skin, pp. 324–329, Copyright 2013, with permission from Elsevier.

and mixed lubrication was the suggested regime. They reported a relationship between sliding velocity and amplitude of the stick-slip peaks and troughs (slower = smaller amplitude). It is assumed that all stationary and stick-slip CoF were for dynamic friction as they were calculated from a range of data but it is not clear how or why these calculations were done. Coefficient of friction values were comparable to those from another study, conducted by the first author and colleagues, at lower sliding speeds and on more participants [70]. The lack of a clear correlation between CoF of the initial sliding phase and sliding velocity was regarded by Derler and Rotaru as support for their assumption that this CoF is related to coefficient of static friction. The friction model for the adhesion mechanism was found to apply to the data in this study.

Veijgen *et al.* [71] carried out a pilot study to test their new friction-measuring device: a small transportable handheld device that applies a normal force via a system using springs, to a rotating cylinder that is in contact with the skin (as in figure 2.12). The outer material of the cylinder can be changed and the device can operate at four different speeds. The *real* normal force was measured along with friction force using piezoresistive force sensors (presumably built into the device). The pilot study was carried out on the left ventral forearm of one young female volunteer because it is a commonly used testing site for friction on human skin and the data could be compared with those from other studies. Different combinations of speeds and loads were used with the stainless steel cylinder, of which surface roughness was measured, and isopropanol was used to clean it >10 min prior to experiments. The authors found that their data for CoF were comparable with those from similar studies, as was the *relationship* between CoF and applied normal load – CoF decreased with increasing normal force.

In 2013, Veijgen *et al.* [72] compared friction between skin and various materials at different hydration levels and temperatures. Four skin sites were tested (two on the forearm and two on the hand) and four materials (PE, PTFE, stainless steel and aluminium), attached to a rotational device described in the paper on their preliminary work [71], were cleaned with isopropanol, just as explained in the pilot study. A total of 31 relatively young participants (both genders) were not asked to do anything to their skin prior to testing, nor were they required to leave their skin unmoisturised – the authors hoped that the knowledge alone (of whether and how the skin had been treated up to 1hr before measurements began) would suffice as long as it was noted, but no further reference was made to this. The applied load range was 0.5-2N and sliding velocity was 1-10 mm · s⁻¹ for a 20-second measurement period.

The skin was not overhydrated by occlusion or the application of a fluid, rather the hydration and temperature were monitored for each participant, using a Corneometer and thermometer. The environment was not controlled either and the authors found that the relative humidity and temperature had a notable effect on the index finger pad and ventral (or volar) forearm respectively, which demonstrates why it is important to control the climate when possible. The relationship between coefficients

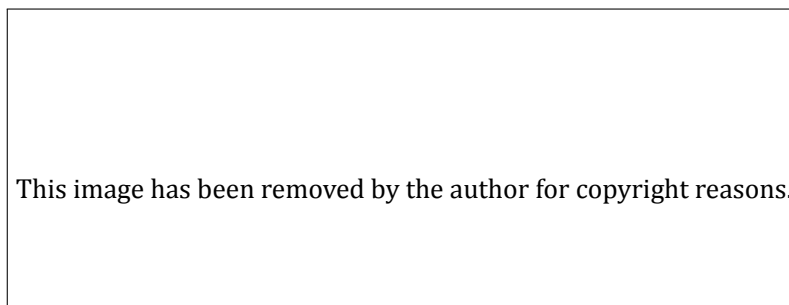


Figure 2.12: Diagram of cylinder rotating on skin from device that measures friction (from Veijgen *et al.* [72])

of static and dynamic friction was highly linear, but both varied greatly between the anatomical regions tested. There was a marked difference in skin hydration at each site between men and women – it was higher for women on both sides (ventral and dorsal) of the forearm – but there was only very little difference in CoF of the forearm sites between the genders. The biggest range of values was observed for ventral forearm skin. The CoF was lowest at the dorsal locations (forearm and hand) and the authors suggested that hair was acting as a lubricant when present in abundance.

Of the materials investigated, PTFE had the lowest coefficient of friction and stainless steel had the highest. Sliding velocity had no impact on the coefficient, which contradicts findings by Derler and Rotaru [69] for measurements on *wet* skin, but CoF did increase as applied load decreased. Without overhydrating the skin Veijgen *et al.* still concluded that skin hydration impacts coefficient of friction, as reported by others, but their data showed only a weak correlation between the two. Similarly, they showed a weak relationship between hydration and temperature of the skin. Reference to adhesion as a mechanism was made without suggesting whether or not it varied among participants in this study due to their different skin hydration levels.

In 2012, Derler and Gerhardt [73] conducted a comprehensive review of the literature on the tribology of human skin, with a specific focus on data from friction measurements. They explained that there are various reasons for measuring friction between skin and other materials – such as surfaces for devices used by consumers and medical applications – hence the range of methodology and instrumentation. Most of the studies mentioned in the review investigated non-textile materials and most used force plates or rotational or torque devices/probes. Some researchers endeavoured to use mechanical skin surrogates due to the repeatability of the methods and data and their ease of use (compared to studies on skin *in vivo*) as will be discussed in §2.5.

The hydration of the skin and its effects on friction have also been investigated and is now considered an important factor when assessing the interaction between the skin and other surfaces. This includes natural moisture from sweat and sebum, as well as applied moisture in the form of lotion or solvent. The effects of age, gender, ethnicity, natural skin temperature and hydration, and skin roughness, among other factors, were also explored. Older studies had a more general approach to measuring friction before much was understood about it and the mechanisms facilitating it. The following work was carried out prior to the review by Derler and Gerhardt; most has been summarised in table 2.2 for convenience.

Tomlinson *et al.* [74] measured friction between the overhydrated index fingers of three or five female participants in their study and a wet surface – it was not clear exactly how many volunteers took part – on a specially designed rig. The rig – described in a previous paper on rugby ball materials and friction with skin [75] – simultaneously recorded normal load and friction force as the participants pulled their finger across the test material surface. There were various test setups for this study, each to investigate a different variable: a range of contact surfaces (PP, HDPE, PVC, steel, aluminium and brass) when the skin was “moist” and applied load was not controlled in any way; restricted force application when pulling a “moist” finger across PVC; wetting the surface of the PVC but not the skin; a range of hydration levels (soaking times) for the skin with dry PVC; maximally overhydrated finger with wet PVC.

After washing fingers to eliminate impurities, a paper towel sprayed or soaked in tap water was used to overhydrate the skin and a dry towel was used to blot the surface dry. The reason given for using *tap* water related to the composition of sweat that leaves the palms, but the source of this water would affect its composition (in terms of solute content) and no comment was made about that. The test material was made wet with a humidifier to distribute the droplets uniformly. Skin moisture level

was measured with a device called Moistsense that converts capacitance readings to an arbitrary value representative of skin hydration.

The friction force was found to increase with skin wetness but peaked before maximum skin hydration for all contacting materials. The lower forces at this stage were considered to be a result of lubrication due to the presence of surface water. André *et al.* [76] and Nonomura *et al.* [77] also observed such a relationship, but other researchers did not [78, 79, 80]. Results comparing materials led to a suggestion that hydrophilicity may have been responsible for the differences in CoF observed. It was speculated that hydrophilic surfaces have a greater ability to form a stable fluid film, thereby increasing lubrication. However, there is no robust evidence to support this theory. When considering mechanisms operating during wet friction, the authors concluded that water absorption dominated and capillary adhesion *may* have contributed, although they accept that the analysis on which these findings were based was rather rudimentary.

Zhu *et al.* [81] investigated the effects of age, gender, skin site and skin hydration on coefficient of friction. In this study, 633 subjects were recruited (333 female, 300 male) for measurements on their dorsal hand, canthus and forehead. Friction was measured with a Frictiometer – and example of which can be seen in figure 2.13 – and skin hydration with a Corneometer after participants had acclimatised in an environmentally controlled room. The units of both CoF and skin hydration were arbitrary, which made little sense considering that CoF is usually reported as the actual value, so the values in this paper would only be comparable to others collected from the same instrument. The Frictiometer had a flat-headed, rotating Teflon probe attached. The rotation speed and normal load were stated (255rpm and 0.7N) but not the length of measurements, whether static or dynamic friction was of interest, or whether the skin was overhydrated in some way.

In females, the coefficient of friction of the dorsal hand and canthus peaked by 40 years and gradually decreased thereafter. For the forehead, it continued to increase with age. The authors stated that the CoF of the dorsal hand ceased to increase by the age of 40 for males and did not change thereafter. The graph presented appeared to demonstrate otherwise, but it is assumed that Zhu *et al.* drew this conclusion based on statistical analysis not presented in any detail in this paper. In fact, many other



(a) Frictiometer without testing material attached



(b) Frictiometer testing material attached

Figure 2.13: Example Frictiometer (reprinted with permission from Courage + Khazaka electronic GmbH) [82]

comments made in reference to the graphs appeared to contradict the authors' analysis, such as the only difference between skin sites observed for males was for 51-60 year-olds. For the most part, there was either no difference in CoF for males and females (forehead), or females had higher coefficients of friction (canthus and dorsal hand). However, this was not so when compared to young boys or very old men, who had high CoF on the canthus and dorsal hand.

Skin hydration was shown to increase in women until middle age before falling until old age. Interestingly, this age dependence of skin hydration was not observed for men. The authors reported that a positive correlation could be seen between coefficient of friction and skin hydration depending on skin site and participant gender. Although, it is not clear how this outcome was determined without explanation of how these values were related methodologically. The Corneometer readings suggest that the skin was not overhydrated with a solvent or occluded and, considering that the readings were arbitrary, it seems rather presumptuous to accept their relationship with friction at face value.

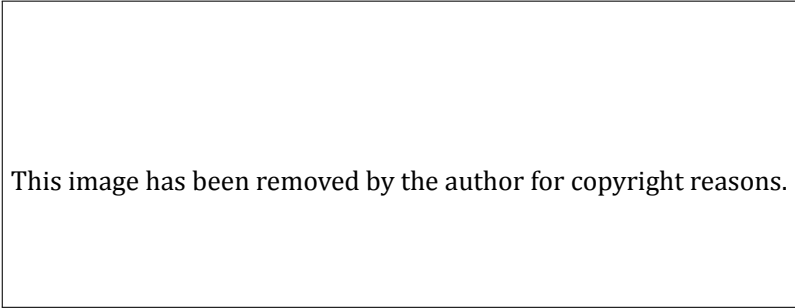
Many other papers contradict the findings by Zhu *et al.* that age and gender have an impact on coefficient of friction [83, 84]. The authors suggest several possible reasons for this:

- the considerably smaller sample size (usually <50 participants compared to 633) does not give a fair representation;
- the range of ethnicities tested (all, rather than one – in this case Chinese) introduced another variable, which has been shown by some [85, 86] to affect skin hydration measurements and therefore possibly CoF;
- the different skin locations tested would be expected to make a difference and the canthus, forehead and dorsal hand are not common test sites.

No attempt was made by Zhu *et al.* to suggest the friction mechanism(s) operating during their measurements.

Man *et al.* [83] measured the hydration of the stratum corneum, pH of the skin surface and the content of sebum in the volar forearms and foreheads of 713 Chinese volunteers (aged 0-94 years). Contrary to Zhu *et al.*, they found that pH of the forehead was lower for those under the age of 70, but stratum corneum hydration (measured with a Corneometer) was higher. Adolescent boys and young men had considerably higher levels than their female counterparts. Skin hydration results were essentially the same for the volar forearm. Marrakchi and Maibach [84] investigated the stratum corneum hydration and transepidermal water loss (TEWL) – among other factors – of nine different sites on the forearm, face and neck of 20 volunteers (10 young, 10 old). Stratum corneum hydration was measured with a Corneometer and TEWL with an evaporimeter. TEWL was lower for the forearms (and two other locations) of the older participants but the difference was not statistically significant. Conversely, the skin hydration was significantly lower in the *young* participants.

Diridollou *et al.* [85] compared the skin water content of the forearms of four different ethnic groups using SkinChip (a capacitance imaging device). The participants were 311 women (aged 18-87 years) of African-American, Mexican, Chinese and Caucasian origin and results were displayed as dryness indices, rather than skin water content values. For ventral (volar) forearm measurements, no significant difference was observed in younger participants (<51 years), but older African-American women did have significantly drier skin than their Mexican and Chinese counterparts. Caucasian subjects produced a skin dryness index in between those of the other groups. Kompaore and Tsuruta [86] found that the permeability of untreated skin to methyl nicotinate was highest in Asians, followed by Caucasians and was lowest in black people. After tape stripping the stratum corneum, black participants



This image has been removed by the author for copyright reasons.

Figure 2.14: Rotating ring device (adapted from [78])

still had the lowest permeability but white and Asian subjects' skin was more similar. It could be assumed that this also relates to the permeability of skin to water and its baseline TEWL.

In 2010, Hendriks and Franklin [78] investigated the effects of contact surface material roughness and environmental conditions on human skin friction with a rotating ring-type technology (see figure 2.14). Twelve volunteers took part – two for the roughness measurements and 10 for skin hydration – all aged 20-24 years old. The anatomical testing sites were on the cheek and three regions on the ventral forearm. No moisturisers or creams were to be applied on the day. Measurements were carried out using probes of different materials and surface roughness, under 2N and with a circumferential speed of $100 \text{ mm} \cdot \text{s}^{-1}$. Preliminary experiments revealed that frictional torque could continue to increase over a 60-second period, but measurements were limited to 30s for the comfort of the participants. It was suggested that continuous measurement for one minute led to superficial stratum corneum cells being removed, resulting in a different surface roughness, reduced barrier function or the creation of a transfer layer on the probe. Skin hydration was, indeed, measured (using a Corneometer) before and after friction measurements, and an increase was observed.

The impact of surface roughness on coefficient of friction was significantly large for all materials in both humid and dry conditions; CoF decreased with increasing R_a for the range tested ($\approx 0.1 - 10\mu\text{m}$). In a humid climate, coefficient of friction was found to be approximately twice that in dry conditions, but also more variable. Correlation between skin hydration and CoF was rather weak, although a relationship was visible, particularly on the forearm. On the other hand, it could be argued that the comparison with cheek skin was unfair: 11/12 participants were men, thereby introducing the possibility of facial hair interfering with friction measurements. The PTFE probe also had a significantly lower CoF than aluminium, regardless of surface roughness, but this was only the case when comparing climate conditions. Due to the different sample sizes of each experiment, it is difficult to tell if this observation was indeed true.

The authors concluded that the stratum corneum softened and swelled, a thin layer of adhesive fluid formed on the skin, and adhesive forces increased when the humidity was higher, all of which led to an increase in coefficient of friction. Not enough was known about *how* exactly each of those mechanisms influenced friction forces for the authors to speculate further. Nonetheless, they do claim that between the concepts of adhesion friction and shear stresses at interfaces with organic films and rough surface contact mechanics, a basic mathematical model could be created to elucidate the behaviour of skin in friction.

Elkhyat and Humbert [87] carried out a study on the effect of hydrophilicity on coefficient of friction and wettability and found that more hydrophobic surfaces typically had a lower CoF. They used glass, Teflon and steel against the volar forearm (number of participants not reported). This contradicts the

findings of Tomlinson *et al.* [74].

Derler *et al.* [88] measured friction between plantar skin (on the sole of the foot) of 14 volunteers – aged 8-63 years – and a selection of substrates with various surface roughness values. The test materials were fixed to a tri-axial force plate in the floor with a steel tank, so that the deionised water used to flood it (1-2mm thick) could be contained. Participants slid one foot 400-500mm across each substrate at a mean velocity of almost $0.5 \text{ mm} \cdot \text{s}^{-1}$, six to seven times, applying roughly the same normal load each time. The skin was not soaked or occluded before measurements and the foot was dried with a towel and air-dried between substrates, although the skin hydration was not monitored. The environment appeared to be partially controlled (approx. 23°C and 30-60% RH).

Mean coefficients of dynamic friction were reported to be in the range 0.117-0.590. The effects of applied load and sliding direction were also investigated later. Derler *et al.* found that applied load and particularly surface roughness did affect dynamic CoF, although there was inevitable variation between participants. As surface roughness of the hard floor coverings increased, so did the contributions of deformation and adhesion mechanisms. The authors speculated that the former may have arisen from abrasion, ploughing and hysteresis, but there was insufficient evidence to support this. Adhesion was thought to have increased on rough surfaces due to greater real contact area from local contacts between asperities.

Table 2.2: Papers on skin friction. (Key: μ = coefficient of friction; μ_d = dynamic μ ; μ_s = static μ ; L = applied normal load; ECR = environmentally controlled room; S-S = stick-slip)

Authors (year)	Contact materials	Anatomical region	Parameters measured/calculated	Methods	Findings/ future work	Participants	Notes (mechanisms, lubrication, etc.)
Gerhardt <i>et al.</i> (2009) [89]	4 woven fabrics – bamboo viscose, PTFE, cotton, polyester	Inner forearm	L; apparent interfacial contact area; mean μ_d ; skin hydration	Rubbed skin of dominant inner forearm against fabrics in a reciprocating motion. Test materials attached to force plate. 15-min acclimatisation in ECR.	L = 11-19N PTFE fabric had lowest μ . No difference between ages or genders – overall range of mean μ was 0.30-0.43.	60 (32 young and 28 old men and women; aged 18-95 years)	Adhesion and deformation – fairly consistent contributions to μ
Darden and Schwartz (2009) [90]	14 fabrics – different combinations of silk, acetate, polyester, nylon, cotton and more	Right index finger	$L > 0.3N$; shear force; μ	60 mm × 60 mm square samples of fabric mounted on rigid PE plates attached to a three-axis dynamometer and amplifier. Swiped finger across material. Tested parallel and perpendicular to fibre alignment. All in an ECR.	Sample and orientation had a significant effect on μ – higher perpendicular to fibres. Overall, mean μ was 0.280-0.624.	1	–

Table 2.2: Continued...

Authors (year)	Contact materials	Anatomical region	Parameters measured/calculated	Methods	Findings/ future work	Participants	Notes (mechanisms, lubrication, etc.)
Kwiatkowska <i>et al.</i> (2009) [79]	2 steel spheres (ø2 mm, ø5 mm)	Inner forearm	Frictional force; TEWL; skin hydration; μ_s ; μ_d	Skin cleaned before each test; measured TEWL and skin hydration during 30-min acclimatisation. Probe (attached to a specially designed machine) moved across skin in reciprocating motion (stroke length 17.6mm) at up to $16 \text{ mm} \cdot \text{s}^{-1}$ under $L = 0.19\text{-}0.5\text{N}$. All in an ECR.	μ ↓ as L ↑, but ↑ as ϕ ↑ ($\mu_s \approx 1.1 - 1.5$ and $\mu_d \approx 0.7 - 1.2$). S-S observed in all tests.	1 (32-year-old woman)	Adhesion (and a little deformation)
Gerhardt <i>et al.</i> (2008) [80]	Plain weave: 50% cotton, 50% polyester	Inner forearm (dominant)	L ; tangential forces; μ_d	No moisturisers applied and hairs were removed on day of testing. Fabric samples were fixed to tri-axial force plate. 15-min acclimatisation before subjects rubbed skin across material in reciprocating motion (ca. $80 \text{ mm} \cdot \text{s}^{-1}$; $L = 14.8 \pm 1.3 \text{ N}$. Repeated on skin soaked in normal saline. All in an ECR.	$\mu_d = 0.42\text{-}0.91$. Level of skin hydration affected women more than men. μ_d ↑ as skin hydration ↑. Same for wet fabric.	22 (31.7 ± 8.4 years)	Adhesion
Derler <i>et al.</i> (2007) [91]	A wool fabric	Index finger	L ; tangential forces; μ_d	Samples of fabric mounted on a dynamometer force plate. Rubbed finger across material for 20s.	Range of mean $\mu_d = 0.27\text{-}0.71$. μ_d not affected by L .	12 (24-61 years; men and women)	Adhesion and maybe deformation

Table 2.2: Continued...

Authors (year)	Contact materials	Anatomical region	Parameters measured/calculated	Methods	Findings/ future work	Participants	Notes (mechanisms, lubrication, etc.)
Adams <i>et al.</i> (2007) [92]	3 probes (spherically tipped); two glass lenses, one PP shell	Inner forearm	Rolling friction; mean μ_d ; "instantaneous" μ	Probe pulled across wet and dry skin in reciprocating motion (stroke length ca. 80mm) at $8 \text{ mm} \cdot \text{s}^{-1}$ under $L = 0.01\text{-}4\text{N}$. Skin and probes cleaned; 30-min acclimatisation. Skin wet with water via syringe. All in an ECR.	μ is independent of L when probe tips are spherical. For wet skin, $\mu \downarrow$ as $L \uparrow$ due to smooth surface created by plasticised SC cells; $\mu_{\text{glass}} \gg \mu_{\text{PP}}$. More stable fluid film with glass than PP – lubrication. Interfacial shear \downarrow but contact area \uparrow , so friction \uparrow . S-S observed. ($\mu_d = 0.226\text{-}2.84$)	1 (young adult male)	Adhesion
Sivamani <i>et al.</i> (2003) [93]	Spherical stainless steel ball, $\varnothing 10 \text{ mm}$	Dorsal skin of finger in vivo; abdomen samples in vitro	L ; μ_d	Probe pulled across skin 5mm in 60s. μ compared for a range of weights (5-45g), skin hydration and lubrication by water and isopropyl alcohol and 2 moisturising creams.	$\mu \downarrow$ as $L \uparrow$; water lowered μ and the alcohol even more so (by drying and shrivelling the skin. $\mu \uparrow$ with moisturiser application. Incorporate other anatomical sites.	?	-

Table 2.2: Continued...

Authors (year)	Contact materials	Anatomical region	Parameters measured/calculated	Methods	Findings/ future work	Participants	Notes (mechanisms, lubrication, etc.)
Egawa <i>et al.</i> (2002) [94]	Steel wires	Inner forearm	TEWL; capacitance; μ	30-min acclimatisation, then measured TEWL and skin hydration. Probe slid across skin at $1.1 \text{ mm} \cdot \text{s}^{-1}$, for 30mm under $L = 0.244\text{N}$. All in an ECR.	$\mu = 0.24 \pm 0.05$. For moist skin, $\mu \uparrow$.	53 (20-51 years; Japanese men and women)	Adhesion
Koudine <i>et al.</i> (2000) [95]	Glass sphere	Inner forearm	Frictional force; μ_s ; μ_d	Skin pulled under probe; $L = 0.05\text{-}0.5\text{N}$ at $0.125 \text{ mm} \cdot \text{s}^{-1}$. Repeated after applying a moisturiser to the skin.	Untreated (dry) $\mu_s \approx 0.25\text{-}0.8$; $\mu_d \approx 0.7\text{-}3.4$. When skin is moist, $\mu \uparrow$.	1	Adhesion
Asserin <i>et al.</i> (2000) [96]	Ruby sphere	Inner forearm	Friction force; μ	Probe (attached to a specially designed machine) moved across skin at constant velocity under $L = 0.2 \pm 0.1\text{N}$.	Frictional force $\propto L$. $\mu = 0.7 \pm 0.07$.	1 (42-year-old woman)	-
Zhang and Mak (1999) [97]	Aluminium ring, nylon, silicone, cotton sock, PA ring	Dorsum and palm of hand, inner and outer forearm, anterior and posterior leg	μ	Portable friction meter applied to testing sites (under 25-100g) at 25-62.5rpm; $L = 0.98\text{N}$	$\mu = 0.37\text{-}0.51$. Within the range of L and rotational speeds applied, both had only negligible effects on μ .	10	Adhesion and ploughing

Table 2.2: Continued...

Authors (year)	Contact materials	Anatomical region	Parameters measured/calculated	Methods	Findings/ future work	Participants	Notes (mech-anisms, lubrication, etc.)
Kenins (1994) [98]	Woven fabrics (wools, cashmere, cotton, polyesters, silk)	Forearm (hairy) and finger (glabrous)	μ_s ; rolling frictional force	Rotational friction test - 5g and 50g weights hung from trailing end of fabric and pulled at $10 \text{ mm} \cdot \text{s}^{-1}$. Comparisons made between: fabrics, skin types, skin hydration, relative humidities.	Friction of glabrous skin is less affected by wetting than hairy skin. All other factors (fabric surface, weight, etc) have less impact on fabric-skin friction.	181 (17-64 years; men and women)	-
Elsner <i>et al.</i> (1990) [99]	Rotating Teflon wheel	Inner forearm, vulva	TEWL; capacitance; μ_d	Portable friction meter applied to testing sites after measuring TEWL and skin hydration; L = 1.96N.	$\mu_d = 0.48-0.66$. Friction can be reduced with wet or dry lubricants but both increase friction when skin is wet. $\mu_{\text{vulva}} > \mu_{\text{forearm}}$ (and same for capacitance).	44 (22-78 years; women only)	-

Table 2.2: Continued...

Authors (year)	Contact materials	Anatomical region	Parameters measured/calculated	Methods	Findings/ future work	Participants	Notes (mechanisms, lubrication, etc.)
Cua <i>et al.</i> (1990) [100]	Rotating Teflon wheel	Forehead, upper arm, inner and outer forearm, postauricular, palm, abdomen, upper and lower back, thigh and ankle	TEWL; capacitance; μ_a	Portable friction meter applied to testing sites after measuring TEWL and skin hydration; L = 1.96N.	Significant positive linear correlation between capacitance and μ_d for old and young, but lots of scatter. No significant difference in μ_d between age groups or genders but TEWL \downarrow for old participants. μ_d varied with body region. $\mu_d = 0.22 \pm 0.07$	29 (24.9 ± 1.1 - 75.3 ± 2.4 years; men and women)	-
Highley <i>et al.</i> (1977) [101]	Motor driven nylon wheel	Inner forearm	Frictional resistance of skin under different hydration conditions	Wheel rotates on skin while L (28.2g) is applied by means of a spring connection. Skin was shampooed and rinsed before testing to minimise variation between subjects.	Wetting skin leads to higher surface friction because of liquid surface tension, and there is more between liquid and stratum corneum. Oil on skin appears to lubricate and hydrate by occlusion (slowing rate of evaporation of moisture transepidermally).	12	Adhesion and lubrication

Table 2.2: Continued...

Authors (year)	Contact materials	Anatomical region	Parameters measured/calculated	Methods	Findings/ future work	Participants	Notes (mechanisms, lubrication, etc.)
Naylor (1955) [102]	PE sphere	Shin	Frictional force; μ	Hairs were removed from skin before testing. The probe (attached to a specially designed machine) moved across the skin at constant velocity. This was repeated after the participant had sweated in a room for some time, and again with oil or water on the skin surface. $L = 5.1 \pm 1.5\text{N}$ in dry (untreated), 6.4N in wet (sweating) conditions.	Frictional force $\propto L$. Dry $\mu = 0.5 \pm 0.02$; wet $\mu = 1.0 \pm 0.1$. When skin is dry, very wet or "greasy", $\mu \downarrow$; when skin is "moist", $\mu \uparrow$.	1	Possibly hydrodynamic or fluid film lubrication

A study carried out by Wong [3, 103], to measure friction between three nonwoven fabrics and the volar forearm skin of five young female volunteers, used a mathematical model developed by Cotten-den (as described in §2.5) to compare two different experimental configurations, both of which are displayed in figure 2.15. Measurements were made on overhydrated (wet) and normal (dry) skin in an environmentally controlled room ($23.0 \pm 2^\circ \text{C}$, $50.0 \pm 5\%$ relative humidity) to reduce the possibility of variations in the data caused by environmental changes. Results showed that the coefficients of static friction varied between participants and a little between nonwoven fabrics. There was a marked difference between coefficients for wet and dry skin – up to 5 times larger for wet skin – but there was a strong positive correlation between values for the different configurations. One participant did seem to be the source of most disagreement between the straight and curved configurations and it was suggested that her considerably hairier arm (compared to other participants) lubricated the skin in the curved configuration. The coefficient of friction was found to be independent of pressure for the range used (0.36-2.23kPa); this was supported by Kondo [104] and Egawa *et al.* [94], but contradicted findings by Comaish and Bottoms [105] or Zhang and Mak [97].

One of the main findings from work on skin friction so far is that coefficient of friction does not change with applied normal force when the skin is dry, but it does when the skin is wet, although there are a few papers that report contradictory results. It is also generally agreed that sliding speed has only a negligible effect on coefficient of friction, and that age, gender and ethnicity have no impact. Interestingly, transepidermal water loss (TEWL) has been shown to vary between people of different ages, genders and ethnicities, and the former two are often linked in their influence on friction. TEWL also changes depending on the skin site (region on the body), as does coefficient of friction. Friction force is always higher when the skin is wet or moist than when dry, and it has been suggested that the increase is a consequence of greater adhesive forces due to smooth contact between skin and the contacting material when the stratum corneum swells with water. However, for the most part, friction force (or coefficient) has not been investigated as a function of skin wetness or hydration. The few studies that have covered friction on skin at a range of hydration levels have also noted that the presence of oil and an abundance of water on the skin surface can lower the coefficient of friction, possibly resulting in

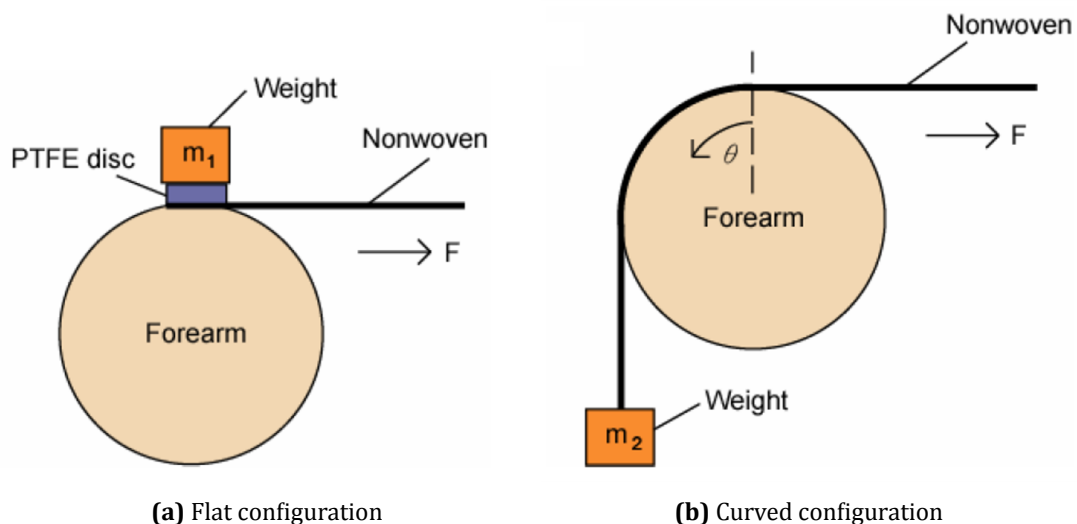


Figure 2.15: Different experimental configurations used by Wong for friction measurements; normal force applied directly to arm through nonwoven in (a), but hangs on end of nonwoven strip in (b). (Image from [3].)

hydrodynamic, fluid film or mixed lubrication; the regime is still unclear. Most consider adhesion to be the principal mechanism for skin friction, but deformation is also mentioned regularly as a potential second mechanism.

2.3.3 Stick-slip

The stick-slip phenomenon is intermittent sliding of one surface against another, continuously alternating between static and dynamic friction. Visually, this is a “jerking” motion between two objects in shear contact. Stachowiak and Batchelor stated that there is a large difference between the actual (instantaneous) sliding velocity – that during “slip” – and the average speed [58]. On a force-displacement graph, stick-slip is represented by a sawtooth curve with multiple peaks and troughs; the force increase to the peaks shows the many instances of static friction (stick) and the sharp decrease in force that follows owes to the brief periods of dynamic friction (slip). Many researchers have shown interest in the phenomenon due to its various implications on daily life, such as earthquakes or undesirable noises produced by vehicle brakes and machinery [106, 107]. Several mathematical models have been tested for different systems, but it should not be assumed that a model created for one would apply to another as this is often not the case [106].

While stick-slip behaviour has also been observed during measurements of friction between human skin and various other materials [92, 108, 109, 110], little has been done to investigate its origins or the primary cause when *skin* is the substrate. In fact, the only known paper to specifically tackle the phenomenon with skin is that by Derler and Rotaru [69]. According to the authors of this paper, it mostly occurs between skin and smooth surfaces in the presence of liquid, so they carried out an investigation on stick-slip between skin (of the index finger) and smooth glass. Their findings were described in §2.3.2, but the main conclusion – in direct relation to stick-slip behaviour – was that increasing the normal force and sliding speed led to a systematic decrease in coefficient of friction for intermittent (stick-slip) sliding.

2.4 Nonwoven Fabrics

There is no universal definition of a nonwoven fabric that fits every situation, possibly due to its broad use in several industries [111]. The term originated from the use of cheaper alternatives to conventional fabrics, which were bonded thermally, chemically or mechanically rather than woven. According to the European Disposables and Nonwovens Association (EDANA) and the Association for the Nonwoven Fabrics Industry (INDA) [112],

“A nonwoven is a sheet of fibres, continuous filaments, or chopped yarns of any nature or origin, that have been formed into a web by any means, and bonded together by any means, with the exception of weaving or knitting.”

There are more complex restrictions for wetlaid webs regarding material composition and fibre dimensions, but the above statement seems to capture the essential definition. Several applications include wrapping cables, protective and normal clothing, car interiors, household products, and there are many more. More than one third of nonwovens are produced for hygiene products. In terms of continence products, they can be most simply described as the teabag-like material that forms the top layer through which urine passes before being “absorbed” by wood fluff pulp and superabsorbent polymers

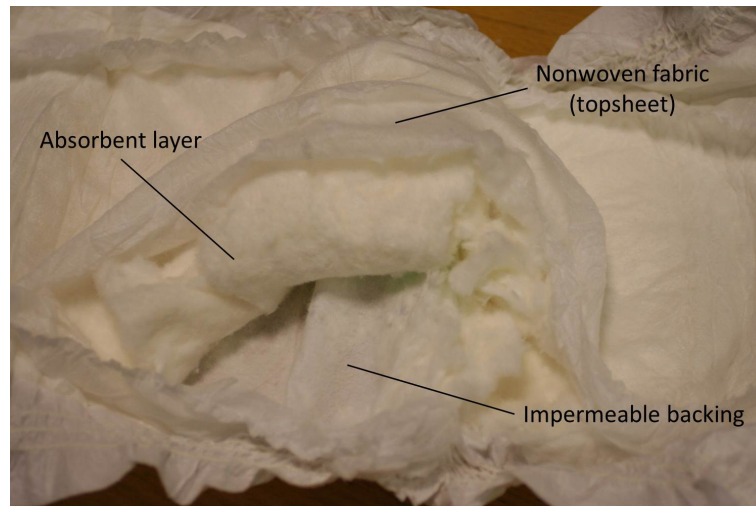


Figure 2.16: Incontinence pad – open to show constituents of pad: nonwoven fabric (top), absorbent layer (centre) and impermeable backing (bottom)

found inside the pad or diaper. It is the part of the product that comes into contact with the skin. In order to understand the application of nonwoven fabrics in continence pads (and diapers), it is perhaps best to put it into context by means of a diagram (see figure 2.16).

One measurement associated with nonwoven fabrics is the linear density of its fibres, the standard international unit for which is decitex (dtex) [113]. Decitex is defined as mass (grams) per 10km [3]. Alternatively, linear density can be measured in denier - mass per 9km - often used with clothing such as tights. Another density measure of nonwovens is mass per unit area ($\text{g} \cdot \text{m}^{-2}$), often written as gsm, and known as *basis weight*.

2.4.1 Manufacturing: formation of webs

Nonwovens can be categorised by general manufacturing process: drylaid, (typically with materials originally used in textiles), wetlaid (mostly using papermaking materials), and polymer-laid (usually implementing substances initially used for making plastics and extruding polymers) [111].

Drylaid nonwovens are either carded or airlaid [114]. During carding, a web of fibres is created from fibre bales which are opened, combined and transported by air to a/several rotating drum(s) (or *cards*). These drums radiate narrow wiry projections or teeth, which act as a comb, spreading the fibres to form the web. (See figure 2.17.) The desired mass of the fabric fibre orientation will determine how the cards are arranged [114]. If the majority of fibres lie in the direction in which they are combed, the web is referred to as parallel-laid, as shown in figure 2.18. Otherwise, they are random-laid. The same equipment can give rise to fabrics with a large selection of varying properties, simply by altering the material, orientation and/or dimensions of the fibres, and the relative speeds of the cards.

The EDANA website states that airlaying is similar to carding in that the fibres are transported by a stream of air to moving machinery where they are converted into a web [114]. In this particular process, very short fibres may be used. Rather than forming fibre webs using drums with teeth, a drum with perforations or a conveyor belt is used. Fibres can only be random-laid, and the resulting web typically has a lower fibre density and softer texture than a carded web. Again, airlaid webs can have a large range of mechanical properties.

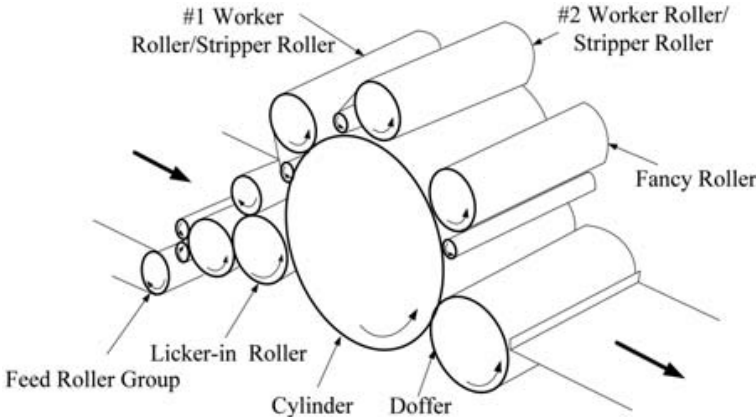


Figure 2.17: Diagram of carding machine (reprinted from Kuo *et al.* [115], Copyright © 2011 Chung-Feng Jeffrey Kuo, Yu-Chung Chou and Tsung-Yi Lin, with permission from SAGE Publications Ltd.)

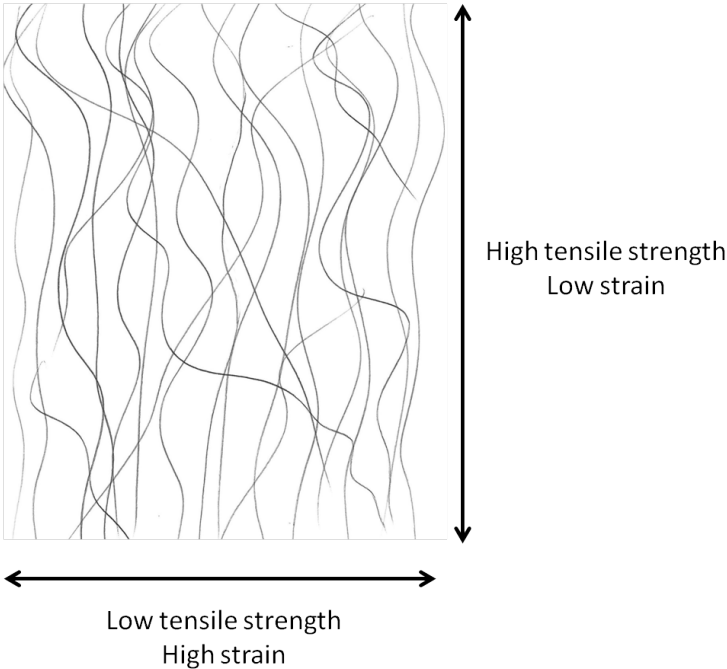


Figure 2.18: Diagram of parallel-laid web

Spunmelt nonwovens are produced from thermoplastic polymers, directly introduced into a web-forming system. They are spunlaid and/or meltblown. In the spunlaid (or spunbond) process, molten polymer granules are converted to filaments by extrusion via spinnerets. These filaments then pass through an attenuator, which cools them before they are placed on a conveyor belt, creating a uniformly laid web. Some bonding initially occurs due to the cohesion of parts of fibres that have not fully cooled. Spunbond nonwovens are generally stronger than those made using other web formation processes, although there is a more restricted choice of raw materials (polymers). Other materials can also be co-extruded with the primary fibre component to improve bonding or add other useful properties to the resulting fabric.

Meltblown webs are initially formed in a similar way to spunlaid webs, except that polymers of low viscosity are used and an airstream at high velocity replaces the conveyor belt. The air dispenses the molten thermoplastic to form a web. The wetlaying process involves a low concentration of fibres in a water "slurry" draining through a mobile/ dynamic wire screen, leaving a web. Rollers compress the web, removing any excess water. (Later on, binder impregnation typically takes place.) Since the fibres are randomly orientated, the web has relatively uniform multidirectional strength. Various materials and fibre dimensions can be used. Some techniques are now being combined, such as spunlaid and meltblown. Many other web-forming techniques exist, some of which incorporate bonding, but these are not likely to be of any importance in this thesis.

There is a large selection of chemical finishes to choose from when manufacturing nonwoven fabrics, depending on the end use of the fabric [116]. Not all are suitable or beneficial for nonwovens used as coverstocks, but examples of those that are include antimicrobial (or biocidal), lubricating or waterproof coatings. However, the latter may be considered redundant in coverstocks, in view of the fact that the majority consist of hydrophobic fibres. A range of finishing *methods* also exist; the most frequently implemented techniques are padding and coating. Padding is essentially treating the nonwoven with a kind of foam or "liquor" while compressing it between rollers. A coating is usually applied to a nonwoven as an aqueous solution or dispersion before being hot-air dried and cured. As nonwovens used as coverstocks are generally non-uniform, it is reasonable to assume that the same applies to their coatings; it is possible for craters or voids to be present in the surfactant layer if the solvent evaporates, but can be rectified by coating the nonwoven several times.

2.4.2 Manufacturing: Bonding

Spunlaid webs are the only webs that have any considerable strength before undergoing the bonding process [117]. It is therefore very important, not only to carry out the bonding, but to select the appropriate process. The latter ultimately affects the properties required for a particular function.

The three groups of bonding techniques are:

- chemical;
- mechanical;
- thermal;

Chemicals used for bonding are usually in liquid form, for example water based adhesives, which are most common. However, powders, foams and occasionally solutions made using organic solvents can also be applied. Impregnation or application of binder in specific patterns to leave an area of bond-free fibres, is known as intermittent bonding.

Mechanical bonding aims to use friction between fibres to strengthen the web and can be split into needlepunching and hydro-entanglement (or spunlacing). The majority of fibre types can be needlepunched,

during which needles pass through the web forwards and backwards, until fibres become entangled. Various webs can be combined using this method, resulting in a nonwoven fabric with a wide range of properties. Where needlepunching uses needles, hydro-entanglement uses fine water jets at high pressure to entangle the fibres. Unlike the former process, the latter is mostly implemented for wetlaid and carded web bonding. The jet configuration can be changed to produce attractive patterns in the nonwoven and the pressure applied can be controlled to increase or decrease its overall strength.

Thermal bonding is, as the name suggests, a method of bonding fibres in a web using heat to partially melt them at the point of the bond. Although the core fibre material can be used for this, its use is not as common as that of a bicomponent fibre or a separate and different fibre with a lower melting point, both of which would already be part of the web at this stage. Temperature is controlled accordingly. Smooth and hot rollers can be used to bind fibres quickly under high pressure. This is called calendaring. High frequency sonic waves can also be used to excite the web fibres, causing their molecules to vibrate and create heat inside the fibres, thereby making the fibres more malleable and easy to bond. During this process, known as sonic bonding, a decorative roller applies pressure to the web. The process of bonding a web all at once by heating with a flow of hot air is called through-air thermal bonding. These webs, however, must contain low melt fibres. The resulting nonwovens are particularly bulky. Nonwovens of *typical* bulk can be produced under high heat and pressure using a “drum and blanket” system.

2.4.3 Mechanical properties

Over the years, the effects of a large variety of mechanical and structural properties on the durability of many textiles (woven, nonwoven and knitted) have been examined separately from the impact of their interaction with skin [118]. There are many different mechanical properties of a nonwoven fabric that are important to its function, such as compressive and tensile strength, and the fabrics are often tested in at least two planes: machine direction and “cross-direction”, which are perpendicular to each other [119]. Petrulis [118] explained that the resistance of a fabric to abrasion is dependent on the material of the constituent fibres. This was based on findings by Amirbayat and Cooke [120] and Ozdil *et al.* [121], who showed that polyester and various other fibre materials had a high resistance to abrasion. The bulk modulus is also an important property as the area of contact between fibres, and potentially at the fabric interface with an opposing material, will be affected under certain normal forces. A low modulus means more deformation at lower loads and, therefore, a larger contact area between fibres and lower pressure. Overall, spunbond nonwovens with randomly orientated fibres also tend to be more durable than those with parallel fibre alignment, which have directional preference.

Various other papers discuss the tensile [122, 123, 124, 125] and compressive [124, 126, 127] properties of nonwovens used for a wide range of applications. However, there appears to be no published work on the mechanical properties of nonwovens specifically for use in absorbent hygiene products. The authors of the aforementioned papers found that:

- the bonding process of a nonwoven (thermal or mechanical) can affect the deformation of the fabric in compression;
- linear density affects the compression of needle-bonded rather than heat-sealed nonwovens;
- nonwovens with smaller fibre diameters, or more “punched” bonds per unit area, appear to have a higher compressive modulus;
- the distribution of an applied force across a nonwoven is not uniform due to variation in its structure – this is the apparent cause of inconsistent measured mechanical properties.

2.5 Skin surrogates

A skin surrogate is a material used as a replacement or a substitute for real, naturally existing skin. Since skin is a relatively complex organ, with many different biomechanical properties relating to its various functions, a surrogate would not be expected to be similar to skin in *every* way. Therefore, different surrogates can be implemented depending on the skin feature or property of interest [4]. With this in consideration, it is in fact evident that most “features” of interest relate to the biology and histology of the skin, rather than physical and mechanical properties. Nevertheless, many authors recognise the importance of both biological and mechanical properties of a skin surrogate in determining its suitability for use in the body, although this may be slightly less important if it is only to be used in a laboratory. Examples of studies on surrogates with clinical and non-clinical uses will be discussed here. The principal purpose of *tissue-engineered skin* in a clinical setting is to re-establish the barrier function of damaged skin and/or encourage wound repair [128], although the mechanical properties are also important. In a recent study by Rolin *et al.* [129], scaffolds made from two different biomaterials were populated with human dermal fibroblasts and exposed to a series of biochemical and mechanical tests. Tensile tests showed that the rigidity of a matrix improves when cells are added and that the modulus of elasticity of the cellularised dermal equivalent was within the range for real human skin.

In a review by Shevchenko *et al.* [130], the production, use, advantages and disadvantages of a range of existing dermal, epidermal and composite tissue-engineered skin substitutes were described. The authors also discussed biomechanical testing of such surrogates, carried out to assess their suitability for use in the body. An example of such testing includes work by Harley *et al.* [131] to investigate the compressive and tensile properties of a commonly implemented collagen-glycosaminoglycan sort of matrix. The reason for research into these biological constructs is that the infiltration of cells from the tissue of interest triggers degradation of the scaffold, consequently compromising its mechanical properties. However, measurements by Harley *et al.* on these scaffolds and a physical model revealed that cross-linking greatly increased the Young's modulus of the structure, which supported work by Powell and Boyce [132] and Garcia *et al.* [133]. The aforementioned researchers studied the impact of cross-linking in more detail: Powell and Boyce found cross-linking to have negative implications on both the mechanical and biological properties, as the result was a brittle and useless scaffold; whereas Garcia *et al.* achieved enhanced stability of the matrix mechanics and eliminated the risk of any associated cytotoxicity. In a similar study, Saddiq *et al.* [134] demonstrated that, following the addition of cells, the positive effects of the cross-linking could be short-lived.

Hong *et al.* [135] measured friction between a sheepskin, used as human skin substitute, and various materials – cotton spunlace (hydroentangled); Tencel spunlace; PP (thermally bonded by a hot cylinder; PP thru-air bonded carded web) (TABCW). The materials were coverstock (nonwoven) materials from baby diapers as the focus of the research was abrasion damage to babies' skin caused by interaction with the top sheet. A 20g weight was applied to the skin surrogate as it was pulled across the nonwoven sample at $4 \text{ mm} \cdot \text{s}^{-1}$ for 10s. Water was dropped on the pad for repeat friction measurements in wet conditions; the coverstock was removed and weighed to record the volume of water held within the fabric. The coefficient of friction for the nonwoven made by PP thermal bonding > cotton spunlace > PP TABCW > tencel spunlace. Surface roughness, which was also measured, revealed that the tencel spunlace nonwoven was rougher than that produced by PP thermal bonding and the PP TABCW fabric was smoothest. Coefficient of friction greatly increased for cellulose spunlaces in wet conditions.

In 2007, Derler *et al.* [91] carried out *in vivo* friction measurements between skin of the medial index finger and a wool fabric meeting Martindale abrasion test specifications. These measurements were also made between the same fabric and seven different materials in an attempt to assess their suitability as mechanical skin surrogates. Most had a coefficient of friction higher than that of dry skin of the medial index finger. Silicone had a coefficient of friction lower than that of the skin and Lorica Soft had a coefficient similar to that of the lowest range on skin. Lorica Soft is an artificial leather made from a polyamide fleece coated in polyurethane (PUR). It is typically used to assess the efficacy of anti-slip coverings for floors on which people walk barefoot. As this study [91] revealed that Lorica Soft had the most similar coefficient of friction to real skin and had a similar surface structure, Cottenden chose to use it for his friction measurements with nonwoven fabrics [4].

In 2008, Gerhardt *et al.* [136] published a paper describing their work on friction between nonwoven fabrics and Lorica Soft, and interfacial pressure across an area between a mattress and pelvic to femoral regions of the body. They stated that there was not yet a surrogate properly validated for simulation of friction and contact between human skin and nonwoven fabrics. Gilchrist *et al.* [137] used an unspecified skin surrogate to investigate the force required to penetrate skin using four different knives. In 2009, Gerhardt and some other colleagues [138] continued to work with Lorica Soft, investigating the effect of lubrication, sliding speed and normal force on friction. The lubricant was an artificial sebum applied to the Lorica Soft in different concentrations, and friction was measured between this and various hard spherical probes of different materials. Shao *et al.* [139] developed and tested one silicone and two multi-layer artificial fingertips, each with a different ratio of elastomer. The fingertips were constructed from an elastomer and silicone gel base mixture forming the tissues closest to the bone, encapsulated silicone for the more superficial tissues, and a thin layer of acrylic for the skin. Friction force between these models and a range of surfaces was measured and compared to real fingertips, showing fairly good agreement for most surfaces.

More recently, Guerra and Schwartz [140] investigated the mechanics of blister formation in the skin using: a transparent silicone rubber to simulate the outer epidermis; a PUR elastomer or neoprene rubber for the dermis; and latex rubber for all subcutaneous soft tissues. None of the studies to date appear to have validated a particular surrogate for use as an appropriate mechanical replacement for the testing of human skin. Lorica Soft has been likened to medial finger skin in terms of coefficient of friction [91], and has a similar roughness to skin at the edge of the hand [138]. However, it must be considered that this skin is different to volar forearm skin, and is likely to have a different range of coefficients of friction when comparing data for real skin with those for Lorica Soft, as will be described later on in this thesis.

Cottenden [4, 141] carried out extensive experimental work with Lorica Soft (LS), measuring friction between it and three nonwoven fabrics. As is the case for much research involving skin surrogates, its use was partly based on convenience – it is adaptable but consistent and readily available for use, unlike human skin. However, the selection of LS specifically owed to the fact that it has surface properties most similar to that of human skin when compared to other surrogates (as found by Derler *et al.* [91]). Although his experimental setup was originally designed for measurements on excised breast skin, only LS was used, but the data were still useful for making comparisons between the fabrics and various other factors. Cottenden found that:

- velocity had very little effect on coefficient of friction (approx. 5% variation);
- friction force increased with increasing applied normal load and coefficient of friction did not vary significantly with applied load;

- only up to about 10% variation was observed with applied load, which could be due to variation within the material;
- Amontons' law was obeyed for the force range used.

Interfacial contact was also examined under an optical microscope, but replacing LS with glass – perhaps the least obvious skin surrogate to be reported. The principle of this work revolved around the use of a high magnification optical microscope to ascertain which nonwoven fibres were in focus and therefore *in contact* with the substrate of interest. More specifically, the depth of field (or distance between the focal plane of the body of interest and the point at which focus is clearly lost) is a valuable tool for correctly positioning the true focal plane at the nonwoven-glass interface and at any level through the depth of the nonwoven. The accuracy of this method improves as the depth of field decreases with increasing magnification, hence the use of a high magnification here. This procedure to quantify fibre contact between a nonwoven fabric and a glass substrate yields only *length* values; nothing in the two-dimensional micrographs is revealed about the *width* of fibre contacts, and so contact *area* cannot be determined. There have been many attempts to model linear elastic half-spaces [142, 143, 144, 145, 146, 147] and quarter-spaces [148, 149, 150, 151], which could be used to estimate contact *area*, but these models were based on materials rather different to skin and nonwoven fabric fibres. As a result, they would be challenging, if at all possible, to implement.

Nonwoven fibres are effectively incompressible (in the plane of their cross-sections) at the range of pressures (0.5kPa-50kPa) used in experiments by Cottenden, and could be likened to convoluted narrow cylinders against a nominally flat elastic surface, where the same fibre may make contact with the surface at various points and with different local contact areas (see figure 2.19). If the skin could deform around the circumference of the fibre, under a certain range of loads and with particular fabric compositions, the contact area would, again, be different. Consequently, calculating the contact area is rather more complex than simply multiplying contact length by fibre diameter. Nevertheless, the method can be used to estimate fibre contact length with human skin, based on the assumption that the stratum corneum behaves in much the same way as the glass slide when a small cylindrical structure is pressed into it. Although this assumption seems rather improbable, it is in fact reasonable for the purposes of estimating contact *length* [141].

Mathematical and physical models of the volar forearm (a common site for *in vivo* friction measurements) were also developed, produced and validated by Cottenden *et al.* [152]. The first experiments were performed on cylindrical models covered in materials dissimilar to skin; the focus, in this case, was the geometry, therefore the contact material was irrelevant. The nonwoven fabric, angles of first point of contact and applied dead weight were all varied across the range of experiments, but not the sliding speed. Two cylinders (circular and elliptical) were incorporated into the system to ensure that a single vertical component (the weight) and a single horizontal component (tangential/shear/frictional force) could be measured and computed easily. The well-known mathematical model used by Gwosdow *et al.* [153] and Cottenden [152], was used to calculate coefficient of static friction for the setup shown in figure 2.20 – see equation 2.7.

$$\mu_s = \frac{1}{\theta} \cdot \ln \left[\frac{F_{\max}}{mg \cdot \sin \theta} \right] \quad (2.7)$$

where θ is angle of arc of contact between skin and nonwoven [radians], F_{\max} is maximum friction force

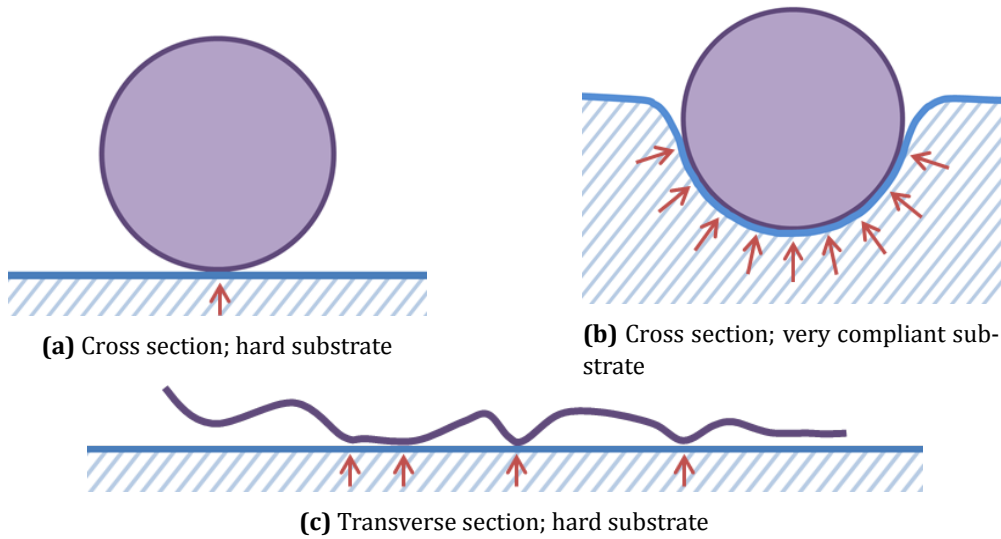


Figure 2.19: Contact between a nonwoven fibre and different substrates; (c) demonstrates multiple contact points of a single fibre

[N] and mg is applied load [N]. In an ideal setup, $\theta = \pi/2$ radians, which simplifies equation 2.7 to:

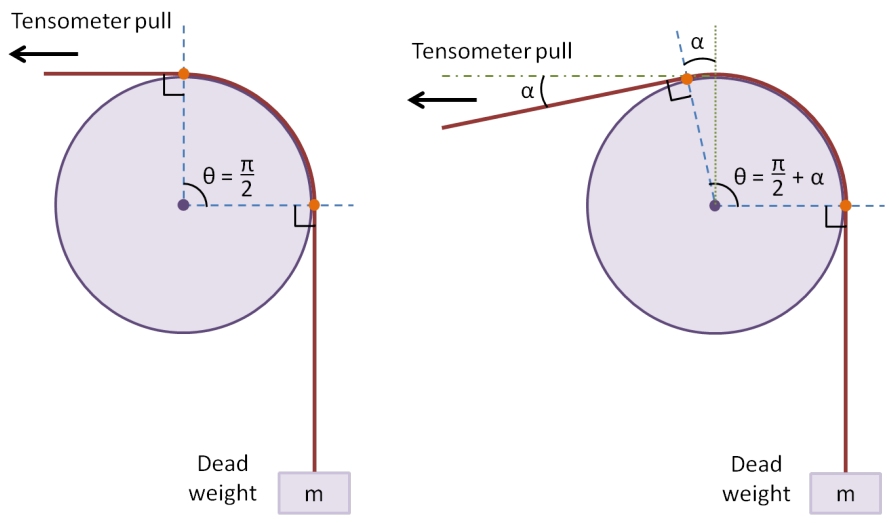
$$\mu_s = \frac{2}{\pi} \cdot \ln \left[\frac{F_{\max}}{mg} \right] \quad (2.8)$$

It was shown that the mathematical model could be applied to any convex surface (i.e. ellipses and cones of varying angles) by performing some practical experiments on a selection of cones [154]. In these models, it is assumed that the “angles of first point of contact” remain constant for the duration of the experiment, that there are no torsional or lateral forces on the fabric, that the fabric is inextensible and that the arm is a rigid cylinder or cone.

The model was further tested by Asimakopoulos [154] who replaced rigid Plaster-of-Paris with foams or gels of different stiffness and studied the impact of surface material (“skin”) and representative underlying tissues. One issue encountered was that the coefficient of friction was changing with the rubber material used on the surface of the physical model due to polishing and abrasion, so the experiments had to be carried out with a material that did not have a rapidly changing friction coefficient. This was important because a varying coefficient of friction would have produced unreliable results, considering that all other factors remained constant for the duration of each test. Remarkably, the highly compliant model arms demonstrated a strong linear relationship between mean dynamic friction force and applied load, as did the rigid models, *despite* the large deformation exhibited by them *and* the nonwoven fabrics. Although the mathematical model assumes the linear regression line (for friction force vs applied load data) passes through the origin, all physical models produced a small offset on the y-axis (see figure 2.21). There was little variation in offset to be attributed to the different model arms, but a more obvious difference between nonwoven fabrics. Asimakopoulos investigated whether these offsets could be explained by an additional force required to bend the fabric around the arm, which would depend on the bending stiffness of the nonwovens. This turned out not to be the case, so it was suggested that the dominating cause was the friction mechanism(s) operating at the interface.

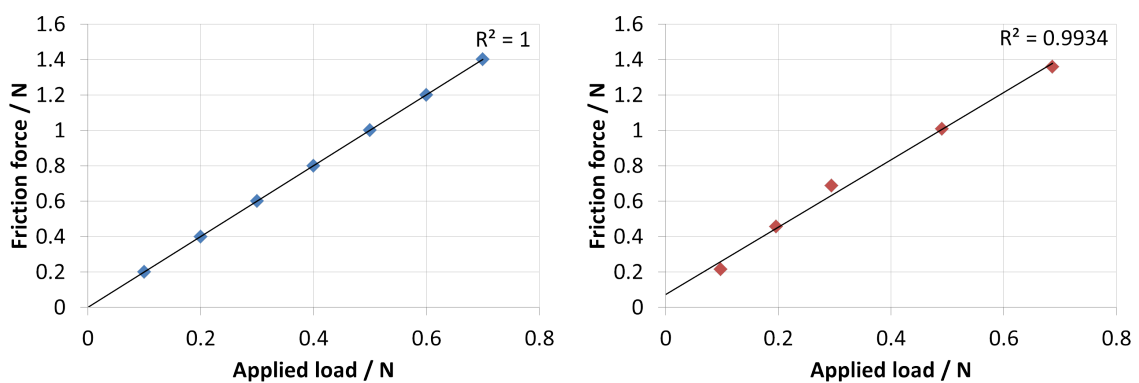
This image has been removed by the author for copyright reasons.

(a) Diagrams of side views of the elliptical cylinders; red line = strip of nonwoven fabric (from [152])



(b) Tangent at first/last point of contact between nonwoven strip and cylinder (orange dots) affects angle of arc of contact (θ); angle is taken between blue dashed straight lines

Figure 2.20: Experimental setup used by Cottenden *et al.* [152]



(a) Friction force passes through origin

(b) Small friction force offset

Figure 2.21: Difference between theoretical model, (a), and physical model, (b), 'friction force vs applied load' relationship

2.6 Summary

A wide range of topics have been covered in this review, from the types and manufacturing techniques of nonwovens, to the mechanical testing of skin (including friction). The key points are summarised here.

Nonwoven fabrics vary enormously in their structure due to the use of a broad range of available materials (polymers) and manufacturing and bonding processes. They are designed for many different applications and are tested according to their use. Nevertheless, the literature on mechanical testing of those used in absorbent hygiene products is rather limited – only few fabrics have been used by few researchers – hence it is difficult to confidently attribute certain features of a nonwoven to certain mechanical properties. Many studies have been conducted with skin surrogates and Lorica Soft has been shown to be most similar to human skin in friction. However, only few nonwoven fabrics have been used with this surrogate, so its suitability to represent skin in friction with coverstocks is not well known.

Measurements of friction between *real* skin and various materials have produced a large selection of results based on body region, age, gender, ethnicity and skin hydration. The wide range of test materials and measurement techniques gave rise to some conflicting data. However, the general consensus seems to be that Amontons' first law of friction is obeyed when the skin is dry (normal). Most measurements have been made between skin and a hard surface (rather than textile). The coefficient of friction with these materials is generally unaffected by sliding speed (even though skin is viscoelastic), age, gender or ethnic origin. On the other hand, TEWL *has* been shown to be affected by the latter three. When skin is wet or damp, the friction force is higher than for dry skin, although the relationship between skin hydration and friction is still not very well understood.

Deformation of the skin mostly depends on the bulk properties of the hypodermis, dermis and epidermis together, but friction seems to be influenced mostly by the stratum corneum (superficial sub-layer of the epidermis). This layer of cells is known to be stiffer than those that lie deeper in the skin and, to an extent, limits the overall deformation of the skin as a whole. Despite this, the effect of skin deformation on friction has not received notable attention in the literature. A minimal amount of work has been carried out to investigate experimentally and model the interface between skin and textiles; as a result, little is known about how friction is mediated, although many have commented on the operating friction mechanisms. Adhesion is the main mechanism associated with skin friction and it has been proposed that its contribution increases when the skin is wet/moist, but there is also a lack of understanding here due to a lack of robust evidence.

2.7 Aims & objectives

The main aim of the work in this thesis is to improve understanding of friction between human skin and nonwoven fabrics, building on work previously done by past PhD students. The ultimate purpose of the project is to aid the improvement of absorbent continence (and similar) products by identifying material properties and manufacturing processes of nonwovens that have a particular impact on their frictional interaction with human skin. This knowledge can then be used to optimise the selection and development of nonwovens so that they are more "skin-friendly", thereby reducing skin damage. In order to achieve these aims, the work has been split into four main strands, the objectives for each are summarised in the relevant sections that follow.

2.7.1 Friction between a skin surrogate and nonwoven fabrics

Measure friction between a wide range of nonwoven fabrics (varying in manufacturing process, polymers and structure) and a skin surrogate: Starting with a large group of (13) new nonwovens, a subset will be chosen using the same methodology implemented by Cottenden to measure friction between nonwoven fabrics and a skin surrogate (Lorica Soft). The subset will consist of fabrics distinct from Cottenden's fabrics and each other, in terms of material and manufacturing properties and/or friction forces.

Measurements of friction on a skin surrogate in a curved configuration: An investigation will be conducted into whether or not the surface of the surrogate undergoes sufficient change, to produce different friction forces with nonwovens, when the interface is curved. It is anticipated that the results of this can be used to help to interpret the data on volar forearm skin *in vivo*.

2.7.2 Friction between excised skin and nonwoven fabrics

Friction tests on a skin surrogate may produce reliably consistent data, but the surrogate only *represents* the surface properties of skin. Real human skin is rather different in many ways – for that reason, it is important to repeat the measurements made on the surrogate on real skin. The data collected here will help to interpret other friction data and will act as an intermediate between measurements on the skin surrogate and human skin *in vivo*. In order to make direct comparisons, the following work must be carried out¹.

Ethics: Research Ethics Committee and Research and Development approvals were obtained by Cottenden before the start of this project. The researcher name and details will be updated; the expected study end date will also be extended.

Measure friction on excised breast skin: With the same apparatus used in skin surrogate-nonwoven friction measurements, these experiments will be repeated on excised skin. Any differences observed between the skin and surrogate will help with the analysis of data on volar forearm skin.

2.7.3 Friction between volar forearm skin and nonwoven fabrics in dry (normal) conditions

This is the first phase of a two-part research study to investigate friction between a broad range of nonwoven fabrics and the volar forearm skin of people of different ages with different skin types. The aim is to determine: (i) if Amontons' law is obeyed; (ii) how friction varies between nonwovens and between subjects, particularly with respect to their age; and (iii) observe the nature and extent of soft tissue deformation accompanying friction between skin and nonwovens, particularly as it varies with the age of participants.

Selection of a subset of nonwoven fabrics: The same large group of nonwovens to be tested with the skin surrogate (see §2.7.1) will also be tested against volar forearm skin to confirm the selection subset for further examination (on participants). The subset will be chosen based on the friction data from both sets of experiments and should encompass a wide range of material and mechanical properties.

Ethics: Research Ethics Committee and Research and Development approvals must be obtained for this study.

¹This work was started but not completed – for reasons explained at the end of chapter 7 – and has been placed in appendices G and H rather than in the main body of this thesis.

Measurements of friction between volar forearm skin and nonwovens: Friction measurements will be made on the volar forearm skin of young and very old volunteers in normal (dry) conditions with the subset of nonwovens. These data will also be compared to the data from the skin surrogate to look for similarities and characteristic trends between them based on their interaction with nonwoven fabrics.

2.7.4 Friction between volar forearm skin and nonwoven fabrics in wet conditions

This is the second phase of the study on friction between human skin and nonwoven fabrics. So far, all friction experiments described are in the absence of fluids. However, this only applies to situations in which urine has not yet leaked into the pad. It is therefore important to introduce fluid into the system and examine its effect on friction across a range of skin types. The same aims (labelled (i)-(iii) in §2.7.3) apply here.

Methodology development and selection of variables: An experimental procedure for measuring friction between volar forearm skin and nonwoven fabrics in wet conditions will be developed. The method must encompass friction at many levels of skin wetness and accommodate the different skin types of study participants.

Measurements on study participants: Having established an appropriate method for introducing water/saline into the system and measuring friction on a range of skin types, measurements will be carried out on participants in the study.

2.7.5 Interfacial contact (fibre footprint)

Information about the fibre footprint between the nonwoven fabrics (used in friction measurements) and a substrate would help to interpret the friction data and to elucidate friction mechanisms.

Fibre footprint between glass microscope slides and a broad range of nonwoven fabrics: Using the same methods as Cottenden, measurements of fibre contact length will be made for nonwovens from the subset selected based on friction measurements. These experiments serve to assess the properties of different types of fabric in relation to their fibre footprint and to help to understand how friction is mediated by the interface.

Application of a mathematical model: The existence of a model to estimate actual contact area will be investigated. Should this modelling work be successful, the contact areas will be compared with contact lengths to check how representative the lengths are of area.

CHAPTER 3

FRICITION MEASUREMENTS ON SKIN SURROGATE

“The great tragedy of science—the slaying of a beautiful hypothesis by an ugly fact.”

— Thomas Huxley, 1825–1895

IN ORDER TO INVESTIGATE the friction between skin and nonwoven fabrics, it was first important to select some materials and develop a suitable method for testing them. As the ultimate aim was to identify potential relationships between friction and certain properties of some nonwovens, it would be useful to study a range of nonwovens that vary in both structural properties and friction behaviour. An assortment of nonwoven fabrics that met these criteria was supplied by SCA Hygiene Products AB in Göteborg, Sweden – a “*leading global hygiene and forest products company*” that provides many of the absorbent hygiene products used worldwide, among other suppliers. With a large selection of 13 new nonwovens to choose from, it was clear that a considerable number of friction measurements would be required to make an informed decision. It would have been inappropriate and unethical to carry out such extensive testing on a volunteer. Instead, these measurements were made using the skin surrogate, Lorica Soft, in preparation for a study with volar forearm skin *in vivo* (see chapters 4 and 5), although some preliminary experiments for method development were also carried out on a volunteer.

Lorica Soft (LS) was used first because it was easy to use, was available at convenience, and was relatively consistent – it produced repeatable friction results with nonwoven fabrics. It had the additional benefit of producing friction data directly comparable with those collected by Cottenden [4] for three other nonwovens, when implemented in conjunction with his rig. As an artificial, polyamide fleece leather, the skin surrogate (Lorica Soft) was, in most respects different to real human skin, but was appropriate for the purposes of this work. Lorica Soft has been shown to be the surrogate (of all those tested) most similar to human skin in terms of surface texture and friction forces. (See §2.5.) It was also more versatile than skin in the sense that its dimensions and orientation were not limited by the source. In this chapter, work to evaluate the new group of nonwoven fabrics, using LS in a flat configuration, is described first. Further experimentation with LS in a curved setup follows, the purpose of which is discussed in the relevant section. Due to the arrangement of chapters in this thesis, methodology and data from measurements on real human skin and the surrogate are kept separate. Nevertheless, the outcome of preliminary experiments on volar forearm skin was borne in mind when analysing results from LS.

3.1 Materials

3.1.1 Skin surrogate

Lorica Soft is the skin surrogate previously described in §2.2.4. It was used in these experiments for the initial analysis of new coverstocks because results obtained with an earlier set proved to be repeatable, therefore making it a reliable material for determining similarity between nonwoven fabrics. It is also worth noting that human skin *in vivo* is more challenging to test because humans lack the ability to remain perfectly still for any period of time, not to mention the interpersonal anatomical variations. There was an added benefit to using a skin surrogate, in that it was readily available for testing. In these experiments, it was important that the skin surrogate surface did not vary *significantly*, as it was anticipated that the nonwoven fabric *would*, and it was the change in nonwoven fabric that was of interest.

3.1.2 Nonwoven coverstock fabrics

This work follows some extensive testing by Cottenden [4] on three nonwoven coverstock fabrics. He was able to identify a potential mechanism present during their frictional interaction with a skin surrogate, applicable to all three nonwovens. However, it was still not known if this mechanism held for a wide range of nonwovens or just for the three fabrics examined. It was particularly difficult to determine, from these data alone, because all three of the fabrics were very similar to one another, varying only in the coating and linear density of the constituent fibres.

Table 3.1 shows a summary of the properties of all the nonwovens considered in this thesis (note that S/C bico refers to the sheath to core ratio of bicomponents fibres – in this case, 30% PE sheath to 70% PP core.) Nonwoven fabrics SF1, SF2, SF7, SF10, SF15, SF16 and DC1 consisted of uncoated hydrophobic fibres; SF9, SF12 and SF18 had hydrophilic surfactants; SF17, DC3 and DC6 were also coated. The presence of a surfactant in dry conditions may have a lubricating effect or increase friction, but the specific surfactant was assumed not to make a difference at this stage. This was expected to become more relevant when investigating friction between volar forearm skin and nonwoven fabrics in the presence of fluid. For full details of the nonwovens used, see table A.1 in appendix A. Nonwoven fabrics SF1 to SF18 were compared due to their wide range of material properties and different manufacturing methods. All of these were tested as described in §3.2.1 and §4.1.1.1 (dry friction only) and a subset of the 13 new fabrics were selected for further examination.

Table 3.1: Manufacturing processes and material properties of all nonwoven fabrics examined in this study

Fabric Code	Fibre Polymer	Fibre Dtex	Fabric Basis Weight / $\text{g}\cdot\text{m}^{-2}$	Fabric Bonding Pattern		Fabric Manufacturing/Bonding
				Area	Points / cm^2	
DC1	PP	2.0	17	12%	-	Spunbond and calendered
DC3	PP	1.4	17	12%	-	Spunbond and calendered
DC6	PP	3.6	17	12%	-	Spunbond and calendered
SF1	PP	2.0	18	18%	50	Spunbond and calendered
SF2	PP	2.0	18	11%	9	Spunbond and calendered
SF3	PET	1.7	50	-	-	Carded and hydroentangled (spunlaced)
SF7	PP	2.5	20	12%	-	Spunbond and calendered
SF9	PP	6	20	12%	-	Spunbond and calendered
SF10	PP	-	18	-	-	Spunbond and calendered
SF11	PP	2.2	18	25%	65	Carded and calendered
SF12	PP	2.2	30	25%	11	Carded and calendered
SF14	PP 95%, Cotton 5%	1.7	30	25%	11	Carded and calendered
SF15	PP	2.0	13	18%	50	Spunbond and calendered
SF16	PP	2.0	25	18%	50	Spunbond and calendered
SF17	PP	6.5	17	12%	-	Spunbond and calendered
SF18	PE/PP S/C bico 30/70	1.5	15	12%	-	Spunbond and calendered

3.2 Comparison of a wider range of nonwoven fabrics: Selection of a subset

The purpose of the work described in this section was to select a subset of representative nonwovens for further testing and to investigate whether inferences made by Cottenden [4] apply to a wider range of nonwoven fabrics. These inferences were: that the main mechanism occurring during friction between nonwovens and Lorica Soft appeared to be adhesion; that displacement rate had very little effect on friction force; and that change in applied load (in the range 0.25N–19.1N) gave rise to a difference in coefficient of friction of less than 10% of the highest value.

Before embarking on a detailed description of the experimental procedure, it should be mentioned that the nonwovens are referred to here and throughout the thesis only by their fabric codes (e.g. 'SF1') for convenience. In order to select the subset of nonwoven fabrics, some preliminary experiments had to be carried out to help to eliminate the most similar fabrics. The friction forces between these nonwoven fabrics and Lorica Soft (LS) were compared to each other and to the data collected on volar forearm skin (as described in §4.1.1.2), and subsequently used to identify the most different fabrics, which were then examined further. (Data on the volar forearm are not discussed in this chapter, rather in chapter 4, in order to maintain a clear presentation of this work.) During this process it was also possible to make some inferences about the relationship between friction force and specific manufacturing processes or material properties of the nonwoven fabrics as shown in table 3.1.

3.2.1 Methodology

Special apparatus, originally designed by Cottenden [4] for the measurement of friction between excised human skin and nonwoven fabrics, was also used here, substituting the excised skin for a skin surrogate called Lorica Soft. It was this same material used by Cottenden that was used for all friction experiments described in this chapter. The apparatus is depicted in figures 3.1 & 3.2 and its components are described in table 3.2 on page 57.

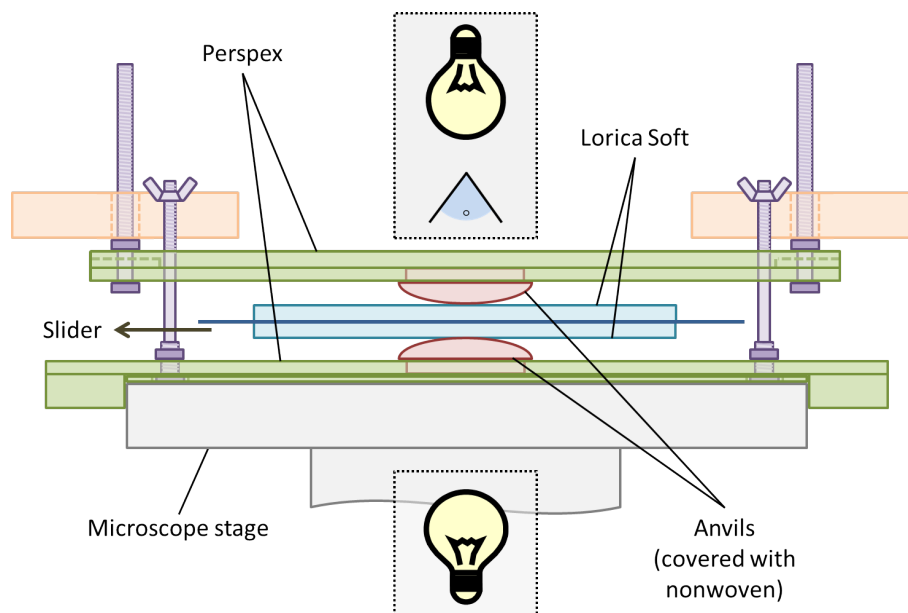


Figure 3.1: Diagram of apparatus used to measure friction between skin (surrogate) and nonwoven fabrics (based on [4])

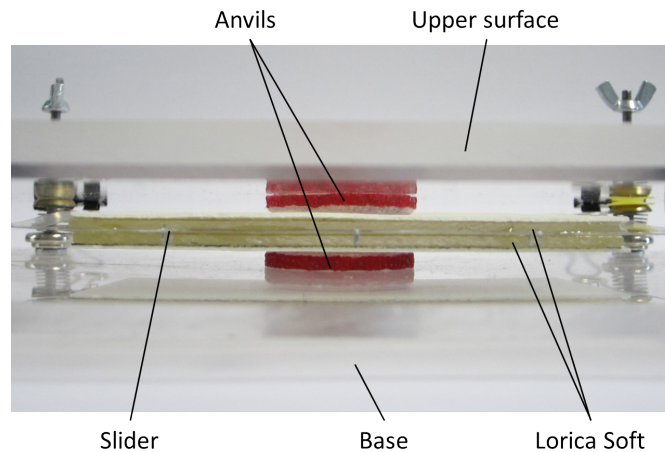


Figure 3.2: Side view of apparatus, focusing on contact between skin surrogate and nonwoven fabric attached to anvils

Lorica Soft (or skin surrogate) on the *slider* – attached to the *tensometer* via a *tensometer connector* and *linkage* – was pulled between two pieces of nonwoven attached to two *anvils*, which were fixed to the *upper surface* and *base* of the apparatus. The two pieces of Lorica Soft and two anvils created a double interface, which greatly reduced the net moments about the points of contact that are observed with a typical single interface when a slider is used. This occurred because, with Cottenden’s design, the moments were *essentially* equal and opposite. Of course, the load applied to the bottom anvil was larger than that of the top one, with the additional weight of the slider¹, although Cottenden attempted to design the slider in such a way that the extra load was limited. The slightly rounded, uni-directional profile of each anvil’s contacting surface enabled uniform pressure distribution in friction. A flat or spherical surface would create a pressure gradient across the interface, but something in between was found to be more appropriate. Also, the pressure distribution depended upon shear stresses; the leading edge (at the front of the anvil in the direction of sliding) was shaped differently to the trailing edge to maintain the uniformity. (A description of how the anvils were manufactured can be found in appendix C of Cottenden’s thesis [4].)

A load was applied to the upper surface, separated from the base by *springs* (with *guiding rods*) and *legs*. Applied loads were selected according to the anvils used – each was produced at a specific pressure and this was taken into consideration during loading. In figure 3.1, the bulbs represent the microscope stage on which the apparatus was positioned, and the microscope camera with which the nonwoven-surrogate interface was visually recorded by Cottenden [4]. However, this no longer bore any scientific importance to the experiments described in *this* thesis as video-recordings with the microscope camera were found to be unhelpful in the analysis of friction data. This is because Cottenden found that the images produced were of no use for fibre contact length measurement, or assessment of dynamic interfacial interaction, due to the lack of clarity (poor resolution). Recording the friction measurements with a normal video camera was attempted instead, but the footage was also uninformative. Nevertheless, the microscope stage was still used, solely to support the apparatus shown in figure 3.1.

¹This was measured (by Cottenden [4]) and the contribution of the slider to the load on the bottom anvil was shown to be up to $\sim 0.5\text{N}$ and decreased by $\sim 0.1\text{N}$ during the course of a 50 mm friction cycle.

Table 3.2: Description of friction apparatus components

Component	Description/purpose
Slider	240 μm -thick acetate sheet to which two pieces of skin surrogate $\approx 50 \text{ mm} \times 100 \text{ mm}$ (one on each side) were glued; disposable if used with real excised skin.
Tensometer	Mechanical testing machine used to apply constant displacement rate to slider/LS across anvils/nonwoven, while simultaneously measuring friction force. [MTT170, Diastron, Andover, UK]
Tensometer connector	Small piece of stiff 0.52 mm polyethylene sheet [RS Components Ltd, Corby, UK] to which linkage attached; kept between tensometer grips.
Linkage	Specially designed larger piece of the same material as connector supported by two flat aluminium rods (rectangular cross-section); supported and connected to slider and tensometer connector.
Anvil	PUR resin discs with one slightly convex face to distribute pressure uniformly across the skin surrogate surface; there were two anvils – one for each piece of skin surrogate attached to the slider; they were a “snug fit” in the upper surface and base.
Upper surface	2 mm, 4 mm and 6 mm perspex sheet and strips; supported the dead weights, applied via two M5 bolts, and held the top anvil in place.
Base	4 mm and 8 mm perspex sheet and strips; designed to fit securely on the microscope [DMLM Leica Microsystems (UK) Ltd, Milton Keynes, UK] stage; held bottom anvil in place.
Springs & guiding rods	Four partially de-threaded M4 bolts acted as rods for four springs [LP 012BC 06 ($k = 0.028 \text{ N} \cdot \text{mm}^{-1}$, $l_0 = 31.75 \text{ mm}$), Lee Spring, Wokingham, UK], which supported the upper surface during loading of the skin surrogate.
Legs	Four bulldog clips to support the upper surface when no load was being applied to the skin surrogate; one of the long hinged components on each clip could be released to remove support.
Wedge tool	A piece of wood shaped to support the slider/acetate so that the skin surrogate and nonwoven fabric on the bottom anvil did not come into contact prematurely; it had two chamfered edges to facilitate its insertion and removal (not shown in figure 3.1).

All friction experiments with Lorica Soft were carried out in an environmentally (temperature and humidity) controlled room: the temperature and relative humidity were maintained at $23.0 \pm 2^\circ \text{C}$ and $50.0 \pm 4\%$ respectively. Apparatus were set up mostly as described by Cottenden [4], including the application of nonwoven fabrics to anvils, attachment of the skin surrogate to the slider, and calculation of the trimming load (the load applied to create initial contact between the fabric and surrogate, without applying a significant force at the interface). Before any dead weights were applied, the only load was the top piece of the apparatus itself. However, the force from its weight was insufficient to compress the springs enough so that the top anvil was *just* in contact with the top piece of Lorica Soft. Small weights had to be applied to induce what could be considered an unloaded contact. In other words, any weights applied thereafter would constitute the *real* applied load.

Once an applied load was chosen according to the pre-made anvils, two pieces of the selected nonwoven fabric were cut to approximately $35 \text{ mm} \times 35 \text{ mm}$ and then attached to the convex side of two anvils

– aligned with the machine direction² parallel to the direction of tensometer pull – using nail varnish as an adhesive on its rim. When the nail varnish dried, the excess nonwoven fabric was removed using scissors. Nail varnish was used because it was easily removed with ethyl acetate, enabling reuse of the anvil. The anvils were orientated in the apparatus such that the machine direction of the nonwovens was parallel to the direction of pull of the tensometer and the same surface of the fabric was always exposed for friction. Lorica Soft was mounted on an acetate sheet which was then connected to the rest of the slider, as shown in figure 3.3.

Each coverstock was tested under two loads (2.6N or 5kPa and 8.1N or 15kPa), at one crosshead speed ($0.5 \text{ mm} \cdot \text{s}^{-1}$) over a distance of 50mm, for 10 cycles. Only two loads – one near the top and the other near the bottom of the range of interest – were used because of the time constraint on measuring friction forces for 13 fabrics. A displacement of 50mm was set in order to collect as much data as possible on the chosen pieces of Lorica Soft without impinging on the edges of the surrogate with the centres of the anvils. Measurements were repeated for 10 cycles as nonwovens SF1-SF18 had never before been tested using the method described in this section, so it was necessary to briefly assess the *wearing-in*³ period and the repeatability of the friction measurements with these fabrics, before eliminating most fabrics. All nonwovens were tested in order of code number (i.e. SF1, SF2, SF3, ...SF18), first under 0.26N, then under 8.1N.

Maximum force, pre- and post-wait periods (phases 2 and 4 respectively – see figure 3.4), pre-cycle gauging and tensometer start and finish positions were important to ensure that measurements were accurate, and that there was time to prepare and reset the apparatus before and between measurements. Maximum force was chosen by first considering the applied load, because if the actual measured force were to exceed the limit set, the tensometer would stop and the experiment could not be completed. However, when it was not obvious whether the friction force would be greater than the applied force, it was reasonable to initially set the maximum value possible for maximum force measured by the tensometer.

The pre-wait period depended on the amount of time required to complete apparatus setup for the *first* cycle after the calibration period (when zero force was measured/set). This was usually considerably longer than the setup between cycles. The post-wait period was typically shorter than the pre-wait period. This was when the upper surface was lifted off the Lorica Soft and rested on the legs, and the wedge tool was used to lift the slider off the bottom anvil, so that the tensometer could return to its start position. All of these parameters were input as tensometer settings, as shown in figure 3.4.

²The machine direction (MD) during manufacture of SF3 was obvious due to its fibre alignment. SF9 and SF11 also had a large proportion of parallel fibres. Some nonwovens exhibited large structural variation, even before friction measurements, visible on a macroscale. Such fabrics included SF1, SF10, SF15, SF17 and SF18. However, all were labelled with MD before receipt.

³*Wearing-in* is the term used to describe changes occurring within a new sample of nonwoven fabric during the first ~ 25 friction cycles as the measured force equilibrates. This can also apply to new pieces of Lorica Soft.

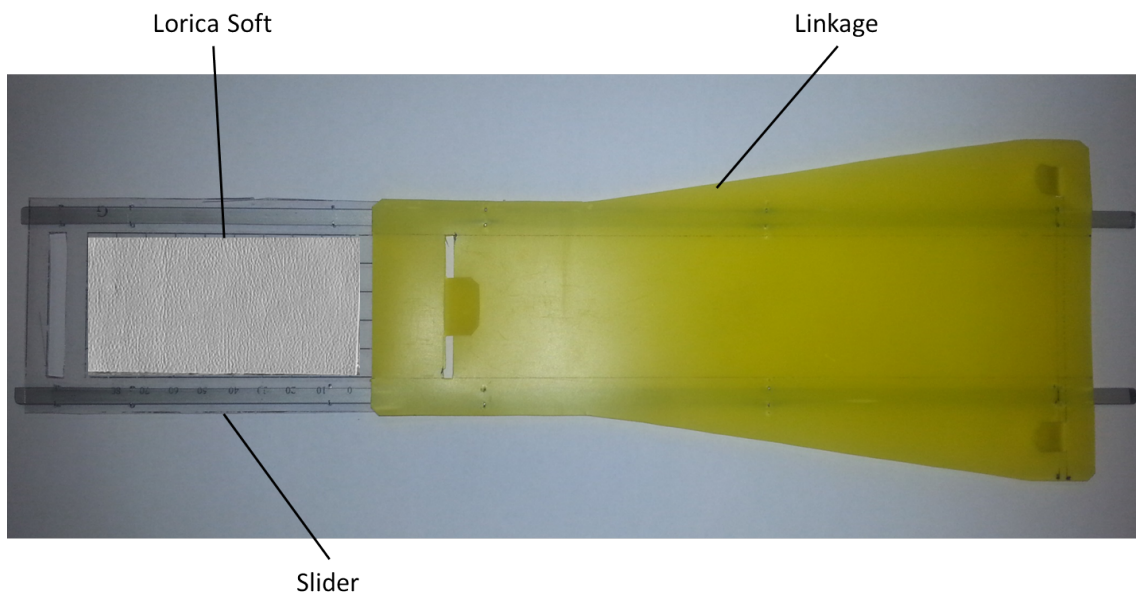


Figure 3.3: Photograph of the slider with Lorica Soft on both sides of the acetate sheet

The screenshot shows a software dialog box titled 'Full Options Test Method'. It contains several sections of settings:

- Motion Options - Set Phase 1 & 3 Units:** Includes radio buttons for 'Units: %' and 'Units: mm'. Below are input fields for: Sample Size (mm): 30., Phase 1 Movement: 0., Phase 2 Static (sec): 40., Phase 3 Movement: 50., Phase 4 Static (sec): 15., and Rate (mm/min): 30.
- Cycle Options:** Includes a 'Cycles:' input field set to 10, and radio buttons for 'Start Each Cycle at Current Position' and 'Start Each Cycle at Origin Position' (which is selected).
- Gauge Force Options:** Includes a 'Gauge Force (gmf):' input field set to 0., and radio buttons for 'Apply Gauging to First Cycle Only' (selected) and 'Apply Gauging to Each Cycle'.
- Force Range Options:** Includes a 'Maximum Force (gmf):' input field set to 1700.
- End of Method Options:** Includes a checked checkbox for 'Return Sample to Pick Up Position'.
- Break Detection:** Includes radio buttons for 'Disabled' (selected) and 'Enabled', with an 'Edit Break Detection' button.
- Carousel Options:** This section is currently empty.

At the bottom of the dialog are four buttons: 'Cancel', 'Save', 'Run After Delay', and 'Save & Run'.

Figure 3.4: Settings applied to tensometer for most friction measurements on Lorica Soft; crosshead speed, number of cycles and phases 2 and 4 sometimes varied during preliminary experiments

The skin surrogate-nonwoven interface was loaded with dead weights on the upper surface of the apparatus. These weights were applied to the apparatus before any contact occurred between the nonwoven fabric and Lorica Soft. The tensometer was left to equilibrate to establish the reference (zero) force for approximately 10 seconds before the slider was placed within its grips (the tensometer connector) and the measurements commenced. The wedge tool was carefully removed from under the slider, allowing the skin surrogate to rest on the bottom anvil. Next, the legs were released and the upper surface was lowered so that the top anvil made contact with the skin surrogate. Between measurements, it was necessary to reset the apparatus to the same position as during the calibration period, so that the tensometer could return to its starting point – without damaging the nonwoven – for each cycle.

3.2.2 Results

The first things to be reported here are the observations made during the experiments – various things that could not be expressed in graphical form and may become more relevant when attempting to explain certain patterns in the data. The surface profiles of Lorica Soft were rather uneven, so the contact area between the skin surrogate and nonwoven fabric was likely to have changed (on a macroscale) with displacement. There also appeared to be a slight peak in the profile of the top piece of LS, distal to the tensometer. The lack of uniformity is something that was recognised by Cottenden [4] as an inevitable consequence of attaching skin surrogate to the acetate using the particular method described in his thesis. However, the effect is more likely to be similar to that of adhering a sample of excised skin to a completely flat surface, as the naturally non-uniform distribution of fat among other tissues causes variations in its thickness over a given area. On a few occasions, a nonwoven briefly rubbed against the Lorica Soft in a direction other than that intended for measurements. Fortunately, this did not appear to have a notable effect on the data.

Despite the sparse distribution of the fibres in SF17, the fabric felt relatively stiff, making it difficult to attach to the anvils, but once attached, there was no longer a problem. SF18 was a particularly thin and lubricious nonwoven. After taking measurements under 8.1N, it was noticed that the piece of nonwoven on one anvil was loose on top and could slide against the convex surface of the anvil. This means that friction was measured at both the nonwoven-anvil and nonwoven-surrogate interfaces. The graph in figure 3.5 is an example of the data collected in each friction test⁴, although graphs varied in shape slightly. There were also differences in static friction force and dynamic force ranges for each fabric, the former of which are compared in table 3.3. Figure 3.6 demonstrates how the static friction force (or “maximum tensometer force”⁵) would fluctuate between cycles, rather than decrease steadily over time. The next six graphs (figures 3.7–3.12) display the friction-displacement curves of each nonwoven at cycles 1, 5 and 10, which were chosen to represent different stages of each friction test, and appear to give an accurate representation of the overall cyclic progression (in terms of force and shape).

⁴Note that all force values plotted are half of the measured values; this is because friction was measured for two interfaces (both nonwoven fabric against Lorica Soft), so the mean force was taken.

⁵Throughout this thesis, the term “(maximum) tensometer force” is used more frequently than “(static) friction force”. This is because the tensometer force may also include another force – perhaps contributed by whichever mechanism is in place – although the dominant force is, indeed, friction.

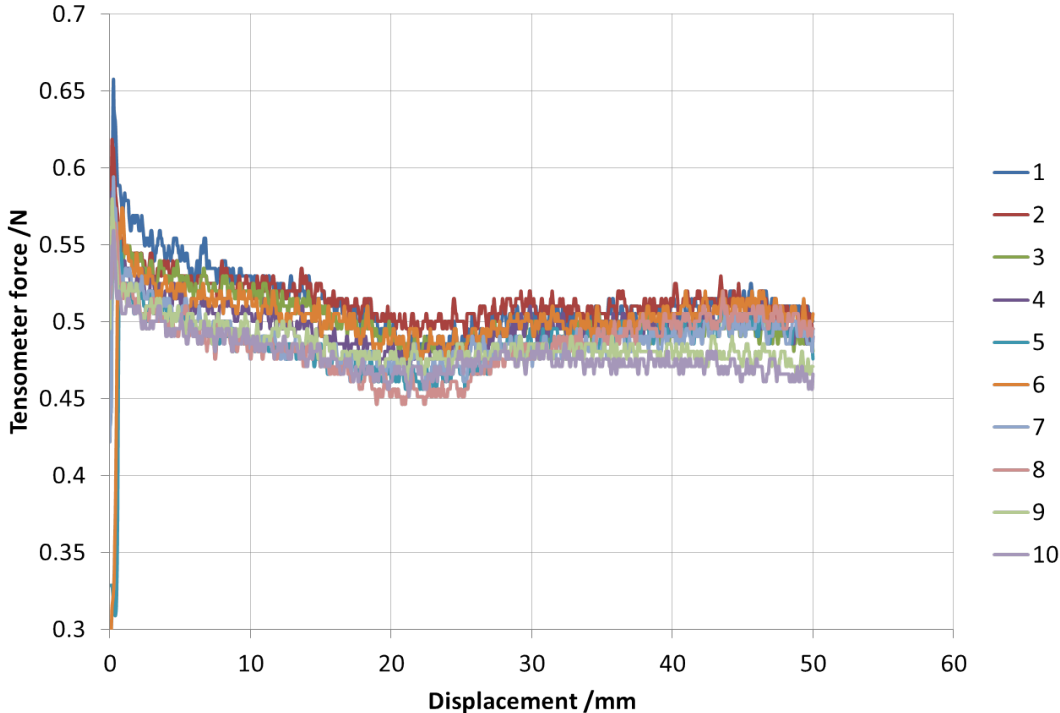


Figure 3.5: Friction between SF9 and Lorica Soft; 2.6 N, 0.5 mm · s⁻¹; each curve represents a different cycle

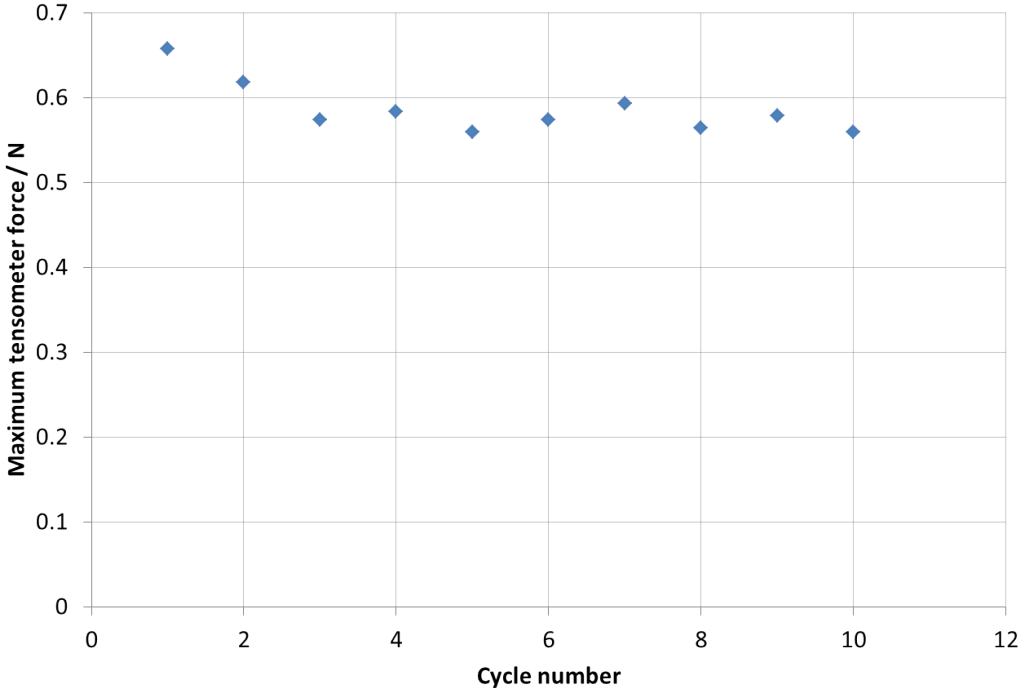


Figure 3.6: Maximum forces measured for each cycle of friction between SF9 and Lorica Soft; 2.6 N, 0.5 mm · s⁻¹

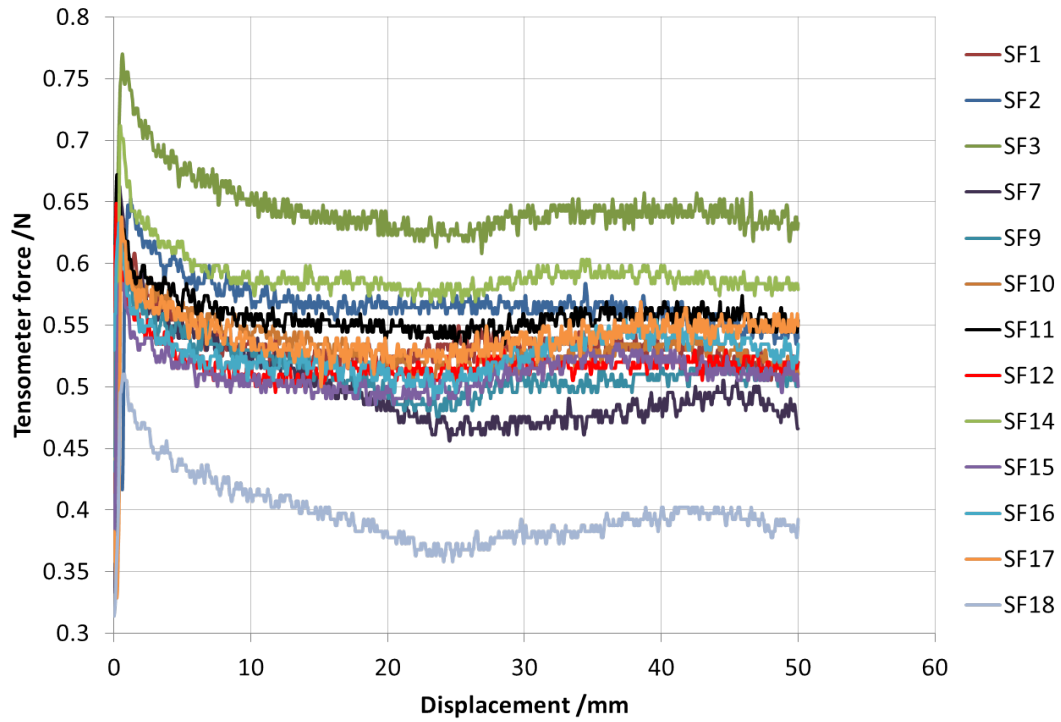


Figure 3.7: Cycle one of friction between Lorica Soft and all nonwovens (SF1–SF18); 2.6 N, $0.5 \text{ mm} \cdot \text{s}^{-1}$

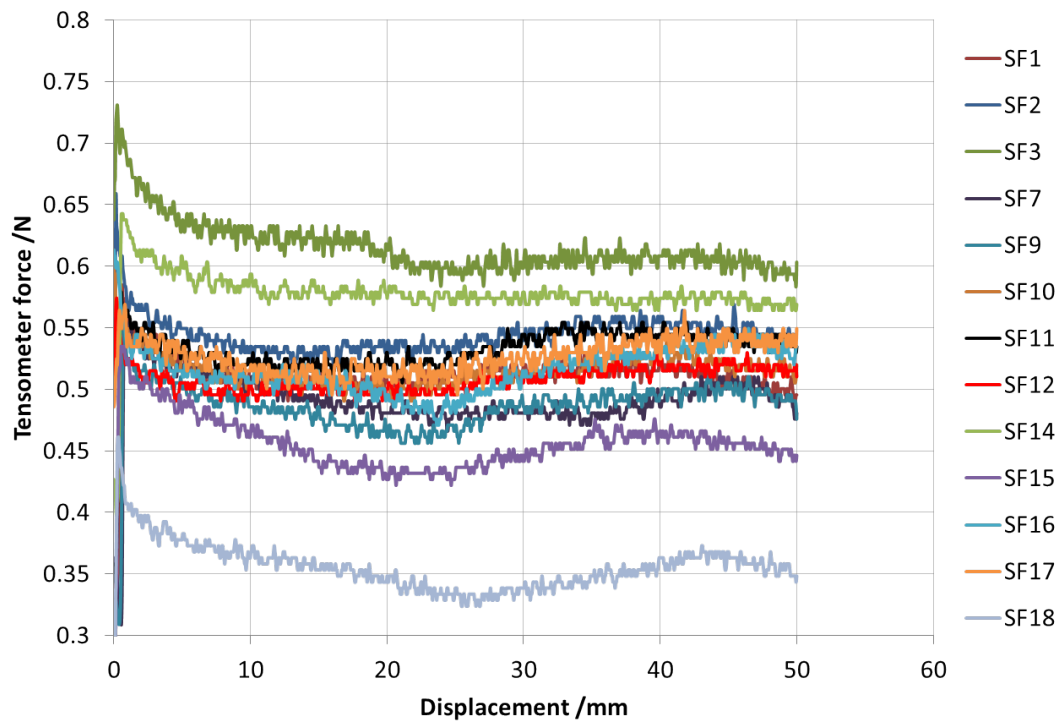


Figure 3.8: Cycle five of friction between Lorica Soft and all nonwovens (SF1–SF18); 2.6 N, $0.5 \text{ mm} \cdot \text{s}^{-1}$

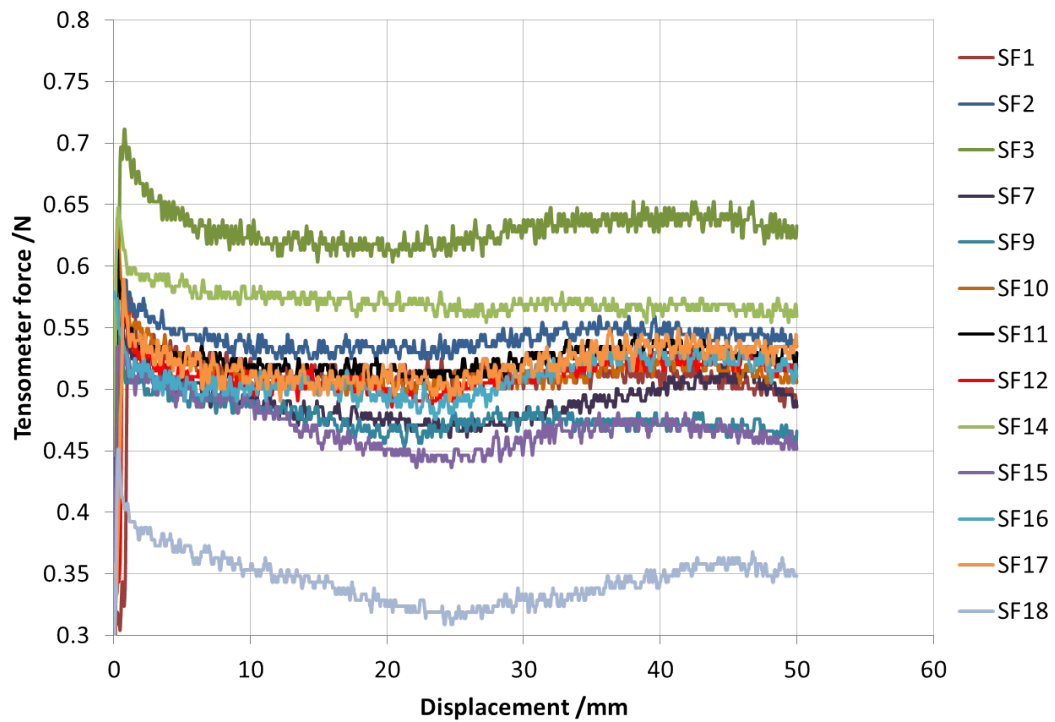


Figure 3.9: Cycle ten of friction between Lorica Soft and all nonwovens (SF1-SF18); 2.6 N, $0.5 \text{ mm} \cdot \text{s}^{-1}$

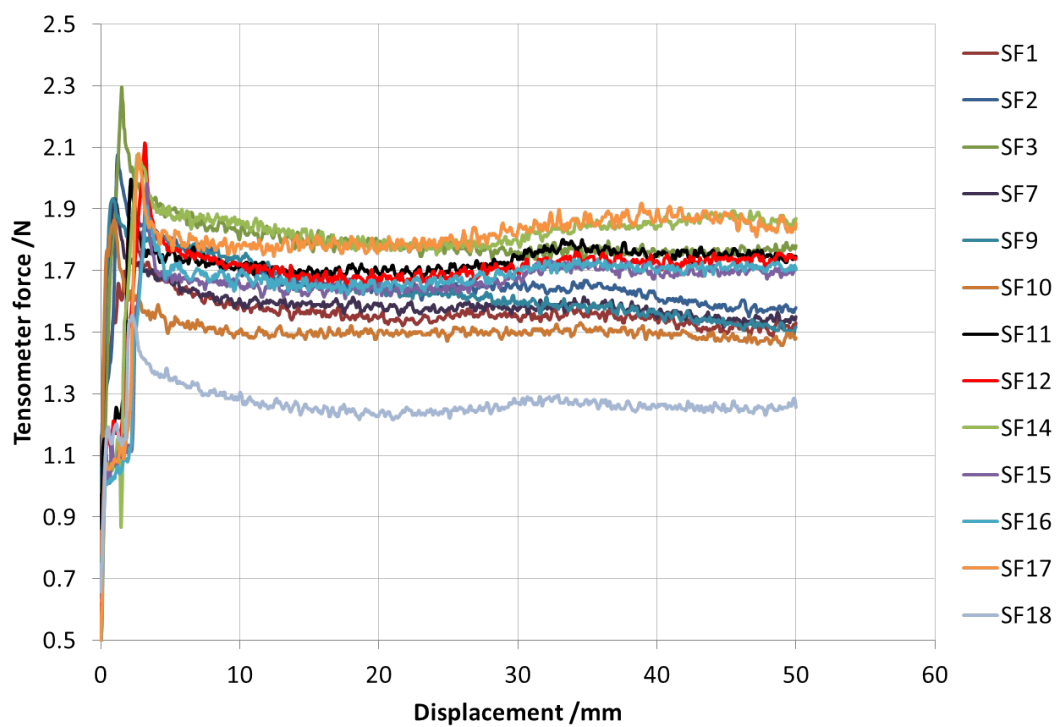


Figure 3.10: Cycle one of friction between Lorica Soft and all nonwovens (SF1-SF18); 8.1 N, $0.5 \text{ mm} \cdot \text{s}^{-1}$

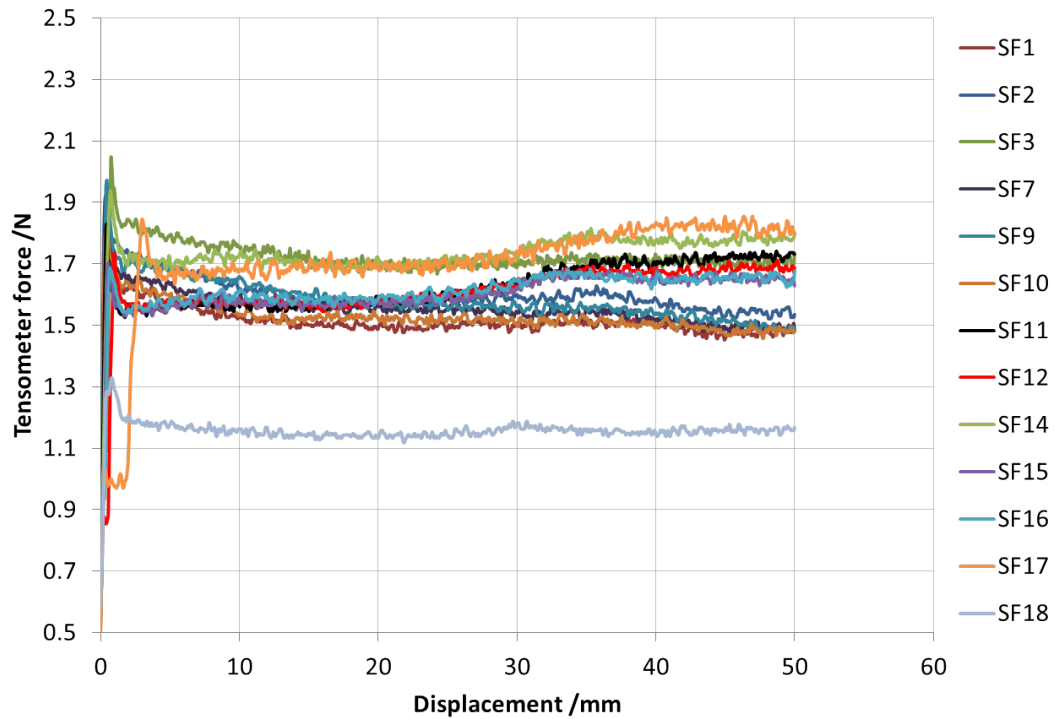


Figure 3.11: Cycle five of friction between Lorica Soft and all nonwovens (SF1-SF18); 8.1 N, $0.5 \text{ mm} \cdot \text{s}^{-1}$

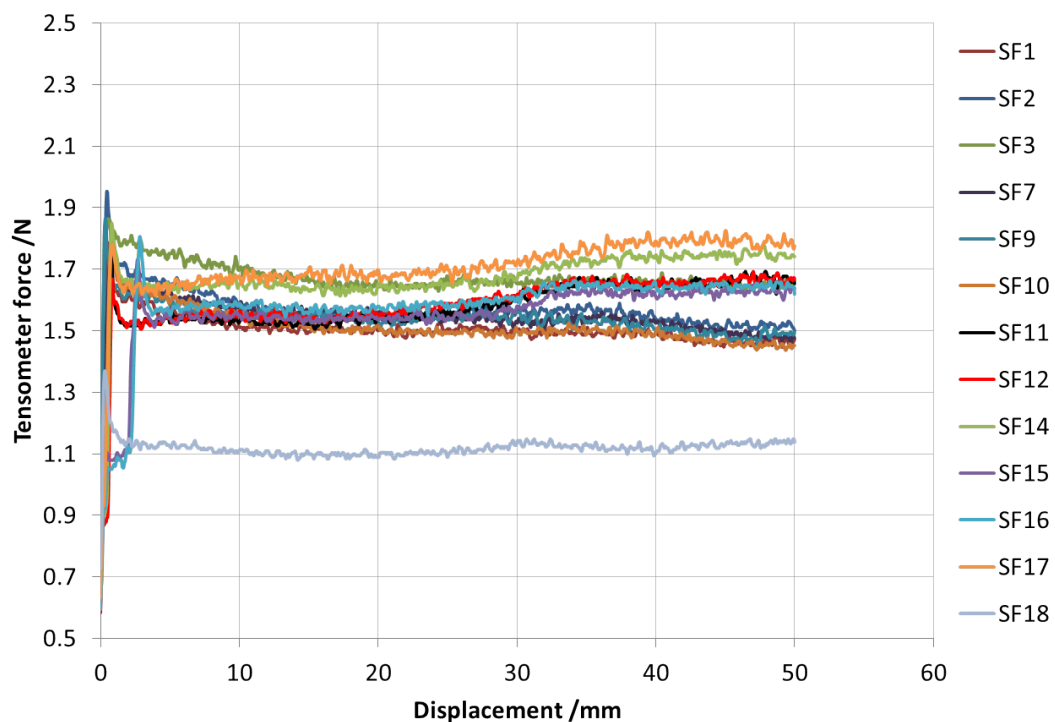


Figure 3.12: Cycle ten of friction between Lorica Soft and all nonwovens (SF1-SF18); 8.1 N, $0.5 \text{ mm} \cdot \text{s}^{-1}$

Table 3.3: Summary of material properties and friction data for all nonwovens; **highest tensometer force**, **second highest tensometer force**, **lowest tensometer force**, **second lowest tensometer force**; *SF18 is PE/PP S/C bico 30/70

Nonwoven (Fabric Code)	Fabric Manufacturing / Bonding			Fibre Polymer(s)				Fibre Linear Density / dtex												Fabric Area Density / g.m ⁻²												Fabric Bonding Pattern						Fibre Surfactant			Maximum tensometer force for a load of:		Nonwoven (Fabric Code)
	Spunbond	Carded	Spunlaced	PP	PE	PET	Cotton	1.5	1.7	2.0	2.2	2.5	6.0	6.5	13	15	17	18	20	25	30	50	11	12	18	25	9	11	50	65	h-phill	lutrasil	none	2.6N	8.1N								
SF1	Spunbond			PP																													0.65	1.85	SF1								
SF2	Spunbond			PP																												0.66	2.06	SF2									
SF3	Spunbond	Carded	Spunlaced				PET																									0.77	2.30	SF3									
SF7	Spunbond			PP																												0.66	1.94	SF7									
SF9	Spunbond			PP																												0.66	1.98	SF9									
SF10	Spunbond			PP																												0.64	1.87	SF10									
SF11	Spunbond			PP																												0.67	2.00	SF11									
SF12	Spunbond	Carded	Spunlaced	PP																												0.65	2.12	SF12									
SF14	Spunbond	Carded	Spunlaced	PP																												0.71	2.07	SF14									
SF15	Spunbond			PP																												0.58	1.98	SF15									
SF16	Spunbond			PP																												0.63	1.91	SF16									
SF17	Spunbond			PP																												0.64	2.08	SF17									
SF18	Spunbond			PP																												0.51	1.56	SF18									

3.2.3 Discussion

Before analysing the data, a few things should be pointed out. Where friction force has been displayed on a graph, it is in fact the mean friction force of two interfaces: the nonwoven on the upper anvil and the top piece of LS; the nonwoven on the lower anvil and the bottom piece of LS. Where there are numbers in the legend of a graph, they refer to the friction cycle number. There are often truncated axes on graphs in order to highlight certain features of curves or to be able to more closely compare each nonwoven, cycle, load or crosshead speed. No useful information has been omitted, nor have anomalies been excluded unless otherwise stated and explained.

The nonwoven samples were not elongated upon application to the anvils, therefore it was expected in some cases that the nonwovens would slide a short distance on the convex anvil surfaces at the start of each cycle. However, this could not have affected the data significantly because, even in the most extreme situation when there was up to 2mm displacement between the anvil and nonwoven, friction was only measured in one direction. For that reason, it can be assumed that the data would have varied only slightly (if at all) in the same way for each cycle. Another thing to acknowledge is that different pieces of each nonwoven fabric were used with each applied load. Cottenden noted that the coverstocks were typically inhomogeneous – in terms of their fibre distribution – and it is very likely that the same amount of variation was found in the new fabrics (SF1-SF18). This is something that must always be considered when discussing possible causes for changes in friction forces or curve shape. As the pieces of LS used in these measurements had already been worn-in, the possibility of wearing-in being the cause for SF3 (tested first) and SF18 (tested last) having the most different friction forces was excluded.

The graph in figure 3.5 shows a typical friction force-displacement relationship, observed with any of the nonwovens tested, as measured by the tensometer. In most cases, the first three cycles had the highest friction forces, after which there was little change with cycle number. Most repeats under each load resulted in very similar “principal” curve shapes, as can be seen in figure 3.5, with only one or few deviations from the mode shape. Each curve also comprised smaller peaks and troughs due to a “remainder friction” as described by Cottenden [4]. It was suggested that these principal and remainder curves (or force variations) were associated with two different components or mechanisms, but this will be discussed later on in this section when all the data have been considered. All friction cycles had a sharp peak (static friction) force at the start, which was almost always highest for the first cycle. The very small width of this peak indicated almost immediate shear between the nonwoven fabric and Lorica Soft from the start of the measurement.

Three of the cycles, for each set of friction measurements with each nonwoven, were chosen for display in this section to simplify comparison of nonwovens. It was thought that the first, fifth and tenth cycles would provide a good range of data to accurately demonstrate the occurrences throughout entire experiments (i.e. these three cycles suitably represented all 10). Even with fewer cycles, there was still a rather large number of nonwovens to compare, therefore the nonwovens under different loads have also been compared on separate graphs.

From the graphs of cycles 1, 5, and 10, under both loads (see figures 3.7–3.12), it can be seen that the order of nonwovens (in terms of magnitude of friction force) was mostly the same for each cycle. Under a normal load of 2.6N, SF3 always had the highest friction force (for all cycles), followed by SF14. SF18 had a notably decreasing friction force with each cycle, which was always considerably lower than all other fabrics - up to 3/5 or 2/3 of that produced by the nonwoven with the highest friction force for an applied load of 2.6N or 8.1N respectively. Considering that SF18 consistently had the *lowest* friction

forces, there was no other nonwoven fabric that always produced the *second* lowest friction force with the skin surrogate for one or both applied loads (2.6N and 8.1N).

For all other nonwovens, the measured tensometer force changed randomly from cycle to cycle (no continuous increase or decrease in force), especially under the higher load. This suggests that the fabrics had very similar frictional interactions with the Lorica Soft, and it appeared that the cycle-to-cycle variation was greater than or equal to variation *between* these particular nonwovens. In all cases, the static friction force for each coverstock only decreased by approximately 0.05N over the 10 cycles, and the same for dynamic friction at any given displacement value – 7.7% or less for SF3 and 13.2% or less for SF18. The shapes of the curves for each nonwoven were very similar between cycles – there was little inter-cyclic variation for each nonwoven. Thus far, all of this would suggest that the manufacturing processes and structural properties played no role in friction against Lorica Soft for most nonwovens. This may have been, in part, due to the fact that most nonwovens were made from fibres of the same polymer (PP) and manufactured using the same two processes.

In order to identify the material properties that may have affected friction between Lorica Soft and the nonwoven fabrics, it was important to first understand *how* these properties may have affected frictional interaction. The manufacturing processes of nonwovens were briefly described in §2.4, where it was clear that the carded nonwovens would have different properties according to their constituents and other features, rather than the specific manufacturing process. However, spunlace (or hydroentangled) nonwovens are known to be soft, compliant and strong in tension, amongst other properties [155]. Considering the fabric compliance, it might be expected that friction force would be higher due to an increasing number of fibres in contact with the skin surrogate, potentially becoming trapped in the small troughs. Alternatively, it may be that fibres would *not* stick because they would be under tension on the anvil during friction measurements.

When comparing friction forces, it can be shown that SF3 had the highest maximum friction force and highest force range under 2.6N, followed by SF14. Nonwovens SF3, SF14 and SF17 had the highest forces when tested under 8.1N. The *lowest* friction force for SF3 (when tested under 2.6N) was greater than most of the *highest* forces for other nonwovens. Most other fabrics were relatively close in terms of their friction forces. Fabrics SF1 and SF12 had exactly the same ranges and maximum friction forces under 2.6N normal force, and SF10 was almost identical to SF1 under both applied loads. SF18 had the lowest force range and maximum force at all times under each load. The principal difference between SF3 and SF18 was their area density (or basis weight), but there was insufficient evidence to infer that this particular property was responsible for the large difference in tensometer force. In fact, other information contradicted the suggestion that any of the known features of the nonwovens directly affected friction. For example, SF3 and SF14 both had very low linear densities, but so did SF18; SF3 and SF14 were made from different materials; SF17 and SF18 had the same proportional bonding area and similar area densities.

As mentioned previously, Lorica Soft had a rather uneven surface. It might be expected that this would be clearly reflected in the friction force-displacement curves, however, this was only partially true. While most curves were generally similar in shape, they were not identical, which suggests that the changes in friction force across the surface of Lorica Soft were also dependent on some other factor. If this factor was a manufacturing process or certain material properties, it should be possible to demonstrate by comparing the data of each nonwoven with their properties. If a group of nonwovens that shared one or more particular processes or properties also showed similarities in graph shape, it may suggest that their common feature(s) contributed to a particular friction mechanism. The same applied to friction force or coefficient, but this will be discussed later on in the section. It should also

be noted that it was the *shape* of the graph rather than the *magnitude* of the friction forces that may indicate which mechanisms were operating.

Looking at figures 3.7, 3.8 and 3.9, there was an interesting curve-shape similarity between SF7, SF9 and SF18. Nonwovens SF3 and SF14 both produced relatively flat curves when tested under 2.6N. SF3 curves remained like this with 8.1N applied load, whereas the curve shape for SF14 became more undulated. The properties of these have already been compared because they had the highest friction forces. Fabrics SF1, SF2, SF11 and SF17 curves all had shallow S-shapes at 2.6N, which became more undulated under the higher load. If all the nonwoven fabrics had the same mechanical properties, it would be expected that curve shape would be the same, based on the assumption that the surface of the skin surrogate also contributed. The particular property of interest is compliance: a more compliant fabric may be more likely to be affected more by a non-uniform substrate surface. However, the experimental setup would not have permitted compliance to have any significant effect on friction as all nonwoven samples were constrained by an adhesive (nail varnish) on the anvils. Therefore, it was not possible to assess the potential impact of compliance on force-displacement curve shape.

The coefficient of static friction, μ_s , was calculated for each friction cycle for each nonwoven, using the standard equation, $\mu_s = F_{\max}/L$, where F_{\max} is maximum tensometer force⁶ (of the cycle) and L is applied normal load⁷. As the configuration of the Lorica Soft and therefore the interface was flat, and only two loads were applied, no angles of arc of contact were involved and it was not necessary to use the gradient of a 'maximum tensometer force vs applied load' plot. The mean coefficient of static friction and standard deviation of each set of 10 friction cycles were calculated for each nonwoven-load combination and these values are presented in table 3.4. Nonwoven SF3 had the highest coefficients of static friction, but also exhibited the greatest variance under 8.1N (as well as SF12). Most nonwovens had similar mean coefficients and standard deviations, further supporting the selection of friction data presented (in figures 3.7-3.12). The values in the table also show that SF18 consistently had the lowest coefficient of friction, as anticipated. Nevertheless, none of the properties listed in table 3.1 stood out as important for determining how the nonwovens would behave in friction.

Following work carried out by Cottenden [4], it was concluded that the dominant mechanism for friction between Lorica Soft and nonwoven fabrics was most likely interfacial adhesion and dissipation,

Table 3.4: Mean coefficients of static friction for all new nonwovens (SF1–SF18) and standard deviations

Applied load / N	Mean coefficient of static friction (& standard deviation)						
	SF1	SF2	SF3	SF7	SF9	SF10	SF11
2.6	0.221 (0.011)	0.236 (0.009)	0.275 (0.008)	0.222 (0.012)	0.221 (0.012)	0.227 (0.009)	0.235 (0.011)
8.1	0.222 (0.005)	0.239 (0.008)	0.256 (0.015)	0.227 (0.008)	0.234 (0.006)	0.220 (0.005)	0.223 (0.009)
	SF12	SF14	SF15	SF16	SF17	SF18	
2.6	0.223 (0.010)	0.248 (0.010)	0.209 (0.007)	0.224 (0.009)	0.221 (0.009)	0.174 (0.008)	
8.1	0.219 (0.015)	0.240 (0.010)	0.216 (0.011)	0.218 (0.010)	0.233 (0.009)	0.169 (0.009)	

⁶That is, the maximum force for one interface, i.e. half of the measured force, as explained in the footnote on page 60.

⁷This was not corrected for the weight of the slider on the bottom anvil – which can be assumed to be 0.5N at the point of maximum tensometer force (static friction) – because the relative differences in μ_s for each nonwoven were more important than the actual values.

and that plastic and viscoelastic dissipation may have had a minor contribution. The components of curve shapes of force-displacement graphs in this thesis support the suggestion that principal and remainder friction were caused by two components of the adhesion mechanism that was in place during friction between nonwoven fabrics and a skin surrogate. Cottenden [4] explained that a combination of smooth and rough contacts at the interface with LS, due to variation in the nonwovens, was a likely source of the different scales of curve-shape variation. It was also proposed that wearing-in was evidence of initial plastic dissipation, which was further supported by the results of experiments – on 13 different nonwovens – reported in this thesis. No measurements were made here to compare different tensometer crosshead speeds, hence no comment can be made regarding viscoelastic dissipation as a mechanism for nonwoven-skin (surrogate) friction.

The key findings of these experiments were:

- Nonwoven SF3 typically had the highest friction forces and SF18 always had the lowest.
- Most nonwovens had similar friction forces when tested against Lorica Soft.
- The shape of force-displacement curves varied between friction cycles (repeats) with no obvious explanation.
- Friction behaviour could not be directly attributed to any specific properties of the nonwovens as listed in table 3.1 or 3.3.

For the above reasons, the initial selection of a subset of nonwoven materials for further investigation was based on differences in coefficients of friction and structural properties separately. The aim was to select a small group of fabrics to represent the entire range of 13. As SF3 and SF18 had the highest and lowest coefficients of friction (with Lorica Soft) respectively, they were selected for more extensive testing. Nonwovens SF14 and SF17 were chosen for their different properties and DC6 (one of Cottenden's fabrics) was included to facilitate comparison between data sets from different experiments. Before a final decision could be made, it was necessary to investigate the friction between all 13 nonwovens and human skin *in vivo*, but only with a limited set of measurements based on the results from experiments with Lorica Soft. This will be discussed in more detail in chapter 4.

3.3 Skin surrogate in a curved configuration

While Lorica Soft (LS) has been considered a reasonable surrogate for skin in friction, it is still very different in many other ways. It was tested with an unsuitable (flat) setup for measurements on human skin *in vivo* (see §3.2), although it was attempted for experiments on *excised* breast skin (see appendix G). The applied loads were also much too large for direct testing on a living volunteer. For these reasons, the effect of making friction measurements with LS in a curved configuration was investigated. Upon studying friction between volar forearm skin and nonwoven fabrics, the coefficient of friction were extracted from the data, based on a model which uses equation 2.7 and makes various assumptions:

- the arm has a fixed position and does not move;
- the nonwoven fabric has a very low density;
- the arm is a uniformly convex prism, (comparable to a cylinder);
- the nonwoven strip has a low bending stiffness, but is an incompressible material⁸ (and is essentially two-dimensional) with no lateral deformation;

⁸with a Poisson's ratio of 0.5

- forces are only applied at the ends of the nonwoven strip and on the arm at the edges of contact with the nonwoven⁹;
- Amontons' law holds for this setup.

It should be noted that most of these assumptions obviously do *not* apply to nonwoven fabrics or the volar forearm, although the mathematical model has been shown to hold for other physical models. This section describes work to test some of those assumptions in that measurements on LS on a cylindrical surface should produce coefficient of friction values in agreement with those on the flat. Using mathematical modelling, Cottenden demonstrated that the geometrical configuration made very little difference to coefficient of friction for real skin [103]. Nevertheless, a change in geometry on a macroscale may cause a significant alteration in surface topography on a microscale. This possible change in surface properties of the skin surrogate may ultimately affect the friction forces measured. Additionally, the nonwoven fabric was pulled against a strip of curved LS attached directly to the tensiometer, rather than a small square sample attached to an anvil. The change in fabric form and the accompanying loss of uniformity in pressure at the interface were considered potential causes for any differences observed in experimental data. For this brief investigation, only nonwovens from the subset (SF3, SF14, SF17, SF18 and DC6) were of interest.

3.3.1 Materials and methods

A solid cylindrical model of the forearm was created by filling a 160mm (long) section of plastic piping ($\varnothing 70$ mm, typically used for plumbing) with Plaster of Paris. An 80 mm \times 215 mm piece of LS was then wrapped around the central portion of the cylinder and attached using a spray-on adhesive [Display Mount Permanent Adhesive, 3M United Kingdom PLC, 3M Centre, Berks RG12 8HT]. The glue was left to set for at least 24 hours before friction measurements began. Initially, 25 friction cycles were run with a strip of SF3 under 50g to wear-in the new piece of LS. Then measurements were made between all five nonwovens in the subset and LS on the cylinder, using the same settings applied during measurements against volar forearm skin in chapter 4 (10g, 20g, 30g, 50g and 70g dead weights; 50mm displacement at $2.5 \text{ mm} \cdot \text{s}^{-1}$ for 2 cycles per load) – see figure 3.13. The decision to use these particular settings followed the development of the methodology for the “dry friction” part of the study, as described in chapter 4. It enabled direct comparison of these data with skin friction data. Measurements were also performed in an environmentally controlled room and one camera was set up to record the angle of arc of contact.

⁹although it is accepted that the distribution of load across this contact is non-uniform

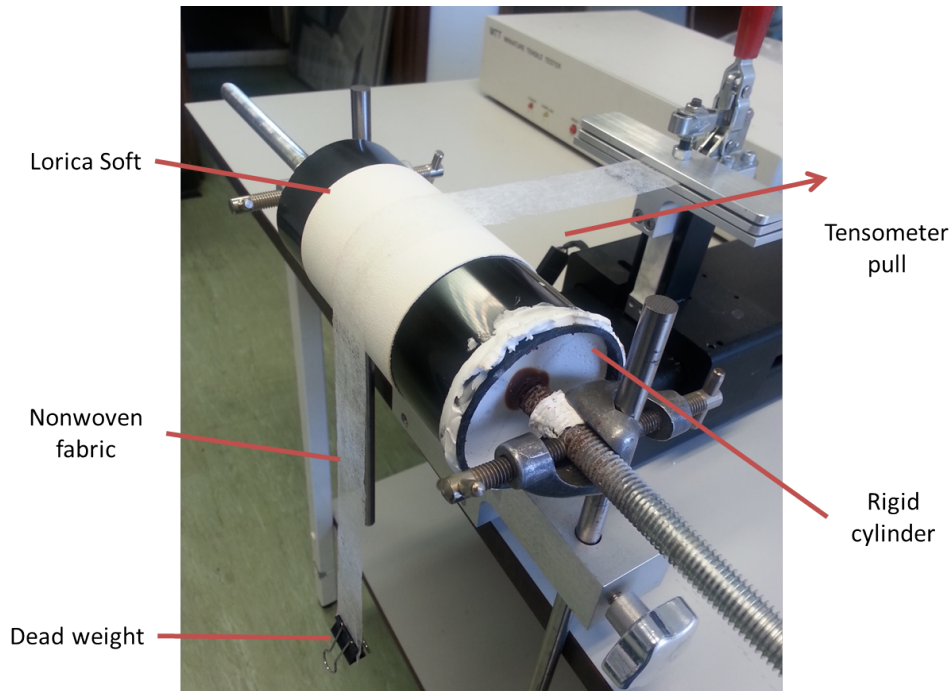


Figure 3.13: Experimental setup for friction measurements between the cylinder covered in Lorica Soft and a strip of nonwoven fabric

3.3.2 Results and conclusions

The force-displacement curves from these measurements had similar shapes to those from measurements made in the flat configuration. The only notable difference in curve shape was that these curves (for LS in a curved configuration) were all relatively flat compared with the common shallow S-shape observed with flat LS – see figure 3.14. For measurements against the curved surface, the tensometer forces were lower than those under 8.1N, but usually similar to those for flat LS under 2.6N despite the fact that the actual applied normal loads (dead weights) were lower and the pressure distribution was not uniform across the curved surface. The coefficients of static friction were also higher for all nonwovens tested in the curved configuration (see figures 3.15 and 3.16), which is further demonstrated by the fact that all data points were above the line of equality in figure 3.16. This may have been caused by an additional force (possibly about 5-20%) required to bend the strip of nonwoven around the cylinder, allowing full nominal contact between the fabric and skin surrogate, or perhaps the fact that the interface was a larger area. However, the high coefficients of correlation and the fact that the extrapolated linear regression lines passed almost exactly through the origin of the graph in figure 3.15, suggested that Amontons' law held for this frictional interaction.

Alternatively, the differences in coefficient of friction may have been a result of a change in topography of the Lorica Soft, with more micro-projections exposed on the convex surface. Another possibility is that Amontons' Law only held for the lower range of applied loads used and that the linearly proportional relationship was lost beyond a certain load. Unfortunately, these theories were mostly speculative due to a lack of supporting evidence at this stage. Time was a limiting factor that prevented further investigation of some of these potential explanations, but it was anticipated that measurements on human skin *in vivo* would help to clarify which were more likely correct. Regardless, the fact that there

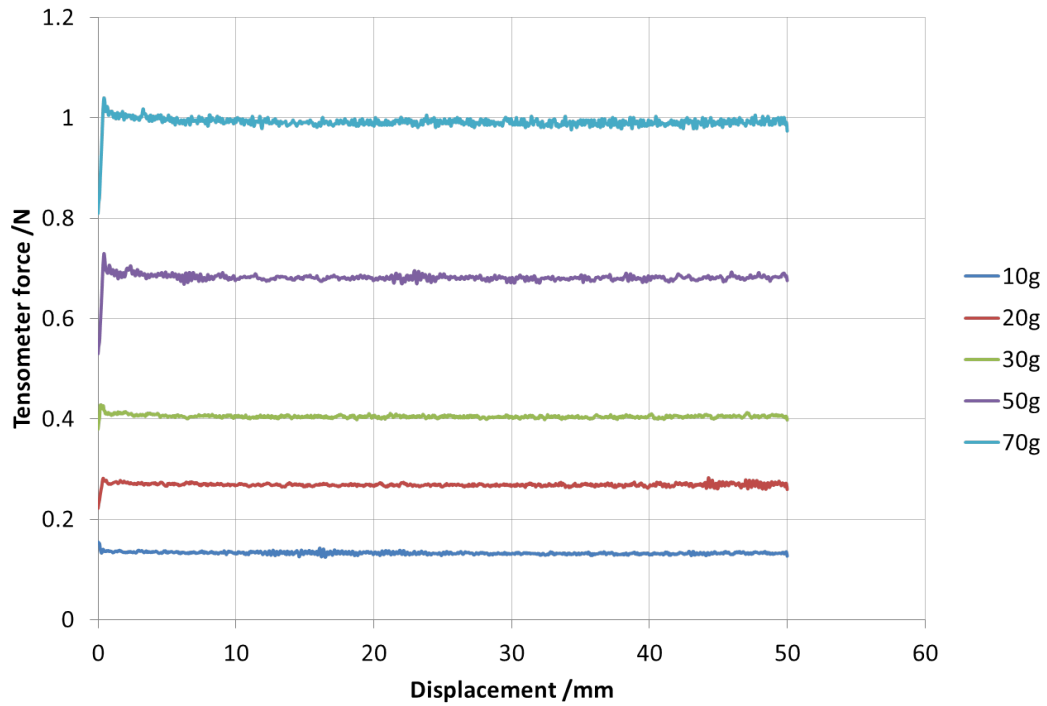


Figure 3.14: Force-displacement curves for SF14 against Lorica Soft wrapped around a cylinder

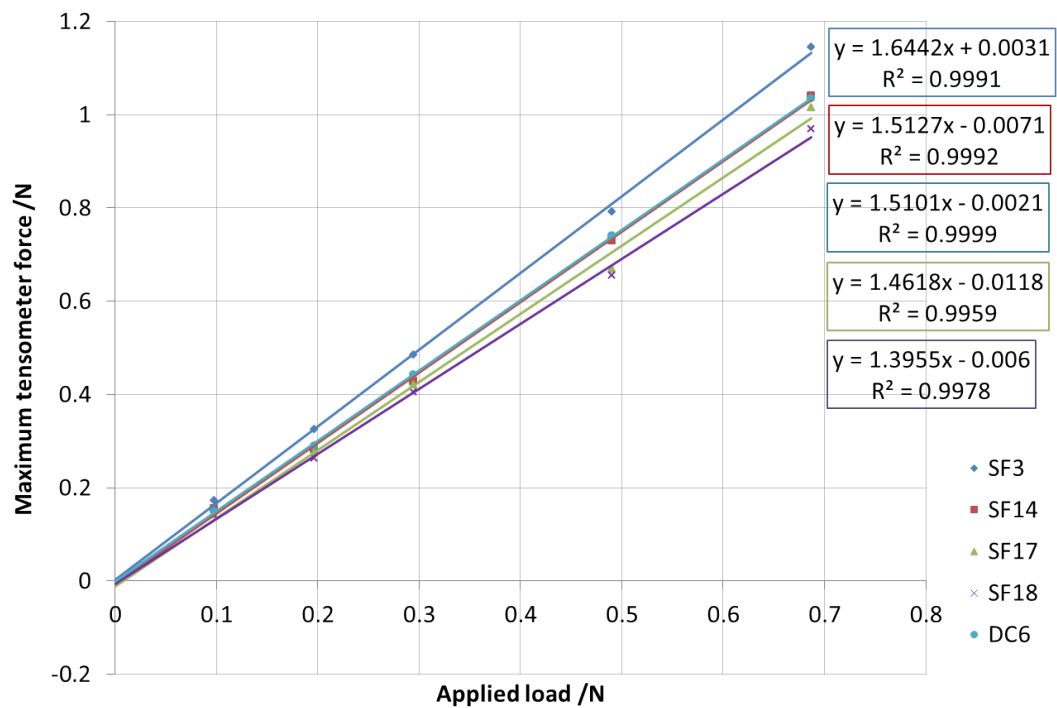


Figure 3.15: Relationship between maximum tensometer force and applied load for all nonwovens against Lorica Soft wrapped around a cylinder

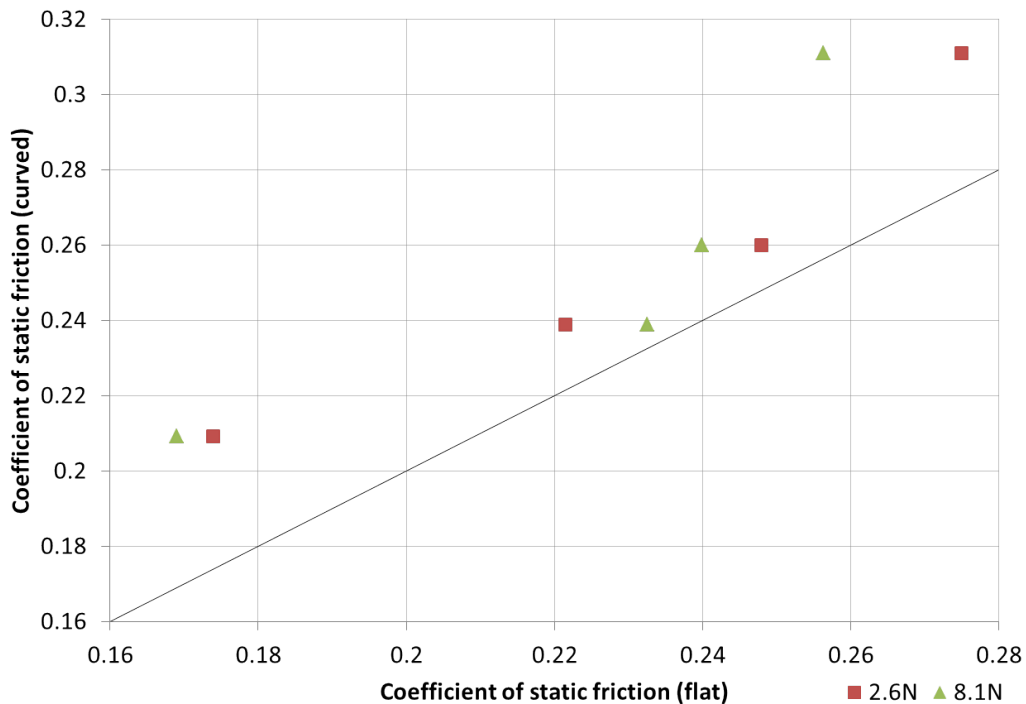


Figure 3.16: Relationship between coefficient of static friction for LS wrapped around a cylinder and flat LS; each pair of red and green points is for a different nonwoven (SF3, SF14, SF17, SF18); black line is line of equality

was good agreement between coefficient of static friction in the flat and curved configurations of LS meant that the data collected in this chapter appropriately represented friction between nonwoven fabrics and the skin surrogate. Therefore, the *relative* observed differences between nonwovens in friction were true for LS and most likely real human skin.

As the bulk of the methodology described in §3.3.1 was the same as that used on participants in the “dry friction” part of the volar forearm skin friction study, it will be possible to eventually make direct comparisons between data collected from Lorica Soft and human skin. In addition to the previously mentioned advantages of making friction measurements on human skin, the impact of underlying tissue can also be analysed, as the Lorica Soft in *this* experiment was wrapped around a *rigid* cylinder. The experiments described in this section only enabled negligible deformation of the skin surrogate (in terms of compression/indentation and shear), whereas measurements on skin will likely divulge an entire range of skin behaviours due to the variable composition of underlying tissue, as much as the bulk viscoelastic properties of the skin itself. All of these factors and more are discussed in chapter 4.

CHAPTER 4

FRICITION MEASUREMENTS ON DRY VOLAR FOREARM

“Confía en el tiempo, que suele dar dulces salidas a muchas amargas dificultades. (Trust in time, as it usually gives sweet solutions to many bitter problems.)”

— Miguel de Cervantes Saavedra, 1547–1616

VERY LITTLE FOCUS has been placed on friction between human skin *in vivo* and fabrics compared with that between skin and other surfaces. Even less work has been carried out on the interaction between *nonwoven* fabrics and skin [136]. The primary aim of the work described in this chapter was to validate the findings of the friction work done so far on the skin surrogate (Lorica Soft) with *in vivo* measurements on volar forearm skin. The particular findings of interest were that: Amontons’ Law held (perhaps within a given force range) – friction force was proportional to applied normal load and did not vary with contact area; tensometer crosshead speed had an insignificant effect on coefficient of friction; and adhesion *may* have been the principal mechanism operating. The effects of participant age and other factors were also investigated.

Measurements of friction force between nonwoven fabrics and volar forearm skin (in wet and dry conditions) on people of different ages and ethnicities were carried out, using the experimental setup displayed in figure 4.1, to compare a range of nonwoven fabrics and applied loads. It was anticipated that the data would indicate whether or not subject age has a significant effect on friction forces. The study followed work done previously by Wong [3] in a study on volar forearm - nonwoven fabric friction, in which she made measurements on young women only. She compared dry and fully overhydrated skin, without considering the effects of excess saline on the surface of the skin or different levels of skin hydration, nor the impact of wetting the fabric. The methods for obtaining the data in *this* study (in dry conditions only) are described in §4.3.2. Experiments relating to these objectives must give an indication of the extent to which the mechanisms and rules identified are common to all people. Consequently, the individuals who participated varied in age and ethnicity – though not in gender, as the requirement for relatively glabrous (hairless) skin typically attracted female volunteers – so that any important features that were identified could be established as likely universal, or not.

This chapter describes all procedures and methods that were employed in the execution of this work, including the identification of subjects, obtaining consent, the recruitment of participants (§4.3.1), and the experimental methodologies for making measurements on volar forearm skin (§4.3.2). Before going on to describe these experiments in any detail, it is important to mention that the volar forearm study (as described in all of the following sections except §4.1.1.1) was carried out with another PhD student/investigator, Vasileios Asimakopoulos. The development and execution of the methodology for friction measurements in dry conditions were achieved with a joint effort, while data processed thereafter was carried out individually according to different research interests.

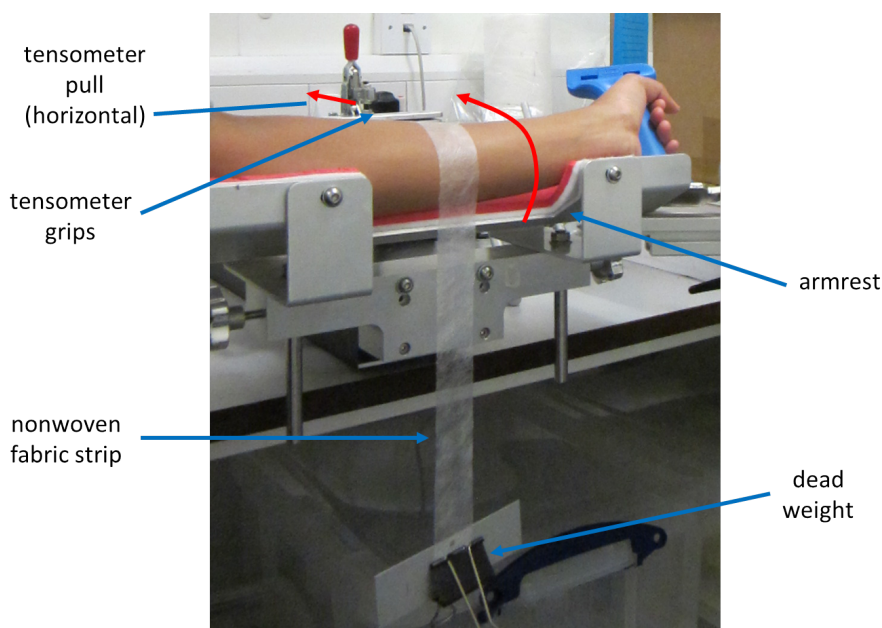


Figure 4.1: The experimental setup for friction measurements between volar forearm skin and a nonwoven fabric

4.1 Materials and method development

The tensometer and nonwoven fabrics SF3, SF14, SF17, SF18 and DC6, as described in §3.2.1, were implemented in the friction experiments on volar forearm skin using the configuration depicted in figure 4.1. These five nonwovens were selected, from a larger set, based on preliminary work described in §3.2 and §4.1.1.1. The experimental methodology presented in this chapter was initially based on work by Wong [3] on volar forearm skin and was adapted to address the aims set out in §2.7.3.

4.1.1 Selection of nonwoven fabrics and other variables

Before any measurements could be made on study participants, a methodology was developed and ethics approval was obtained. The aim of the method development was to determine a suitable set of variables to fairly compare a group of nonwoven fabrics based on friction data and observations of their interaction with human skin. All preliminary experiments were carried out with volunteer SF00 – see table 4.2 for more information.

4.1.1.1 Methodology

Friction was measured between strips of nonwovens SF1–SF18 (13 in total – see summary table 3.1) and volar forearm skin at a single crosshead speed ($2.5 \text{ mm} \cdot \text{s}^{-1}$) and under three loads – 0.30N (30g), 0.48N (50g) and 0.99N (101g) – for three cycles per load. Loads were applied in a random order – not the same for each nonwoven – and a table to show order of load application can be found in table C.1 of appendix C. Prior to this, some preliminary testing was carried out on SF1 in order to select an appropriate crosshead speed, applied loads and number of repeats necessary to ensure that friction data obtained – within the available measurement session time – was accurate; hence the use of the

aforementioned variables. The nonwoven fabric strip¹ dimensions were originally 580 mm × 30 mm in order to ensure good clearance between the forearm and the weight attached to the vertical end of the coverstock. This was later changed to a length of 450mm, in line with that used by Wong [3].

The selection of experimental variables was based on results from the preliminary testing, and is therefore explained in the corresponding results section (§4.1.1.2). Nonwovens were tested in the same order as they are listed in table 3.1, followed by repeats again on SF2 then SF1 at the end. The repeats served to reveal any changes that may have taken place in the skin over the duration of the measurements: if the second set of data on SF1 and SF2 were significantly different to the first set, this would suggest that changes had occurred within the skin; if not, variation in data between nonwovens could be attributed to actual differences in the individual coverstock test pieces. The loads applied during the measurements between Lorica Soft and SF1–SF18 (see §3.2.1) were not used here because they were too high (2.6N and 8.1N) for measurements between the volar forearm – without causing discomfort to the participant – and the nonwoven fabric – without rupturing or permanently deforming the nonwoven before the experiment was complete.

4.1.1.2 Results and conclusions

Below are the results of the preliminary tests during which the experimental variables were chosen (figures 4.2 & 4.4-4.6). The reason for comparing the three crosshead speeds relates to earlier work. Speeds of $0.5 \text{ mm} \cdot \text{s}^{-1}$ and $1.5 \text{ mm} \cdot \text{s}^{-1}$ had previously been used in experiments with Lorica Soft, including that described in §3.2.1, and $2.5 \text{ mm} \cdot \text{s}^{-1}$ was the speed used by Wong in a similar study to this one. It was important to test the effect of crosshead speed on friction because measurements may change due to the viscoelastic properties of skin, which would mean that the speed used would have to be the same as that for Lorica Soft. However, using the highest speed would enable more measurements to be made within a given time period, and data would be more comparable to that collected by Wong.

As can be seen in figure 4.2, there was little change in friction force between the volar forearm and SF1 with crosshead speed, other than the slight decrease (<10% for both static friction and dynamic friction) with increasing speed from $0.5 \text{ mm} \cdot \text{s}^{-1}$ to $2.5 \text{ mm} \cdot \text{s}^{-1}$. Overall, the crosshead speed had very little effect on coefficient of friction, so the highest speed was chosen for future use, for the reasons previously explained. Increasing applied load led to an increase in measured friction force, as expected, and had an insignificant effect on coefficient of friction. The highest load used (0.99N or 101.0g) substantially deformed the arm and several of the fabrics, as demonstrated in figures 4.3a, 4.3b and 4.3e. Deformation to the fabric was often extreme and usually took some time to reverse when the load was removed. Furthermore, some discomfort was experienced with some nonwovens, particularly SF17. For these reasons, the maximum load was reduced and the 0.99N load was excluded after further testing confirmed that this was an inappropriate upper limit.

The change in tensometer force over three cycles was very small for all nonwovens – typically <5% – so it was clearly unnecessary to have this many repeats for each applied load and nonwoven. The biggest difference in force was observed between the first two cycles at $0.5 \text{ mm} \cdot \text{s}^{-1}$. Nothing was different experimentally during the first cycle, but it may be that the fabric adjusted to the setup – a sort of brief wearing-in. For the most part, one cycle per load would suffice, provided no errors were made during an experiment, however, it would not be sensible to rely on only one reading. As a result, it was decided that two cycles should be run per applied load-nonwoven combination and the second cycle used for calculations of coefficient of friction. Between this conclusion and the reduction of the

¹Each strip was cut so that its length was parallel to its machine direction – the direction in which it was manufactured.

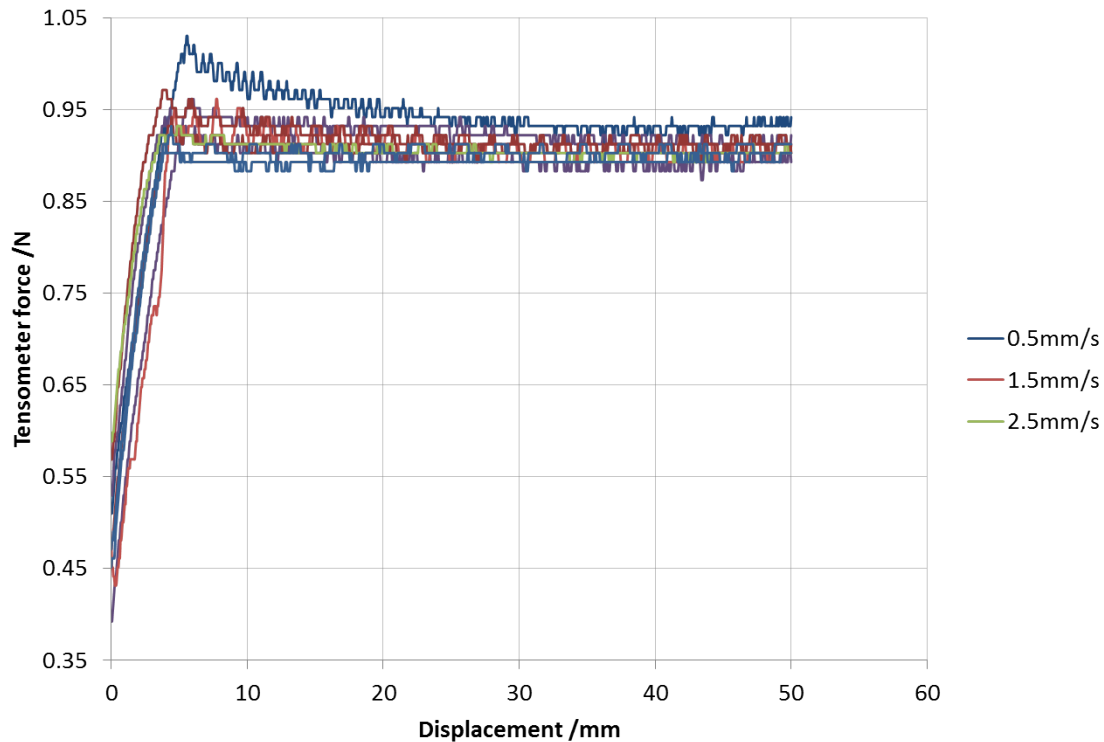


Figure 4.2: Comparison of friction between nonwoven SF1 and volar forearm skin under 0.48N at three crosshead speeds, for three cycles each

nonwovens to be tested, it was decided that the number of applied loads (or dead weights) could be increased to five: 0.10N (10g), 0.20N (20g), 0.30N (30g), 0.48N (50g) and 0.69N (70g).

The following set of graphs (figures 4.4-4.6) serve to compare the behaviour of nonwovens SF1-SF18 against volar forearm skin under different loads. Where the first “linear” phase is displayed on the force-displacement graphs, there was no slippage between the skin and nonwoven fabric. The peak in force, eventually reached after approximately 5mm displacement (as measured by the tensometer), represents the static friction force. The small peaks and troughs that follow in the plateau were present in all nonwoven curves, but varied in amplitude. Due to the variation in size, it was assumed that they could be attributed mostly to skin-nonwoven interaction rather than noise from the tensometer because quantisation of the force measurement by the equipment was proportional to the force limit set. It also suggests that they did not relate to the surface profile of the volar forearm. In that situation, one would anticipate some consistency in the dimensions.

Figure 4.4 compares the friction-displacement curves of all nonwovens tested under a load of 0.30N. SF17 had the highest friction force, while SF18 had the lowest. This was the case for all loads (see figures 4.5 and 4.6), with some variation in ranking of other nonwovens in the middle force range. In all three force-displacement graphs, SF2 had the longest initial “linear” phase before reaching static/maximum tensometer force, closely followed by SF17, which also had the highest maximum force. Nonwoven SF2 was the first fabric in a set of 12 to be tested in one day; it may be that the changes in the skin were responsible for the differences observed between SF2 and other nonwovens, which was emphasised at the highest load (see figure 4.6). During each measurement, rucking of the skin was observed to the sides and ahead of the nonwoven fabric contact with the volar forearm, and was felt underneath the nonwoven (see figure 4.3d). However, the degree of rucking between or adjacent to the nonwoven-skin interface appeared not to have a significant effect on coefficient of friction, suggest-

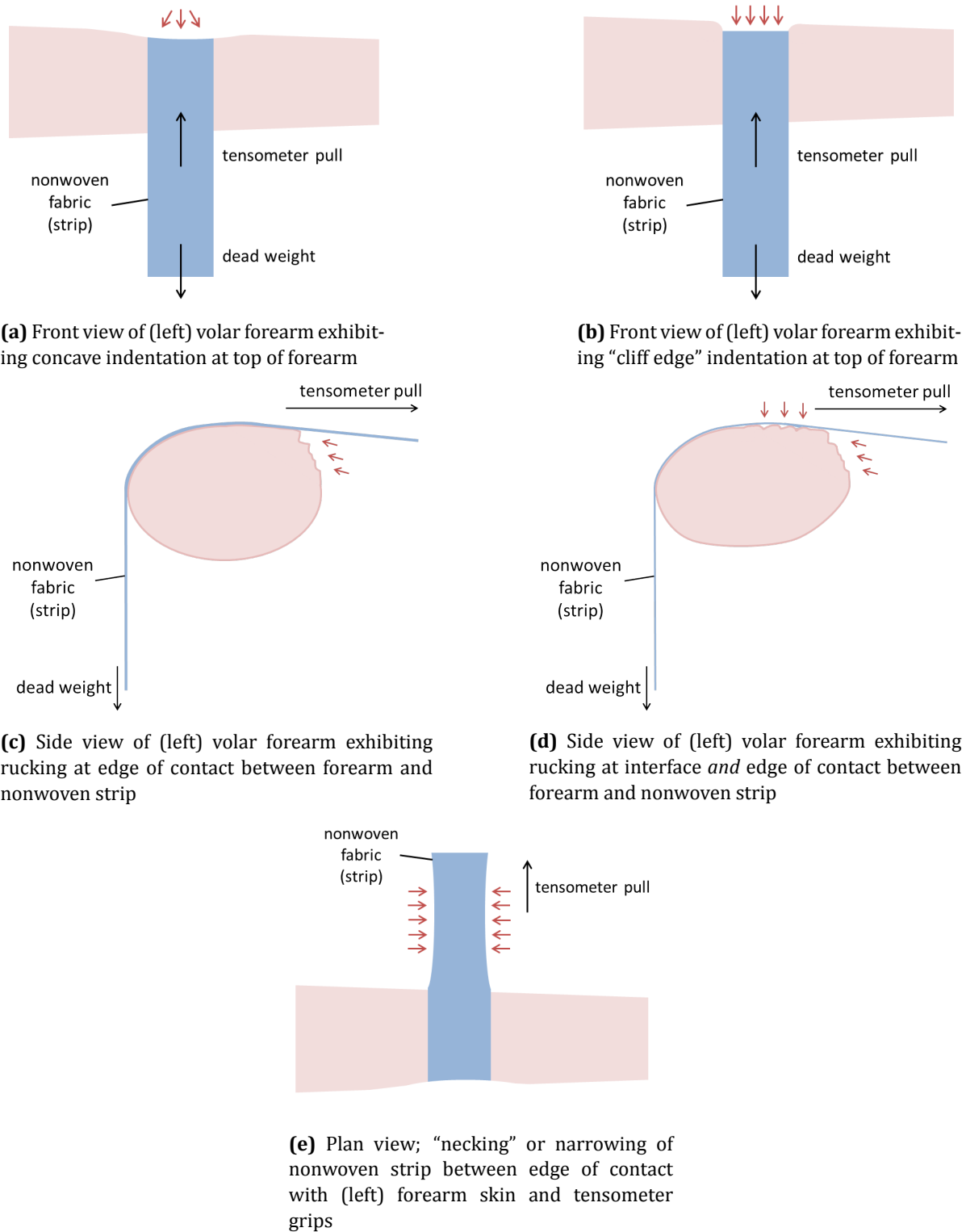


Figure 4.3: Various examples of deformation observed in volar forearm and nonwoven fabric during friction measurements

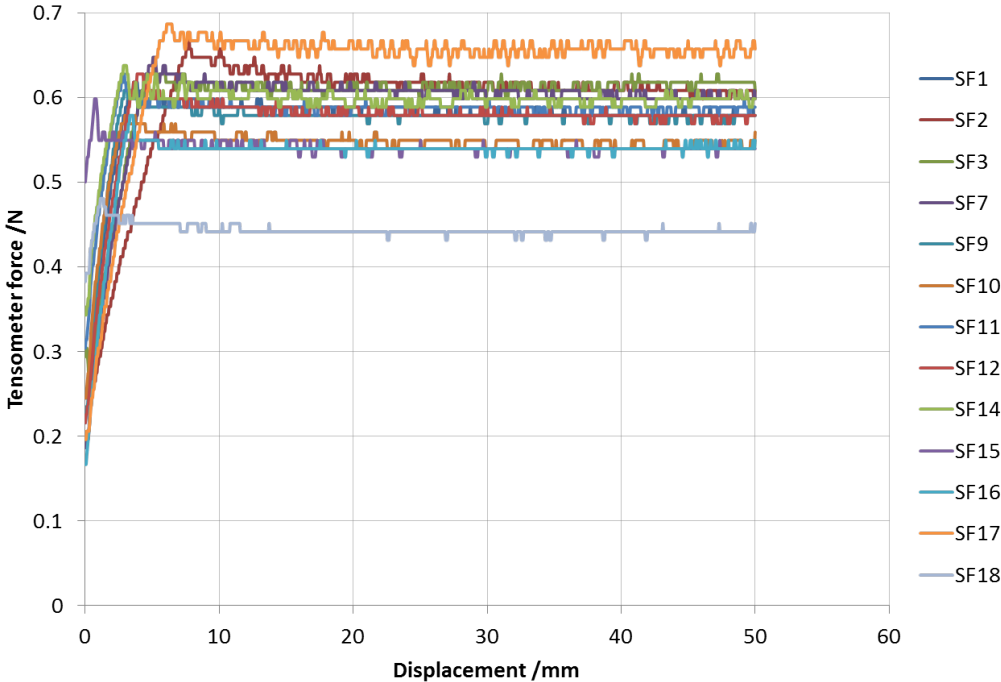


Figure 4.4: Friction force vs displacement for all nonwovens under an applied load of 0.30N (cycle 2 only) with a chosen crosshead speed of $2.5 \text{ mm} \cdot \text{s}^{-1}$

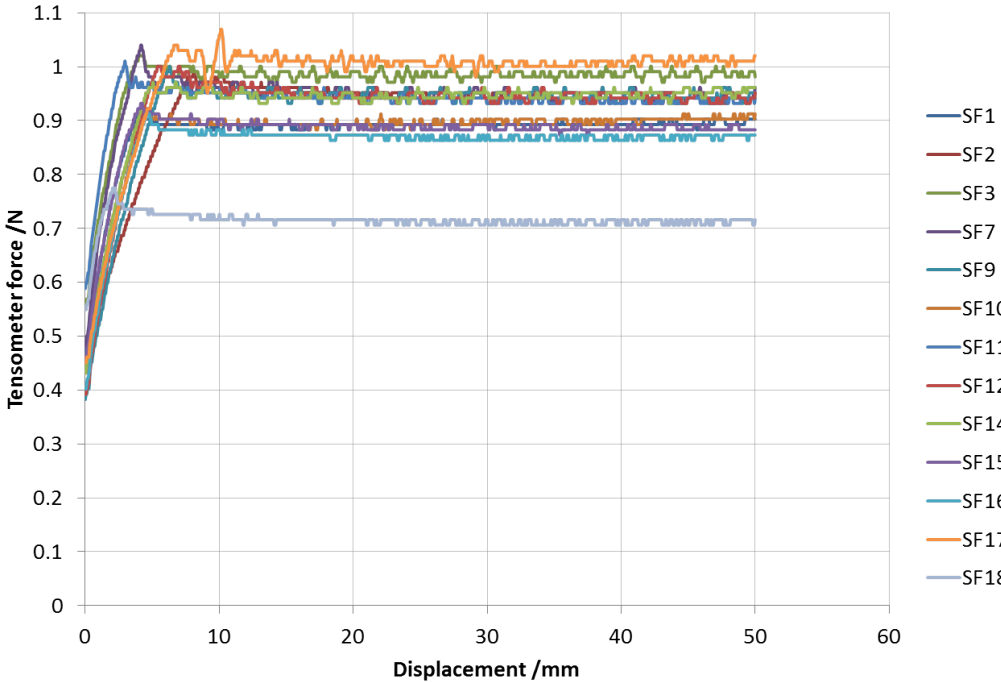


Figure 4.5: Friction force vs displacement for all nonwovens under an applied load of 0.48N (cycle 2 only) with a chosen crosshead speed of $2.5 \text{ mm} \cdot \text{s}^{-1}$

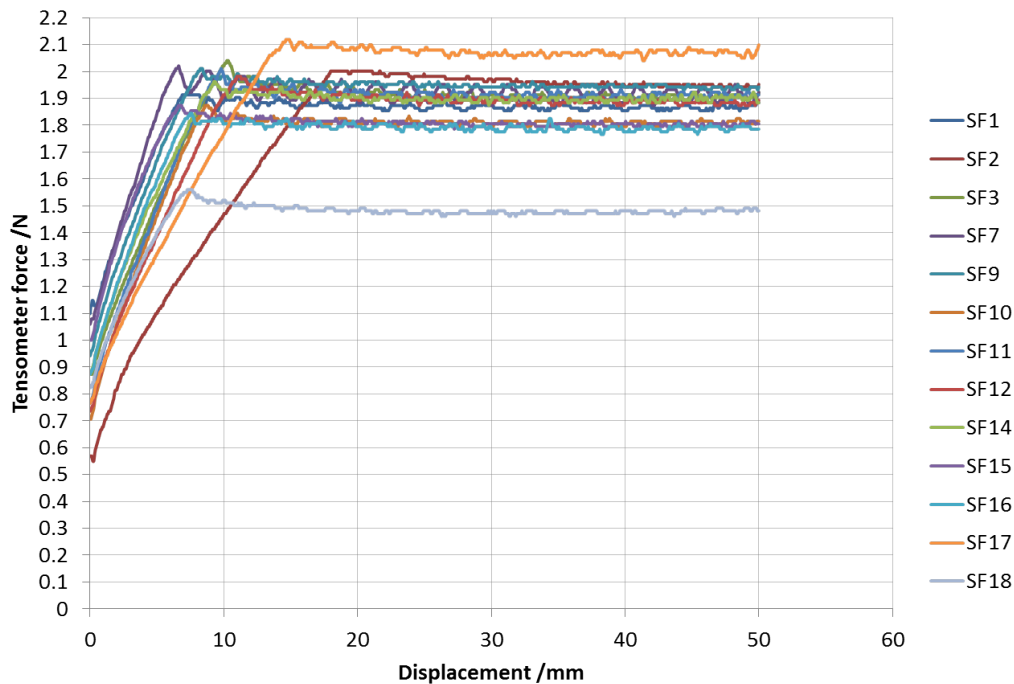


Figure 4.6: Friction force vs displacement for all nonwovens under an applied load of 0.99N (cycle 2 only) with a chosen crosshead speed of $2.5 \text{ mm} \cdot \text{s}^{-1}$

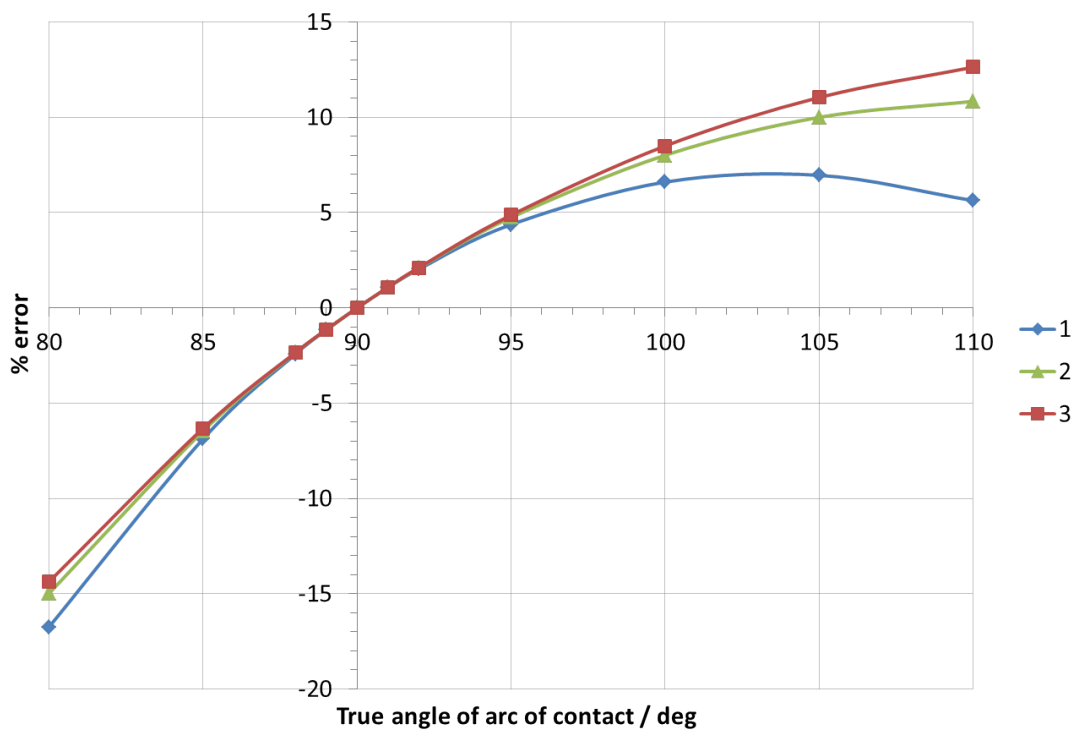
ing that – conveniently – corrections did not need to be made for older (or more flaccid) skin friction calculations.

The lack of a significant difference in the overall graph shape emphasised the consistency of measurements made on the volar forearm and supported the use of one representative coefficient of friction per nonwoven for comparison. For that reason, the coefficients of static friction have been calculated – using the mathematical model developed by Cottenden [152] (see equation 2.7 on page 46) – and are displayed in table 4.1². In the case of these coefficients, the angle of arc of contact was taken as 90° ($\frac{\pi}{2}$ radians) for convenience, and the section of nonwoven connected to the weight was considered to be perpendicular to the direction of travel. However, it was also considered that the angle of arc of contact may change by a few degrees toward the end of the experiment – particularly at the highest applied load – or due to varying participant arm size. In order to assess the potential error that may arise from the assumption that the angle was 90° throughout, some calculations were carried out for an angle difference of $\pm 10^\circ$. Figure 4.7 displays the result of angle change on percentage error for one applied load; the graphs for the other (higher) normal forces were almost identical, both in shape and magnitude. Depending on the difference between the true angle of arc of contact and 90° , and whether this difference was caused by an arm that reduced or increased the angle, the error could reach 10-15%. It was therefore decided that a correction to the tensometer force should be applied when the angle of arc of contact was more than 5° different from 90° .

²Coefficient of static friction was calculated from the gradients of graphs of maximum tensometer force against applied load, rather than individual (F_{max}/mg) values. Therefore, the ‘gradient error’ has also been included: these are standard deviation values calculated for the corresponding aforementioned gradients. There were three data points (from repeat friction measurements), for each applied load for all nonwovens, and one linear regression line for each nonwoven fabric. R^2 values were never lower than 0.99 for all data presented in the table.

Table 4.1: Coefficients of static friction for 13 nonwoven fabrics; highest value in red and lowest value in blue

Nonwoven	Coefficient of static friction (& gradient error)
SF1	0.40 (0.04)
SF2	0.42 (0.03)
SF3	0.44 (0.04)
SF7	0.42 (0.03)
SF9	0.44 (0.01)
SF10	0.39 (0.04)
SF11	0.45 (0.02)
SF12	0.43 (0.02)
SF14	0.42 (0.02)
SF15	0.41 (0.06)
SF16	0.40 (0.06)
SF17	0.46 (0.02)
SF18	0.29 (0.03)

**Figure 4.7:** Effect of angle of arc of contact (see figure 2.20b) on percentage error in coefficient of static friction when the angle is assumed to be 90°; each curve is for a hypothetical gradient from a 'maximum tensometer force vs applied load' graph, representing effect on error in addition to angle; 1 = gradient of 1.5, 2 = gradient of 2, 3 = gradient of 2.5

At this point, any association of coefficient of friction with manufacturing processes or material properties would have been purely speculative; it is for that reason that no such correlation between the two has been made. In conclusion, nonwovens SF17 and SF18 were selected for more extensive testing, on a larger set of participants, due to their consistently high and low friction forces respectively. Fabrics SF3 and SF14 were also chosen to ensure a wide range of structural properties were covered. Cottenden's NW6 was also added to the subset of fabrics as a reference for comparison (as mentioned in §3.2.3), but is referred to, in this thesis, as DC6 for clarity.

4.2 *The effect of inter-strip area density variation on friction*

Due to the natural lack of uniformity of nonwoven fabrics, in terms of area density or distribution of fibres, it was considered appropriate to investigate the potential impact of this variation on measured friction. It was important to determine the implication of assuming that varying area density had little or no effect on friction force *before* commencing measurements on participants. Investigating the effect of inter-strip variation also helped to determine whether there was need to use more than one strip of the same fabric to get a reliable set of data. It was anticipated that the results would highlight any dependency of friction force on area density, thus suggesting reason for variation between nonwovens or sample of the same material, or indicating that there is no relationship between the two.

4.2.1 *Methodology*

For most of the nonwovens of interest, it was difficult to identify a length that would be in contact with the skin for the duration of the cycle. Nonwoven SF17, however, was the most variable, so sections of strips were selected for comparison, as shown in figures 4.8 and 4.9. They were chosen according to visible differences in area density – a “middle section”, 140mm in length, was marked out first (see figure 4.8). SF17(3) had the highest density ($21.4 \text{ g} \cdot \text{m}^{-2}$), followed by SF17(2) ($18.1 \text{ g} \cdot \text{m}^{-2}$), and SF17(1) had the lowest ($12.6 \text{ g} \cdot \text{m}^{-2}$). Friction measurements were made between each of these strips of SF17 and the volar forearm skin of SF00, under dead weights of 30g, 10g and 50g – in that order – at $2.5 \text{ mm} \cdot \text{s}^{-1}$ for five cycles per load. The first set of measurements (SF17(2), 30g) were repeated at the end to check for changes in the skin over the experimental period and TEWL was measured at the start and end of the experiment.

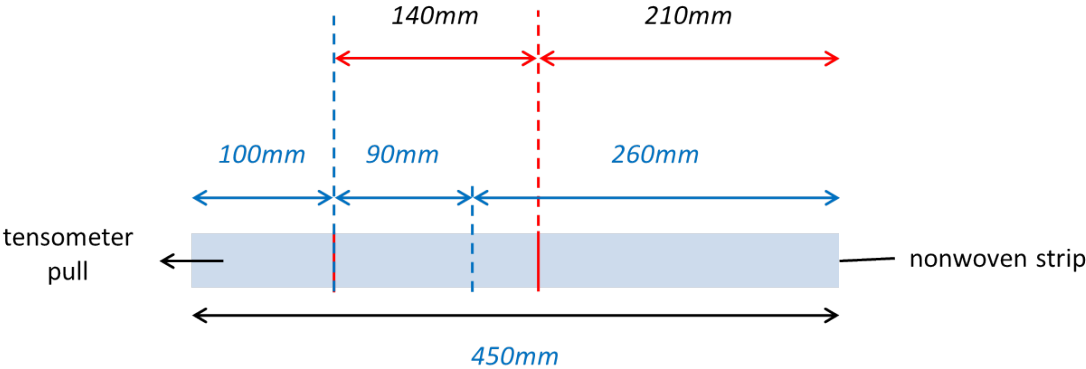


Figure 4.8: Diagram to show how strips were marked – middle 90mm initially in contact with skin, and after 50mm displacement, total length of contacting nonwoven is 140mm; black dimensions show actual marked lengths

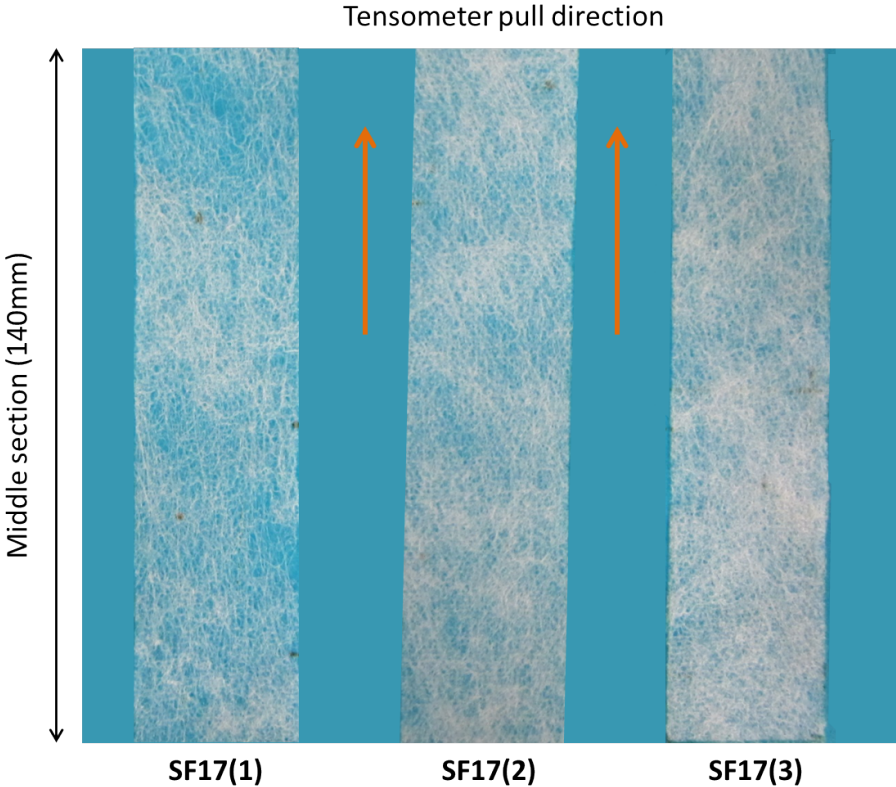


Figure 4.9: Middle (140mm) section of strips of SF17 used for friction measurements; (1) “low” density ($12.6 \text{ g} \cdot \text{m}^{-2}$), (2) “medium” density ($18.1 \text{ g} \cdot \text{m}^{-2}$), (3) “high” density ($21.4 \text{ g} \cdot \text{m}^{-2}$)

4.2.2 Results and conclusions

Below is a force-displacement graph (figure 4.10) for all three strips of nonwoven. It is clear that variation in area density – on this scale – had no significant effect on tensometer force. It may be that the fibres rearranged themselves in order to distribute the load and maintain the same pressure, i.e. a greater proportion of fibres were in contact at a lower density. In addition to the variation in area density of the middle sections of these three strips of nonwoven, there was local variation within the middle sections. If such non-uniformity could be detected during friction measurements, not only would this have shown in the coefficient of friction values for each strip, but measured tensometer force would have varied with displacement; this was not the case.

Figure 4.11 shows the effect of applied load on tensometer force for each nonwoven. The slight decrease in gradient (and therefore coefficient of friction – 0.49, 0.48, 0.47) could be attributed to “polishing” of the skin, rather than sample area density. This assumption is supported by the very slight decrease in “friction” force observed when the same measurements were repeated on SF17(2) at the end of the experiment. It implies that coefficient of friction does not depend on the nominal contact area (Amontons’ law holds for skin-nonwoven friction in these circumstances), and is partially supported by a study by Comaish and Bottoms [105], which showed that coefficient of friction did not change with contact area for wool, although it did for polyethylene. While the data from this short experiment showed that area density of nonwoven strips is not a factor for concern in the friction study, further investigation by microscopy was required. The method and its outcome are described in chapter 6.

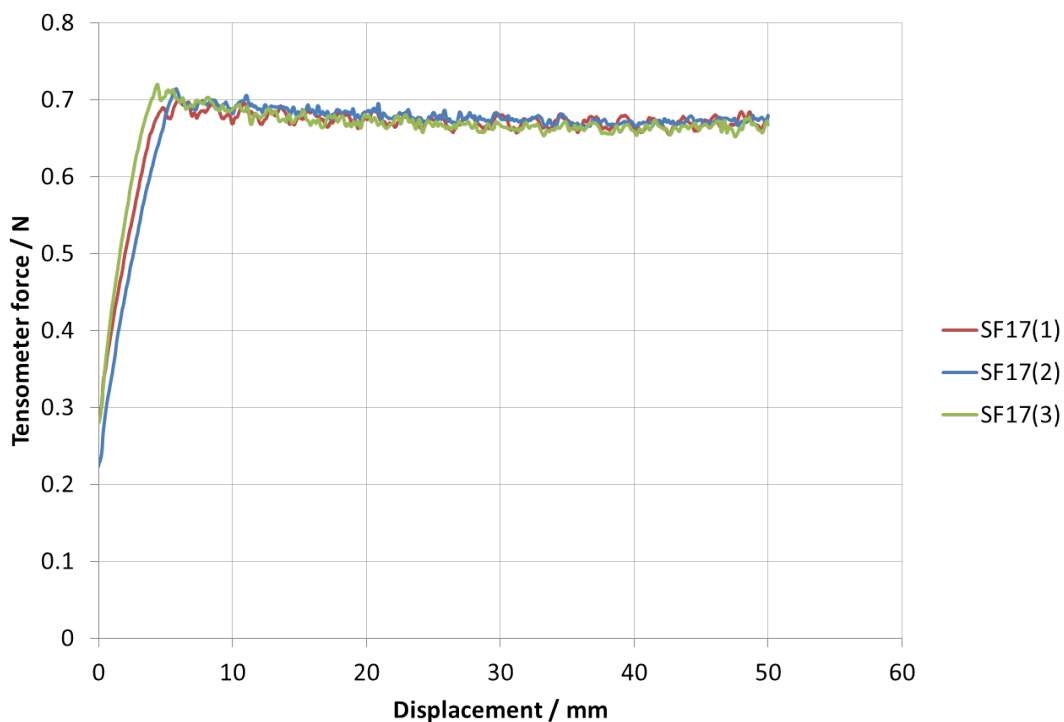


Figure 4.10: Cycle 5 of all three nonwovens under 30g

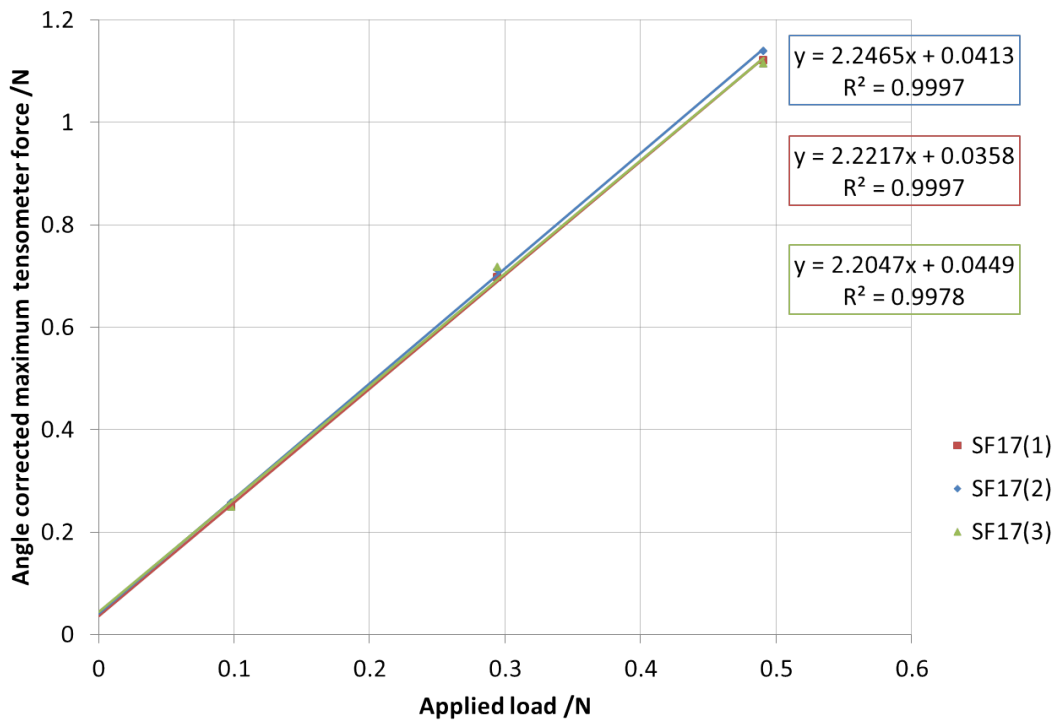


Figure 4.11: Tensometer (“friction”) force against applied load for all three strips of SF17

4.3 Volar forearm study

Having determined the appropriate variables for further experiments with the subset of nonwoven fabrics, the research study on friction with volar forearm skin *in vivo* began. The volar forearm is a good proxy for skin of the diaper region and is a fairly flat and hairless part of the body and is easily accessed for taking measurements. This made it well suited to these experiments: in this exploratory work it was more important that the skin was uniform and simple than that it was from the diaper area. The overall aims of the study were to compare friction forces for all five nonwovens against a range of skin types and to observe the effects of age, skin compliance and hydration on friction force and skin behaviour. As this chapter focuses on friction on normal (“dry”) volar forearm skin, only the experimental procedures for *these* measurements are described here. Subsequent work on skin-nonwoven friction in wet conditions will be reported in chapter 5. Before any work on volunteers could begin, approval from a Research Ethics Committee (London Stanmore REC) was obtained.

4.3.1 Ethical considerations, identification of subjects and consent

It was required that all participants were at least 18 years of age, self-consenting and had relatively little hair on their volar forearms. The participants must not have had an active skin condition that made the surface of their skin rougher than it would normally be (e.g. eczema, psoriasis), or have a known allergy to nonwoven fabrics. Volunteers were sought from outpatients of the Incontinence Clinic of Whittington Health NHS, residents of Cheverton Lodge Care Home, and UCL students and staff. Full versions of the protocol, information sheets, consent forms, GP letter and advertisement material can be found in appendix B.

The video cameras used to record the strip of nonwoven fabric being pulled across the participant's forearm only recorded the forearm and so the participant was not identifiable from images. Experimental data taken from each participant was stored on university computers and a laptop, but were labelled with alphanumeric codes in order to anonymise the sources. Personal details (such as name, address and phone number) were stored on a password-secure university computer, accessible only to the investigators and chief investigator.

Identification and initial contact with prospective incontinence clinic participants was made by the clinic staff, who distributed copies of the participant information sheet (PIS; see appendix B). Those interested then spoke to an investigator who explained the study further and answered any questions they had. Patients who still wished to participate, after at least 24 hours' consideration, contacted the investigators to arrange a session. The consent form was signed on the (first) day of participation, before beginning the experiment. This same process applied to residents of the nursing home, except that the general manager identified and made the initial contact with potential participants. All students and staff were invited to participate by poster adverts and received PIS on request (see appendix B). Those interested in participating contacted the investigators for more information and/or to arrange a measurement session. They were also required to sign consent forms in the same way as other participants. Recruitment continued until sufficient data were gathered; the expected number of participants needed was about 20, not to exceed 30. The participants were split equally into two groups (18-64 yrs and 65+ yrs) to compare "young" and "old" skin.

4.3.2 Methodology

Nineteen volunteers were recruited to take part in this study (all but SF00); details of potential scientific importance can be found in the summary table (4.2).

For most participants, measurements took place in an environmentally (temperature and humidity) controlled room (ECR) in the Department of Medical Physics and Bioengineering, UCL Archway Campus. Friction measurements on the skin of nursing home residents took place in the home itself: it was not *essential* for the dry skin friction measurements to be taken in the ECR, so measurements made at the nursing homes were not expected to be affected significantly by the lack of environment control. However, in order to have better control of the temperature and humidity, to reduce the chance of variation in skin hydration (i.e. for convenience of data analysis), and to more easily monitor environmental change, measurements were made in the department for all other participants.

A hygrometer and a thermometer were set up in the testing room in the nursing home to record changes in temperature and humidity, from approximately 20 hours before measurements began, to the end of the last day of measurements made there. Fortunately, the conditions in the testing room ($23.3^{\circ}\text{C} - 25.5^{\circ}\text{C}$ 44-50% relative humidity) were very similar to those in the ECR ($23.0 \pm 2^{\circ}\text{C}$, $50.0 \pm 4\%$ RH). For all participants, photographs of their volar forearm skin were taken at the beginning and end of the measurement session, both to keep a record of the appearance of the testing site, and to ensure that there was no visible change/damage to their skin. All measurements were made on the left forearm, with the exception of six participants, identified in table 4.2, for whom it was not practical to use that arm (e.g. those who had suffered a stroke).

Table 4.2: Participant details

Subject code	Gender	Age in years ³	Ethnicity	Arm used	Physical description of skin
SF00	Female	24	Mixed other	Left	Smooth skin; slim arm but not bony; very low compliance of skin.
AD02	Female	56	White European	Left	Smooth skin; low compliance.
MM03	Female	50	White European	Left	Smooth, relatively large volar forearm; very low compliance of skin.
MS04	Female	27	White European	Left	Smooth skin; slim arm; very low compliance.
RJ05	Female	60	White European	Left	Slim arm; slightly wrinkled skin with low compliance.
SF06	Female	80	White European	Left	Smooth skin with few wrinkles and relatively compliant; slim arm but not bony.
HJ07	Female	71	White European	Right	Very wrinkly, very slim, bony arm (virtually no underlying tissue); very compliant skin.
MD08	Female	93	White European	Right	Slightly wrinkly, large arm (lots of underlying tissue); very compliant (indentation, not rucking).
JJ09	Female	79	White European	Right	Very wrinkly, slim arm with lots of veiny prominences; very hairy back of forearm; very compliant.
DJ10	Female	90	White European	Right	Very wrinkly skin with some sagging; large arms; very compliant skin.
AB11	Female	95	White European	Right	Large arm; wrinkly skin; compliant (indentation more than rucking).
MG12	Female	76	White European	Left	Slightly wrinkly skin; low compliance.
KG13	Female	30	Asian	Left	Smooth skin; slim arm; very low compliance.
MT14	Female	88	White European	Right	Slightly wrinkly skin; low compliance.
DA15	Female	73	White European	Left	Slightly wrinkly, large arm; compliant (indentation more than rucking).
LC16	Female	27	Black British	Left	Smooth skin; slim arm; very low compliance.
MH17	Female	84	White European	Left	Relatively wrinkled and very compliant skin; slim arm with some bony and veiny prominences.
CB18	Female	44	Black African	Left	Smooth skin; large arm; low compliance.
DF19	Female	21	Mixed Other	Left	Smooth skin; slim arm but not bony; very low compliance of skin.
AK20	Female	20	Asian	Left	Smooth skin with very low compliance.

The procedure for making measurements was as follows:

1. Begin the 30-minute acclimatisation period with the participant's forearm exposed to the environment.
2. Meanwhile, position the forearm in the armrest and ensure that the strip of nonwoven fabric is set up in the tensometer grips as demonstrated in figure 4.12.
3. Mark the testing site by drawing a straight line (a ballpoint pen with washable ink) or attaching one strip of surgical tape [3M Micropore Surgical Tape, 50 mm × 5 m, 3M Poland Sp. z o.o., 05-830 Nadarzyn, Poland] to the skin on each side of the nonwoven.
4. Remove the strip from the arm, and at the end of the acclimatisation period, measure the water vapour flux density (WVFD) using the DermaLab evaporimeter [Cortex Technology, Denmark] continuously for 2 minutes.

³at time of participation

5. Measure friction between the first nonwoven and the skin for two cycles per applied load, starting with the 10g dead weight (then 20g, 30g, 50g, 70g); use the tensometer settings displayed in figure 4.13 and record measurements for all five loads using the three video cameras [*two* Panasonic HC-V100 Full HD Digital Camcorder, Panasonic Corporation of North America, Secaucus, NJ 07094; *one* Sony Handycam DCR-SR52E, Sony Corporation, Tokyo, Japan] as set up in figure 4.14.
6. Repeat step 5 for the remaining four nonwoven fabrics.
7. Repeat step 4.

As shown in figure 4.14, camera 3 was used to record the angle of arc of contact between the nonwoven fabric and volar forearm. Camera 1 was used to monitor the behaviour of the skin and nonwoven on top of the forearm and camera 2 recorded skin-nonwoven interaction at the front. All recordings from all cameras contained audio notes on observations made that may not be clear from visual footage alone.

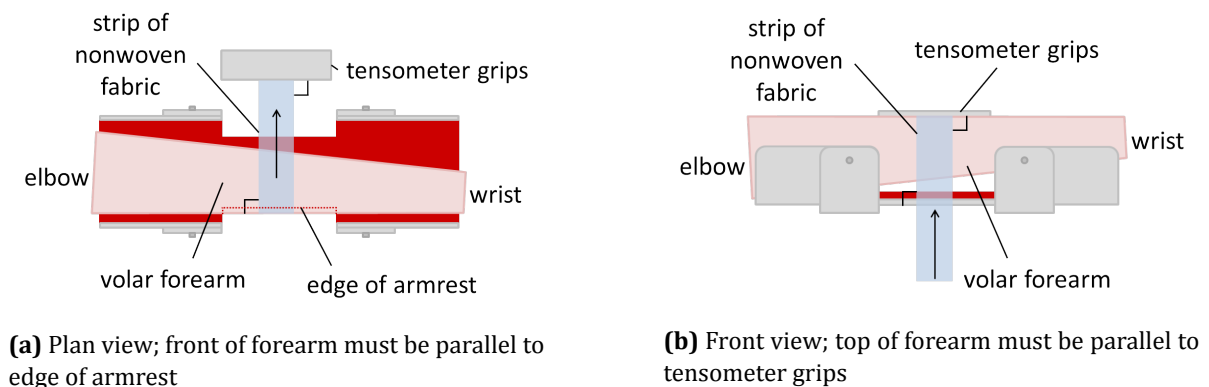


Figure 4.12: Experimental setup for friction measurements – diagram of nonwoven fabric strip on forearm in armrest; arrows indicate direction of tensometer pull

The screenshot shows a software dialog box titled "Full Options Test Method" with the following settings:

- Motion Options - Set Phase 1 & 3 Units:**
 - Units: mm
 - Sample Size (mm): 30.
 - Phase 1 Movement: 0.
 - Phase 2 Static (sec): 10.
 - Phase 3 Movement: 50.
 - Phase 4 Static (sec): 5.
 - Rate (mm/min): 150.
- Cycle Options:**
 - Cycles: 2
 - Start Each Cycle at Current Position
 - Start Each Cycle at Origin Position
- Gauge Force Options:**
 - Gauge Force (gmf): 0.
 - Apply Gauging to First Cycle Only
 - Apply Gauging to Each Cycle
- Force Range Options:**
 - Maximum Force (gmf): 100.
- End of Method Options:**
 - Return Sample to Pick Up Position
- Break Detection:**
 - Disabled
 - Enabled
 - Button: Edit Break Detection
- Carousel Options:** (Empty)

Buttons at the bottom: Cancel, Save, Run After Delay, Save & Run.

Figure 4.13: Settings applied to tensometer for all friction measurements under 10g, 20g and 30g; only “maximum force” was increased for higher applied loads.

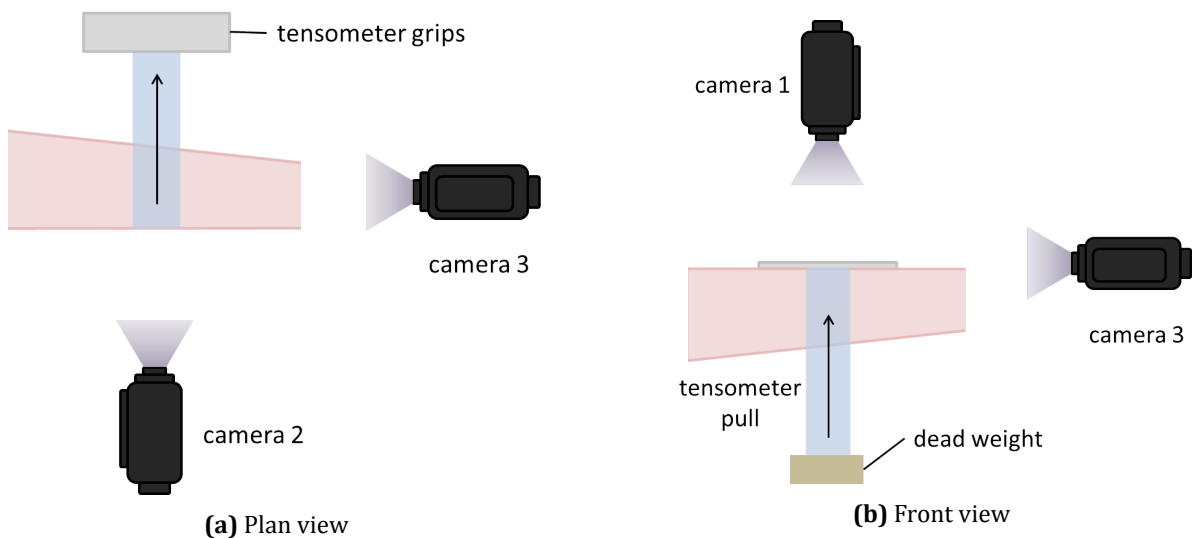


Figure 4.14: Camera setup for friction measurements; camera 1 records from plan view, 2 from front view and 3 from side view; arrows indicate direction of tensometer pull

4.3.3 Results

Raw data were initially presented in the form of force-displacement graphs, before being processed for more extensive analysis. Various features of these graphs could be attributed to certain events and skin behaviours. It was necessary to calculate coefficients of (static) friction for each participant-nonwoven combination for a fair comparison of fabrics and to investigate the impact of subject age and other factors. In this section, examples of these are given, including descriptions of observations relating to the behaviour of both the skin and nonwoven fabrics.

As displayed in figure 4.15, force displacement curves obtained from the measurements described in §4.3.2 resulted in a mostly linear initial increase in force followed by a plateau. The peak force was the static friction force, which was immediately succeeded by dynamic friction as the fabric moved across the volar forearm skin. This particular example was typical for participants with very low compliance (high modulus) in their skin – usually young – but the key features were the same for all subjects. In most cases, the tensometer force at zero displacement was equal to the applied load. Where this did not happen, the strip of nonwoven had either been inadvertently put under excess tension between the tensometer grips and the forearm when set up (resulting in an initial force value greater than the dead weight) or was slack between the tensometer grips and the forearm (resulting in an initial force value less than the dead weight).

Figure 4.16 shows a graph for a participant experiencing stick-slip at all applied loads. Each peak and trough corresponded to a separate incidence of static-dynamic friction transition; the difference between these forces increased with increasing applied load. The effect of rucking (folding of the skin) is demonstrated in figure 4.17 by the low gradient of the initial part of the curve, relative to other force-displacement graphs, or the long displacement before static friction force is reached. Participants with high compliance skin and a tendency to ruck did not have the same linear initial stage of force-displacement curves as those with firm skin (high modulus). In this example, peak force was not reached until ≈ 18 mm displacement at the highest load. Images of other participants' arms (see figure 4.18), coinciding with static friction force, demonstrate different extents of rucking, but all resulted in a similar graph.

It seems likely that all three examples given (figures 4.15-4.17) displayed rucking of the type shown in figure 4.3c, although there were also a few occasions when figure 4.3d was an accurate representation of the behaviour observed. During the measurements, a wide range of skin behaviours (deformation) and skin-nonwoven interactions were observed for all participants. As expected, the younger participants (mostly 50 years or younger) had firm skin with relatively little deformation in the form of rucking or indentation – in some cases, none of one or both of these were observed. “Torsional displacement” (displacement of the skin relative to the underlying tissue of the forearm) was seen in all participants to some extent. The skin of the older participants (half of whom were aged over 80 years) displayed a wider range of behaviours. Some elderly participants had skin with a considerably wrinkly appearance, yet had very little deformation, induced either by the weight attached to the end of the strips of nonwoven, or the friction between the nonwoven and the skin. Others had skin that moved or deformed with very little applied pressure.

Graphs of maximum tensometer force against applied load were plotted from raw data. Taking the maximum measured force from each load, they were then corrected for angle of arc of contact – a decision made after studying video footage of measurements – because the angle was often $5-10^\circ$ greater than 90° . Examples of these corrected plots can be seen in figures 4.19-4.21 (and the full set in appendix D). They are a representative set, covering the youngest and oldest participants, as well as the subject with the highest friction forces. *All* produced linear graphs like these, with small offsets where the linear regression lines met the y-axis.

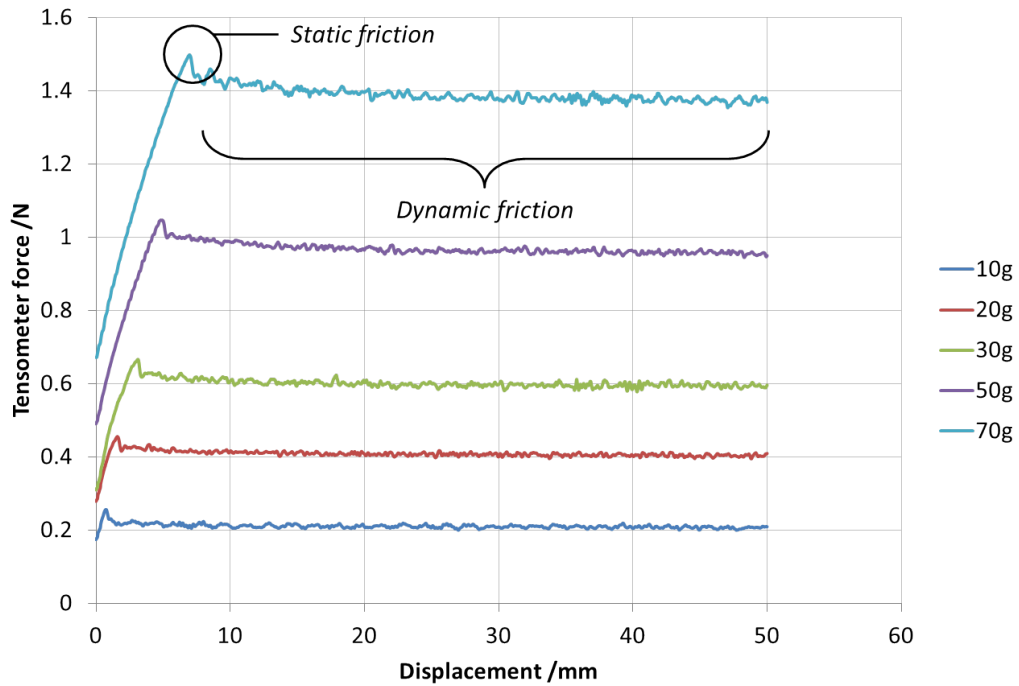


Figure 4.15: Example force-displacement curves for a participant with negligible skin deformation; SF14 under all (five) applied dead weights with participant MS04

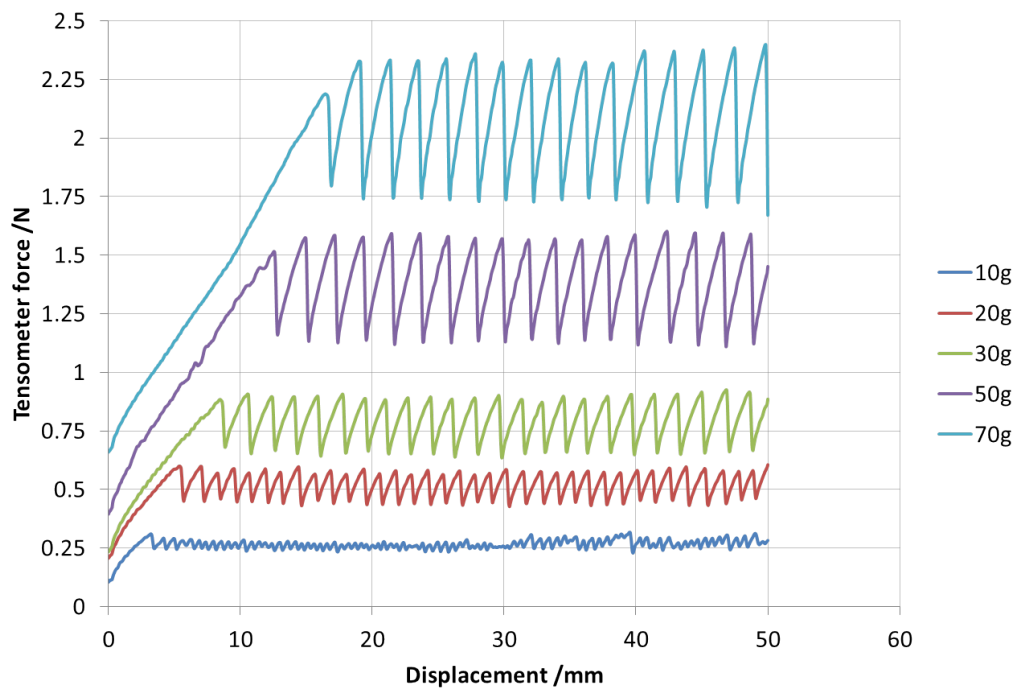


Figure 4.16: Example force-displacement curves for a participant displaying "stick-slip" behaviour; SF17 under all (five) applied dead weights with participant RJ05

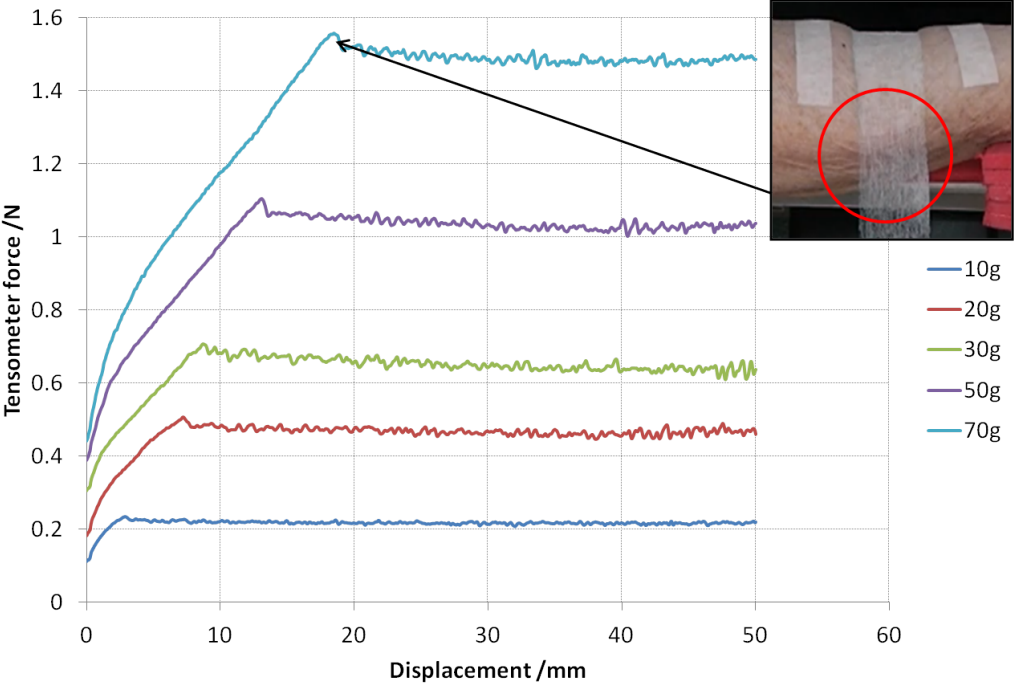


Figure 4.17: Example force-displacement curves for a participant displaying rucking; SF17 under all (five) applied dead weights with participant DJ10

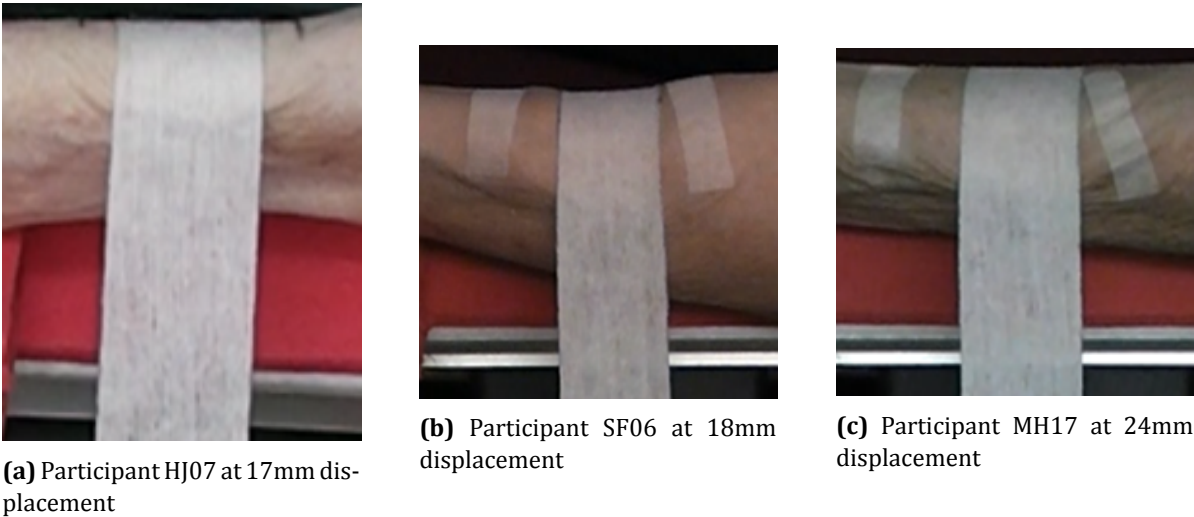


Figure 4.18: Examples of rucking of volar forearm skin with SF3 under 70g

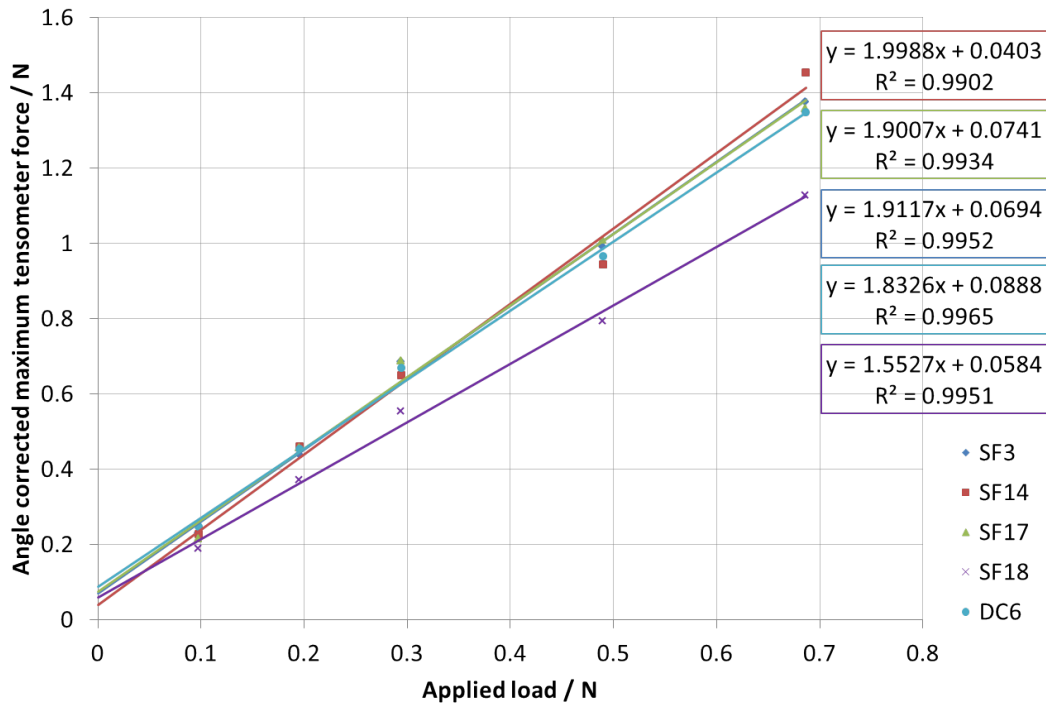


Figure 4.19: Youngest participant data (AK20) – maximum tensometer force against applied load for all non-wovens

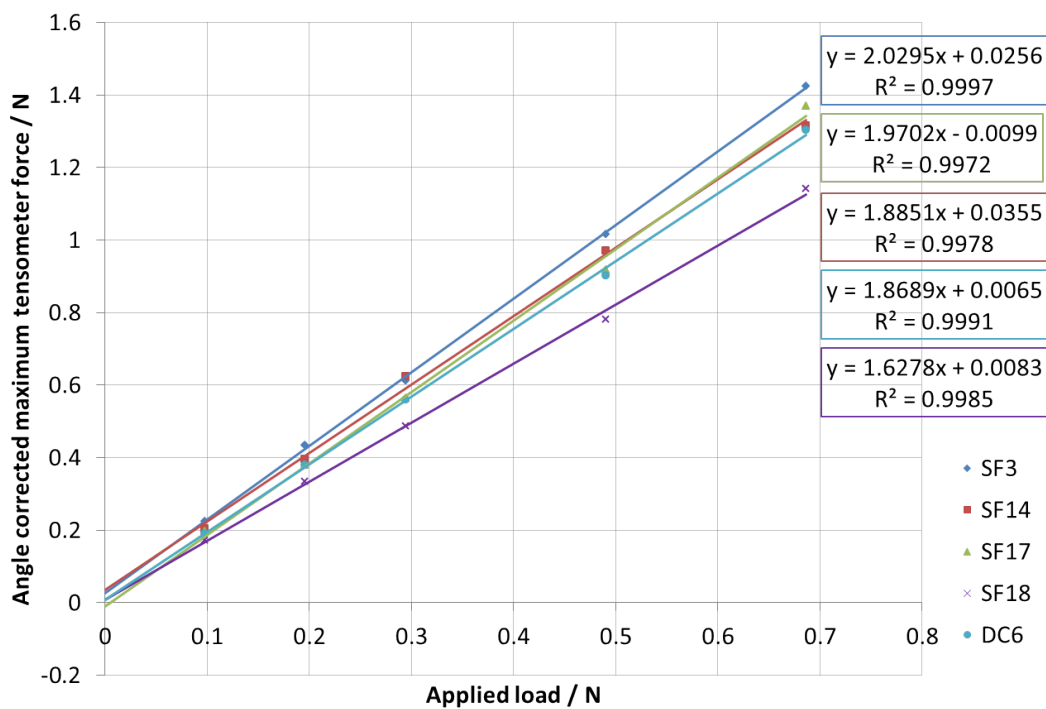


Figure 4.20: Oldest participant data (AB11) – maximum tensometer force against applied load for all nonwovens

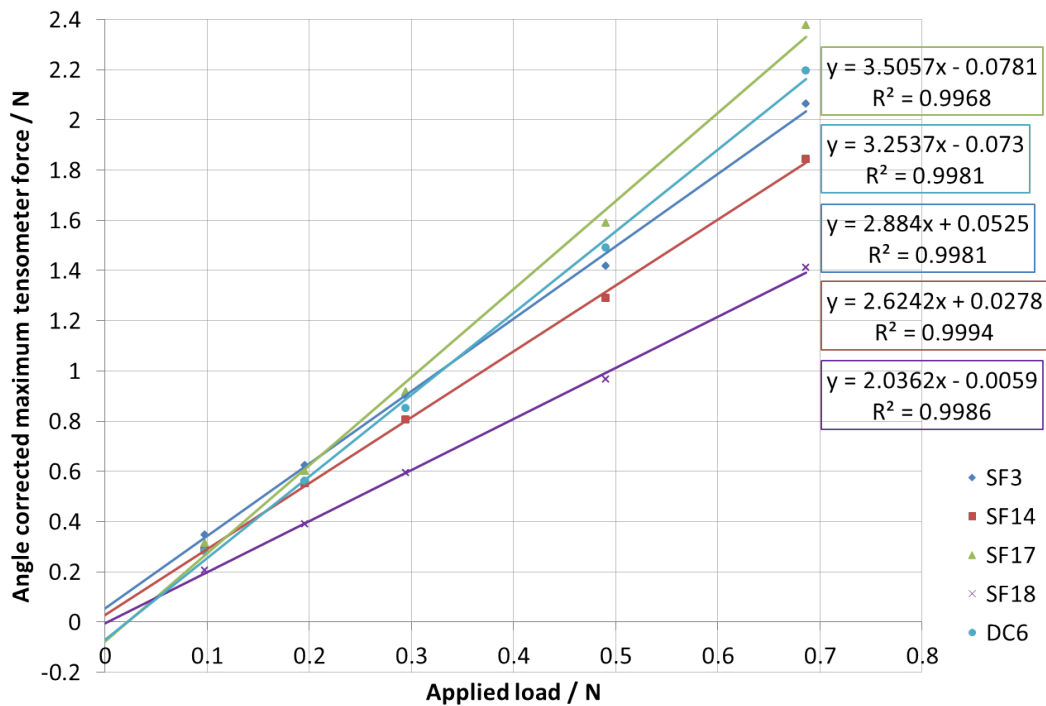


Figure 4.21: Data from participant (RJ05) with highest tensometer forces – maximum tensometer force against applied load for all nonwovens

Coefficients of static friction (μ_s) have been included in table format, along with a table ranking the fabrics according to μ_s (see tables 4.3 and 4.4). The data are colour-coded to indicate where the offset⁴ was greater than the error in the offset and therefore likely to be real. Participant RJ05 always had the highest μ_s with all nonwovens and nonwoven SF18 always had the lowest μ_s with all participants. The overall ranking of nonwovens from highest to lowest coefficient of (static) friction was: SF3, SF17, DC6, SF14, SF18. On average, SF3 had the highest CoF with most participants, whereas the ranks for the other nonwovens (apart from SF18) were rather interchangeable.

⁴The intercept where the linear regression line of friction force - applied load graphs met the y-axis (friction force), i.e. at zero applied load.

Table 4.3: Coefficients of friction for all participants and all nonwovens; **red values are highest** and **blue values are lowest** for a given nonwoven

Nonwoven	Mean coefficient of static friction																			
	AD02	MM03	MS04	RJ05	SF06	HJ07	MD08	JJ09	DJ10	AB11	MG12	KG13	MT14	DA15	LC16	MH17	CB18	DF19	AK20	
SF3	0.533	0.446	0.506	0.624	0.548	0.422	0.529	0.437	0.558	0.408	0.440	0.456	0.473	0.486	0.399	0.496	0.493	0.525	0.375	
SF14	0.447	0.374	0.453	0.562	0.504	0.407	0.469	0.397	0.418	0.353	0.468	0.406	0.403	0.408	0.401	0.436	0.418	0.503	0.401	
SF17	0.474	0.371	0.454	0.739	0.574	0.397	0.493	0.394	0.494	0.390	0.471	0.457	0.475	0.465	0.367	0.486	0.451	0.643	0.372	
SF18	0.314	0.284	0.323	0.416	0.383	0.285	0.380	0.334	0.391	0.273	0.328	0.313	0.373	0.340	0.279	0.334	0.297	0.347	0.259	
DC6	0.447	0.348	0.411	0.685	0.505	0.359	0.473	0.418	0.467	0.354	0.450	0.427	0.477	0.440	0.354	0.471	0.434	0.621	0.354	

Table 4.4: Nonwoven fabrics ranked by coefficients of friction for all participants; **pink values mean offset > offset error**

Nonwoven	Rank (1 = highest μ_s , 5 = lowest μ_s)																			
	AD02	MM03	MS04	RJ05	SF06	HJ07	MD08	JJ09	DJ10	AB11	MG12	KG13	MT14	DA15	LC16	MH17	CB18	DF19	AK20	Mean
SF3	1	1	1	3	2	1	1	1	1	1	4	2	3	1	2	1	1	3	2	1
SF14	4	2	3	4	4	2	4	3	4	4	2	4	4	4	1	4	4	4	1	4
SF17	2	3	2	1	1	3	2	4	2	2	1	1	2	2	3	2	2	1	3	2
SF18	5	5	5	5	5	5	5	5	5	5	5	5	5	5	5	5	5	5	5	5
DC6	3	4	4	2	3	4	3	2	3	3	3	3	1	3	4	3	3	2	4	3

4.3.4 Discussion

Friction measurements between volar forearm skin and nonwoven fabrics produced some very interesting – and sometimes surprising – data, all of which will be discussed in this section. Each aspect of the data – from raw force-displacement curves and observations of skin behaviour, to fully processed coefficients of friction – may reveal something important about skin-nonwoven interaction and contribute to the understanding of friction at this interface. Starting with force-displacement graphs, it was clear that the starting tensometer force, in some cases, was not equal to the applied load, which related to the way in which the nonwoven strip was placed on the arm. The occasional and unintentional application of additional tension to nonwoven strips, when applying them to the volar forearm, may have had some minor implications. In such a situation, the starting tension in the strip would limit its extension capacity during friction and may have affected the deformation of the skin and the nonwoven itself. However, it was unlikely to have made a significant impact on the tensometer forces overall. On the other hand, placing a slack/loose strip of nonwoven on the volar forearm would have resulted in an initial force owing only to the extension of the strip. Tensometer force caused by friction between the fabric and skin would only have taken effect once the strip was taut. Again, the extent of tautness was too small to have had a significant overall effect on friction.

As mentioned in chapter 2, Amontons' first law of friction stated that friction force and applied load are directly proportional. Despite such large variations in behaviour, the applied load - "friction" force relationship was surprisingly linear in every case, with coefficients of determination never less than 0.99 for these data (except on one occasion for participant MH17). This, combined with the very small offsets on the y-axis where the regression lines almost passed through the origin, was evidence that Amontons' Law held for dry friction measurements, regardless of the viscoelasticity of skin. The offsets, however, did present some uncertainty, so it was important to investigate further. It is already widely accepted that adhesion is the main mechanism operating during skin-fabric friction. Nevertheless, should the offsets be real, it may suggest the presence of another mechanism or source of force acting at the interface in addition to friction.

As is clear from the example graphs in figures 4.19-4.21, the offsets of regression lines, showing the relationship between friction and applied load, were mostly positive. This initially suggested that the probability of error in the offsets was relatively low, but the error was calculated (using standard deviation) for each offset to check this quantitatively. It could be assumed that, when $\text{offset} > \text{offset error}$, the offset was likely to be real/significant. As demonstrated in table 4.4, SF3 and SF14 'friction vs load' graphs had significant offsets (highlighted bold pink) with all but two participants. For SF18, offsets appeared to be real in just over half of all cases, compared to just under one third for SF17 and DC6. It was not immediately obvious why this should be, so various theories were considered. Eventually, the most likely theory – that the additional force arose from that required to bend the fabric around the volar forearm for full nominal contact – was explored. Following a set of bending stiffness experiments performed by Asimakopoulos [154], it was found that there was a clear positive correlation for most participants between fabric bending stiffness and the offsets of graphs created from the *volar forearm* skin friction data. However, this correlation did not necessarily indicate cause – further investigation was required here (see 'Physical models' in §7.3).

In most cases, the skin of each participant behaved according to obvious anatomical features. For example, torsional displacement was observed in almost every situation, but the movement of skin relative to the underlying tissue varied; when a volunteer's skin was more flaccid, the displacement was typically more. This was often complemented by rucking, which also depended on the compliance or

elasticity of the skin. The sizes of the folds were determined by both the type and volume of underlying tissue. Participants with very little fat or muscle in their forearms often formed smaller rucks than those with lots of fat, possibly because the skin was less restricted by these tissue structures. However, wrinkles also affected the size of skin folds when they were present; they created creases along which small rucks could form. Rather predictably, indentation of the forearm was deeper when there was more underlying soft tissue – most likely fat, rather than muscle.

The particular kind of indentation – concave or “cliff edge” (figures 4.3a and 4.3b respectively) – appeared to depend on the combination of the nonwoven used and the size and shape of participant arm. For example, DC6 was a relatively robust fabric that was rather resistant to lateral deformation, which, when in contact with a large arm with soft, compliant tissues, usually led to “cliff edge” indentation. In all situations, the load applied to the arm also influenced the depth of the indentation, although visually this change was negligible when there was little underlying tissue, or most of it was muscle, and skin compliance was limited.

There were few instances of stick-slip (10/95 participant-nonwoven combinations), with no obvious explanation for its occurrence. The scale of the stick-slip varied depending on participant-nonwoven combinations and sometimes applied load. From all data where this behaviour was observed, it could be inferred that the phenomenon was the result of an especially large difference between static and dynamic friction forces. This would mean that dynamic friction occurred very briefly until the force required to maintain the displacement of fabric against skin was too high, and sliding ceased at the interface – see the troughs in figure 4.16. At this point, displacement continued – but not between the skin and nonwoven – until the static friction force (peaks on graphs) was reached again. This pattern repeated itself and rarely dissipated during the measurement period. Derler and Rotaru [69] have investigated the stick-slip phenomenon (in wet conditions only) and found that its occurrence was usually linked with lower coefficients of friction than those in its absence. The magnitude of stick-slip also depended on the sliding velocity of skin against the contacting material (glass). Many papers – including this one by Derler and Rotaru – suggest that stick-slip only transpires when conditions are wet [69, 77, 92, 109], which contradicts the findings of work described in this chapter. Nevertheless, the ultimate cause of this behaviour is still unknown, as are its potential implications for skin health.

Examination of the “dry” friction data and videos revealed that there was no obvious relationship between age and friction forces, age and skin behaviour, or skin behaviour and friction forces. Certain features of force-displacement curves were attributed to specific skin behaviours, but coefficients of static friction, between each participant and each nonwoven, could not be explained by the condition, WVFD or general behaviour of a person’s skin.

After calculating the coefficients of static friction for all study subjects, these values were plotted against participant age – see figure 4.22. RJ05 (60 years old) had both the highest coefficient of friction with all nonwovens and the largest *range* of coefficients, but there was no correlation between age and μ_s . Perhaps coincidentally, RJ05 also displayed the most extreme stick-slip behaviour of all participants. Since the reason for this phenomenon is currently unknown, and more supporting experimental data are lacking, it could only be speculated that the magnitude of μ_s influences or is affected by stick-slip behaviour.

It could be suggested that since tensometer force was essentially directly proportional to applied load, and that applied load affected the extent of deformation (i.e. indentation, torsional displacement and rucking) of the skin, it would be logical for tensometer force to depend (at least partly) on skin deformation. As the data obtained appeared to contradict this theory overall, it was necessary to review the data more closely to check. This was done by comparing the pre-static-friction displacement val-

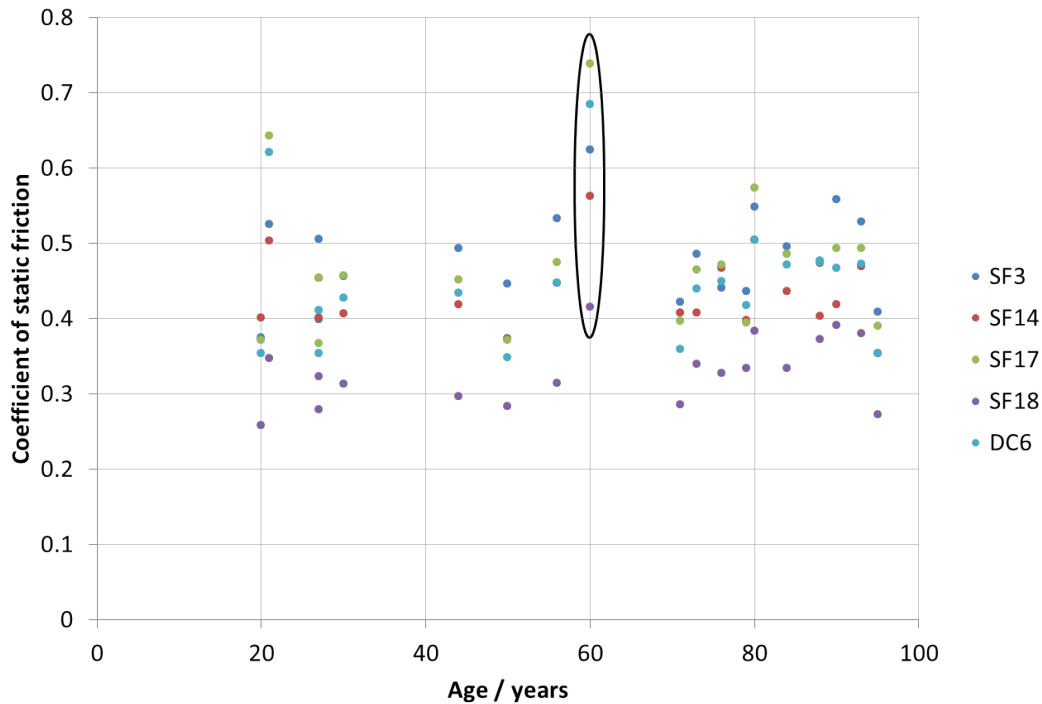


Figure 4.22: Relationship between participant age and coefficient of static friction

ues, under the 70g dead weight, for all nonwovens and participants.⁵ These displacement values were considered to be a suitable representation of skin compliance in the most extreme case (i.e. under the highest load). Results are displayed in figure 4.23.

It is immediately apparent, looking at figure 4.23, that there was no relationship between coefficient of static friction and the displacement of the skin up to that point. It implies that the extent of deformation did not affect measured force, although the *change* in tensometer force during this initial period was not taken into account. However, the extent of deformation did change slightly with each fabric: nonwovens SF3 and SF17 were associated with the greatest skin deformation, which demonstrates that the properties of the nonwoven also played a role in the time taken to reach static friction force. Based on these observations, there are two possible explanations for the events during dry friction measurements that led to the creation of figure 4.23 : (i) the extent of deformation (or apparent displacement of the skin before slip) depends largely on the compliance of the skin as a bulk and that of the underlying tissue; (ii) the increase in friction force depends more on the surface properties of the stratum corneum and its interaction with the nonwoven fabric.

Taking all into account, a brief analysis of the properties of the nonwovens, in relation to friction measurements, can now be carried out. The fibre materials and manufacturing processes, in combination with bonding area and number of points, may be expected to indicate how compliant a nonwoven fabric is. Highly compliant nonwovens could *potentially* be more susceptible to changes due to microscopic variations in the topography of the skin. However, with an anticipated extremely low contact area, this was unlikely to make a difference. Nonwovens SF3 and SF14 were both created from a mesh

⁵It was not possible to calculate the gradient of the initial slope of the force-displacement curves for all participants due to the varying linearity.

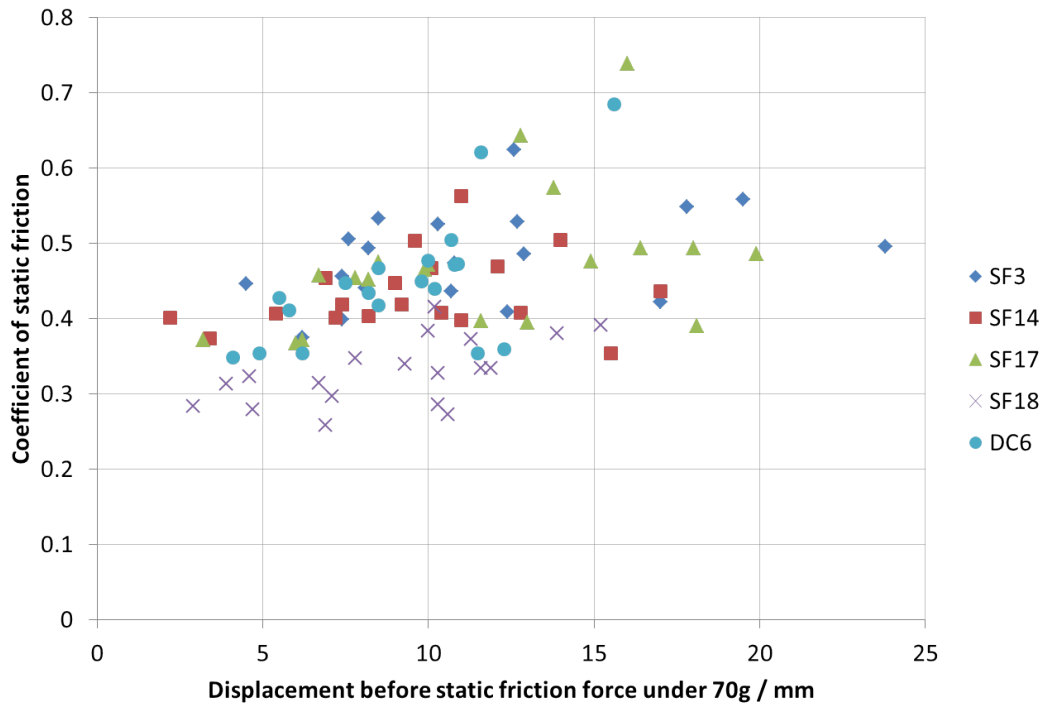


Figure 4.23: Relationship between skin deformation before slip and coefficient of static friction

of fibres; SF14 was thermally bonded by calendaring but SF3 was hydroentangled. It appeared that the relatively high strength in tension of SF14 was due to the fact that it was bonded at a high pressure and that it had the largest bonding area of all five nonwovens. These properties and the high area density made it less compliant than other nonwovens.

In SF3, the fibres were visibly preferentially aligned with the machine direction of the fabric. The nonwoven was anisotropic and had a comparatively high unidirectional tensile strength and bending stiffness, possibly enhanced by the high basis weight (area density). As DC6 was bonded thermally and at a high pressure, it was rather “robust” in nature (low Poisson’s ratio), similar to SF14. This was not the case for SF17 and SF18 and, considering their low densities, they were the most compliant. It was evident that there was still very little difference between the offsets of the nonwovens, but that SF14 had the smallest and DC6 had the largest overall. A much smaller proportion of the offsets for DC6 and SF17 (6 out of 19) were greater than the calculated error, compared to SF18, SF14 and SF3, with 10, 12 and 13 out of 19 offsets respectively. As SF18 has a bending stiffness more similar to SF17 and DC6, and much lower than SF14 and SF3, this also supports the argument that the offset is independent of bending stiffness but affected by some other factor – possibly deformation of the skin-nonwoven interface.

The linear densities of the nonwoven fibres did not appear to relate to the friction force at slip, but may have been a good indication of roughness in terms of sensation, the extremes being SF17 (coarse) and SF18 (soft/smooth). With the exception of SF18, there was also a direct link between fibre diameters and linear density, which may be an important potential measure of predicted comfort. The presence of surfactants may have contributed to fibre roughness on a scale that could not be detected by the tensometer, but this was not considered crucial to the study and was therefore not investigated. Due to the minimal bonding information for these five nonwovens, it would have been a challenge to assess their ability to maintain their integrity, if not for the observations made during measurements.

4.3.4.1 Lorica Soft compared with dry (normal) volar forearm skin friction data

The first obvious difference between friction measurements on Lorica Soft and human skin was the shape of the force-displacement curves. Static friction force was reached almost immediately with the skin surrogate (both flat and wrapped around a rigid cylinder), whereas there were several millimetres displacement (typically > 2 mm) before sliding began on skin. This was essentially due to the compliance of skin and its underlying tissues, which deformed to move in the direction of tensometer pull *with* the strip of nonwoven, unlike Lorica Soft (LS). The extent of this pre-slip deformation varied between participants and depended on applied normal force (dead weight), but did not change appreciably with load on the surrogate. It was clear that the physical (cylindrical) model was very different to the volar forearm and met the assumptions required by the mathematical model that the real arm did not. Nevertheless, *both* experimental setups showed a linear proportional relationship between friction force and applied load, and that coefficient of static friction did not depend on apparent contact area, thus demonstrating that Amontons' law held.

Force-displacement graphs for volar forearm skin were more similar to those produced by curved LS than flat LS, which suggests that the forearm is better represented by a smooth, rigid cylinder than a flat undulated surface. However, the relationship between coefficient of static friction (μ_s) for flat and curved LS (as shown in figure 3.16) indicates that flat LS still produces similar values to curved LS. These coefficient of friction values (just under 0.2 to just over 0.3) were generally *lower* than those for volar forearm skin *in vivo* (0.26 to 0.74), but the order of the nonwovens – when ranked according to μ_s – was the same: SF3 had the highest μ_s , SF18 had the lowest and the other nonwovens (SF14, SF17 and DC6) were interchangeable. Hence, for the purposes of identifying relative differences between nonwovens and selecting a subset for further testing on real skin, Lorica Soft was a suitable choice of surrogate.

It should also be noted that, on graphs of 'maximum tensometer force vs applied load' for Lorica Soft wrapped around a rigid cylinder, the linear regression lines essentially all go through the origin. The offsets for the different nonwovens are negligible, unlike some of those for volar forearm data, further supporting the suggestion that the offset may be dependent on the deformation of the fabric and/or skin. As expected, the behaviour of the nonwoven strip was influenced by the properties of the interacting surface. Samples of fabric deformed less – in the form of "necking", lateral folding and extending along its length – when pulled against Lorica Soft on the cylinder than against volar forearm skin. It is likely that this difference in deformation of the nonwoven is a consequence of the difference between both the moduli and surface properties of the skin/stratum corneum and skin surrogate. Similarly, no stick-slip was observed during friction measurements on LS, possibly due to its low compliance and the rigid Plaster-of-Paris cylinder to which it was attached.

Although this block of work has given rise to a number of interesting findings, it is by no means an *ideal* model of friction between perineal skin and a coverstock on an incontinence pad, partly because of the deliberate exclusion of liquid. A more realistic representation of this interaction would involve the introduction of a urine substitute to wet the skin and/or nonwoven fabric, building upon the foundation of data from friction measurements on dry (normal) skin. This constitutes the next block of work and the second part of the study, which will be described in chapter 5.

CHAPTER 5

FRICTION MEASUREMENTS ON WET VOLAR FOREARM

“Life isn’t all about swimming—it’s about fresh air and family and happiness!”

— Jason Falloon, 1998-

This chapter has been removed due to its commercially sensitive content. It will be made available in the full version of this thesis, which will be published at a later date.

CHAPTER 6

FIBRE FOOTPRINTS OF NONWOVENS AGAINST A SUBSTRATE

“We have found a strange footprint on the shores of the unknown.”

— Arthur Eddington, 1882–1944

THE MEASUREMENT OF FIBRE CONTACT LENGTH between nonwoven fabrics and skin is important for the analysis of the interface, and should be compared with friction data, in order to help to provide an explanation for why most nonwovens yield similar coefficients of friction with human skin or a skin surrogate. Visualisation and quantification of contact at the interface, under a range of pressures, should provide more insight into the way in which friction between nonwovens and human skin is mediated by the interface and possibly the type of mechanism(s) operating during such interaction. In this chapter, work implementing Cottenden’s method for examining fibre footprint [4] is described and discussed. The principles of this work were explained in §2.5 of the literature review. Various alternative techniques to measure or estimate contact area were also considered, such as mathematical modelling of quarter-spaces and imaging the interface using optical coherence tomography or micro computed tomography. None of these were appropriate for examining the skin-nonwoven interface; hence no attempt was made to test them. The only other potential alternative to the existing microscopy method to be explored was one applying Fourier Transform Infrared (FTIR) Spectroscopy. Based on the theory that a total contact area could be calculated from spectra of a simple material, if calibrated with the microscopy technique, some preliminary experiments were carried out with FTIR Spectroscopy. Unfortunately, time was a limiting factor that prevented this exploratory work from continuing any further. Instead, the microscopy method was used alone to analyse nonwoven fibre footprints.

This chapter describes work carried out to study the fibre footprints of a subset of nonwoven fabrics on glass microscope slides (as a surrogate for skin). Real skin or Lorica Soft could not be used because they are opaque, which would prevent imaging of the interface under the microscope. First, the effect of pressure on *total* fibre contact length (assumed to be proportional to total contact area) and contact length *distribution* were investigated, followed by the impact of the local area density of a nonwoven. In both experiments, fibre contact lengths were measured and analysed under the assumption that they were representative of and similar to those in actual skin-nonwoven contact. This was based on some mathematical modelling carried out by Cottenden [141], who demonstrated that there were negligible differences between the *stratum corneum* and glass as substrates, due to their high elastic moduli relative to the applied pressures used in the work presented in this chapter. These pressures were also low compared to fibre stiffness, so the calculated height of bulges in the fibres – that form

at the interface with a substrate when a nonwoven is compressed – was negligible compared to fibre diameter [4]. Between bulge height and substrate stiffness, it was clear that no *indentation* would occur, whether pressed against human skin or a glass slide, and so fibre contact length against glass would be suitably representative of that against skin.

6.1 Materials & Methods

Cottenden [4] measured the fibre contact lengths of areas of samples of three nonwoven fabrics against glass slides using an optical microscope. It was found that total contact length increased with applied load; the relationship was linear when the x-axis (pressure) had a logarithmic scale. The plan here was to repeat these measurements with a broader range of nonwoven fabrics than Cottenden [4], varying in manufacturing process, polymer, structure and coefficient of friction. During preliminary experiments, all five nonwovens of the subset selected from the 16 in table 3.1 were examined. After further testing, in both microscopy and friction, it was decided that only SF17, SF18 and DC6 should undergo extensive testing using microscopy, as with wet friction measurements. The reasons for this are explained in §?? and §6.1.2.2. In this section, experimental procedures for measuring and analysing fibre footprints are described, starting with a calibration technique necessary for interpreting data about the depth measurements within the fabrics.

6.1.1 Equipment calibration and fibre diameter measurement

The thickness of a microscope slide [Thermo Scientific, Menzel-Gläser, Gerhard Menzel GmbH, Braunschweig, Germany] was measured with calipers [M310-25, Mitutoyo, Japan] and then with a microscope camera [DFC 320, Leica Microsystems (UK) Ltd, Milton Keynes, UK] connected to the microscope [DMLM microscope, Leica Microsystems (UK) Ltd, Milton Keynes, UK]. Without, cleaning the slide, it was placed on the microscope stage and the image (using the camera with QWin software [QWin, version 3.2.0, Leica Microsystems (UK) Ltd]) was focused on one of the surfaces; this was determined by dust particles visible at the surface. The number of microscope stage depth divisions was set at zero here. The opposite surface was then also put into focus, counting the number of divisions moved to achieve this. After repeating the previous step twice more, a mean value of the thickness (/divs) of the slide was taken; this value, combined with mean thickness (in micrometres) measured with the calipers, was used to calculate a unit conversion constant (the denominator of the following equation).

$$[\text{Thickness in } \mu\text{m}] = \frac{[\text{Total no. of divisions}]}{[\text{Microscope slide thickness /div}] / [\text{Microscope slide thickness / } \mu\text{m}]}$$

The diameters of nonwoven fabric fibres were then measured, using the microscope setup, in the same way as the thickness of the microscope slides. These values were then converted to their equivalent in micrometres, using the aforementioned equation, and are displayed in the first row of table 6.1. Although mean values of fibre diameter were calculated from repeat measurements on the same fibre, the diameters varied for different fibres within each nonwoven, hence the measured *range* of diameters has been included for each. The expected average fibre diameter¹ is also included in the table (in the second row).

¹The linear densities (given in table 3.1 – see ‘Dtex’ column) and estimated volume densities (based on the constituent polymers) of the fibres were used to calculate expected average fibre diameter.

Table 6.1: Fibre diameters of nonwoven fabrics in the subset

Nonwoven	SF3	SF14	SF17	SF18	DC6
Measured range of fibre diameters / μm	7-12	10-15	25-30	12-17	15-20
Expected average fibre diameter / μm	12.5	15.1	29.6	19.7	22.0

6.1.2 Investigating the effect of applied pressure on fibre footprint

6.1.2.1 Micrograph collection

As the initial aim of this investigation was to compare fibre footprint data for a range of nonwoven fabrics, including one used by Cottenden (DC6), the microscopy method he designed was implemented first with DC6. The procedure was to be as follows:

1. Carefully clean the microscope slides using ethanol and a soft cloth.
2. Place a 30 mm \times 30 mm sample of nonwoven fabric between them on the base component of the apparatus displayed in figure 6.1.
3. Apply pressure by placing weights directly on the top slide (*0.5kPa and 1.5kPa*) or the top component of the apparatus (*5kPa and 15kPa*) – see figure 6.1.
4. Viewing the *upper* surface of the sample against the *top* slide under the microscope, via the computer screen, put the image in focus and check that the sample is flat and level; if it is not, insert shims where needed in order to make it level.
5. Ensuring that the image is correctly focused, scan the sampling area (approximately 4.5 mm \times 4.5 mm, true area 4316 $\mu\text{m} \times$ 4272 μm .) automatically with the Mosaic tool in QWin, which splices together the 12 small micrographs that make up the larger one.
6. Save the image in TIFF (tagged image file format).

A fresh sample of nonwoven was used for each repeat under each applied pressure. This served to avoid the collection of misleading or spurious data that can occur if the sample is nudged when weights are added or changed, resulting in inaccurate or non-uniform pressure application. There is also the issue of permanent deformation of the fabric: if a lower pressure is applied after a high one, the total fibre contact length often remains the same; if increasing pressure is applied, the increase in contact is gradual. The former might be rectified by removing the sample from the apparatus, repositioning it and re-applying the weights, but this might be the equivalent of using a new sample of nonwoven, thus defeating the object of reusing a sample. Also, it would not guarantee that the deformation of nonwoven sample (caused by compression) had been reversed. The latter method would not necessarily demonstrate the true relationship between pressure and total contact length, especially if the sample is disturbed during the addition of a load. The final reason for using a new sample of fabric for each repeat owes to the impracticality of changing the experimental setup for the different ranges of applied pressure on one sample (see step 3 of the procedure).

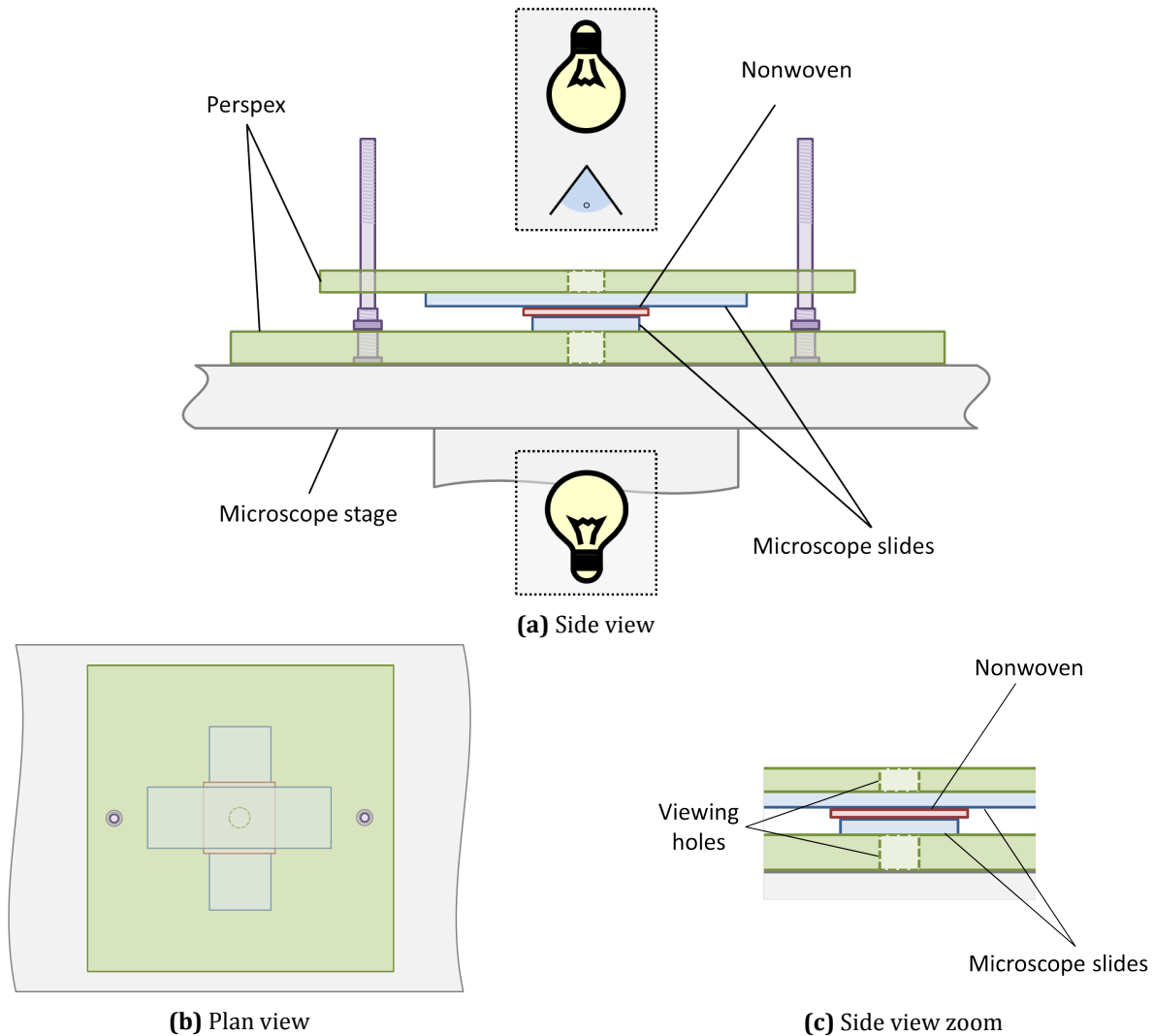


Figure 6.1: Diagram of equipment used to measure contact length of nonwoven fibres against glass

6.1.2.2 Alterations to the method

In preliminary experiments, while experiencing equipment malfunction, there was a change to the image collection process that led to an important discovery. By collecting micrographs manually (i.e. moving the stage by hand, rather than automatically), the time taken to gather all 12 individual images per sample was considerably longer and the fibres were progressively more out of focus. After further investigation, it was discovered that two things were happening:

1. fibres were moving out of the focal plane, reducing the *apparent* total contact length;
2. the *actual* contact length was increasing.

This was because of fibre settling (see figure 6.2). The *apparent* total contact length decreased with time and at a rate that varied from sample to sample. Depending on the applied pressure, and the nonwoven fabric, it *appeared* that no fibres were in contact with the top slide after as little as 10 minutes after load application. However, the *actual* contact length of each nonwoven increased for up to 20 minutes, which meant that this was the length of time required for fibres to settle in the samples

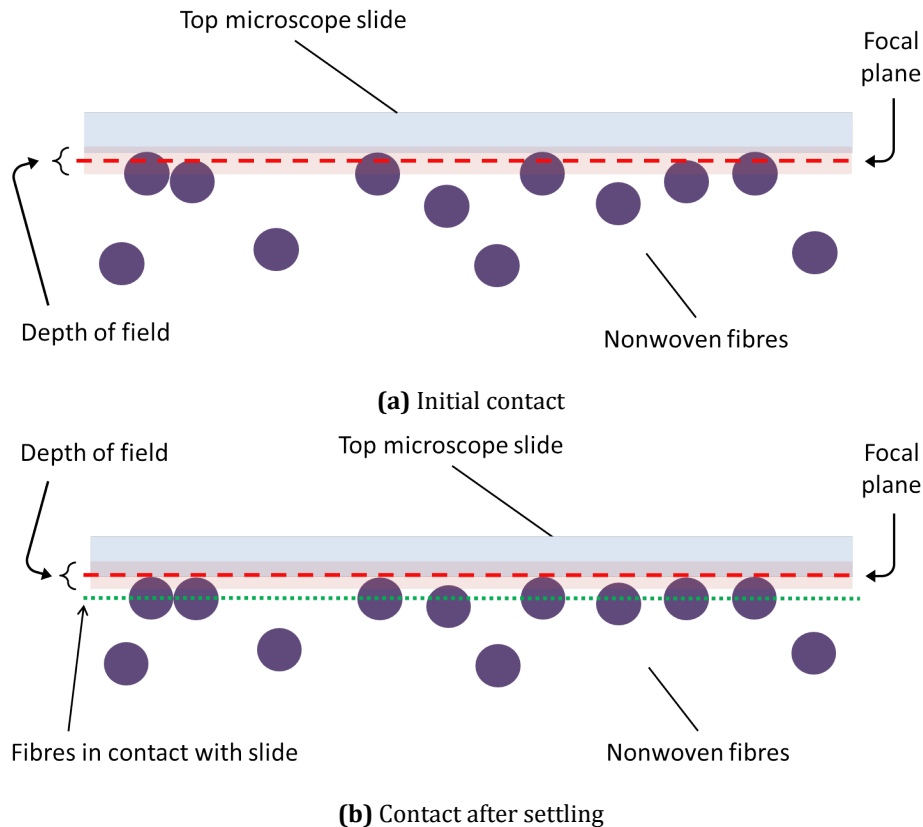


Figure 6.2: Diagram to demonstrate effect of fibre settling. Fibres in contact with slide are in focus in 6.2a, where focal plane is in correct position, but out of focus in 6.2b, where slide and fibres move below focal plane. Apparent fibre footprint *decreases* in 6.2b, but actual footprint *increases* as nonwoven is compressed. (While this diagram is not to scale, the effective depth of field in this setup has been shown to vary between 19 μm and 24 μm for nonwoven fibres with mean diameters of roughly 14–22 μm , with the largest diameter apparently exceeding its respective depth of field [4]. The fibre diameters of the nonwovens studied in *this* chapter were similar to that largest diameter, suggesting that they too were larger than their effective depths of field.)

of nonwovens used. As a consequence of this brief investigation, a step was added to the method described in §6.1.2.1 to include a period of half an hour² for fibre settling before assessing if the sample is level and flat, and then collecting micrographs.

6.1.2.3 Image processing

There were several stages required to convert the raw micrographs into an image from which contact lengths of fibres could be measured. These involved a combination of manual and computational methods as computers lack the ability to distinguish between useful information and artefacts on an image. All of the steps are presented in the form of a flowchart (see figure 6.3) and further details of the different stages of image processing are given in appendix F.

²20 minutes would probably suffice, but 30 mins ensured that fibre settling had ceased.

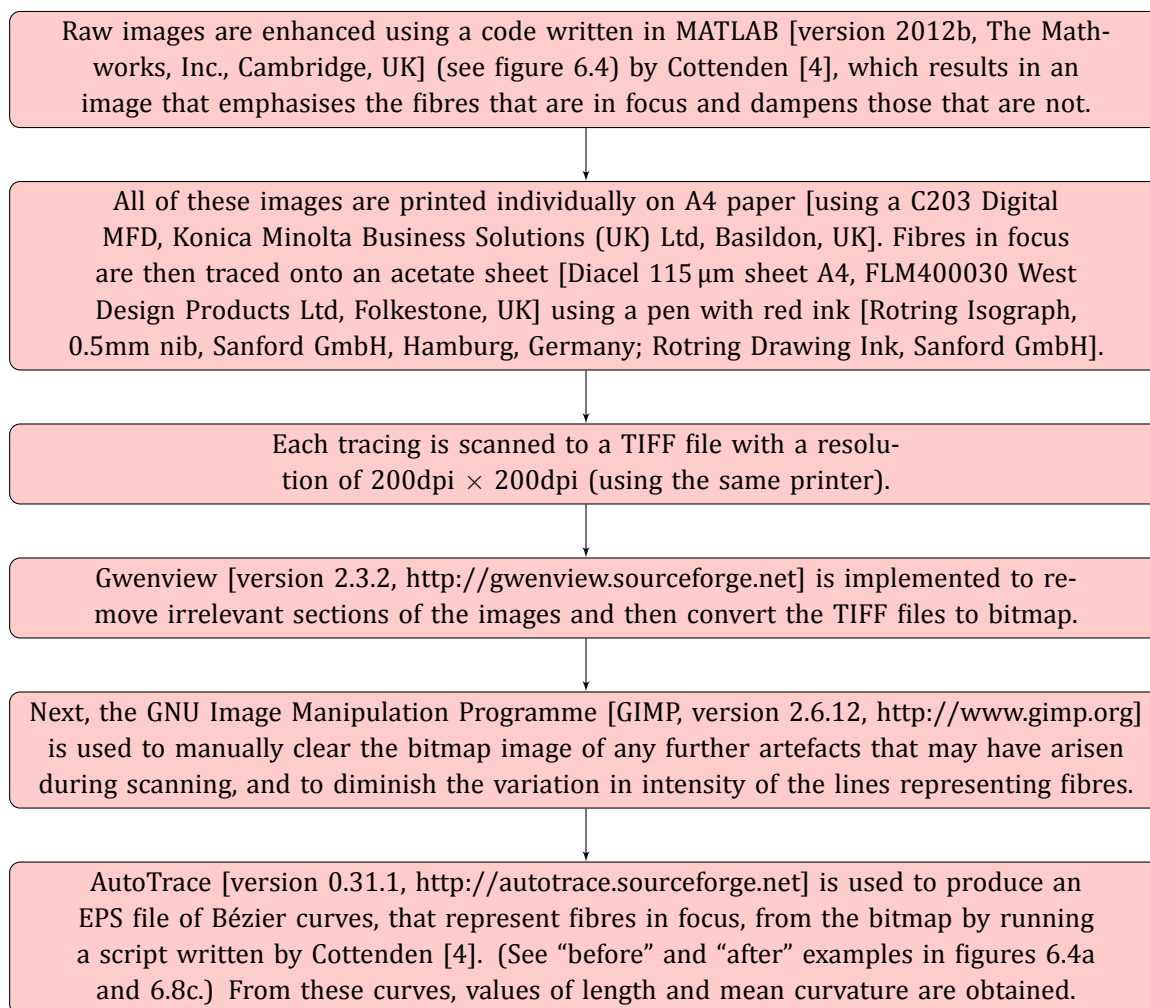
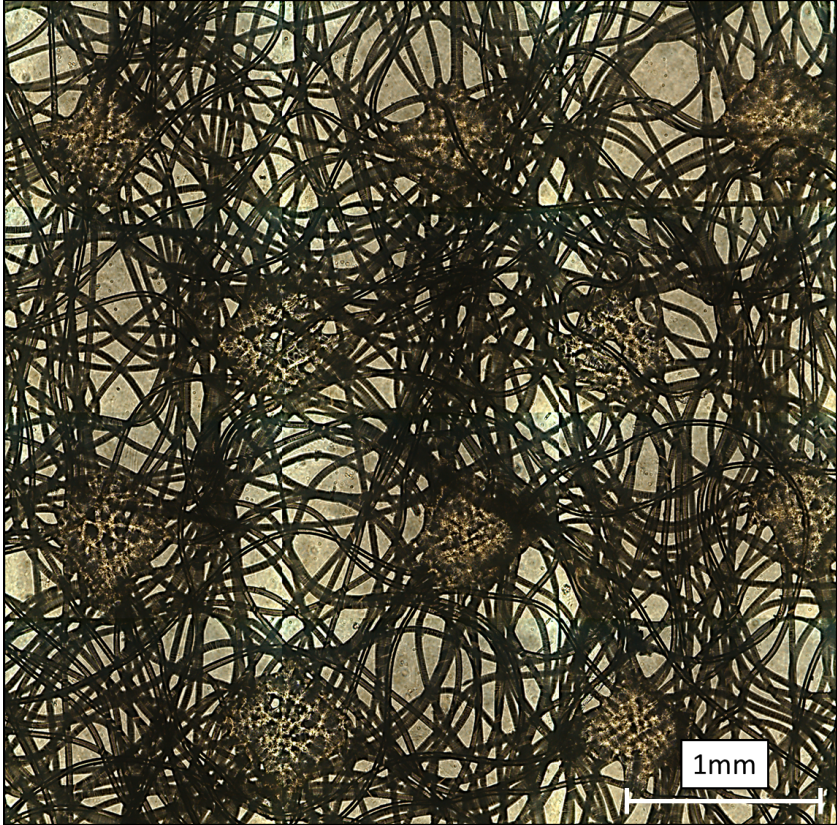
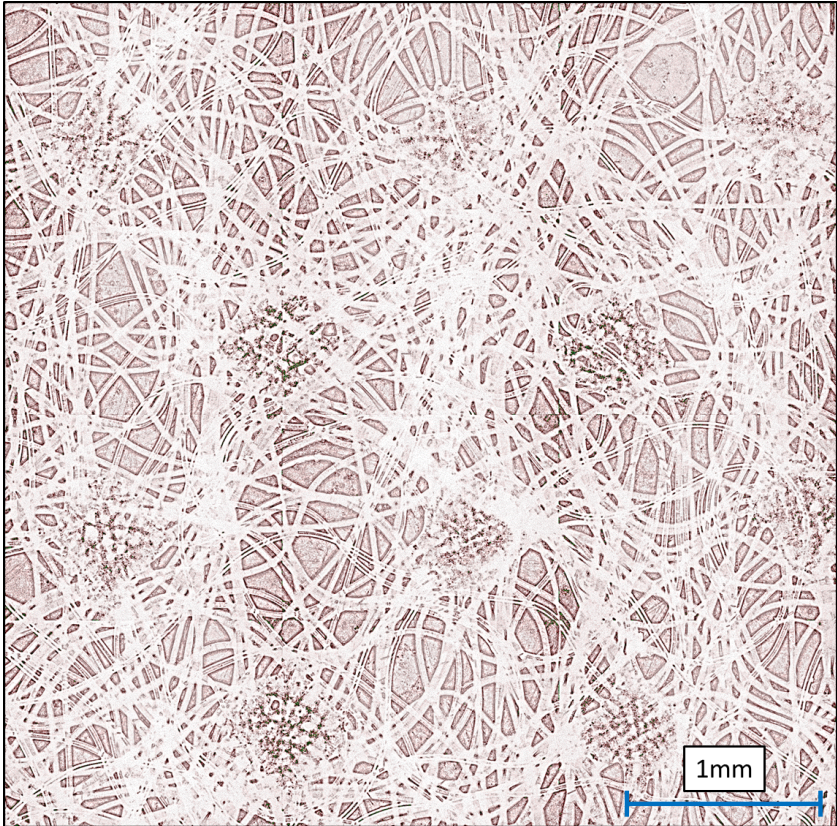


Figure 6.3: Flowchart to describe image processing

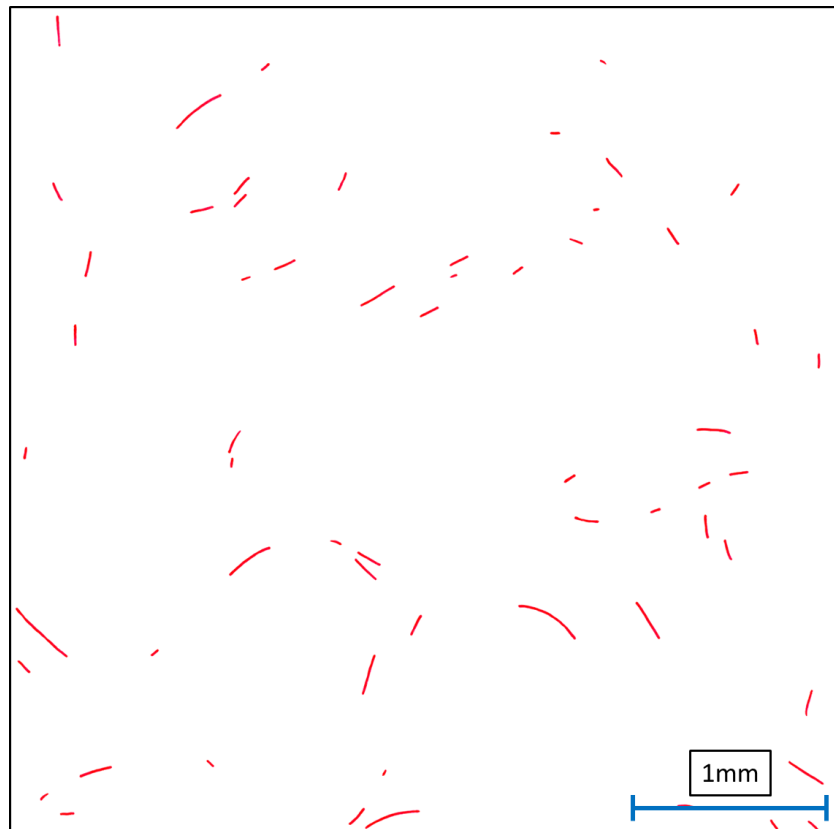


(a) Micrograph



(b) After processing in MATLAB

Figure 6.4: Images of a sample of nonwoven SF17 under 1.5kPa at various stages in the processing sequence. *Continues...*



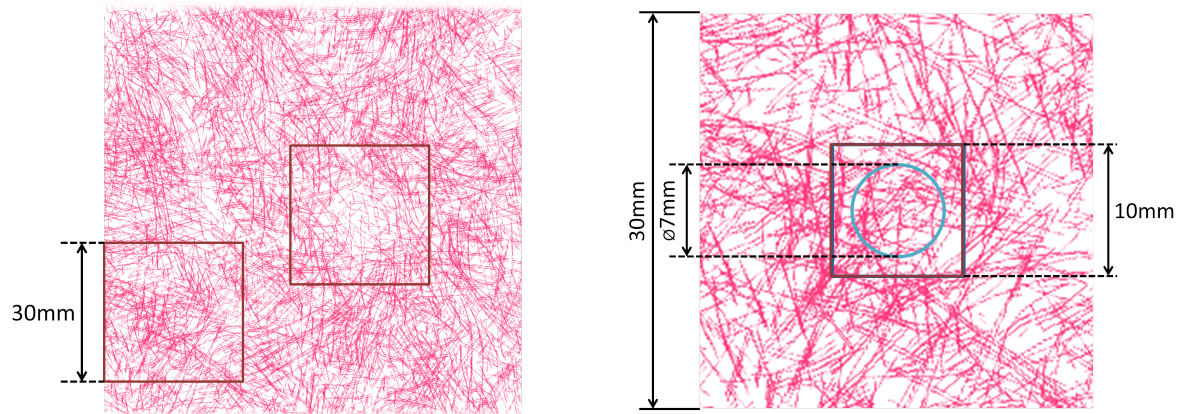
(a) After tracing and scanning

Figure 6.5: Continued.

6.1.3 Investigating the effect of local area density on fibre footprint

The importance of investigating the impact of various local area densities – of a nonwoven fabric – on its total contact length stems from the fact that friction forces appear not to be affected by fabric area density. As explained in §4.2, low, medium and high density portions of nonwoven were pulled against volar forearm skin to test this theory, but no significant difference was observed between the measured friction forces. In order to understand how friction was mediated by nonwoven samples of varying density under the same applied load, it was imperative that the fibre footprints of similar samples were examined. If the total length of fibres on the microscope slide increased with increasing area density, it would mean that the total true pressure of fibres against the skin would depend on the density of the sample. Alternatively, if the area density of different samples had no effect on total contact length, it would suggest that the nonwoven deformed to withstand the applied load and possibly maintain the pressure at the interface.

It may also explain variation in fibre footprint of different samples of the same nonwoven, as well as the differences in frictional interactions between nonwoven fabrics and skin. Ideally, contact and friction at the skin-nonwoven interface would be studied simultaneously, where particular fibre footprints could be associated with particular friction forces. This would also remove the complication of non-uniform pressure distribution across the volar forearm. For obvious reasons, there was no prac-



(a) Selecting samples from large piece of nonwoven

(b) A sample of nonwoven – dimensions and focus points

Figure 6.6: How samples of nonwoven were selected for area density; the square in 6.6b highlights central region where area density must be the same as similar samples; circle represents “viewing hole” of top piece of apparatus and outer boundaries of possible scanning area

tical method for accurately measuring contact in conjunction with friction, nor was it possible with a skin surrogate, as discovered by Cottenden [4].

Samples were selected based on qualitative (visual) judgement of area density. Sampling sections – 30 mm × 30 mm – of “high”, “medium” and “low” density were sought from a large piece of nonwoven (see figure 6.6a) SF17 as this material was particularly inhomogeneous. It was most important that the central region of the sample, minimum area 10 mm × 10 mm, was the same for all samples of the same qualitative density, as this was the portion of the sample to be examined under the microscope – see figures 6.6b and 6.7. Measurements were carried out as previously described; then samples were weighed whole before cutting out and weighing a 7 mm × 7 mm square³ from the centre. This was done using a microbalance [XP6, Mettler-Toledo (Schweiz) AG, Im Langacher, 8606 Greifensee, Switzerland] in the Department of Chemistry, UCL. It was essential to measure the mass of each sample to be able to make accurate comparisons between the total contact length and the sample area density or local area density of the scanned region. The weighing could not be carried out before making fibre footprint measurements because it involved cutting the samples, thereby destroying them.

³A square was cut out, rather than the circle, shown in figure 6.6b, for convenience and accuracy of cutting.

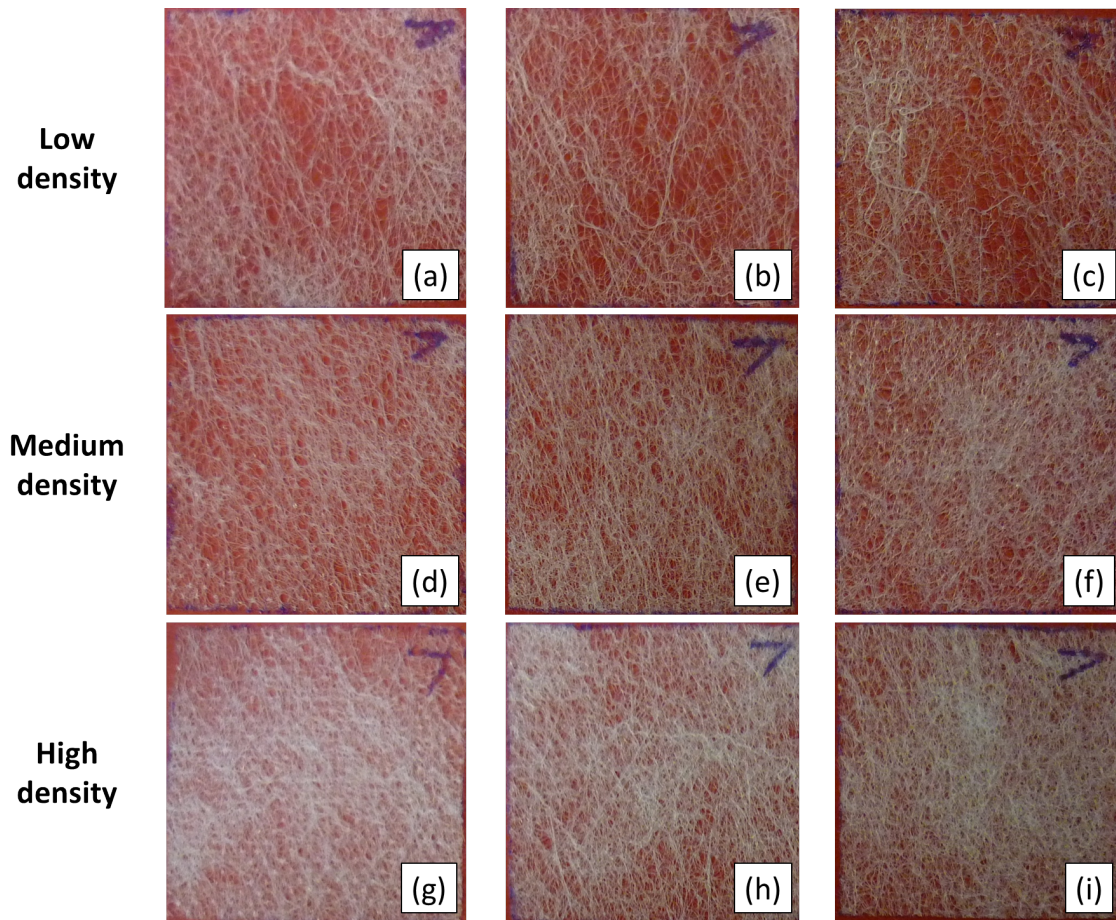


Figure 6.7: All samples of SF17 (whole, 30 mm × 30 mm) used for the area density test

6.2 Results

In this section, all data collected using the methods described in §6.1 are presented for analysis, having been processed using the techniques also described in §6.1. The main focus of data collection was the effect of applied pressure on fibre footprint, so these data are presented first (§6.2.1). Studying the impact of local area density on total contact length was also of interest; the results are presented next (§6.2.2). Although the nonwoven samples examined were not the same ones used in friction measurements (to investigate the effect of area density), the relationship between friction and fibre footprint will still be discussed in §6.3.3.

6.2.1 Investigating the effect of applied pressure on fibre footprint

Figure 6.8 displays examples of the end result of processing images collected using the microscope. Each image was for one sample of each nonwoven under 1.5kPa. These EPS images provided a way to qualitatively analyse the contact, while the corresponding numerical data – fibre contact length values – provided a basis for quantitative analysis. Information about the fibre lengths and distribution, for different nonwovens under different pressures, was immediately observable from the images, but was more easily scrutinised in numerical form – see figures 6.9-6.14. Nevertheless, one thing that could

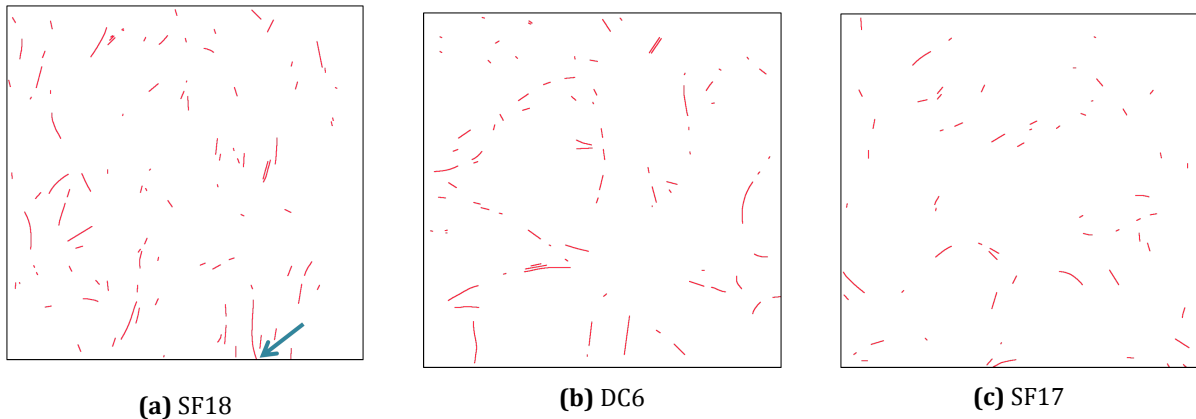


Figure 6.8: Fully processed (EPS) images of samples of nonwovens under 1.5kPa; the arrow indicates where a fibre met the edge of the image

only be determined visually, from raw data, was how many and where fibres intersected the edge of the “sampled” area. This was important for reasons to be explained in §6.3.4 and an example can be seen in figure 6.8a.

Figures 6.9-6.11 show the effect that applied pressure had on total fibre contact length for each nonwoven; each data point was from a different sample and the associated error was based on the reproducibility of the total contact length values for the same image⁴. These graphs provided a general insight into the behaviour of nonwovens under pressure and the differences between their structures. In addition to this, it was anticipated that the individual lengths and distribution of fibres in contact with the slide would help to make a more in depth assessment of the different nonwoven fabrics, when combined with information about their specific structures. Although the EPS images – the final visual output of image processing – enabled a qualitative analysis, it was useful to plot the actual length values (see figures 6.12-6.14). The first two of these figures are example frequency distribution graphs; the final figure is an array of all frequency distributions for easier comparison across pressures and nonwovens. (Note that *relative* frequency was plotted on the y-axis for each of these graphs: that is the frequency as a proportion of the total number of contacts.)

⁴Three tracings of the same MATLAB-enhanced micrograph (see step 2 of figure 6.3) were produced and compared for repeatability; the percentage error in total contact length value, due to the subjectiveness of determining which fibres were in focus, was calculated.

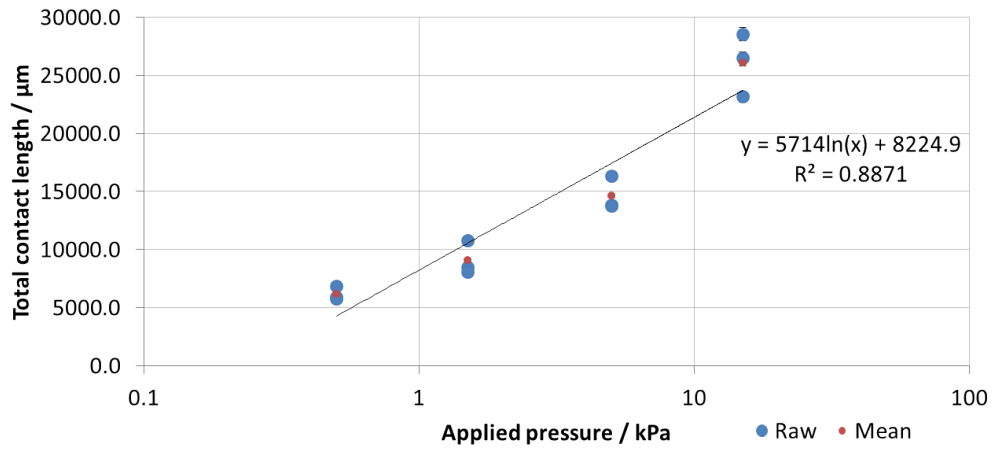


Figure 6.9: Relationship between total contact length and pressure for DC6

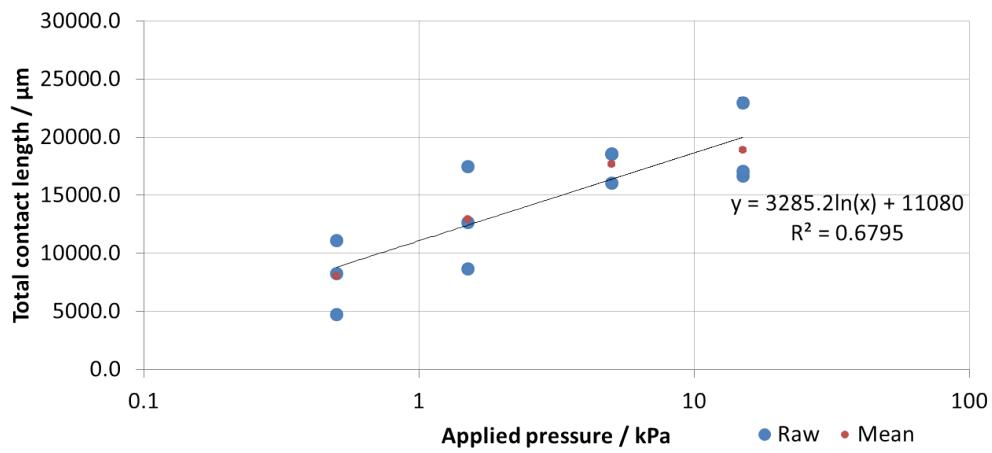


Figure 6.10: Relationship between total contact length and pressure for SF18

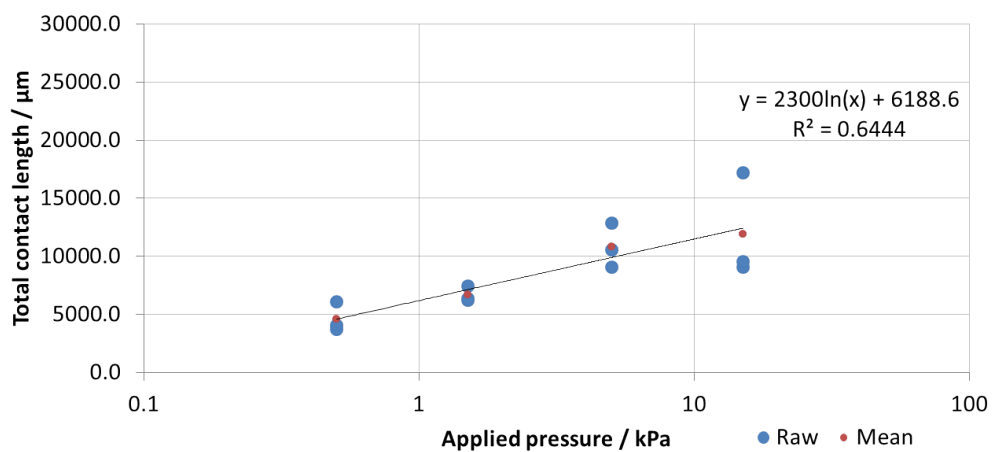


Figure 6.11: Relationship between total contact length and pressure for SF17

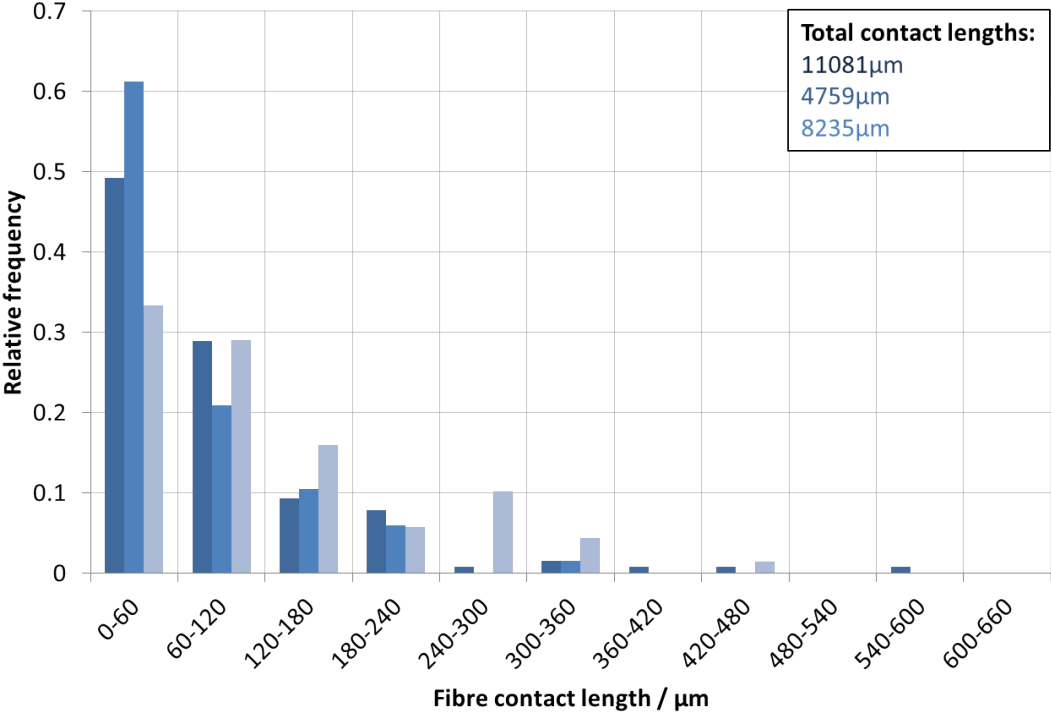


Figure 6.12: Fibre contact length distribution for three samples of SF18 under 0.5kPa

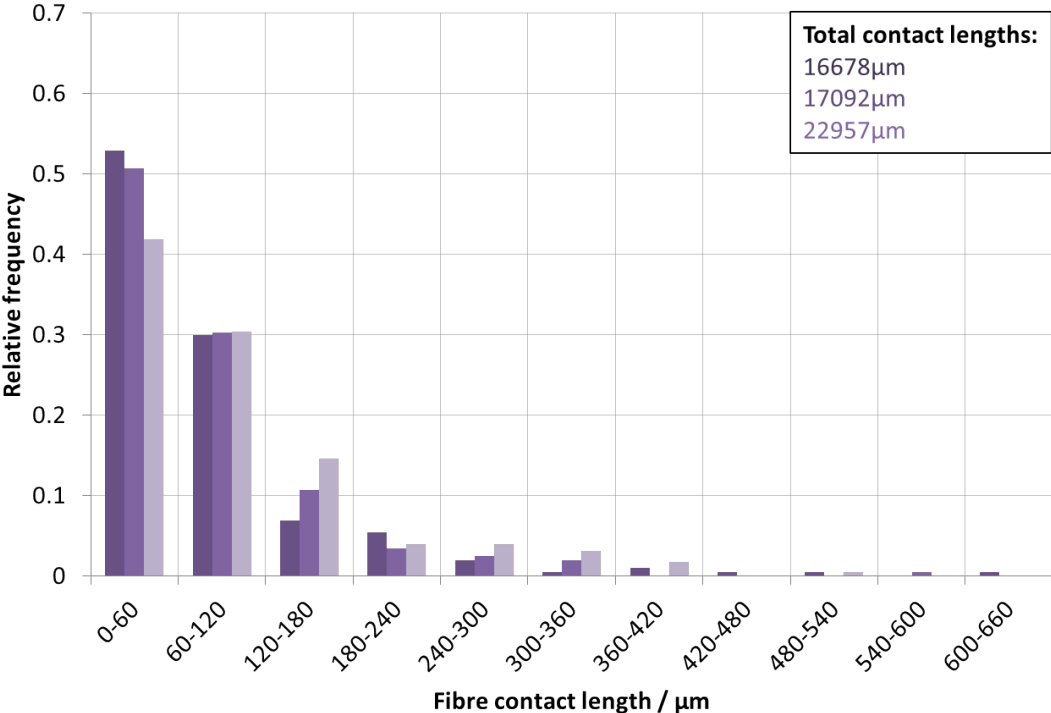


Figure 6.13: Fibre contact length distribution for three samples of SF18 under 15kPa

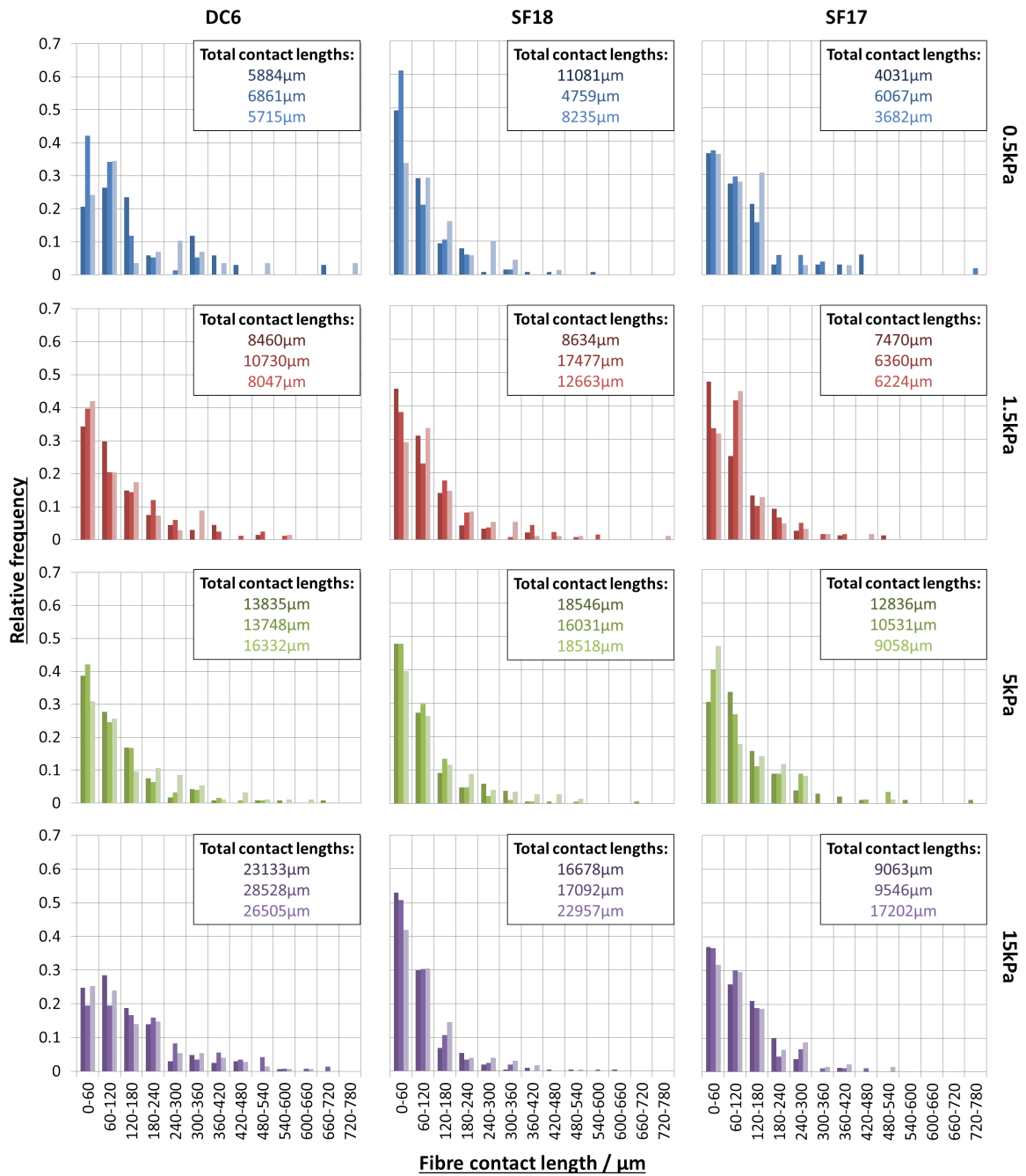


Figure 6.14: Relative frequency distributions of fibre contact length for all pressures and nonwovens tested; all axes have the same scale (x = 0-780 μm, y = 0-0.7 and relative frequency = frequency/total no. of fibre contacts) as in the previous two figures

6.2.2 Investigating the effect of local area density on fibre footprint

As all measurements for the area density test were carried out under the same pressure, all contact length data could be presented on one graph. First, the effect of the area density of whole samples on fibre footprint was studied, hence figure 6.15. Total contact length was also plotted against the area density of the central portion of the sample, as shown in figure 6.16. For reasons that will be explained in §6.3, the proportional difference in area density was calculated using equation 6.1.

$$\frac{\text{local area density of whole sample} - \text{local area density of sample centre}}{\text{local area density of whole sample}} \tag{6.1}$$

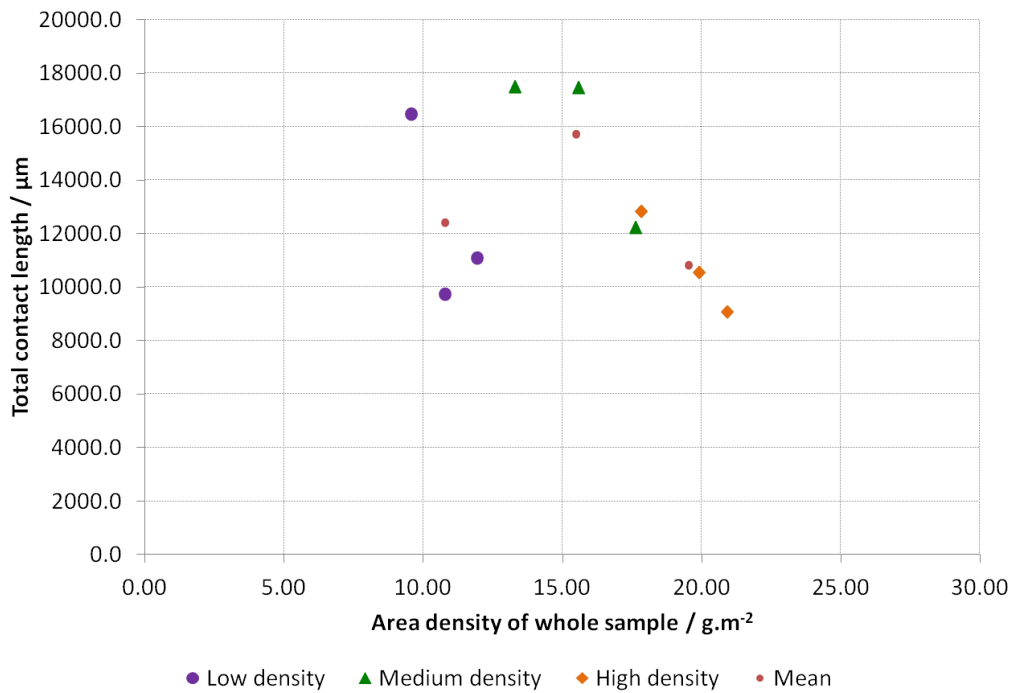


Figure 6.15: Relationship between total contact length and local area density of whole samples of SF17 under 5kPa

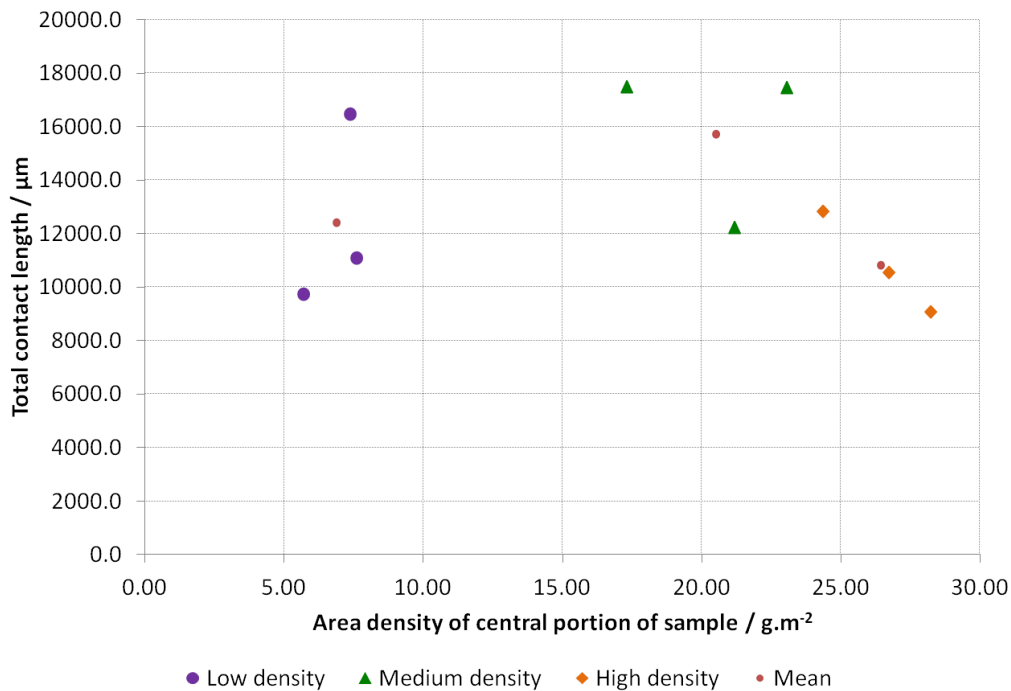


Figure 6.16: Relationship between total contact length and local area density of central portions of samples of SF17 under 5kPa

6.3 Discussion

Before and during the collection of the data presented in the previous section 6.2, it was anticipated that this microscopy technique would enable cross-evaluation of the nonwovens examined by producing contact length values representative of a true contact area. It was also predicted that this information would, in turn, provide an insight into how friction is mediated by the skin-nonwoven interface and how this may relate to the properties of the nonwovens. In this section, all of the data relating to fibre footprints of nonwoven fabrics against a skin surrogate (microscope slide) are analysed, starting with the effect of applied pressure (§6.3.1). Next, the impact of local area density on the total contact length of a nonwoven sample is discussed (§6.3.2), followed by suggestions of how the experiment could be improved, focusing on data analysis (§6.3.4). Any direct links between fibre footprint and friction data will be discussed in §6.3.3.

6.3.1 Investigating the effect of applied pressure on fibre footprint

Of the three nonwovens tested, DC6 showed the greatest (relative) increase in total contact length with increasing applied pressure, and the least change occurred with SF17. In all three graphs, (see figures 6.9-6.11, there was a strong positive correlation and the relationship between contact and the log of pressure was linear. At the lowest pressure, all nonwovens produced a total contact length of approximately 5 mm for at least one 30 mm × 30 mm sample. The fabric with the largest total contact at the highest pressure was DC6. Overall, SF18 displayed the most inter-sample scatter, suggesting that variation in the material (e.g. local area densities) was responsible for more of the changes in contact length than the pressure itself. In fact, there was generally more overlap here, from one pressure to the next,

than for SF17, which may have been a consequence of greater material variability or purely based on chance – something that occurred during sample selection. Considering the fact that samples of SF17 with visually similar area densities were chosen, it appears that the latter was more likely, assuming that basis weight had any effect. This is something that will be discussed in more detail in §6.3.2.

Before analysing the data for these three nonwovens any further, it is important to make reference to those collected by Cottenden [4]. As with any experimental procedure that relies on human judgement, there was a risk of error in both data collection and processing. It was necessary to adjust the microscope stage height so that the microscope slide-nonwoven interface was in focus across the entire area, and later, to consistently assess which fibre portions were in focus for tracing. The former was easily checked during preliminary testing and the latter by making multiple tracings of the same processed micrograph. After assessing repeatability of the method, the subjectivity of distinguishing between fibres in and out of focus was evaluated. Cottenden compared his tracings with those of various volunteers, but as the purpose here was to ensure comparability of old and new data for DC6, old MATLAB-processed micrographs were traced. Repeatability was calculated to be 98-99.5% and differences based on subjectivity were consistently 30-35%⁵; both were computed from *total* contact length values.

The relationship between total contact length and pressure for DC6, displayed in figure 6.9, was very similar to that found by Cottenden. It would, therefore, be reasonable to assume that the relationships for SF17 and SF18 were also comparable, despite the probability that Cottenden would have produced larger total contact length values from the same MATLAB images. For the purposes of this thesis, it was deemed acceptable to make relative comparisons between the nonwovens based on the data presented in this chapter.

Figures 6.12 and 6.13 display relative frequency distribution data for samples of SF18 under the lowest (0.5kPa) and highest (15kPa) pressures plotted from raw fibre footprint data. The main difference was the increase in the *number* of contacts, although there were a few new longer contacts. Overall, there was no change in the proportion of individual lengths, i.e. the distribution was essentially the same. It is clear from the full set of graphs for SF18 in figure 6.14 that this was the pattern for all applied nominal pressures. This particular pattern implies that fibre movement within the samples was rather restricted. The shapes of the fibre contact length distributions were similar for SF17 and DC6, most of the contacts being short in length (0 – 120 μm) and covering mostly the same range of lengths. Nonwoven DC6 had the longest fibre contacts – up to 1440 μm (not shown in figure 6.14) – and its distribution appeared to be the most affected by a relative increase in individual fibre contact length. Between 0.5kPa and 1.5kPa, and 5kPa and 15kPa, there was a slight ostensible shift in distribution, suggesting that the increases in total contact length were, in part, due to increases in *individual* fibre contact lengths. This was further supported by the greater frequency of short contacts for SF18, despite the lower total values.

It is important to remember that there were 12 samples per nonwoven, or three per pressure, which inevitably increased the chance of inter-sample variation. Nonetheless, comparisons could be made between samples at each pressure. Following closer examination of the graphs in figure 6.14, the relative frequency distribution was most skewed for SF18 and least for DC6 (with the exception of 0.5kPa), but it could be argued that this may change if more samples were to be compared. This observation was complementary to total contact length data. Unfortunately, the scanning area was limited – roughly 25 mm^2 compared to a 625 mm^2 sample size, which equates to approximately 4%. It may have been

⁵Cottenden's total fibre contact lengths were always higher, although not necessarily the *number* of contacts.

the case that the total contact lengths of entire samples were the same, under a certain pressure, but that the scanned sections were particularly unrepresentative of the whole test piece. This was evident when studying smaller (5 mm^2) images, with varying fibre length and density within the area.

Considering the properties of the nonwoven fabrics, it might be expected that the fibre material (polymer), manufacturing process and bonding would, together, affect the overall compliance of the nonwoven. It could be assumed that a fabric with a low nominal compliance would be less affected by an increase in applied pressure, as was SF17. Nonwovens SF17, SF18 and DC6 were all spunbond and calendered (bonded thermally under pressure), which suggests that they should all have had considerable strength without further treatment. All three nonwovens had the same proportion of bonding area. Fibres of SF17 and DC6 were all made from polypropylene (PP) and those of SF18 had a PP core with a polyethylene sheath. Although all of the above provided a good explanation for the physical appearance and texture of the fabrics, it did not reflect their behaviour under pressure in terms of total contact length. It may, in fact, have related to something as simple as layering: SF17 appeared to have the fewest layers of fibres, which also had the largest diameters. These factors combined provide a more feasible explanation for the low dependence of total fibre contact length of SF17 on applied pressure.

Linear density could be accepted as a good indication of fibre diameter and therefore widths of contacts, but it was not particularly useful here because contact widths could not be measured on a microscale. In the case that they could be measured or estimated, they would be negligible relative to the contact *lengths*. All three nonwoven fabrics were coated with a surfactant, but this did not affect the fibre footprint measured using the microscopy technique, despite the possibility that it would have had an impact on contact on a nanoscale. If anything could be gleaned from the results of this experiment, it would be that nonwoven DC6 – the fabric most influenced by nominal pressure – would most likely be the best choice if the aim was to maintain the *true* pressure at a skin-nonwoven interface, although that also assumes the relationship between fibre footprint and applied pressure is always the same.

It might be anticipated that area density, considered alongside manufacturing process, bonding (distribution and number of points) and fibre polymer, influenced fibre contact length distribution. This is because these properties would affect the ability of fibres to form different length contacts with a surface. The basis weights were very similar – $15 \text{ g} \cdot \text{m}^2$ for SF18, $17 \text{ g} \cdot \text{m}^2$ for SF17 and DC6 – and unfortunately no information was available on the number of bonding points per unit area to be able to make this comparison. Based on previous observations of fibre layering and low area density, it was anticipated that SF17 would produce the longest individual contacts, but this was not the case. Nevertheless, it would be irresponsible to place too much emphasis on these data, simply because the lack of uniformity of nonwovens could lead to different frequency distributions and total contact lengths when testing different samples.

One thing that remained constant – and could therefore not affect fibre footprint – was the substrate material (glass microscope slides). This means that, not only was the variation between contact lengths of samples real, the relative differences in footprint between applied nominal pressures were *representative* of contact between nonwoven fabrics and human skin (or Lorica Soft). As explained by Cottenden, the principal influence on fibre footprint is the mechanical properties of the nonwoven fabrics as a whole, due to their low compressive moduli relative to that of the substrate and individual fibres [141]. This applies to skin as a substrate as much as glass or artificial leather (LS) and the expected differences between the total contact lengths for each of these would be negligible, at least for the pressure range and experimental setup used. Further, Cottenden demonstrated this via mathematical modelling of the interface as a linear elastic half space [4, 141], which also applied to the data

presented here as the nonwovens examined did not vary too greatly from those described in that paper. To conclude, the contact length data presented in this thesis were characteristic of those that would be collected for skin, including inter-sample variation, regardless of the use of glass as a substrate.

6.3.2 Investigating the effect of local area density on fibre footprint

Taking into account the visibly obvious non-uniform nature of the nonwovens investigated in this chapter, and the results of exploring the impact of area density on friction, it was imperative that the same was done for fibre footprints. As the inconsistencies in SF17 were especially clear, samples with different local densities were selected by eye, but it was difficult to obtain a sample with the same particular density across its whole area, let alone several with a common density. Ideally, samples with uniform densities would have been weighed before use, or the relevant regions weighed without destroying whole samples. As this was not possible, it was anticipated that qualitative sample selection would be adequate for the task at hand, but that quantitative assessment of local area density would be necessary for data analysis.

Figures 6.15 and 6.16 demonstrate why this decision was sensible. Data points were colour-coded according to their qualitative densities: purple = low density; green = medium density; and orange = high density. More overlap was observed for whole samples than for central portions of samples, but this was acceptable because it was the centres that were scanned under the microscope. Considering the two sets of densities separately, it was evident that there was no relationship between them and total contact area. This is perhaps unsurprising following the lack of relationship with friction forces and the minimal effect of nominal pressure on total contact for SF17. However, the differences between figures 6.15 and 6.16 suggest that there may, in fact, have been a hidden connection between local area density and total contact length.

In §6.1.3, figure 6.7 showed not only the differences between selected samples, but also the variations within each. It was visibly evident that samples (f)-(i) were slightly denser in the centre, (b) and (c) were clearly denser outside the central 49 mm², and (a), (d) and (e) were relatively uniform. The potential implication of testing a sample with a lower density in the centre was that the pressure was not equally distributed across the sample, and the nominal pressure at the centre was lower than that on the rest of the piece of nonwoven. The reverse (high density centre) may have resulted in a higher pressure being applied to the centre. Data from figures 6.15 and 6.16 were combined to check the probability of these two situations. Calculating the proportional difference in area density between the whole and centre of each sample gave an indication of which scanned areas may have been exerted to more or less pressure than intended. Interestingly, but unsurprisingly, all “low density” samples had lower densities at their centres and the smaller the difference in density in proportion to the whole sample, the larger the total contact length. This implies that there *was* a relationship between area density and fibre footprint, contrary to earlier analysis. However, this appeared not to be so for the other samples of SF17. With these conflicting findings from data on only nine samples of SF17, it was impossible to determine whether fibre contact length was influenced by or dependent on local area density.

A sample of nonwoven fabric with varying *volume* density can, for the purposes of analysing its mechanical properties, be likened to a composite made from materials of different densities. Depending on the orientation, either uniform strain or uniform stress can be applied and the other will vary throughout its volume – a similar idea to Voigt and Reuss models (see figure 6.17). According to the

Voigt model, strain is constant across the loaded area:

$$\epsilon_t = \epsilon_a = \epsilon_b, \tag{6.2}$$

where ϵ is the strain across the total area (t) under load and across the areas of the constituent materials (a and b) with different densities.

Since Young's modulus, $E = \frac{\sigma}{\epsilon}$ (where σ is stress) and a nominal pressure, P , is applied across the whole sample, equation 6.2 can be written:

$$\frac{P}{E_t} = \frac{\sigma_a}{E_a} = \frac{\sigma_b}{E_b}.$$

If $E = kD$, where D is area density and k is a constant,

$$\frac{P}{D_t} = \frac{\sigma_a}{D_a} = \frac{\sigma_b}{D_b},$$

and

$$\sigma_a = \frac{P \cdot D_a}{D_t}$$

or

$$\sigma_b = \frac{P \cdot D_b}{D_t}.$$

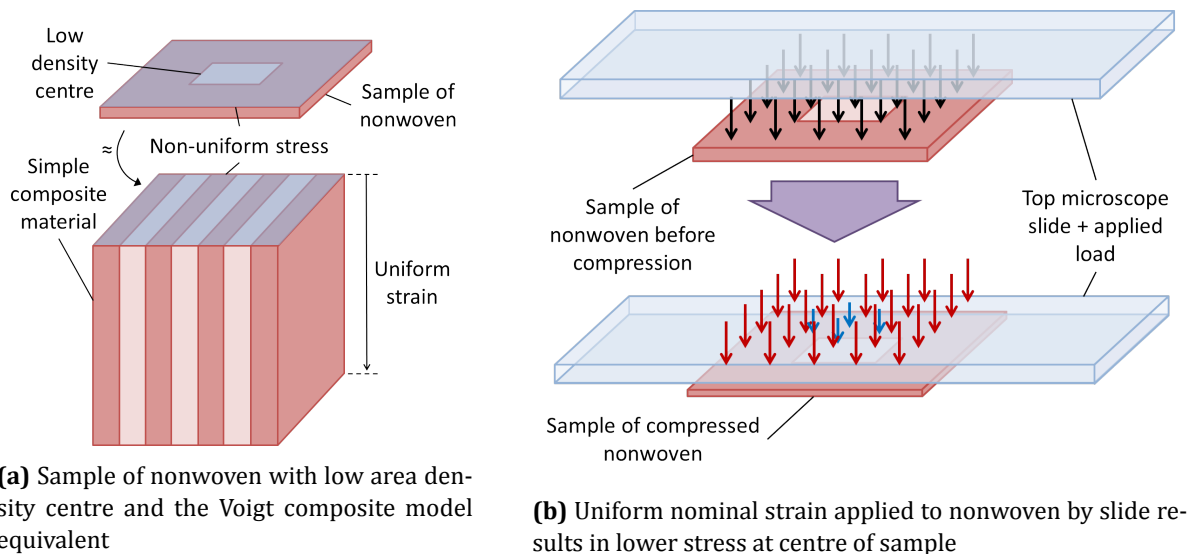


Figure 6.17: Distribution of pressure on a sample of nonwoven with a lower density centre; **black arrows** represent nominal pressure, **red arrows** are for higher localised pressure and **blue arrows** for lower localised pressure

In the case of nonwovens, the higher density regions have the higher “modulus” of elasticity and vice versa for low density regions. This means that the strain would be limited by high densities or *possibly* the thickness of low density areas. If it is assumed that area density is proportional to volume density, the distribution of nominal normal stress will differ greatly across the interface. In contrast, if volume density is relatively constant, the nominal pressure will essentially be uniform, even though the *true* pressure will not. The thickness of SF17 was measured under a nominal pressure of 0.4kPa

for 10 different regions and varied from 0.19mm to 0.24mm. It resulted in a mean volume density of $66.1 \text{ kg} \cdot \text{m}^{-3}$, with considerable fluctuation. Unfortunately, the raw values were calculated from one area density value (the basis weight), so this is inconclusive, but an area-volume density relationship may be inferred when comparing SF17 values with those of other nonwovens – see table 6.2. Not only were the volume densities *not* proportional to the area densities, the variation (standard deviation) between the latter was greater than that of the former. This implies that it is the true pressure that is primarily affected by varying area density.

Table 6.2: Thickness and densities of nonwoven fabrics in the subset

Nonwoven	Thickness / mm	Std dev	Area density / $\text{g} \cdot \text{m}^{-2}$	Volume density / $\text{kg} \cdot \text{m}^{-3}$
SF3	0.689	0.009	46.9	68.1
SF14	0.508	0.016	33.2	65.4
SF17	0.221	0.016	14.6	66.1
SF18	0.169	0.015	15.0	88.8
DC6	0.230	0.020	18.1	78.7

Results from experiments described in §6.1 suggested that the SF17 fibre footprints were less affected by nominal pressure than the other nonwovens tested. It is not clear whether this was the case because of non-uniform distribution of pressure across these samples, or that there was no distinct relationship between area density and contact length for the aforementioned reason. Either of these would depend on some structural property (or properties) of SF17, which could not be identified in the absence of similar fibre footprint data for other nonwoven fabrics. Although SF18 was also a visibly variable material, it would have been a very time-consuming – and not necessarily fruitful – task to select samples of different local area densities for investigation. Furthermore, DC6 had the most uniform structure and would have been unsuitable for this experiment.

Considering that these data were representative of skin-nonwoven contact, it can be assumed that the relationship – or lack thereof – between nonwoven local area density and total contact length would remain unchanged by applied pressure. Whether the total fibre contact length of a sampled area was less than it ought to be because the nominal pressure was not uniformly distributed, or the pressure genuinely had no effect on contact length, both are possible explanations for the insignificant differences in friction force measured in the complementary friction measurements. If true contact length was affected by local area density, it may be that the true pressure applied to the nonwoven fibres varied to compensate, without changing the friction forces. In the opposite situation, it may be that the nonwoven sample deformed to maintain the nominal pressure throughout its structure, also maintaining the friction force. For pad-wearers, this would mean that a nonwoven with a lower total contact length would have a high pressure at the fibre-skin interface, regardless of friction force. Unfortunately, it is unknown *which*, if either, would have the greater impact on skin damage: high localised pressure or high friction forces between the skin and nonwoven.

6.3.3 Relationship between fibre footprints and friction data

Before analysing friction data alongside fibre footprint data, it is important to remember that not all fabrics tested in dry friction measurements were examined under the microscope. This means that comparisons can only really be made here between nonwovens SF17, SF18 and DC6. Ideally, the friction measurements between dry volar forearm skin and nonwoven fabrics would have been recorded under

a microscope to monitor the contact at the interface during sliding. This would have enabled a more direct comparison between the sets of data, but there is no known practical and effective method of measuring such skin-nonwoven contact thus far. A similar experiment was conducted by Cottenden [4] with the flat skin surrogate, but the resolution was too poor for the footage to be useful.

The data in chapter 4 suggest that Amontons' law holds for friction between volar forearm skin and nonwovens and is in line with other studies that suggest adhesion as the contributing mechanism [80, 89, 91, 92, 94, 95, 97]. If the magnitude of adhesive forces is related to the friction force offset size at zero applied load, it could be stated that, on average, nonwoven SF18 has the highest adhesive forces of the three examined under the microscope and DC6 has the lowest. Adhesive forces could also be associated with total contact area, however, the order of nonwovens when ranked for offset is not the same as for total contact length. The local area density of a nonwoven (SF17) had no significant effect on friction force, but the impact on fibre footprint was inconclusive. Amontons' second law of friction states that the coefficient of friction is independent of nominal contact area, but fibre footprint measurements are closer to *true* contact area, so no further comments can be made relating to that.

It is accepted that skin deformation was only observed on a macroscale and that the surface of the SC on a microscale is unknown in both wet and dry conditions, but it is assumed, based on work by Hendriks and Franklin [78] that the surface is smoother when wet. In the case of contact between nonwoven fabric fibres and skin, it is anticipated that a smoother surface (due to swollen stratum corneum cells) would enable a greater total contact area.

The gradients of total fibre contact length against pressure did not correlate with the average 'maximum tensometer force vs applied load' gradients or the coefficients of static friction for wet skin, which suggests that either:

- friction depended less on pressure than total fibre contact length did;
- the area studied under the microscope was too small to get a fair estimation of contact;
- or the real contact between fibres and skin was less dependent on applied load and more dependent on the mechanical properties of the fabric as a whole and its ability to deform under pressure.

Fabric area density appeared to have no effect on friction between nonwovens and human skin but fibre footprint measurements were inconclusive. With this in mind, it was considered that, where area density varies, the fabric might deform locally to accommodate the load and/or facilitate friction so that the true contact pressure remains the same. None of the other manufacturing processes or structural properties of the nonwovens are useful in the comparison of friction and fibre footprint data.

6.3.4 Improvements for future analysis

Total contact length data were not affected by incomplete fibre contacts at the boundary of the scanned region, but the *frequency distribution* of individual contact lengths may have been misleading. To accept the frequency data at face value would be to assume that contacts at the edge of the sampling area did not extend beyond this boundary. This was often not the case, meaning that many contacts were longer than they appeared within the sampled region, thus introducing an error in calculations. In order to calculate the associated error, it is necessary to measure contact lengths for a much larger area and compare this to data from smaller sections of the same area. If done manually, this would take a very long time, not to mention the complexity of making the relevant calculations by hand.

To avoid wasting time this way, a BASH script, written by D. J. Cottenden, could be applied to images eight times the area of normal sampling areas. The script would take the large EPS image file (after

processing it as described in §6.1.2.3) and another EPS file containing a reticule, as inputs, and then output correction matrices and bins for grouping data. The purposes of the bins and matrices would be to group the data appropriately and apply corrections to the grouped frequency data respectively. Depending on the particular nonwoven, a different set (or *matrix*) of correction factors would need to be applied, hence varying bin widths. To test this, three micrographs were produced – one per nonwoven – by scanning an area eight times that of normal sampling areas, under a nominal pressure of 0.19kPa. This pressure was chosen for practical reasons: the testing rig (see figure 6.1) could not be used when scanning an area larger than 5 mm × 5 mm because it would obstruct the light source; the total height and width of the dead weights applied directly to the top slide had to be restricted to avoid collision with the microscope lens during scanning.

The micrographs were processed as described in §6.1.2.3 before the final EPS images were processed further, using the method described above, in conjunction with raw contact length data from each nonwoven under 0.5kPa. The results of this are presented in figures 6.18-6.20. If these figures are compared to figure 6.14, it can be seen that, while there are similarities in the shape of the frequency distributions, the unequal bin widths and their associated varying x-axis limits make it difficult to assess the true distribution of contact lengths. The challenge would be to create a histogram for corrected relative frequency densities with more reasonable data grouping. Also, provided the procedure for data collection could be modified to investigate the pressures used in this thesis, these corrections could be applied to all the data. It would also be useful to limit the number of bins for grouping data, to facilitate their analysis. Due to the constraints of time, the method was not developed further, but would be worth modifying in the event that this work is continued.

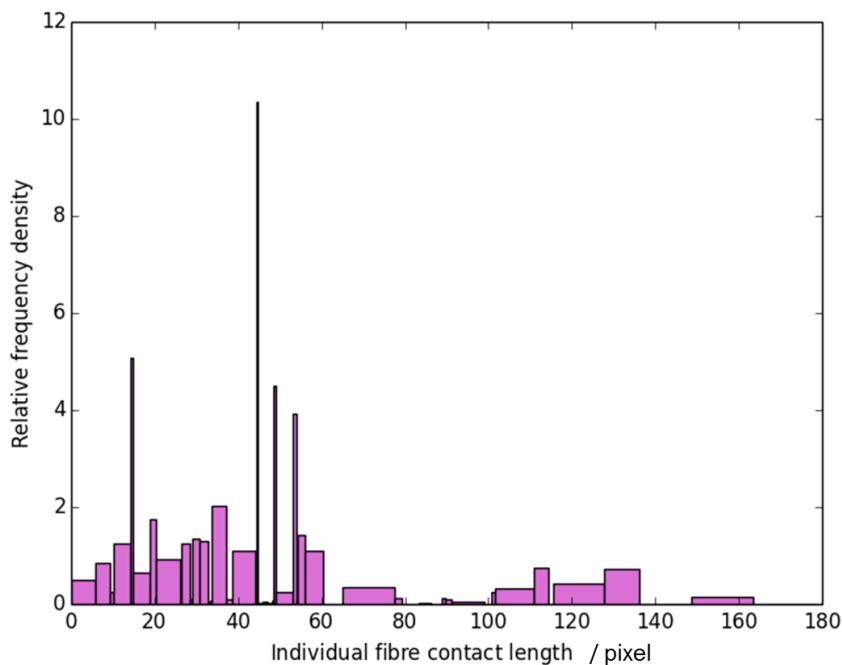


Figure 6.18: Corrected fibre contact length frequency data for one sample of DC6 at 0.5kPa

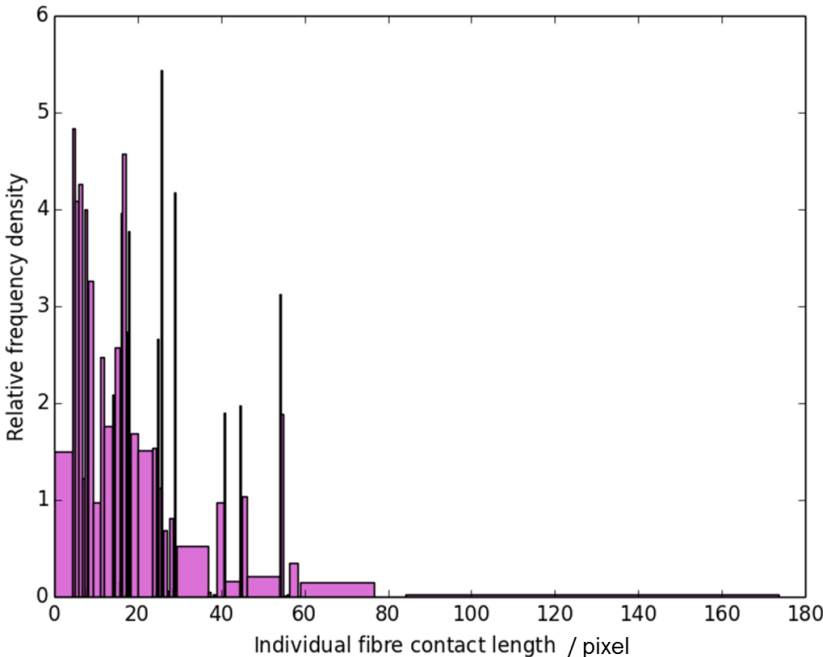


Figure 6.19: Corrected fibre contact length frequency data for one sample of SF18 at 0.5kPa

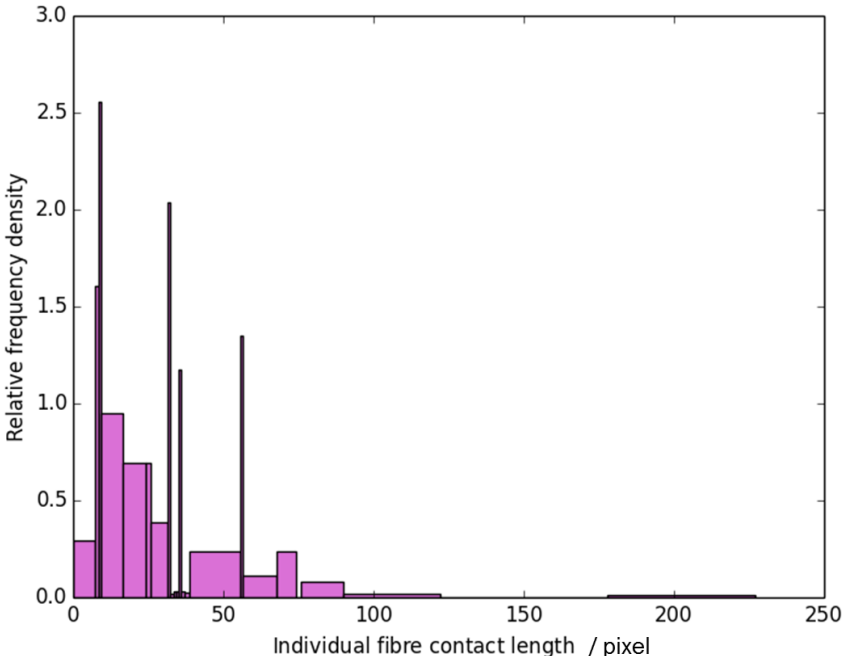


Figure 6.20: Corrected fibre contact length frequency data for one sample of SF17 at 0.5kPa

CHAPTER 7

CONCLUSIONS

“...on fait la science avec des faits comme une maison avec des pierres; mais une accumulation de faits n’est pas plus une science qu’un tas de pierres n’est une maison. (...science is made with facts as a house with stones; but an accumulation of facts is no more a science than a heap of stones is a house.)”

— Henri Poincaré, 1854–1912

EACH STRAND OF WORK in this project, described in chapters 3 to 6, was carried out separately and the results were analysed in stages. Data from groups of experiments were discussed in their individual chapters and compared with those from other chapters, so it is not necessary to provide any more than a brief outline of the conclusions of the project here. This outline is accompanied by an evaluation of the project objectives and suggestions of further work.

7.1 *Summary of conclusions*

A number of interesting findings have arisen from the work described in this thesis – some of which were particularly unexpected – as described in the relevant previous chapters. This section summarises the main conclusions drawn from all strands of work, which have been divided accordingly.

7.1.1 *Friction between nonwoven fabrics and Lorica Soft*

LS was an appropriate surrogate for volar forearm skin for the relative comparison of a large group of nonwovens and in the selection of a smaller representative set of fabrics as the relative differences between nonwovens were similar when tested against human skin.

The different geometries of the surface of Lorica Soft (LS) – flat and curved – did not significantly affect the static coefficient of friction, although it did produce different force-displacement curves. This implies that the geometric configuration of the skin surrogate was only of importance during dynamic friction.

7.1.2 *Friction between nonwoven fabrics and volar forearm skin in dry conditions*

Amontons’ law held for friction between volar forearm skin and a broad range of nonwoven fabrics irrespective of skin compliance and participant age. There was a remarkably linear and proportional relationship between applied normal force and friction force for *all* participants of *all* ages, which it was also independent of compliance of the skin and underlying tissues (wrinkled and flaccid versus smooth and firm).

Relative friction data for a range of nonwovens against one person's skin was typically representative of similar data for many people as the ranking of nonwovens in the subset (by μ_s) was broadly the same for all participants.

The offsets on graphs of friction force against applied load were usually smaller than experimental error and positive. Those larger than the error may be related to the friction mechanism (e.g. adhesion), deformation of the nonwoven or skin, or some other unknown contributing factor.

There was no discernible relationship between nonwoven area density and friction force. This suggests that skin-nonwoven friction is independent of apparent contact area – if area density is indicative of skin-nonwoven contact area during friction – or that a higher proportion of fibres are in contact with the skin for low density samples.

No single nonwoven manufacturing process or property can be attributed to differences in coefficient of friction. The particular combination of manufacturing processes and properties of SF18 resulted in low friction forces (and coefficients). Linear density of a fabric or fibre diameter might be good indicators of how it feels – a measure of comfort – against the skin, though this would require further investigation. Looking for trends between skin-nonwoven friction and structural and mechanical properties of the nonwovens was rather challenging, partly because of the inhomogeneity of the fabrics and partly due to the variation in the data between participants.

The behaviour of the skin and underlying tissues were not always dependent on the age of the participant. Many forms of soft tissue deformation were observed, such as rucking and indentation, as well as the stick-slip phenomenon. Some behaviours were identifiable on force-displacement graphs but the extent of deformation was not always reflected in the friction force.

Some nonwoven fabrics were more susceptible than others to deformation Under the highest loads used in this part of the friction study (0.48N and 0.69N), the strips of nonwoven often deformed laterally. The most robust nonwoven, with the highest resistance to lateral deformation, appeared to be DC6 (the same one used by Cottenden [4]).

7.1.3 Friction between nonwoven fabrics and volar forearm skin in wet conditions

This section has been removed due to its commercially sensitive content. It will be made available in the full version of this thesis, which will be published at a later date.

7.1.4 Fibre footprints of nonwoven fabrics against a glass slide

Total contact length increased linearly with logarithmic pressure for all nonwovens and the gradient was different for each one. There was some scatter caused by variation between samples of nonwoven. Fabric DC6 showed the most dependence on applied pressure, with the highest gradient, whereas SF17 changed the least.

The distribution of fibre contact lengths mostly remained the same with increasing pressure although there was some shift for DC6; as pressure increased from 0.5kPa to 15kPa, there was a small increase in the number of longer contacts for this nonwoven. This was most likely due to the mechanics of the micro-structure.

No clear relationship between total fibre contact length and local area density was established in this work as analysis of the data was inconclusive. This may have been due to limitations of the method, such as the inability to control the distribution of pressure across a sample of nonwoven.

Friction data for all nonwovens appear to be independent of their true contact areas with skin based on total fibre contact length data. This does not contradict nor support the evidence that Amontons' law holds for friction between volar forearm skin and these nonwovens. It suggests that applied load is distributed throughout the entire structure of a nonwoven sample so that not all is translated to increase the contact area, but the true pressure at the points of contact varies depending on the nonwoven and particular sample.

7.2 Evaluation of the project based on objectives achieved

The aims and objectives of the work carried out in this project were set in §2.7 at the end of the literature review. This section is an assessment of which of the objectives were attained.

7.2.1 Friction between a skin surrogate and nonwoven fabrics

Examination of a broader range of nonwoven fabrics: The force-displacement curves for friction between Lorica Soft and the wider range of nonwovens (used in this project) were consistent with those for Cottenden's [4] nonwovens. A subset of five fabrics for further testing was successfully selected using this method in conjunction with measurements on real skin.

Measurements of friction on a skin surrogate in a curved configuration: Coefficients of static friction for flat and curved LS were similar, but not the raw data traces. Whether or not a curved surrogate undergoes sufficient change at the surface to produce different friction forces with nonwovens could not be determined. Nonetheless, LS wrapped around a solid cylinder was also useful in the selection of the subset nonwovens.

7.2.2 Friction between volar forearm skin and nonwoven fabrics in dry (normal) conditions

Selection of a subset of nonwoven fabrics: As mentioned previously, five nonwovens were selected for further examination (on participants) based on the friction data from both skin and the skin surrogate. The decision was also made based on the structural properties of the fabrics, including as large a variety as possible.

Ethics: Research Ethics Committee and Research and Development approvals were successfully obtained for this study (on dry and wet volar forearm skin) in September 2011.

Measurements of friction between volar forearm skin and nonwovens: Friction measurements were made on the volar forearm skin of 19 volunteers (aged 20–95 years) in normal (dry) conditions with the subset of nonwovens, using a similar method to Wong [3]. The data were compared to those from the skin surrogate, the conclusions of which, can be found in §4.3.4.1.

7.2.3 Friction between volar forearm skin and nonwoven fabrics in wet conditions

This chapter has been removed due to its commercially sensitive content. It will be made available in the full version of this thesis, which will be published at a later date.

7.2.4 Interfacial contact (fibre footprint)

Contact length between microscope slides and new nonwovens: The fibre footprints of three out of five nonwovens in the subset were examined using a slightly adapted version of the method used by Cottenden [4]. The data were comparable with those obtained by him and revealed some interesting information about the behaviour of nonwovens under pressure, although analysis was restricted by limitations of the methods.

Application of a mathematical model: No appropriate mathematical model to estimate actual contact area was found.

7.3 Future work

As always, answering one question in research opens the door to many more. Although the work in this project produced many interesting results, there are certain strands that would benefit from further investigation. The principal areas of interest for future work are summarised below.

Human skin friction This text has been removed due to its commercially sensitive content. It will be made available in the full version of this thesis, which will be published at a later date.

Physical models An MSc student in the Continence and Skin Technology Group, Cristina Bogatu, ran experiments on physical models of the volar forearm, simplifying and separating different features used in previous work (by Asimakopoulos [154] and Karavokyros [156]). She used rigid cylinders of various diameters with a low friction surface and sheets of acetate with different bending stiffness to investigate the offsets on graphs of friction force vs applied load [157]. This setup complied with all assumptions made by the mathematical model. The data from these measurements were compared with some for rigid cylinders with a high friction surface, as well as friction between nonwoven and acetate strips and a high friction surface on a compliant cylinder. She found that the bending stiffness of the conforming material was not the cause of the offset, but it may relate to the biaxial deformation of the nonwoven strip on the cylinder (or arm). This work could be continued by using strips of fabric of different dimensions and actively measuring their deformation on the cylinder, which could then be compared to similar measurements on volar forearms.

Fibre footprints Until now, there has been no need to estimate or measure fibre contact *area*, as measurements of total contact *length* were appropriate for investigating fibre footprints against glass and were considered suitably representative of area. Although the method was also deemed apposite for estimating contact with skin, it would be interesting and may be useful to develop an alternative method for investigating actual skin-nonwoven contact. Such a method may involve the use of a linear-elastic quarter-space (mathematical) model or a different imaging technique like Fourier Transform Infrared (FTIR) Spectroscopy. Some work with FTIR Spectroscopy was attempted during this project (as explained in chapter 6) and would be worth further investigation.

Other work Measuring friction between *excised* skin and nonwoven fabrics in the absence – and possibly presence – of fluid is another possible option for further investigation of skin deformation in friction. The contribution of the underlying tissue to friction could be eliminated by removing (excising) the epidermis and dermis from part of the body. Ideally, the stratum corneum would be isolated from the rest of the skin and tested separately, but the more practical and feasible next step would be to measure friction on the skin as a whole. It is anticipated that the data obtained from these experiments

would help to explain the deformation observed in friction measurements on skin *in vivo* and to determine the size of the effect of skin without subcutaneous tissue on force-displacement curves. This work was attempted on excised breast skin before the volar forearm friction study began, but little progress was made due to a limited supply of skin (see appendices G and H). It was tested in a flat configuration using the equipment described in §3.2.1 but could equally be tested in a curved configuration, wrapped around a rigid cylinder, for example.

APPENDIX A

NONWOVEN FABRICS: A COMPREHENSIVE TABLE OF MATERIAL PROPERTIES AND MANUFACTURING PROCESSES

THE FOLLOWING TABLE (A.1) contains all known details of all 14 nonwovens used in preliminary testing (DC6-SF18) and two others used by Cottenden [4] (DC1 and DC3) in addition to DC6. Missing information is represented by '-'. The fabric codes bear no special meaning; nonwovens were simply labelled with the initials of the researcher who originally tested them (DC = David Cottenden, SF = Sabrina Falloon) and a randomly assigned number. In the 'Manufacturing/Bonding' column, manufacturing processes are listed first, then bonding techniques. PP, in the 'Polymer' column represents polypropylene, PET is polyethylene terephthalate and PE is polyethylene; S/C bico refers to the sheath/core ratio of a bicomponent fibre. Two of the surfactants (final column) have been named, but it is not known whether they are hydrophilic or hydrophobic.

Table A.1: Full details of nonwoven fabrics used in this study and a previous study [4]

Fabric code	Material no.	Fabric Manufacturing/Bonding	Fibre Polymer	Fibre Dtex	Fabric Weight / $g \cdot m^{-2}$	Area	Fabric Bonding Pattern		Fibre Surfactant
							Points / cm^2	Shape	
DC1	103-237-1	Spunbond and calendered	PP	2.0	17	12%	-	-	-
DC3	103-237-3	Spunbond and calendered	PP	1.4	17	12%	-	-	Siltasol
DC6	103-237-6	Spunbond and calendered	PP	3.6	17	12%	-	-	Siltasol
SF1	18NN/SS4FW-01	Spunbond and calendered	PP	2.0	18	18%	50	round	none
SF2	18NN/SS4BW-01	Spunbond and calendered	PP	2.0	18	11%	9	rod	none
SF3	sawatex*2621/2021	Carded and hydroentangled (spunlaced)	PET	1.7	50	-	-	-	-
SF7	article code 272	Spunbond and calendered	PP	2.5	20	12%	-	-	none
SF9	article code 350	Spunbond and calendered	PP	6	20	12%	-	-	hydrophilic
SF10	18NN/SS4FW-01	Spunbond and calendered	PP	-	18	-	-	-	none
SF11	Terpo 18 phil	Carded and calendered	PP	2.2	18	25%	65	standard	-
SF12	TricTrac 30 phil	Carded and calendered	PP	2.2	30	25%	11	oval	hydrophilic
SF14	Tricot 30 XL	Carded and calendered	PP	1.7	30	25%	11	-	-
SF15	13NN/SS4FW-01	Spunbond and calendered	Cotton 5%	2.0	13	18%	50	round	none
SF16	25NN/SS4FW-01	Spunbond and calendered	PP	2.0	25	18%	50	round	none
SF17	103-269-1	Spunbond and calendered	PP	6.5	17	12%	-	-	lutrasil
SF18	103-261-1	Spunbond and calendered	PE/PP	1.5	15	12%	-	-	hydrophilic

APPENDIX B

RESEARCH ETHICS COMMITTEE APPLICATION: VOLAR FOREARM FRICTION STUDY PROTOCOL

THIS CHAPTER COMPRISES the supporting documents for the Research Ethics Committee application for the study of friction between nonwoven fabrics and volar forearm skin. The application form itself was too long (29 pages) to include and would not have added to the value of this appendix. Some of the supporting documents varied according to the source of participants for which it was intended; all versions of such documents have been included. The supporting documents for the REC application are presented in the following order: protocol, participant information sheets, letter to the GP, consent forms and finally advertisement material (for recruitment of participants into the study).

Protocol for a study of friction between volar forearm skin and nonwoven fabrics

Sabrina Falloon¹, Alan Cottenden¹, James Malone-Lee², Mary Rabbitte³

¹Department of Medical Physics & Bioengineering, University College London, UK

²Department of Medicine, University College London, UK

³Cheverton Lodge Care Home

20 July 2011, version 2.1

Full title of study An experimental study of the friction between excised, healthy, blemish-free human skin and nonwoven coverstock fabrics, preparatory to theoretical modelling of this interaction.

Short title A study of friction between human skin and nonwoven fabrics

Chief investigator Prof. Alan Cottenden

Co-investigators Miss Sabrina Falloon, Mr Vasileios Asimakopoulos

Sponsor University College London

Abstract

Wearers of incontinence pads and sanitary towels frequently experience skin abrasion due to friction. The Continence and Skin Technology Group has worked for some years to develop techniques for measuring this friction *in vivo*. In order to deepen our understanding of how this friction works, we now need to conduct a study on real skin *in vivo*.

This study will involve performing some mechanical tests on a *relatively* hairless area of the forearm of volunteers with nonwoven coverstock fabrics. There will of course be interaction between the participants and investigators, but no identifiable information will be included in the study. All participants will have given informed consent before taking part in the study.

Contents

1 Introduction	2
1.1 Background.....	2
1.2 Aims and objectives.....	2
2 Methodology	3
2.1 Identification of subjects and consent.....	3
2.2 Experimental methodology.....	4
2.3 Health and safety.....	5
2.4 Projected timing.....	6
3 Ethics	6
4 Expertise	7
References	7

1 Introduction

The work described in this document involves measuring friction between nonwoven fabrics (similar to tea bag material and commonly used against the skin in incontinence pads) and the volar forearm of adults of different ages. It is the latest of a series of *in vivo* and *ex vivo* experimental studies, having the overall aim of understanding and modelling friction between incontinence pads and skin, so paving the way for the development of more skin-friendly products. The proposed work will use methodologies developed and successfully used in earlier studies, giving a high level of confidence that it will yield fruitful data.

1.1 Background

Approximately five million people in the UK are known to be incontinent of urine, and the prevalence is anticipated to increase further as the growing population ages [1]. Whilst many sufferers can be at least partially cured, the significant minority who cannot be fully cured require products to manage their condition. The most common product type is absorbent pads, but can lead to skin damage, often in the form of Incontinence Associated Dermatitis (IAD), of which friction is a major contributor.

The friction mechanisms that occur here must first be identified and modelled before products can be improved to be less damaging to the skin.

So far, many clinical studies have been carried out to determine the prevalence, severity, duration and location of IAD in incontinent nursing home populations [2]. A methodology has been developed for measuring friction between nonwoven fabrics and volar forearm skin [3] - skin on the underside of the lower arm, commonly used as a proxy for the diaper area of the skin. Mechanisms of friction between nonwoven fabrics and a skin surrogate (Lorica Soft) have also been investigated and significant progress has been made toward identifying them [4].

In a current study, I aim to determine whether the friction mechanisms that characterise interaction between Lorica Soft and nonwoven fabrics, also apply to real skin. I am doing this on excised breast skin. *Breast* skin is used because it is mostly smooth and hairless, and it is available in quite large pieces from mastectomy operations. *Excised* skin is used because it has the ability to remain completely stationary throughout testing, and it can also be placed in the apparatus used to test Lorica Soft. This provides a direct comparison between material surfaces (real skin and the skin surrogate) and acts as an intermediate between skin surrogate and real skin *in vivo*. However, properties of the skin change with time once excised, so further testing on human skin *in vivo* is also necessary.

1.2 Aims and objectives

The aim of this study is to validate the findings of the friction mechanism work done so far with *in vivo* measurements on volar forearm skin. This will involve measuring friction force between nonwoven fabrics and volar forearm skin (in wet and dry conditions) on people of different ages and genders, using a range of nonwoven fabrics and pressures.

The methods for obtaining these data are described in §2.2. Experiments relating to these objectives must give an indication of the extent to which the mechanisms and rules identified are common to all people. Consequently, the individuals who participate will vary in age, and if possible, should vary in ethnicity and gender so that any important features that are identified can be established as likely universal, or not. However, though this would be desirable, it is not of primary importance for the present project.

2 Methodology

This section describes all procedures and methods that will be employed in the execution of this work, including the identification of subjects, obtaining consent, the recruitment of participants (§2.1), and the experimental methodologies for making measurements on volar forearm skin (§2.2). The timing of different stages in the recruitment of subjects and the experiments are given in §2.4.

2.1 Identification of subjects and consent

This study will involve working with volar forearm skin *in vivo*. The volar forearm is a fairly flat and hairless part of the body and is easily accessible for taking measurements. This makes it well suited to our experiments: in this exploratory work it is more important that skin is uniform and simple than that it is from the diaper area.

Criteria for *inclusion* in this study are as follows.

- The participant is aged 18 (years) or over.
- The participant has little or no hair on their volar forearms - see fig1.

Criteria for *exclusion* from this study are as follows:

- The participant is under 18 years old.
- The participant has hairy volar forearms - see fig1.
- The participant has an active skin condition that makes the surface of their skin rougher than it would normally be (e.g. eczema, psoriasis).
- The participant has a known allergy to nonwoven fabrics.

Volunteers will be sought from outpatients of the Incontinence Clinic of Whittington Health NHS, residents of Cheverton Lodge Care Home, students and staff from the Clerkenwell Building, and students and staff from UCL.

2.1.1 Incontinence clinic participants

Identification and initial contact with prospective participants will be made by their doctor, Prof James Malone-Lee (JML), in routine appointments with his patients, during which he will give them an information sheet to read. The patient will then be asked if they would like to speak to an investigator – Sabrina Falloon (SF) or Vasileios Asimakopoulos (VA) will explain the study further and answer any questions they may have. The patient will be given at least 24 hours to consider their decision. If they are happy to participate, the patient should contact one of the investigators. The participant will come to the 3rd floor of the Clerkenwell Building on an arranged date when an investigator will go through the details of the study again with them and the consent form will be signed. Some participants may take part in the experiment on the same day as one of their future outpatient appointments. However, if a participant comes outside their usual appointment, transport will be arranged or travel expenses will be reimbursed.

2.1.2 Nursing home participants

This same process applies to residents of the nursing home, except that the general manager, Mary Rabitte (MR), will identify and make the initial contact with potential participants, and consent will be obtained in the home rather than the Clerkenwell Building.

2.1.3 Students and staff participants

All students and staff from the Clerkenwell Building will be invited to participate by poster adverts and will receive information sheets on request; students and staff of UCL will receive their invitation in a generic e-mail with an attached PIS. They will all need to contact the investigators to register their interest in participation in the study and direct all their questions to them. They will also be required to sign consent forms in the same way as other participants.

Recruitment will continue until sufficient data have been gathered; the number of participants needed is expected to be about 20, and will not exceed 30. The participants will be split equally into two groups (18-64 yrs and 65 yrs +), but no precise figure is possible due to the exploratory nature of this work.



Figure 1: Image of forearm skin: people with MORE hair on the *underside* of their forearm than shown in the photo above will NOT be considered for participation in the study.

2.2 Experimental methodology

The experimental methodology presented here is mainly the result of work by Rebecca Wong (WKRW) on volar forearm skin. WKRW did very similar experiments but she focused on young female subjects, whereas in this study, people of all ages (above 18) and both genders are considered. Methodology used by WKRW has been adapted to address the aims set out in §1.2. All reasonable measures have been taken to anticipate any issues that may arise. The experimental methods required to achieve the objectives stated in §1.2 are detailed below.

2.2.1 Dry friction

Most measurements will take place on the participant's volar forearm in an environmentally (temperature and humidity) controlled room in the Department of Medical Physics and Bioengineering, UCL Archway Campus. It is not essential for the dry skin friction measurements to be taken in there, so measurements made at the nursing homes will not be affected by the lack of environment control. However, for convenience, measurements will be taken in the department for all other participants.

For consistency: Baseline measurements of trans-epidermal water loss (TEWL) on the volunteers' arm will be taken with an evaporimetry device in order to help us to make conclusions about the friction values produced by their skin with nonwoven fabrics. This is because we know that skin hydration affects friction values and some people's skin may naturally lose water at a faster rate than others' [5]. The instrument used is non-invasive and consists of a small probe, which will be placed gently on the skin and will remain in position for approximately 3 minutes for baseline measurements.

In the nursing home, the temperature of the room will also be measured, using a standard commercially available room thermometer, so that these friction measurements can be fairly compared with those made in the environmentally controlled room. Photographs of the volunteers' arm will be taken in order to characterise the surface wrinkling and topography of the skin. This will be performed in good lighting conditions with a high-resolution digital camera.

For skin friction measurements: The skin friction measurements will be carried out using a piece of equipment called a Tensometer (MTT175 Miniature Tensile Tester, Dia-Stron Ltd.), which has an armrest to position and support the participant's arm. A strip of nonwoven fabric (similar to the stay-dry topsheet of a pad) with a light weight (no more than 100g) attached will be pulled across the skin by the Tensometer, while the same machine measures the force required to do this and the distance the material moves.

Skin friction measurements will be taken on the volunteers' dry arm under various loads and repeated at least three times. Each friction test will be video recorded in order to demonstrate any gross physical differences between participants' skin in the study. Photographs will also be taken of the participant's volar forearm before and after the measurements.

2.2.2 Wet friction

Friction measurements on over-hydrated (wet) skin will be carried out as described above, but prior to carrying out the experiment, the arm and/or nonwoven fabric will be hydrated. Hydrating the skin may take up to 20 minutes each time and hydrating the fabric will take no longer than 10 seconds. Each friction measurement will take up to 1 minute and TEWL may be measured between each of these or just at the end, depending on the individual participant.

2.3 Health and safety

Both investigators have had the appropriate training and experience to use the equipment (described in this protocol) proficiently, and have tested this method on models many times.

There is a very low chance that participants may present with reddening of the skin or a rash as a result of contact with the nonwoven fabric, but should this persist or occur repeatedly, medical advice will be sought. A similar study (involving the same measurements with the same materials) has been carried out successfully with no sign of adverse skin reactions.

The arm rest was specifically designed to support an arm comfortably and the chair on which the participant sits will be adjusted to suit the comfort of the individual. (The chair will have a backrest, armrests and adjustable height for both safety and comfort.)

No significant health and safety issues are raised by this study. Typical laboratory risks still apply - such as chemical, mechanical and electrical hazards - but this will be managed by good laboratory practice. Chemicals are stored safely in locked cupboards and participants will not come into direct contact with any dangerous electrical equipment.

2.4 Projected timing

The purposes of this section are to clarify the timings of participant recruitment and experiment completion, and to give an approximate guide to the start and end dates of the work. This work is expected to start immediately after ethics approval has been obtained. Participants will be recruited throughout the study from all 'groups' (i.e. incontinence clinic, nursing home, students and staff from Clerkenwell Building, students and staff from UCL). Students and staff in the Clerkenwell Building are most available to receive information and will therefore most likely be recruited first, having been given a PIS. All potential participants will have had a period of at least 24 hours to consider whether or not to take part. This means that experiments may go ahead the following day for Clerkenwell Building staff and student participants.

Patients from JML's clinic will have a longer period between first receiving information and actually taking part. This depends on the gap between appointments (typically 8-12 weeks), as some patient participants will prefer to take part on the same day as an appointment for their convenience. However, those who prefer not to do this can participate sooner. Investigators will travel to the nursing home to take measurements on residents there, in which case the time between residents receiving information and participating will depend mainly on the daily schedule at the home. While it is not possible to specify an end date for this study, the work will continue until at least the minimum amount of data has been collected from the minimum number of participants. It is estimated that it will take up to the end of September 2013.

3 Ethics

This study involves interaction between the investigators and participants prior to, during and sometimes after experiments. This is because all participants will need to arrange a time and date with the investigators for the friction measurements to be taken, and this may need to be repeated.

In consequence of this, the primary ethical requirement is to obtain informed consent from participants. As described in §2.1, this will be managed by the investigators. At least 24 hours will be given to the prospective participants in which to consider the information, before they are given the opportunity to take part when written consent is sought (§2.1).

The data obtained by the experiments will have an alphanumeric code and will be entirely untraceable to the participant, but will be kept on password-secure computers. Minimal personal details will be kept in separate files containing information such as gender, ethnicity, and age of the participant, as well as a general description of the condition of the skin. These files will also be stored on password-secure computers in either the laboratory or office, both of which have code-locked doors. Our practice with experimental data of this type is to keep them in long term storage for 20 years with personal data in separate files.

4 Expertise

Prof. Alan Cottenden is a Medical Physicist with over 25 years' experience working on incontinence technology. He has managed, directed, or participated in around 25 clinical trials of incontinence products and clinical studies involving *in vivo* measurements on skin.

Sabrina Falloon is a PhD student in the Continence and Skin Technology Group, a joint venture of the departments of Medical Physics & Bioengineering and Medicine at UCL. Her previous training is in medical engineering. Her first supervisor is Alan Cottenden.

Prof. James Malone-Lee is Professor of Medicine at University College London, and has been working on incontinence for about 25 years. In this time he has overseen 15 clinical trials, and has considerable experience in this respect.

References

- [1] Thomas, S., Billington, A. and Getliffe, K. (2004). Improving continence services a case study in policy influence. *Journal of Nursing Management*. **12**(4), pp. 252-257
- [2] Abrams, P., Cardozo, L., Khoury, S. and Wein, A. eds. (2009). *Incontinence: 4th International Consultation on Incontinence, Paris July 5-8, 2008*. 4th Ed. Health Publication Ltd.
- [3] Wong, W. K. R. (2008). A study of evaporation and friction on hydrated forearm skin [PhD thesis]. University College London.
- [4] Cottenden, D. J. (2010). A multiscale analysis of frictional interaction between human skin and nonwoven fabrics [PhD thesis]. University College London.
- [5] Warriar, A.G., Kligman, A. M., Harper, R. A., Bowman, J. and Wickett, R.R. (1996). A comparison of black and white skin using noninvasive methods. *J. Soc. Cosmet. Chem.* **47**, pp. 229-240

University College London
Department of Medical Physics and Bioengineering
Continance & Skin Technology Group

Archway Campus
Clerkenwell Building
Highgate Hill
London
N19 5LW
England



University College London Continance & Skin Technology Group
study into friction between volar forearm skin and nonwoven
fabrics

Participant Information Sheet: Outpatients

(1 August 2011 Version 1.5)

What is the purpose of this study?

People who use sanitary towels or incontinence pads sometimes get sore skin caused by friction (rubbing) against the surface of the pads. We need to understand how this friction occurs in order to develop pads which are kinder to the skin.

The purpose of this study is to find out how the friction between the skin and the fabric which forms the surface of the pads works.

Who is organising and funding the study?

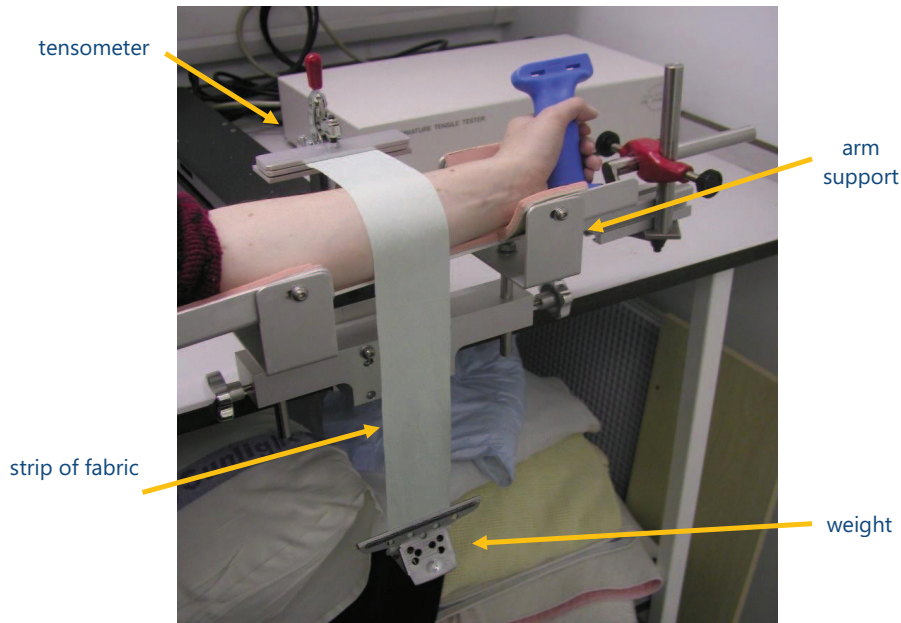
This study is organised by research staff at University College London. The study is funded by SCA Hygiene Products AB (a pad manufacturer) and University College London.

Why have I been chosen?

We need up to 30 volunteers to take part in this study. We know that different people's skin reacts differently to fabrics, therefore we need to measure friction on men and women of different ages. These tests will tell us if some fabrics cause more friction than others. This knowledge will ultimately help pad manufacturers to develop pads that are kinder to the skin.

What types of experiments will you be doing?

The experiments we will be doing will measure the force needed to make fabric slide over your skin. You will be asked to sit with your arm supported on an arm rest as shown in the photograph below. The fabric will be pulled gently and slowly across your arm by a device called a tensometer. Each test will take less than one minute and will be repeated several times. You will be asked to keep your arm as still as possible during the tests.



We will also measure water loss from your skin which can affect friction.

We may need to dampen your skin and/or the fabric as we would like to know more about the effect of moisture on friction.

A photograph of your arm will be taken before and after each test. A video record will be made as the strips of fabric are being pulled across your arm. Only your forearm, the fabric and equipment will be in the shot. It will not be possible to see your face.

Skin moisture can be affected by how relaxed or excited you feel, so reading material and videos will be provided to help you relax during the tests. You are also welcome to read a book or magazine, or watch a DVD of your own choice.

In total the tests will take approximately two hours including breaks. Depending on the results obtained, we may have to repeat the tests at a later date; this would be no later than 6 months after the initial tests. It is unlikely that you will be required to participate for a third time.

The tests will be done at our department on the 3rd floor of the Clerkenwell Building. We will arrange the tests for a day that is convenient for you. This could be when you are coming to see Professor Malone-Lee. If it does not coincide with a clinic appointment, we will pay your travel costs.

Do I have to take part?

No, you do not have to take part. You do not have to give a reason and it will not affect your care in any way.

What if I change my mind?

You are free to change your mind and withdraw from the study at any time up to or during your participation.

What are the possible disadvantages or risks of taking part?

If your skin is sensitive to the fabrics, you may experience some minor irritation where the fabric touches your skin. There are no other anticipated risks or side effects associated with taking part in this study.

What are the possible benefits of taking part?

There are no immediate or direct benefits to you from taking part. Longer term, you and/or others may benefit from any improvements to fabrics that are used in incontinence pads and sanitary towels as a result of this study.

Confidentiality

Your participation in this study will not involve accessing any of your medical information. Only your name and age will be passed to us from the outpatients staff. Results from this study will be made anonymous so they cannot be linked to you. Your GP will be informed of your participation in the study **only** if you consent to this.

What will happen to the results of the study?

Results from the study will be published widely (in print/conferences) but will be completely anonymous and untraceable back to you. Your personal details will be stored securely and separately from the results gathered from the tests in accordance with the University's policy. A summary of the results will be sent to you after the completion of the work.

What happens if something goes wrong?

If you have a concern about any aspect of this study, you should ask to speak to the researchers who will do their best to answer your questions (contact details at the end of this document). If you remain unhappy and wish to complain formally, you can do this through the NHS Complaints Procedure (or Private Institution). Details can be obtained from the hospital.

Who has reviewed the study?

The study has received ethics approval from the London Stanmore Research Ethics Committee.

What happens next?

Any questions you may have should be answered satisfactorily by the researchers. If you wish to take part, you will be asked to sign a consent form. You will be given a copy of the signed consent form.

Thank you very much for your help.

Sabrina Falloon

Tel: 020 7288 3771

E-mail: sabrina.falloon.10@ucl.ac.uk

Vasileios Asimakopoulos

Tel: 020 7288 5150

E-mail: v.asimakopoulos@ucl.ac.uk

University College London
Department of Medical Physics and Bioengineering
Continance & Skin Technology Group

Archway Campus
Clerkenwell Building
Highgate Hill
London
N19 5LW
England



University College London Continance & Skin Technology Group
study into friction between volar forearm skin and nonwoven
fabrics

Participant Information Sheet: Nursing Home Residents

(1 August 2011 Version 1.6)

What is the purpose of this study?

People who use sanitary towels or incontinence pads sometimes get sore skin caused by friction (rubbing) against the surface of the pads. We need to understand how this friction occurs in order to develop pads which are kinder to the skin.

The purpose of this study is to find out how the friction between the skin and the fabric which forms the surface of the pads works.

Who is organising and funding the study?

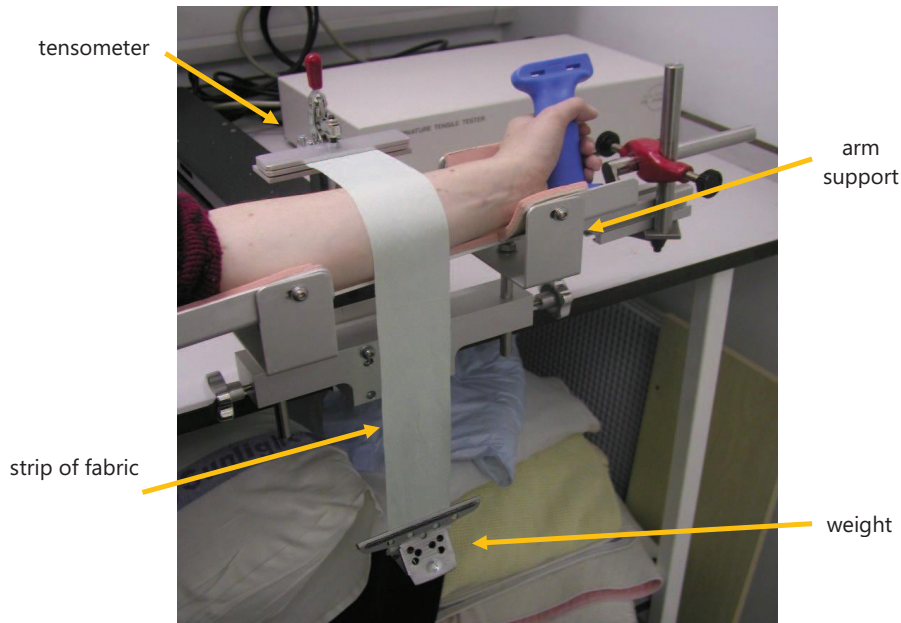
This study is organised by research staff at University College London. The study is funded by SCA Hygiene Products AB (a pad manufacturer) and University College London.

Why have I been chosen?

We need up to 30 volunteers to take part in this study. We know that different people's skin reacts differently to fabrics, therefore we need to measure friction on men and women of different ages. These tests will tell us if some fabrics cause more friction than others. This knowledge will ultimately help pad manufacturers to develop pads that are kinder to the skin.

What types of experiments will you be doing?

The experiments we will be doing will measure the force needed to make fabric slide over your skin. You will be asked to sit with your arm supported on an arm rest as shown in the photograph below. The fabric will be pulled gently and slowly across your arm by a device called a tensometer. Each test will take less than one minute and will be repeated several times. You will be asked to keep your arm as still as possible during the tests.



We will also measure water loss from your skin which can affect friction.

A photograph of your arm will be taken before and after each test. A video record will be made as the strips of fabric are being pulled across your arm. Only your forearm, the fabric and equipment will be in the shot. It will not be possible to see your face.

Skin moisture can be affected by how relaxed or excited you feel, so reading material and videos will be provided to help you relax during the tests. You are also welcome to read a book or magazine, or watch a DVD of your own choice.

In total the tests will take approximately two hours including breaks. Depending on the results obtained, we may have to repeat the tests at a later date; this would be no later than 6 months after the initial tests. It is unlikely that you will be required to participate for a third time.

The tests will be done at Cheverton Lodge Nursing Home. You will not have to leave the nursing home to take part in this study.

Do I have to take part?

No, you do not have to take part. You do not have to give a reason and it will not affect your care in any way.

What if I change my mind?

You are free to change your mind and withdraw from the study at any time up to or during your participation.

What are the possible disadvantages or risks of taking part?

If your skin is sensitive to the fabrics, you may experience some minor irritation where the fabric touches your skin. There are no other anticipated risks or side effects associated with taking part in this study.

What are the possible benefits of taking part?

There are no immediate or direct benefits to you from taking part. Longer term, you and/or others may benefit from any improvements to fabrics that are used in incontinence pads and sanitary towels as a result of this study.

Confidentiality

Your participation in this study will not involve accessing any of your medical information. Only your name and age will be passed to us from your nursing home manager. Results from this study will be made anonymous so they cannot be linked to you. Your GP will be informed of your participation in the study **only** if you consent to this.

What will happen to the results of the study?

Results from the study will be published widely (in print/conferences) but will be completely anonymous and untraceable back to you. Your personal details will be stored securely and separately from the results gathered from the tests in accordance with the University's policy. A summary of the results will be sent to you after the completion of the work.

What happens if something goes wrong?

If you have concerns about any aspect of this study, please contact one of the researchers (see details below). If you are unhappy with the way you have been dealt with, or in the unlikely event that you suffer any harm, please speak to your nursing home manager.

Who has reviewed the study?

The study has received ethics approval from the London Stanmore Research Ethics Committee.

What happens next?

Any questions you may have should be answered satisfactorily by the researchers. If you wish to take part, you will be asked to sign a consent form. You will be given a copy of the signed consent form.

Thank you very much for your help.

Sabrina Falloon

Tel: 020 7288 3771

E-mail: sabrina.falloon.10@ucl.ac.uk

Vasileios Asimakopoulos

Tel: 020 7288 5150

E-mail: v.asimakopoulos@ucl.ac.uk

University College London
Department of Medical Physics and Bioengineering
Continance & Skin Technology Group

Archway Campus
Clerkenwell Building
Highgate Hill
London
N19 5LW
England



University College London Continance & Skin Technology Group
study into friction between volar forearm skin and nonwoven
fabrics

Participant Information Sheet: Students & staff

(1 August 2011 Version 1.4)

What is the purpose of this study?

People who use sanitary towels or incontinence pads sometimes get sore skin caused by friction (rubbing) against the surface of the pads. We need to understand how this friction occurs in order to develop pads which are kinder to the skin.

The purpose of this study is to find out how the friction between the skin and the fabric which forms the surface of the pads works.

Who is organising and funding the study?

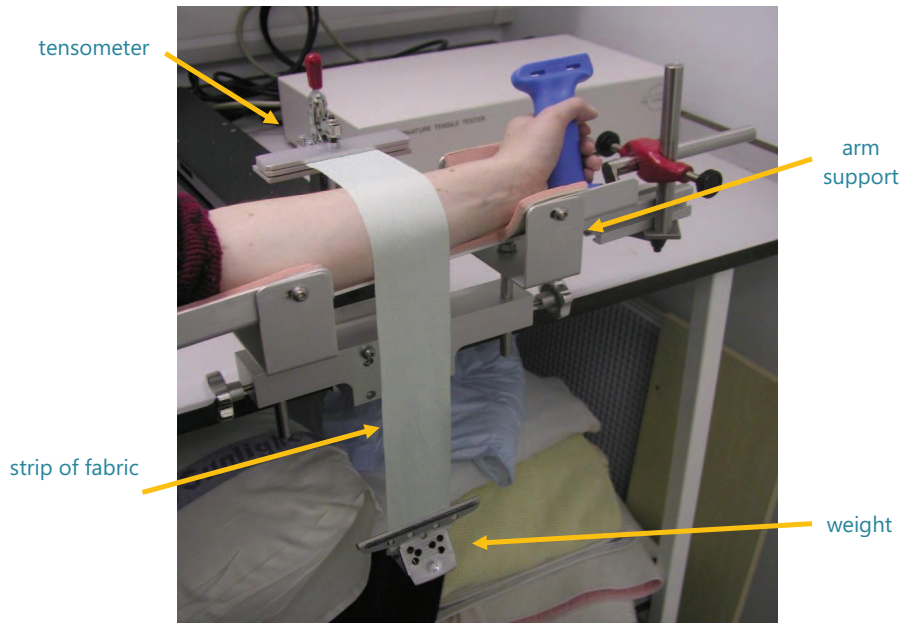
This study is organised by research staff at University College London. The study is funded by SCA Hygiene Products AB (a pad manufacturer) and University College London.

Why have I been chosen?

We need up to 30 volunteers to take part in this study. We know that different people's skin reacts differently to fabrics, therefore we need to measure friction on men and women of different ages. These tests will tell us if some fabrics cause more friction than others. This knowledge will ultimately help pad manufacturers to develop pads that are kinder to the skin.

What types of experiments will you be doing?

The experiments we will be doing will measure the force needed to make fabric slide over your skin. You will be asked to sit with your arm supported on an arm rest as shown in the photograph below. The fabric will be pulled gently and slowly across your arm by a device called a tensometer. Each test will take less than one minute and will be repeated several times. You will be asked to keep your arm as still as possible during the tests.



We will also measure water loss from your skin which can affect friction.

We may need to dampen your skin and/or the fabric as we would like to know more about the effect of moisture on friction.

A photograph of your arm will be taken before and after each test. A video record will be made as the strips of fabric are being pulled across your arm. Only your forearm, the fabric and equipment will be in the shot. It will not be possible to see your face.

Skin moisture can be affected by how relaxed or excited you feel, so reading material and videos will be provided to help you relax during the tests. You are also welcome to read a book or magazine, or watch a DVD of your own choice.

In total the tests will take approximately two hours including breaks. Depending on the results obtained, we may have to repeat the tests at a later date; this would be no later than 6 months after the initial tests. It is unlikely that you will be required to participate for a third time.

The tests will be done at our department (see address at the top of page 1). If you are not already expecting to come to the Archway Campus on the day that you participate, your travel costs will be reimbursed.

Do I have to take part?

No, you do not have to take part. You do not have to give a reason.

What if I change my mind?

You are free to change your mind and withdraw from the study at any time up to or during your participation.

What are the possible disadvantages or risks of taking part?

If your skin is sensitive to the fabrics, you may experience some minor irritation where the fabric touches your skin. There are no other anticipated risks or side effects associated with taking part in this study.

What are the possible benefits of taking part?

There are no immediate or direct benefits to you from taking part. Longer term, you and/or others may benefit from any improvements to fabrics that are used in incontinence pads and sanitary towels as a result of this study.

Confidentiality

Your participation in this study will not involve accessing any of your medical information. Results from this study will be made anonymous so they cannot be linked to you.

What will happen to the results of the study?

Results from the study will be published widely (in print/conferences) but will be completely anonymous and untraceable back to you. Your personal details will be stored securely and separately from the results gathered from the tests in accordance with the University's policy. A summary of the results will be sent to you after the completion of the work.

What happens if something goes wrong?

If you have a concern about any aspect of this study, you should ask to speak to the researchers who will do their best to answer your questions (contact details at the end of this document). If you remain unhappy and wish to complain formally, please contact the Chief Investigator, Professor Alan Cottenden, who will forward your complaint to the appropriate person. You can contact him at:

3rd floor, Clerkenwell Building
Highgate Hill
London
N19 5LW
Tel: 020 7288 5670

Who has reviewed the study?

The study has received ethics approval from the London Stanmore Research Ethics Committee.

What happens next?

Any questions you may have should be answered satisfactorily by the researchers. If you wish to take part, you will be asked to sign a consent form. You will be given a copy of the signed consent form.

Thank you very much for your help.

Sabrina Falloon

Tel: 020 7288 3771

E-mail: sabrina.falloon.10@ucl.ac.uk

Vasileios Asimakopoulos

Tel: 020 7288 5150

E-mail: v.asimakopoulos@ucl.ac.uk

UNIVERSITY COLLEGE LONDON
DEPARTMENT OF MEDICAL PHYSICS AND BIOENGINEERING

Continence and Skin Technology Group
3rd Floor, Clerkenwell Building
Archway Campus
Highgate Hill
London
N19 5LW



UCL

<<GP NAME>>

<<GP ADDRESS>>

<<DATE>>

Version 1.3

Re.: <<PATIENT NAME>> - Notification of participation in a study of friction between volar forearm skin and nonwoven fabrics

Dear <<GP NAME>>,

The above named patient has consented to take part in a study on friction at the interface of volar forearm skin and nonwoven fabrics (the kind routinely used as coverstocks on incontinence pads, diapers and sanitary towels). This study is being carried out by the Continence and Skin Technology Group at University College London as part of two individual PhD projects. It is funded by UCL and SCA Hygiene Products AB in Sweden, and has been approved by London Stanmore Research Ethics Committee.

Each participant will have a strip of nonwoven fabric pulled across their volar forearm by a Tensometer (pulling machine), while a computer simultaneously measures friction forces between the fabric and skin. All procedures are non-invasive and participants are free to withdraw from the study at any time.

Please do not hesitate to contact either of the investigators for any further information or if you have any concerns regarding your patient's participation.

Thank you for your support in this venture.

Yours sincerely,

Sabrina Falloon, MEng, AMIMechE
PhD Student / Investigator

Tel: 020 7288 3771
E-mail: sabrina.falloon.10@ucl.ac.uk

Vasileios Asimakopoulos, BSc, MSc
PhD Student / Investigator

Tel: 020 7288 5150
E-mail: v.asimakopoulos@ucl.ac.uk

**UCL Department of Medical Physics and Bioengineering
Continenance & Skin Technology Group**

Archway Campus
3rd floor, Clerkenwell Building
Highgate Hill
London
N19 5LW



**University College London Continenance & Skin Technology Group study into
friction between volar forearm skin and nonwoven fabrics**

Participant consent form: Outpatients – confidential

(prepared 1 August 2011, Version 1.8)

Chief Investigator's name: Alan Cottenden

Chief Investigator's address: Continenance & Skin Technology Group, Third Floor, Clerkenwell Building,
Highgate Hill, London N19 5LW

To be completed by the participant:

Please initial
the box:

1. I have read the participant information sheet (version 1.5, dated 01/08/2011)
2. I have been given enough information about the study and all my questions

_____ _____
Member of staff providing information Position

3. I understand that my participation is voluntary and that I am free to withdraw at any time without giving any reason, without my medical care or legal rights being affected.
4. I consent to audio visual recordings and photographs of my forearm being taken for this study.
5. I agree to the investigators sending a letter to my GP about my participation.*
6. I agree to take part in the study.

*Giving consent to this part is not required for participation in the study.

Participant:

Person taking consent:

Signature: _____ Signature: _____

Print name: _____ Print name: _____

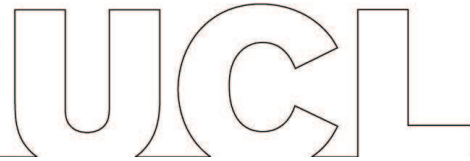
Date: _____ Position: _____

Date: _____

When complete: one copy for participant; one copy to go in participant's medical records; original to go in study notes.

**UCL Department of Medical Physics and Bioengineering
Continenance & Skin Technology Group**

Archway Campus
3rd floor, Clerkenwell Building
Highgate Hill
London
N19 5LW



**University College London Continenance & Skin Technology Group study into
friction between volar forearm skin and nonwoven fabrics**

Participant consent form: Nursing Home Residents – confidential

(prepared 1 August 2011, Version 1.5)

Chief Investigator's name: Alan Cottenden

Chief Investigator's address: Continenance & Skin Technology Group, Third Floor, Clerkenwell Building,
Highgate Hill, London N19 5LW

To be completed by the participant:

Please initial
the box:

1. I have read the participant information sheet (version 1.6, dated 01/08/2011) about the study that was given to me.
2. I have been given enough information about the study and all my questions have been given a satisfactory answer.

Member of staff providing information

Position

3. I understand that my participation is voluntary and that I am free to withdraw at any time without giving any reason, without my medical care or legal rights being affected.
4. I consent to audio visual recordings and photographs of my forearm being taken for this study.
5. I agree to the investigators sending a letter to my GP about my participation.*
6. I agree to take part in the study.

*Giving consent to this part is not required for participation in the study.

Participant:

Person taking consent:

Signature: _____ Signature: _____

Print name: _____ Print name: _____

Date: _____

Position: _____

Date: _____

When complete: one copy for participant; one copy to go in participant's care notes; original to go in study notes.

**UCL Department of Medical Physics and Bioengineering
Continenace & Skin Technology Group**

Archway Campus
3rd floor, Clerkenwell Building
Highgate Hill
London
N19 5LW



**University College London Continenace & Skin Technology Group study into
friction between volar forearm skin and nonwoven fabrics**

Participant consent form: Students & staff – confidential

(prepared 1 August 2011, Version 1.5)

Chief Investigator's name: Alan Cottenden

Chief Investigator's address: Continenace & Skin Technology Group, Third Floor, Clerkenwell Building,
Highgate Hill, London N19 5LW

To be completed by the participant:

Please initial
the box:

1. I have read the participant information sheet (version 1.4, dated 01/08/2011) about the study that was given to me.
2. I have been given enough information about the study and all my questions have been given a satisfactory answer.

_____ Position _____
Member of staff providing information

3. I understand that my participation is voluntary and that I am free to withdraw at any time without giving any reason, without my medical care or legal rights being affected.
4. I consent to audio visual recordings and photographs of my forearm being taken for this study.
5. I agree to take part in the study.

Participant:

Person taking consent:

Signature: _____ Signature: _____

Print name: _____ Print name: _____

Date: _____ Position: _____

Date: _____

When complete: one copy for participant; original to go in study notes.

University College London
Department of Medical Physics & Bioengineering

3rd Floor, Clerkenwell Building
Archway Campus
Highgate Hill
London
N19 5LW



Continence and Skin Technology Group study of friction between nonwoven fabrics and human skin

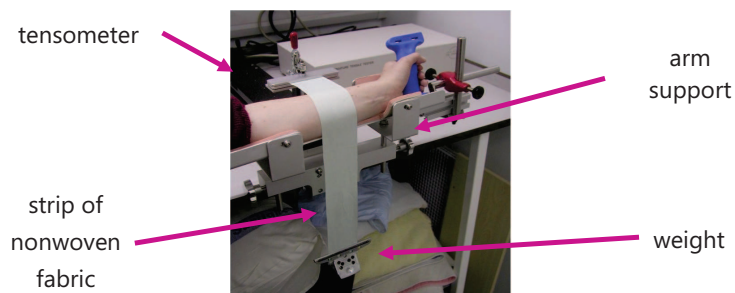
Volunteers needed!

TO ALL **STAFF AND STUDENTS:**

We are two PhD students carrying out a study on friction between human skin and nonwoven fabrics (the kind used as coverstocks on incontinence pads, diapers and sanitary towels) in order to better understand interaction between the two. It is anticipated that the results of this study will contribute to the improvement of non-woven fabrics, making them more 'skin-friendly'.

We need 10 volunteers **between the ages of 18 and 64 years** to take part and we are hoping that you will be one of them! Your participation would involve sitting in our lab while we make measurements on your volar forearm (underside of your lower arm). *See photograph below.* This would be done in no more than two 2-hour sessions and you are welcome to bring a book or DVD to pass the time!

If you are interested in taking part, **please contact one of us in person, by phone or by e-mail and ask for an information sheet!**



Many thanks,
Sabrina and Vasileios

020 7288 3771 - sabrina.falloon.10@ucl.ac.uk / 020 7288 5150 - v.asimakopoulos@ucl.ac.uk

Version 1.2

Dear all,

We are two PhD students carrying out a study on friction between human skin and nonwoven fabrics (the kind used as coverstocks on incontinence pads and sanitary towels) in order to better understand interaction between the two. It is anticipated that the results of this study will contribute to the improvement of nonwoven fabrics, making them more 'skin-friendly'.

We need 10 volunteers **between the ages of 18 and 64 years** to take part and we are hoping that you will be one of them! Your participation would involve coming to the **Archway Campus** of UCL and sitting in a room while we make measurements on your volar forearm (underside of your lower arm). This would be done in no more than two 2-hour sessions and you are welcome to **bring a book or DVD** to pass the time!

All travel costs will be **reimbursed** and refreshments will be provided! If you are interested in taking part, **please read the information sheet** attached to this e-mail and then send an e-mail to sabrina.falloon.10@ucl.ac.uk or v.asimakopoulos@ucl.ac.uk, or call one of the numbers at the bottom of this message.

Many thanks,

Sabrina and Vasileios

Continence & Skin Technology Group
Archway Campus
University College London
+44(0)20 7288 3771 / +44(0)20 7288 5150

APPENDIX C

ORDER OF LOAD APPLICATION: VOLAR FOREARM FRICTION

NORMAL LOADS WERE APPLIED to the volar forearm during preliminary friction experiments (as described in §4.1.1.1) in the order shown in table C.1.

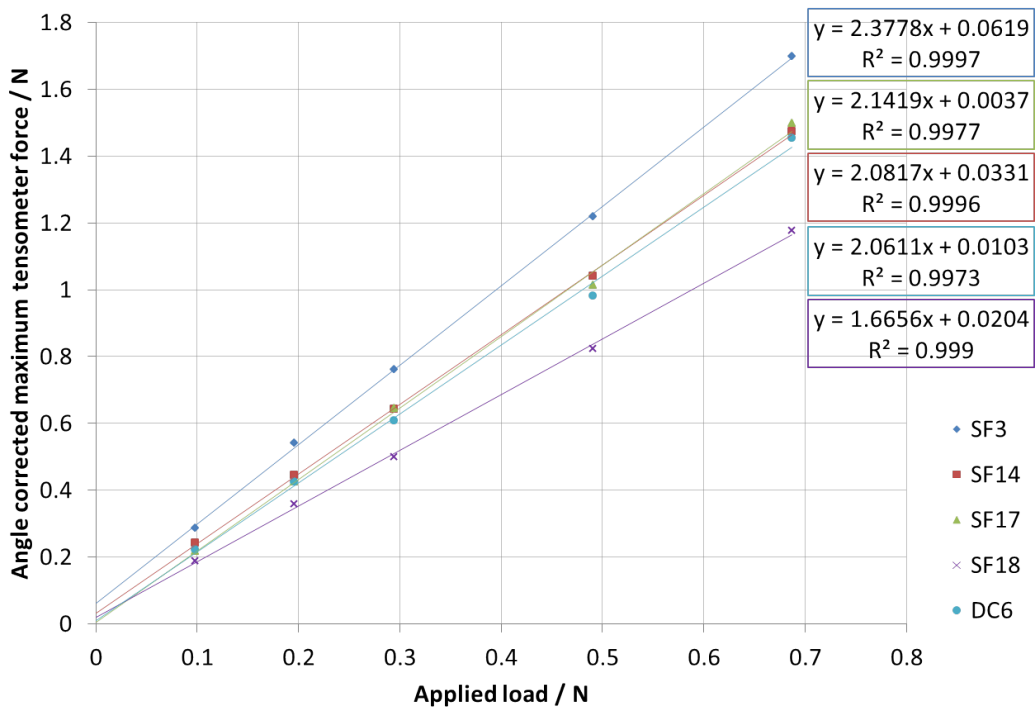
Table C.1: Order of load application for each nonwoven sample

Nonwoven	0.30N	0.48N	0.99N
SF1	1	3	2
SF2	2	1	3
SF3	1	2	3
SF7	2	3	1
SF9	2	1	3
SF10	3	1	2
SF11	3	2	1
SF12	1	1	2
SF14	2	1	3
SF15	2	3	1
SF16	1	3	2
SF17	1	2	3
SF18	3	2	1
SF2	3	1	2
SF1	-	1	-

APPENDIX D

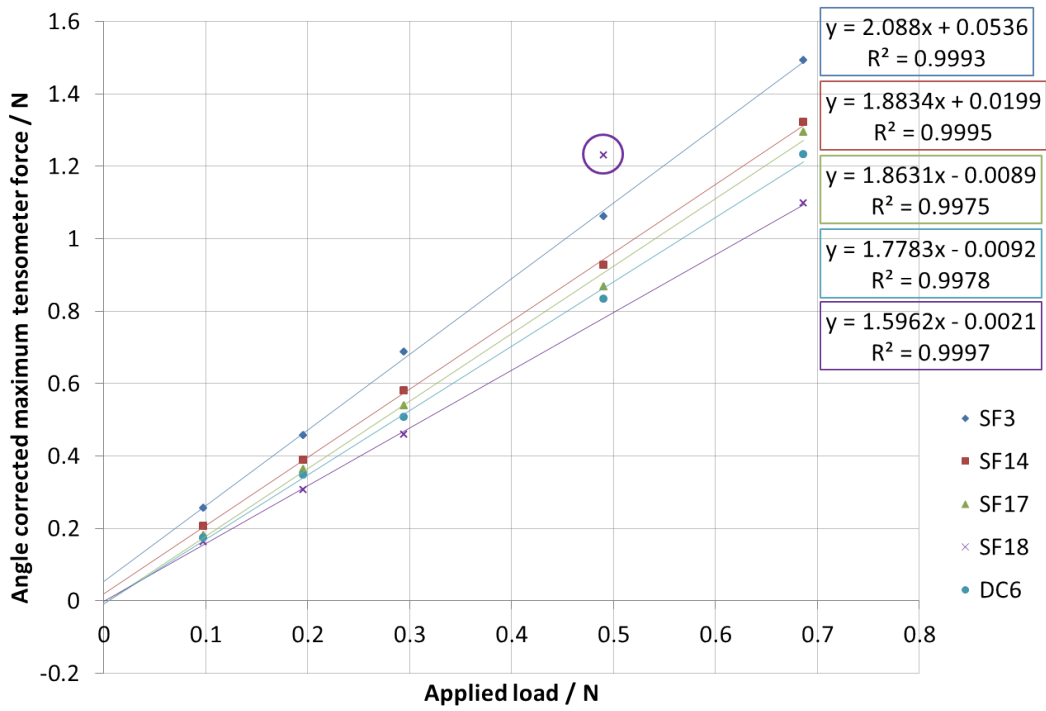
A FULL SET OF DRY FRICTION DATA: MAXIMUM TENSOMETER FORCE VS APPLIED LOAD

ALL THE GRAPHS of maximum tensometer force against applied load from dry friction measurements with volar forearm skin have been included in this chapter. Maximum tensometer forces were identified as the first peak on force-displacement graphs (static friction force) and were corrected when the angle of arc of contact, between the volar forearm and the strip of nonwoven fabric, was less than or greater than 90° . The gradients of the graphs in this chapter (and the angles of arc of contact) were later used in equation 2.7 to calculate the coefficients of static friction. (Note that the code under each graph is the participant code – see table 4.2 for more details.)

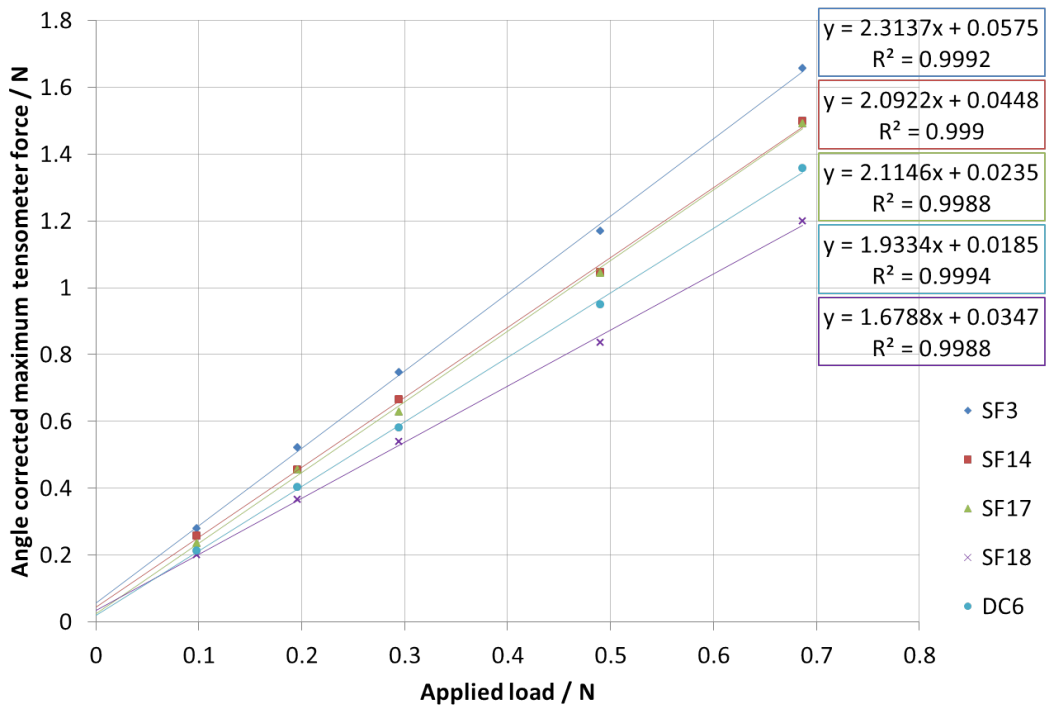


(a) AD02

Figure D.1: Maximum tensometer force against applied load for all nonwovens and study participants. *Continues...*

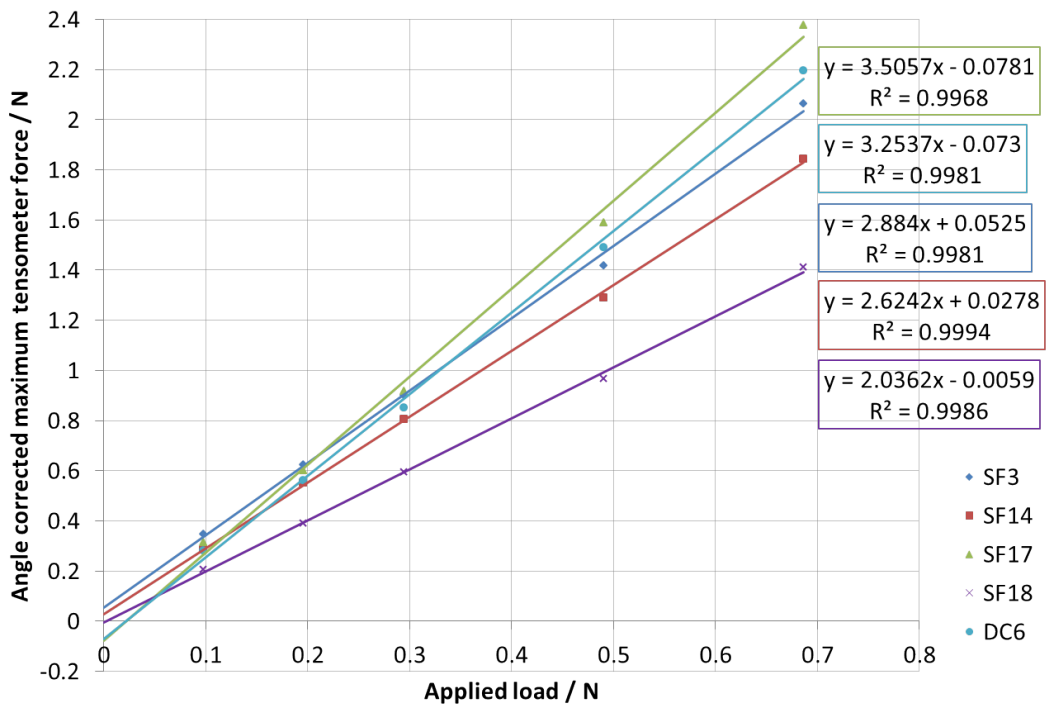


(b) MM03 – circled data point was anomalous (incorrect load application)

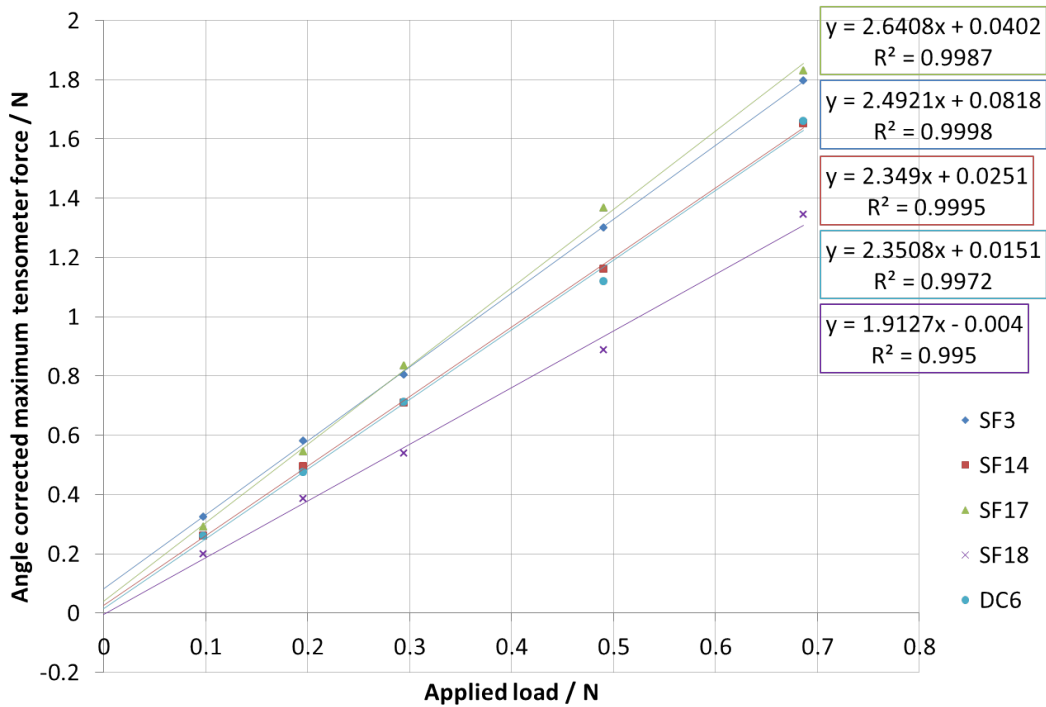


(c) MS04

Figure D.1: Continues.

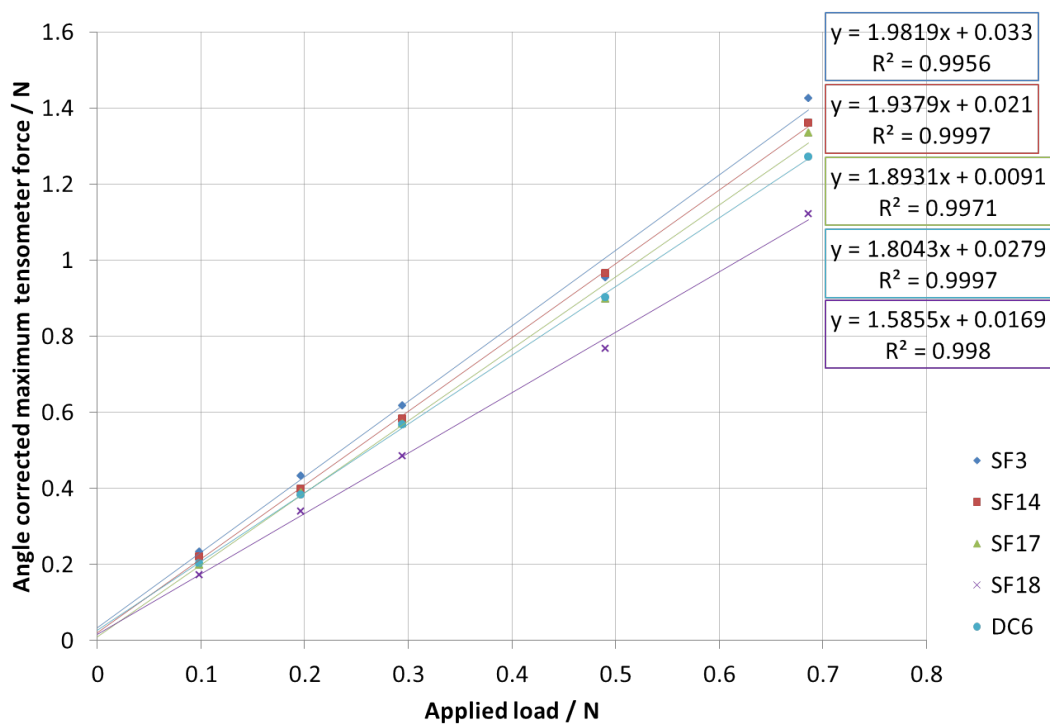


(d) RJ05

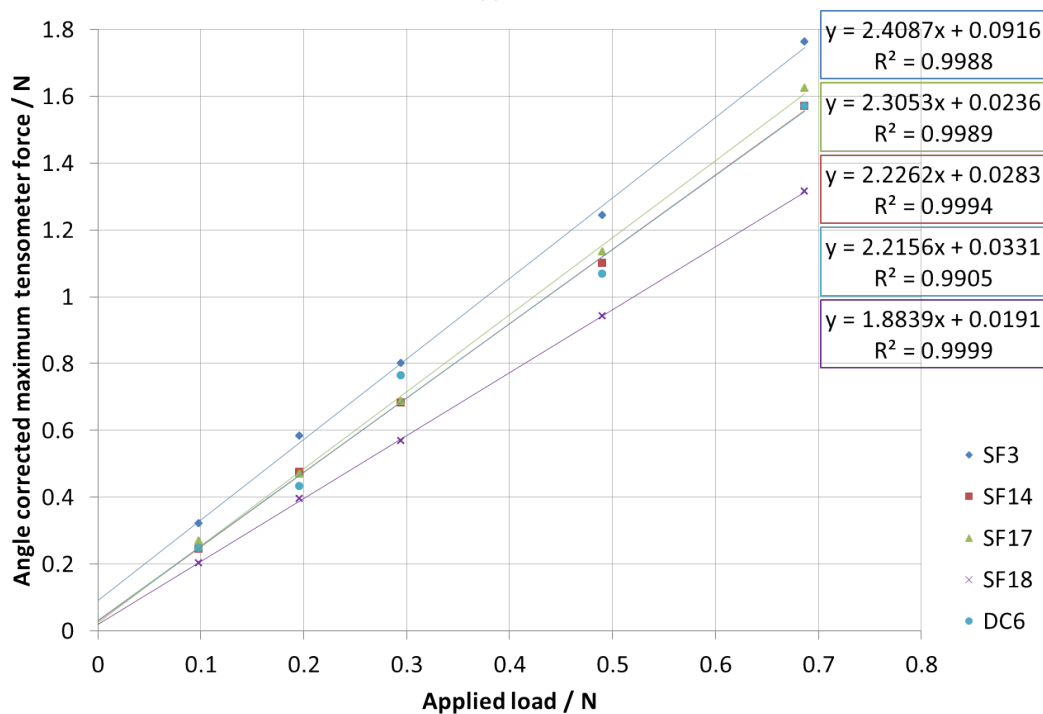


(e) SF06

Figure D.1: Continues.

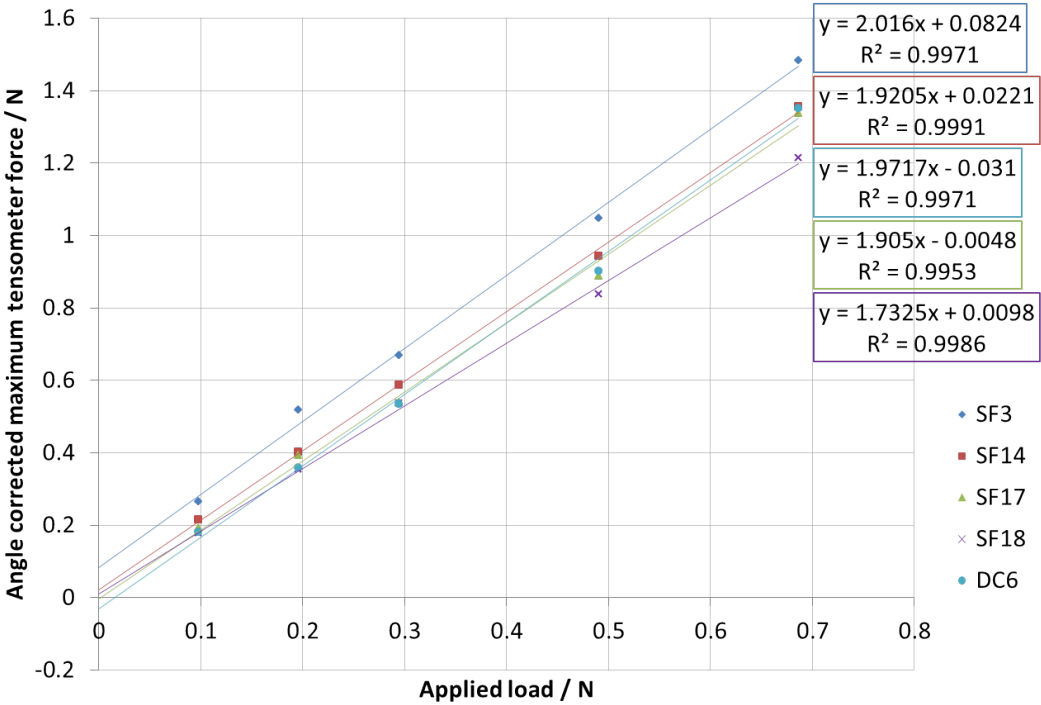


(f) HJ07

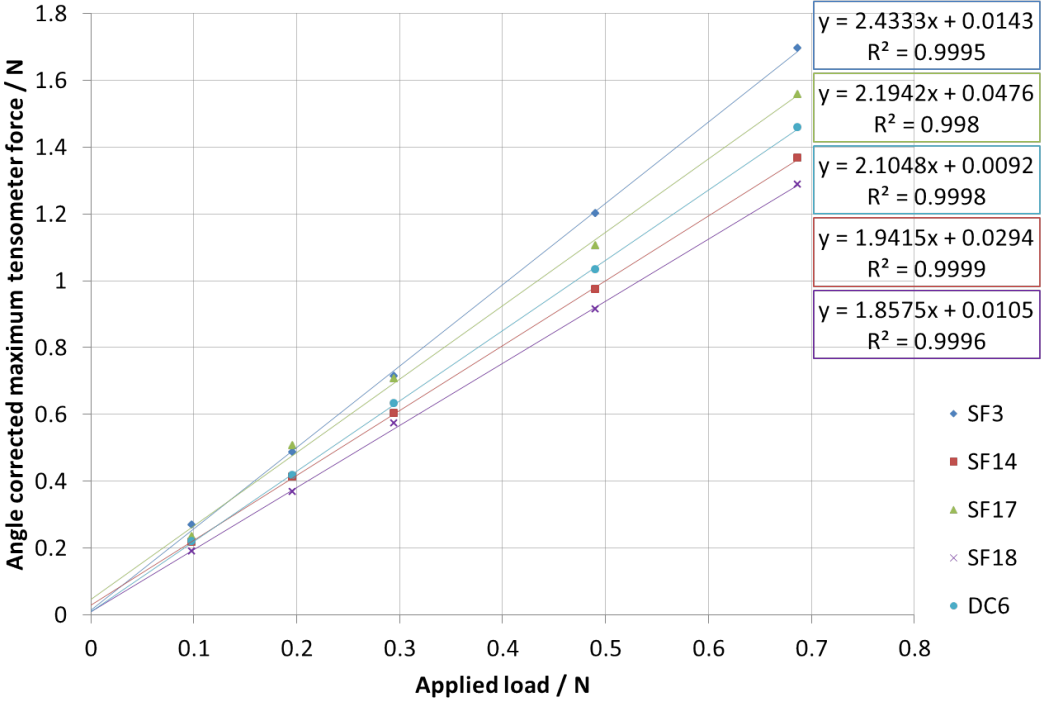


(g) MD08

Figure D.1: Continues.

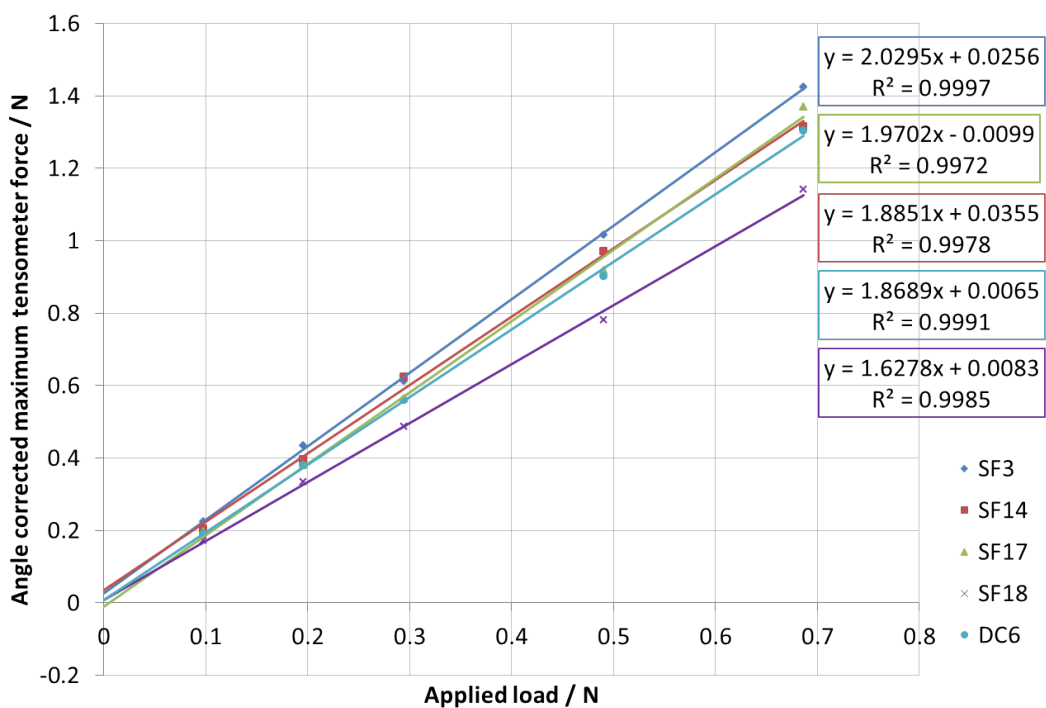


(h) JJ09

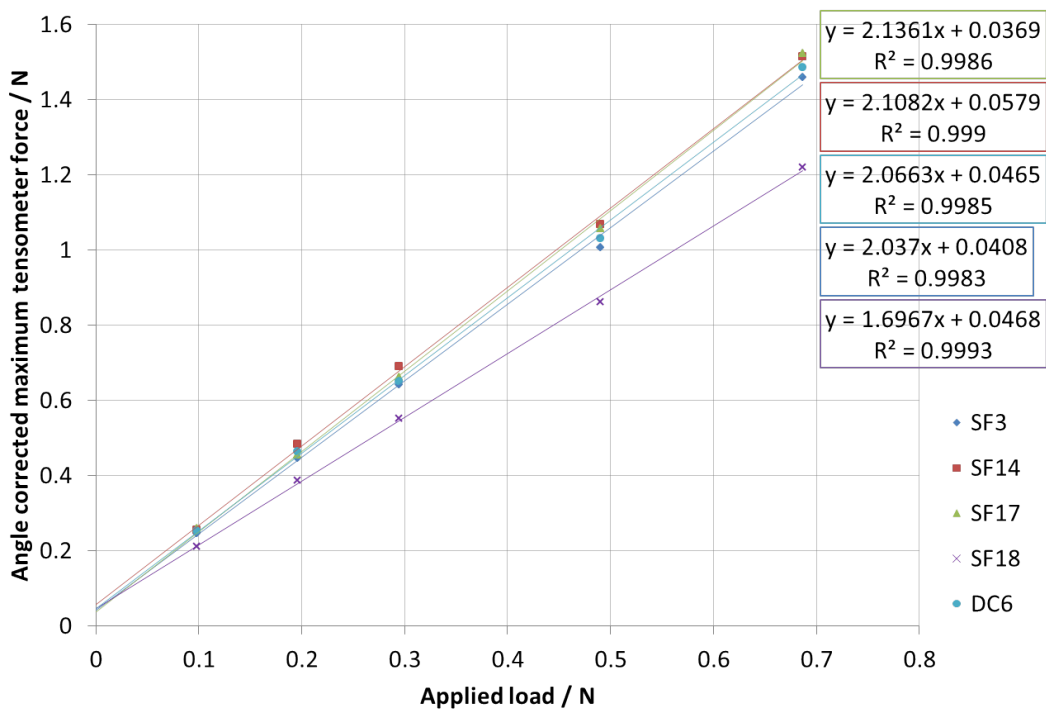


(i) DJ10

Figure D.1: Continues.

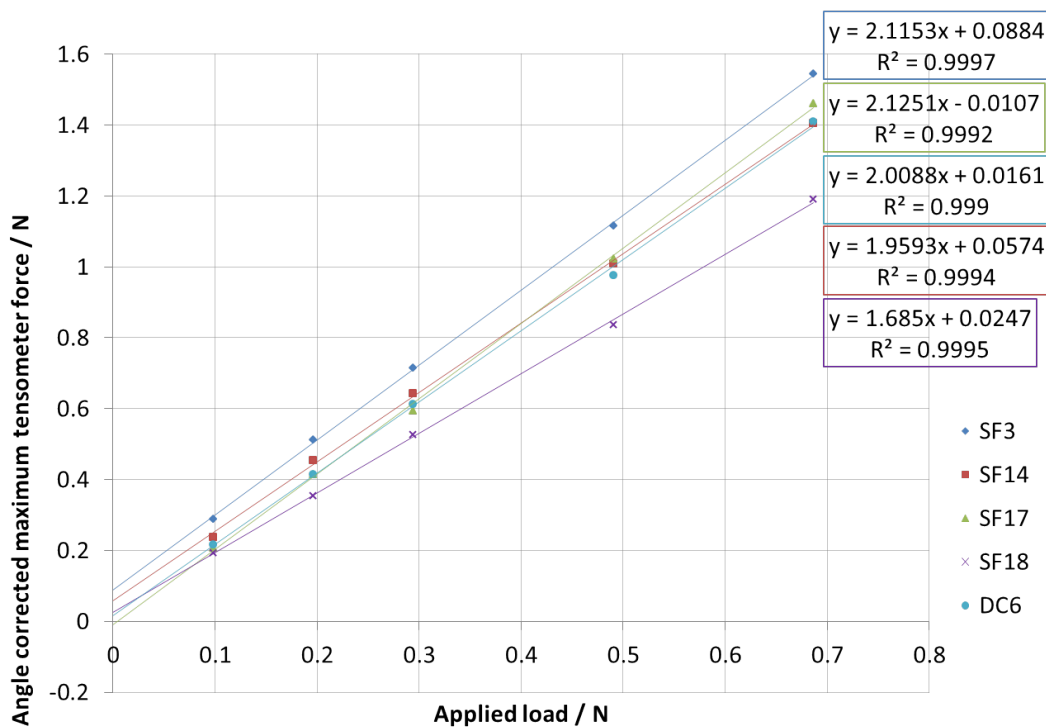


(j) AB11

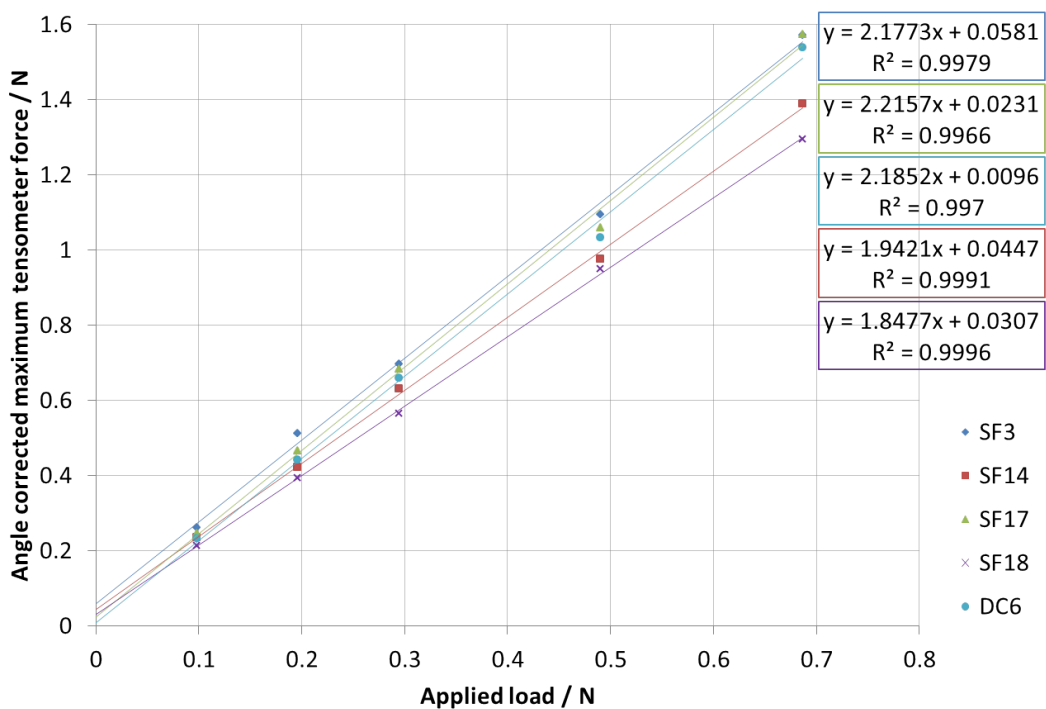


(k) MG12

Figure D.1: Continues.

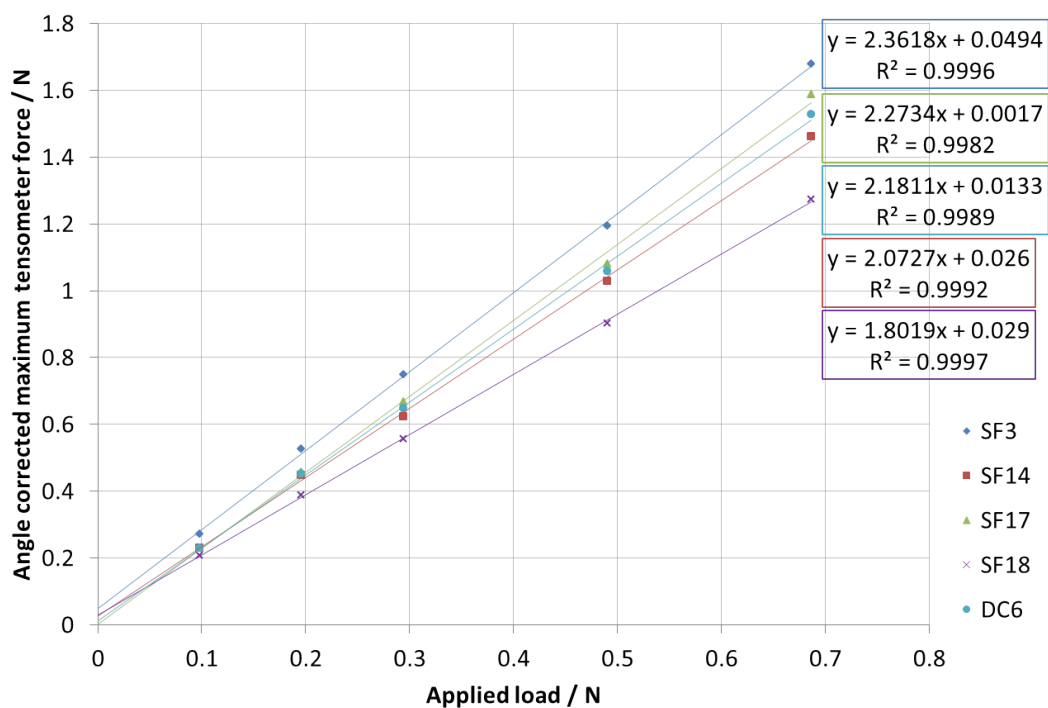


(l) KG13

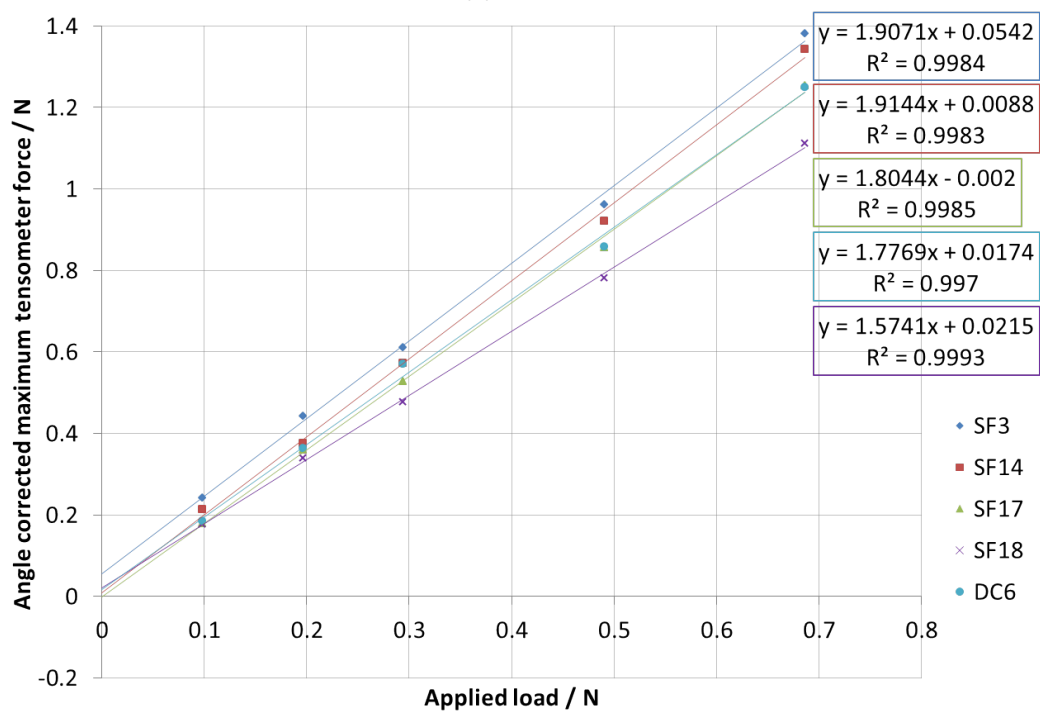


(m) MT14

Figure D.1: Continues.

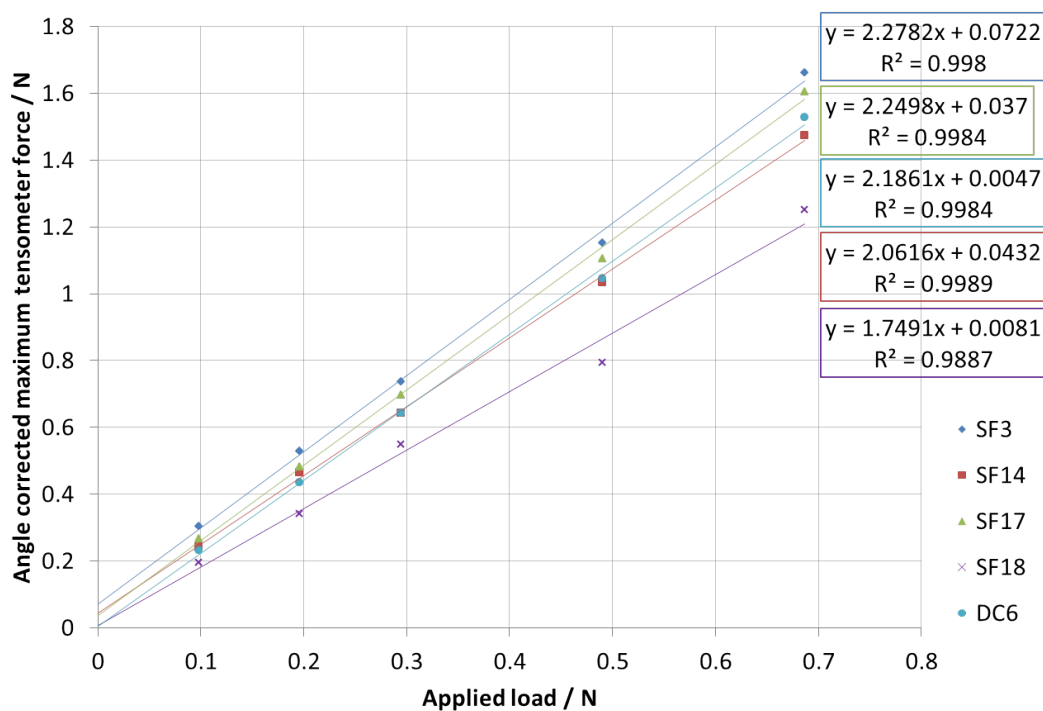


(n) DA15

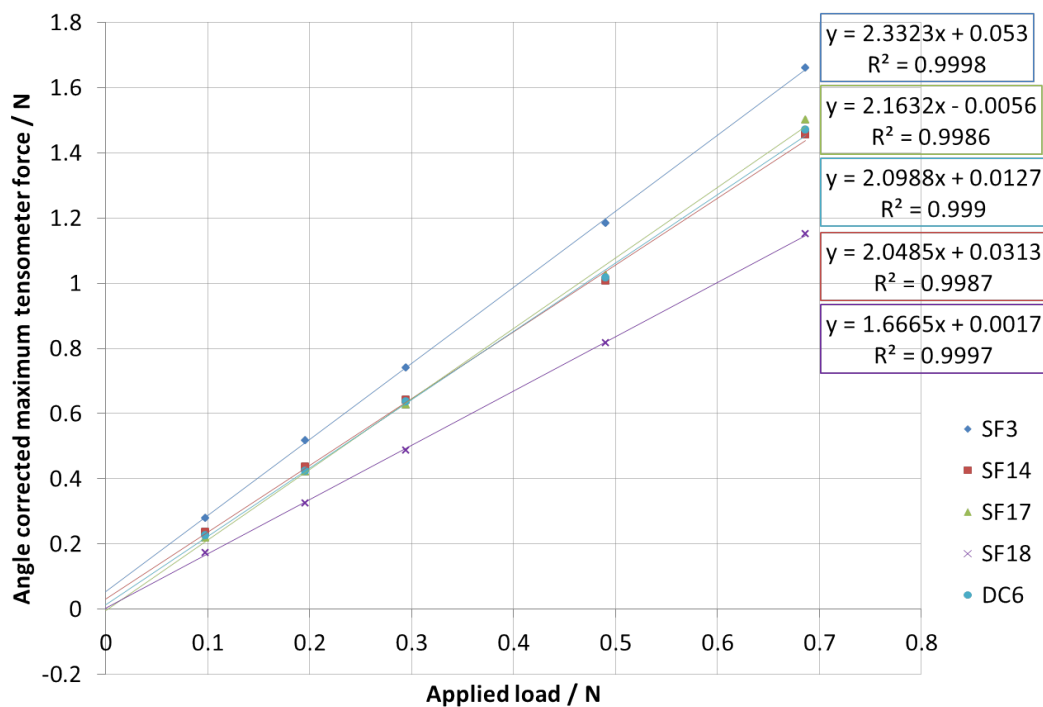


(o) LC16

Figure D.1: Continues.

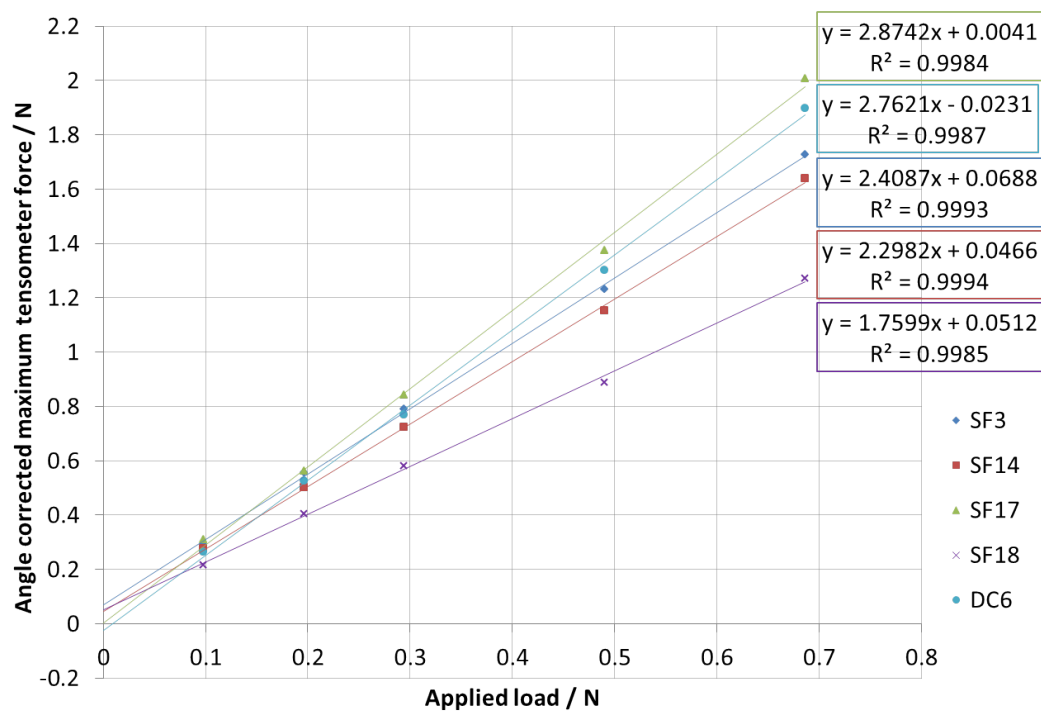


(p) MH17

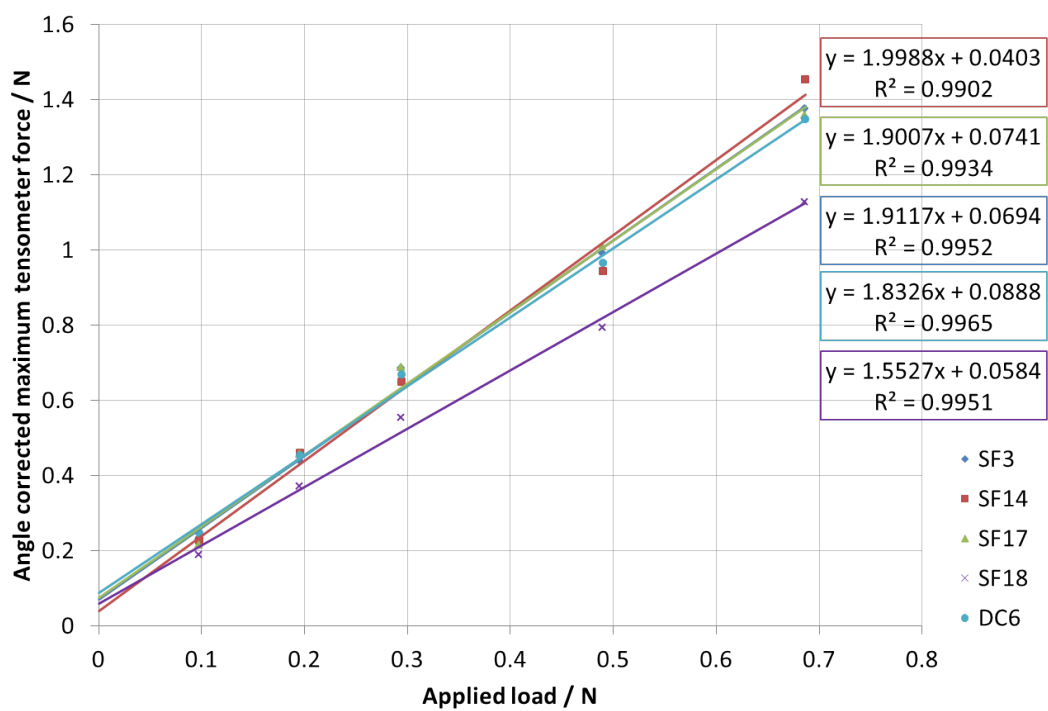


(q) CB18

Figure D.1: Continues.



(r) DF19



(s) AK20

Figure D.1: Continued.

APPENDIX E

A FULL SET OF WET FRICTION DATA: MEASURING FRICTION AS A FUNCTION OF SKIN WETNESS (GREYSCALE)

This appendix has been removed due to its commercially sensitive content. It will be made available in the full version of this thesis, which will be published at a later date.

APPENDIX F

PROCESSING OF FIBRE FOOTPRINT IMAGES

AS EXPLAINED IN CHAPTER 6, there are many steps to processing fibre footprint images for analysis. The first involves the use of a MATLAB code to enhance the fibres that are in focus in the micrograph and is described in more detail in §F.1. The last uses a BASH script to produce Bézier curves, that represent fibre contacts, and their corresponding length values; this is explained in §F.2. All other steps in between (tracing, scanning, cropping and cleaning the image of artefacts that were introduced during tracing or scanning) were described in sufficient detail in chapter 6 (§6.1.2.3).

F.1 Enhancing raw micrographs

In order to facilitate the tracing of fibre segments in focus in the micrograph, it is necessary to create an image file in which such segments would be considerably clearer (with sharper edges) relative to all other fibres partially visible in the image. This is done by applying the code in figure F.1 to each micrograph (saved in TIF format) using MATLAB software.

```
file_name = input('TIFF file? ', 's');
focus = imread(file_name);
output_file_name = strcat(file_name, '_ngrad.tif');

green = focus(:, :, 2);
[greenx, greeny] = gradient( single(green) );
green_grad = sqrt(greenx.^2 + greeny.^2);
green_grad_norm = green_grad ./ max(max(green_grad)) .* 256;

colours = [linspace(1,0.5,64); linspace(1,0,64); linspace(1,0,64)]';
imwrite( green_grad_norm, colours, output_file_name );
```

Figure F.1: MATLAB code used to enhance raw TIFF images of fibre footprints collected using the microscope. The green channel is selected and the modulus of the gradient is written into a new TIFF file. This code was created and first used by Cottenden [4].

F.2 Extracting the numerical data

Following the completion of the step described in §F.1 and all subsequent steps that lead to the production of a “clean” bitmap image, the curves representing fibre contacts (all of which are a single colour)

are quantified in terms of their lengths and mean curvatures [4]. The name of the bitmap file is inserted into the BASH script – displayed in figure F.2 – and the output is an Encapsulated PostScript (EPS) image file and corresponding numerical data. The BASH script displayed here is a rather simple description of the full code, but essentially summarises how it works, which involves running two different programmes consecutively: AutoTrace, then epstodist.

AutoTrace is the freely accessible programme that is implemented to fit Bézier curves to the input (bitmap) file and save the output in the EPS format. Cottenden [4] wrote a basic library in C++, which was used to create the *epstodist* programme that extracts fibre contact length and mean curvature values from the EPS file produced in AutoTrace. The EPS file contains a preamble (including various articles of metadata and some other information) and several “strokes” (representing individual fibre contacts) that have associated information on their start and end points and shapes [4]. When epstodist is run on this file type, it creates its own stroke objects, for which it then computes arbitrary length and mean curvature values. A text file, containing these data, is automatically produced and then the arbitrary values are converted to their real lengths and curvatures in Microsoft Excel (or other data processing software). This is done by drawing a straight line of known length (i.e. the same width or height as the micrograph) on the tracing and determining the conversion factor from the true and arbitrary lengths.

```
#!/bin/bash
echo Autotrace script

if [ -z "$1" ]; then
    echo usage: $0 file_name.bmp
    exit
fi
input_file=$1
autotrace -report-progress -color-count 2 -background-color FFFFFFFF -filter-iterations 20 \
    -centerline -tangent-surround 3 -output-file ${input_file%'.bmp'}.eps $input_file

echo Traced to ${input_file%'.bmp'}.eps

epstodist ${input_file%'.bmp'}.eps

echo Line lengths output to ${input_file%'.bmp'}.eps.dist
```

Figure F.2: Simple BASH script run on a bitmap image of a fibre footprint that was “cleaned” as described in step 5 of figure 6.3. It converts this image into an EPS file of Bézier curves and then produces a set of individual fibre contact lengths and mean curvatures. This code was created and first used by Cottenden [4].

APPENDIX G

FRICITION MEASUREMENTS ON EXCISED HUMAN SKIN

A CONSIDERABLE AMOUNT OF EXPERIMENTAL WORK has been carried out using a skin *surrogate* (Lorica Soft) which produces consistent results in friction measurements, but in real situations, non-woven fabrics are used against *real* skin. The results obtained so far have shown that Lorica Soft is a suitable representative of real (volar forearm) skin in friction against a range of coverstocks when predicting the relative friction forces for each nonwoven. While the comparison between data from the skin surrogate and human skin *in vivo* has been useful, measurements on the volar forearm are substantially affected by the underlying tissues, so it would be useful to examine friction and deformation of skin alone. A study of friction between excised skin and the same nonwoven fabrics used with volar forearm skin was planned – and approved ethically – with the aim of providing an intermediate between the friction on the skin surrogate and real skin *in vivo*. Preliminary measurements began on skin from a small selection of participants, but the study ended early due to a slow and insufficient supply of skin. Nonetheless, this appendix serves to describe the preliminary work that *was* carried out, which may prove useful to any related future work.

The advantage of using skin *ex vivo*, rather than *in vivo*, is that it can be tested in a flat configuration and until it has worn or dried out, and it does not move spontaneously. *Breast* skin was specifically chosen for use in these experiments as it is relatively smooth and hairless, and is sometimes available in large quantities appropriate for making measurements with the existing apparatus. As the anvils were originally designed for the skin surrogate (as explained in chapter 3), it was also necessary to compare its global compressive modulus with that of excised breast skin. This should give some insight into the impact on measured friction force of using these anvils on skin. First, the development of friction measurement techniques for excised skin and nonwoven fabrics will be described, including skin preparation and the results and observations. Next the developed friction method will be described, and finally procedures for performing compression tests are summarised.

G.1 Friction measurements

G.1.1 Materials

Only two nonwoven fabrics (DC6 and NW3¹) were used in this experiment because it was expected that the same correlation in results – or the lack thereof – for two nonwoven fabrics would apply to all others. It is also expected that this would be evident in results from the chapter 3 – particularly focusing on the range of forces and graph shapes within the entire group of all (16) nonwovens tested.

¹This was a nonwoven used by Cottenden [4] in friction against Lorica Soft. It was not part of the subset of nonwovens used against volar forearm skin, but these experiments began before the subset had been selected.

The excised skin used was obtained during mastectomies on consenting breast cancer patients. (A full copy of the ethics approval for this study, including information sheet and consent form, can be found in appendix H.) Most (approx. 90%) of the subcutaneous fat initially attached to the skin samples was removed by a surgeon before using them in the experiment. Each sample of skin was rinsed with cold tap water and dabbed dry before use.

G.1.2 Methodology development

Preliminary experiments involved developing a method to attach the excised skin (two pieces - one on each side) to a piece of acetate (table 3.2) and observing any common behaviour occurring during friction tests. Details of this are explained below, followed by the finalised method in §G.1.3.

G.1.2.1 Experimental procedure

Attaching skin to the slider:

1. A rectangular frame made from corrugated plastic was cut to size, so that the centre hole was slightly smaller than the original skin dimensions (see figure G.1).
2. Surgical tape was then attached to the rigid frame using double-sided tape – the idea being that surgical tape adheres well to human skin but can also be removed with relative ease.
3. The skin was stretched to its original dimensions as marked when still attached to the patient, and the edges were glued to surgical tape, stratum corneum-side down. (The purpose of the frame was to maintain the skin in its extended state² before attaching it to a sheet of acetate, part of the experimental apparatus.)
4. Superglue was applied to the entire area of the subcutaneous side of the skin.
5. The acetate sheet was placed on it carefully and this was repeated for the piece of skin on the opposite side.
6. Pressure was applied in the form of dead weights (200g) for a little over one hour.

Once the skin had been attached to the slider, the same general methodology described in §3.2.1 was applied to the excised skin. As the settings for each preliminary test were different (applied load and tensometer crosshead speed), they have been summarised in the §G.1.2.2 for simplicity and clarity (§G.1.2.2). Unlike the experiments with Lorica Soft, these could *not* be carried out in the environmentally controlled room because of the use of human tissue. Instead, all work on excised skin was executed in a laboratory licensed for testing of biological substances [Room 204, Research Laboratory, 2nd floor, Clerkenwell Building N19 5LW].

²When skin is removed from the body, it loses its natural resting tension and retracts to a much smaller size, curling inwards and leaving very little of the subcutaneous side showing.

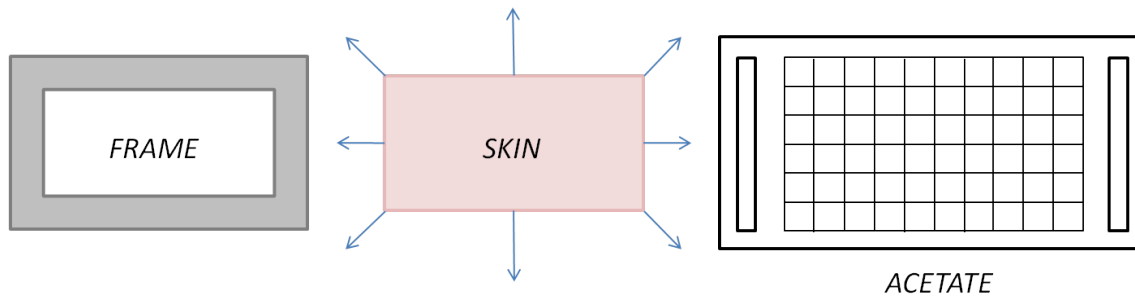


Figure G.1: Diagram to illustrate materials used to mount skin on slider

G.1.2.2 Preliminary results

First, it should be noted that it is rather challenging to restore the original dimensions of the skin, particularly in a direction parallel to the long sides of the samples. Considerably higher tensile forces (which are not quantified here as it was not necessary to measure them) were required to deform the skin samples across their width rather than length. It has been considered that the reason for this may relate to orientation of the skin on the body, such that skin is said to be stiffer perpendicular to the spine in the thoracic and abdominal regions, than it is parallel to the spine [35]. This is linked to the directions of Langer's lines on the body, which, for breast skin, implies that samples taken from the edge of the breast will extend more perpendicular to the edge than parallel (see figure 2.5). However, this has not been found to be the case experimentally. It is also worth mentioning that double-sided and surgical tapes are similarly adhesive – both stick well to skin but are detachable. Therefore, it is not necessary to use both.

Below are the results of the friction measurements between a nonwoven fabric (NW3) and the first two excised skin samples obtained. Here, the attachment of the skin pieces to the slider and their ability to remain in position were the primary concerns. This was mostly successful, although the very first sample did become partially detached from the slider, as shown by figure G.2. It should be noted that the methodology for the first two samples was not exactly as described previously; this is because parts of the protocol had to be developed in order to ensure their practicality, such as attaching skin to the slider. The preliminary experiments were also important for making initial observations about the behaviour of the skin and its experimental implications.

Preliminary test 1

- Applied load: 2.6N (270g)
- Crosshead speed: $30 \text{ mm} \cdot \text{min}^{-1}$ (or $0.5 \text{ mm} \cdot \text{s}^{-1}$)
- Nonwoven fabric: NW3
- Age and ethnicity of donor: 66 years, White European
- Size(s) of samples: $60 \text{ mm} \times 30 \text{ mm}$ and $80 \text{ mm} \times 30 \text{ mm}$

Pre-friction observations Many issues arose with the use of this sample:

1. The skin had some long hairs protruding from it (not all of which could be removed completely).
2. Both pieces were extremely difficult to stretch back to their original size and one was narrower – and too narrow for the anvils – than its pair once on the slider.

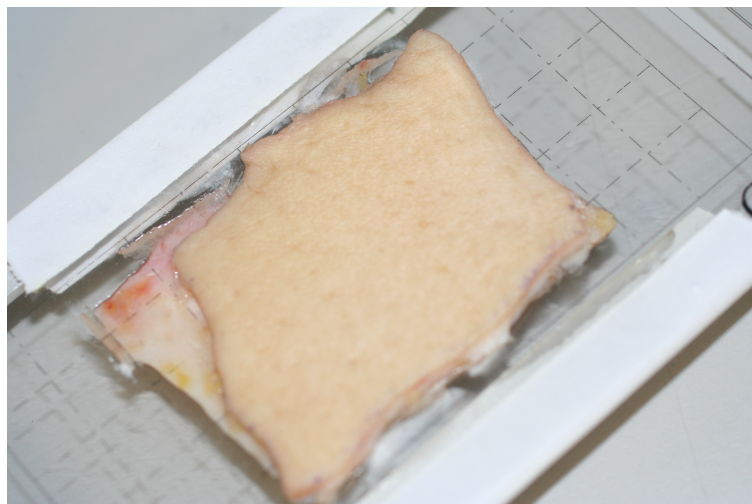


Figure G.2: Photograph of skin attached to acetate sheet with one detached corner after measurements

3. The moist subcutaneous tissue made it particularly difficult to adhere to the acetate (slider), despite multiple attempts to dry it. The rubber gloves (worn for health and safety reasons) came into contact with the subcutaneous side several times, resulting in the loss of adhesive properties of the double-sided tape or surgical tape³. The effect was perhaps similar to that of contact between sellotape and oil.
4. After attaching the skin to the acetate with super-glue (despite applying weights while the glue set), the skin slowly began to shrink again from the edges inwards.

Practical issues: The slider caught the nut on the underside of the top face of the apparatus during every cycle, after about 15-20mm displacement. This was not immediately obvious, but when noticed, it was not possible to fix during the experiment and time restrictions meant that the experiment could not be repeated. This event usually led to a sharp increase in force (see figure G.3), and for some cycles, the slider was almost completely removed from the tensometer grips. Unfortunately, the cause of the anomaly in cycle 7 is unknown.

Friction measurement observations: During the experiment, there was more rucking of the skin than expected. This was to such an extent that for some cycles, the anvil appeared to move not very far across the skin surface, and instead only moved with the skin (sticking) for a distance of about 5-10mm before moving across the skin surface (slipping). This corresponds with the initial “toe” region, where there was a large increase in force over approximately 5mm, and the start of the next almost-linear region of the graph.

³This was the tape used to adhere the edges of the upper (SC) side to a rigid frame (to make sure that the skin was stretched to the correct size) before gluing the underside to the acetate.

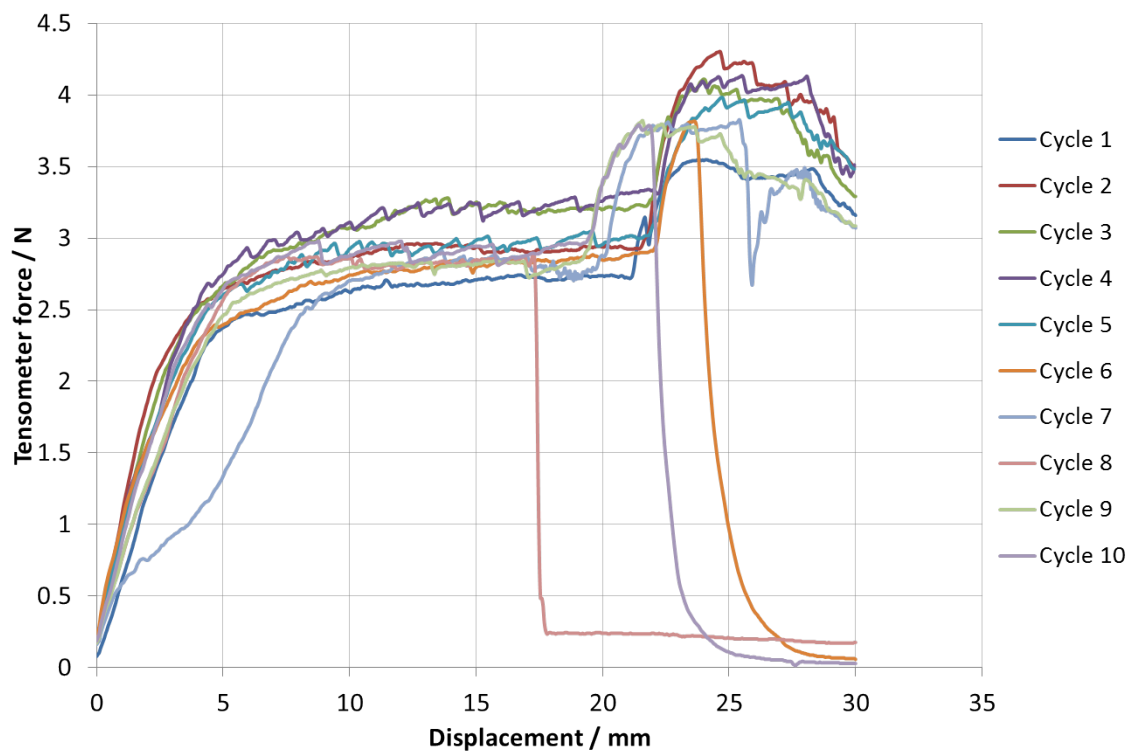


Figure G.3: Preliminary experiment 1

Preliminary test 2

- Applied load: 9.81N (1000g)
- Crosshead speed: $90 \text{ mm} \cdot \text{min}^{-1}$ (or $1.5 \text{ mm} \cdot \text{s}^{-1}$)
- Nonwoven fabric: NW3
- Age and ethnicity of donor: 62 years, Black African
- Size(s) of samples: $60 \text{ mm} \times 30 \text{ mm}$ (both)

Pre-friction observations: This sample was not as difficult to handle as the first one. Both pieces of skin were equal in size and were stretched to almost their original size when in tension on the body. The anvils fit comfortably on the skin.

Practical issues: Unfortunately, the first friction cycle must be ignored because the slider slipped out of the tensometer grips (which were not closed properly).

Friction measurement observations: This sample of skin displayed more rucking than the first sample, which may have been due to the larger load applied or perhaps due to natural physical properties of the donor's skin that made it more flexible or wrinkled.

A strange white substance began to appear on the skin after the third cycle. During the experiment, it was initially thought that this substance may have been the nonwoven fabric "rubbing off" (rather unexpected). However, upon further examination, it turned out to be desquamation ("flaking off") of the stratum corneum cells. This sample was not exposed to the environment outside its container for much longer than the first sample, so it is possible that this was simply a feature of the donor's skin,

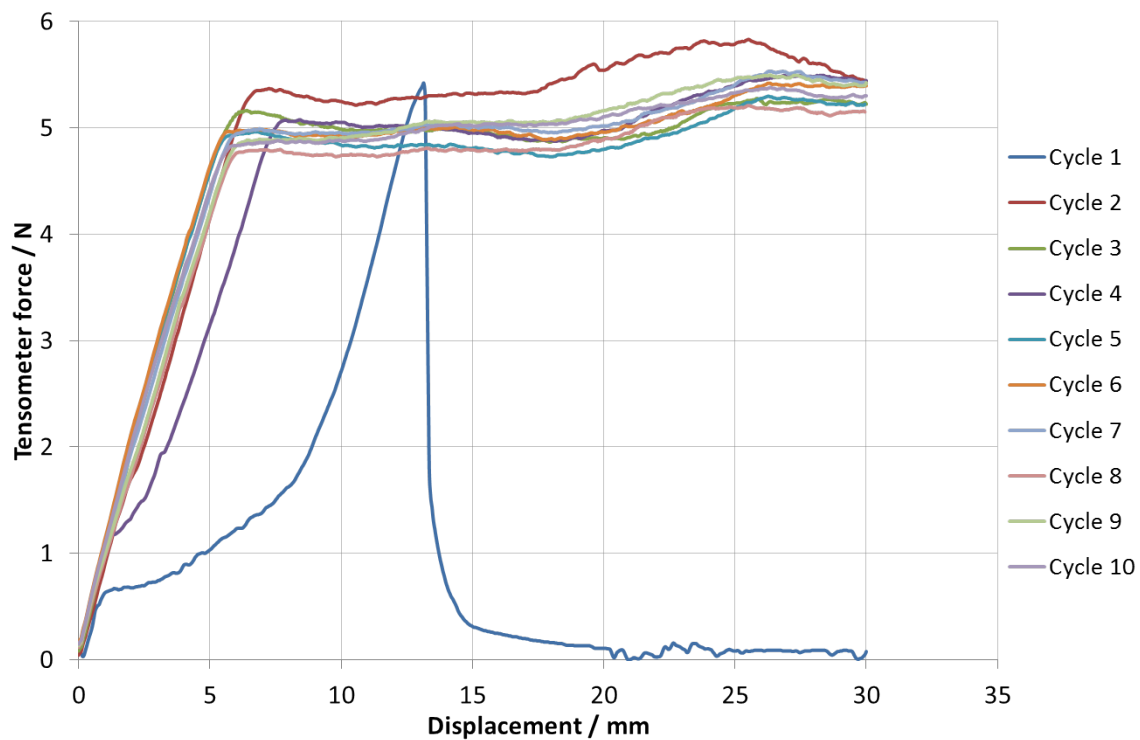


Figure G.4: Preliminary experiment 2

causing it to dehydrate more quickly. Alternatively, the increased load and crosshead speed may have been the key contributors to the flaking of the skin.

Figure G.4 demonstrates the repeatability of the technique as the curves for each cycle are much more similar, both in force magnitude and shape; overall a more successful attempt than the first preliminary friction measurements on excised skin. Again, there was a sharp increase in friction force during the first 5 mm displacement, but this time, all curves (except for the anomalous cycle 1) reached a plateau, with only a small peak toward the end. It is believed that the final peak related to edge effects: continued rucking of the skin as the anvil reached the end of the set displacement, relatively close to the proximal (tensometer) edge of the skin.

G.1.3 Developed methodology

It should first be mentioned that the methods presented in this section depended very much on the results of the preliminary experiments, which were described in §G.1.2.2. As the method for preparing the skin and attaching it to the acetate sheet was very successful, it remained the same for subsequent work. However, surgical tape was no longer used, for reasons explained in §G.1.2.2.

G.1.3.1 Experimental procedure

The next step was to explore the possibility of variation in the friction data over three applied normal loads (0.25N, 2.6N and 8.1N). Tensometer crosshead speed was set at $1.5 \text{ mm} \cdot \text{s}^{-1}$. Considering the

interesting observations made throughout the preliminary experiments and the phenomenon occurring within the first 10mm displacement, it was thought that video-recordings of each measurement would be highly useful. The purpose of video-recording was to enable the association of characteristic changes on the friction force-displacement curves with a visible physical variation. Therefore, all measurements described here were recorded with a video camera [Sony Handycam DCR-SR52E, Sony Corporation, Tokyo, Japan]. The skin and acetate were also marked along one edge (parallel to the tensometer pull direction) at the centre, and two other points on either side of the centre. It was expected that this would provide some information about local deformation (tension and/or shear) in the skin during friction measurements, particularly at the start of the measurement.

Details of the donor:

- Age (years): 64
- Ethnicity: Mixed (black and white)
- Size of samples: 40 mm × 40 mm
- Condition of skin: Nodules of fat on subcutaneous side; few small hard lumps within dermis, not visible to the naked eye.

G.1.3.2 Results

Only one sample (pair of pieces) of excised skin was obtained for friction measurements due to reasons mentioned at the start of this chapter. Consequently, only a brief discussion of this data is included in this section.

Looking at the toe region of the graph in figure G.5 between 0.3 and 0.6N (within the first 5mm displacement), curves are relatively linear; there is a clear, sharp increase in friction force for each cycle. It appears that this was due to sticking between the skin and nonwoven fabric, during which no actual relative movement (slip) took place. Here, the anvil moved *with* the skin. These first 5mm displacement induced the initial rucking, which persisted for the remainder of each friction cycle. There was no visual evidence (to the naked eye) of the stick-slip mechanism. However, when it is considered that the extent of the rucking in the skin did not decrease and the anvil continued to move across the surface of the skin, it would be expected that stick-slip existed on some smaller scale. This may have given rise to the small variations in the region of the graph after 5mm, rather than noise from the tensometer alone.

The same applied to figure G.6, except that the toe region appears to be split into two separate linear regions on the graph – the first at 0-2mm displacement, the second at 2-6mm. It also extended slightly: 1mm beyond that at 0.25N. The first cycle had a large trough at 7.5-9.5mm due to one corner of the skin (proximal to the tensometer) slipping and becoming partially unglued from the acetate. From approximately 10mm displacement onwards, there was a clear increase in friction force with each consecutive cycle (with the exception of cycles 4 and 5, where the reverse appears to be true or there is overlap). This is something that was not seen with friction between Lorica Soft and nonwoven fabrics.

Again, under 8.1N, there appears to be two linear regions to the toe of the graph – the first at 0-2.5mm displacement and the second at 2.5-7.5mm (figure G.7). Cycle 1 has a larger “toe region” where the skin took longer to reach the second linear phase (of friction force against displacement) during this cycle than any other. The toe region relates to excessive sticking of the skin to the anvils before slipping, perhaps larger in the first cycle due to the slow recovery of skin. After about 10mm displacement, there is a general *decrease* in friction force from one cycle to the next, contrary to the results under an applied load of 2.6N.

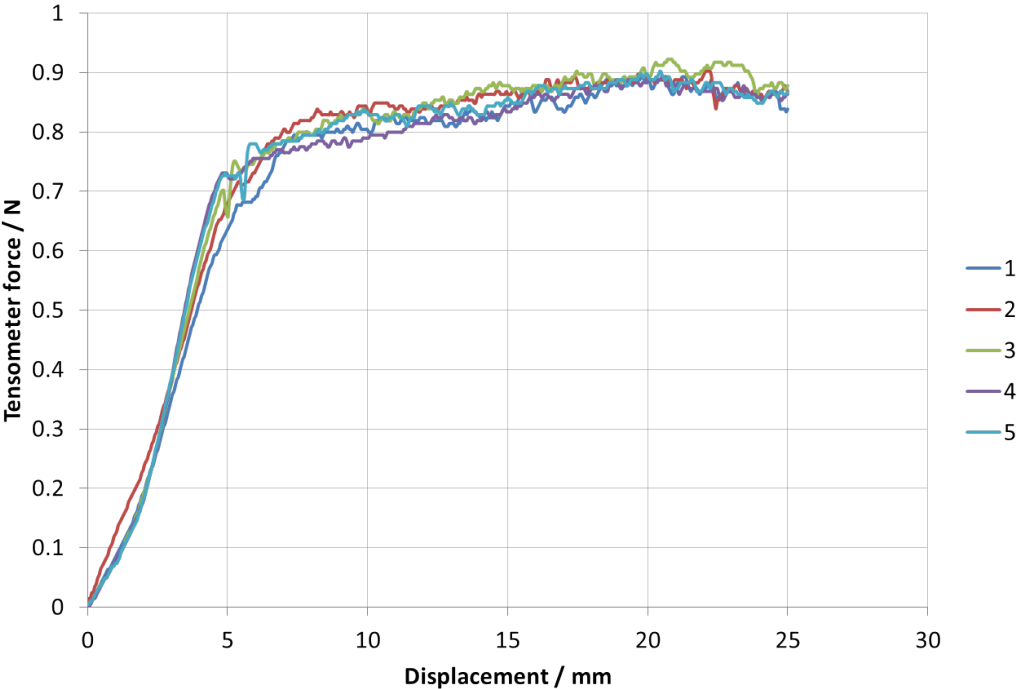


Figure G.5: Friction forces between nonwoven fabric DC6 and excised breast skin under 0.25N

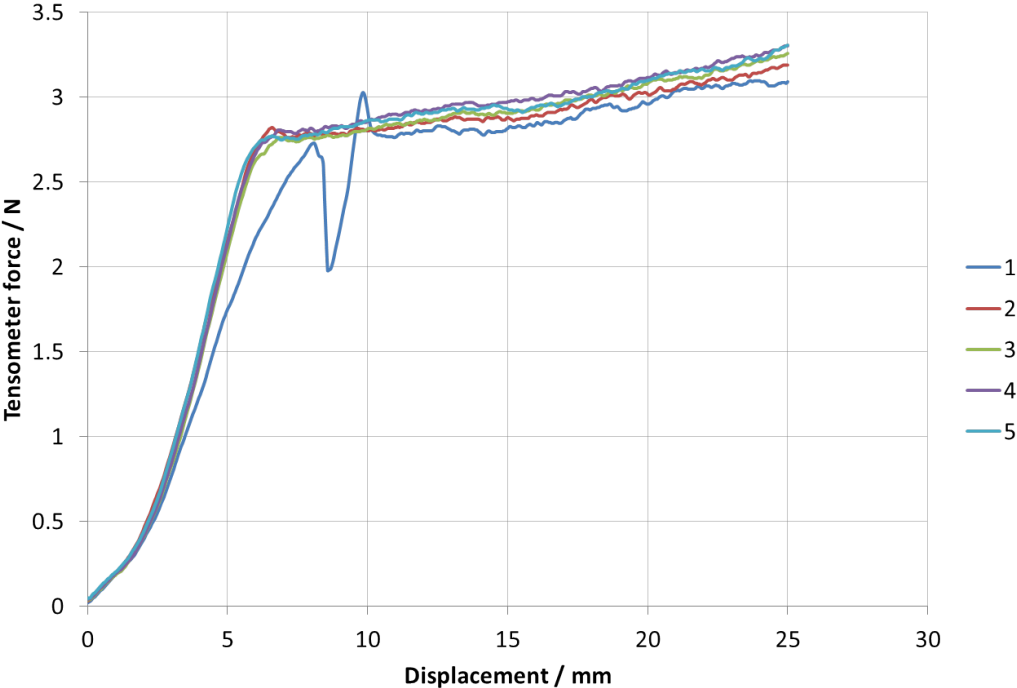


Figure G.6: Friction forces between nonwoven fabric DC6 and excised breast skin under 2.6N

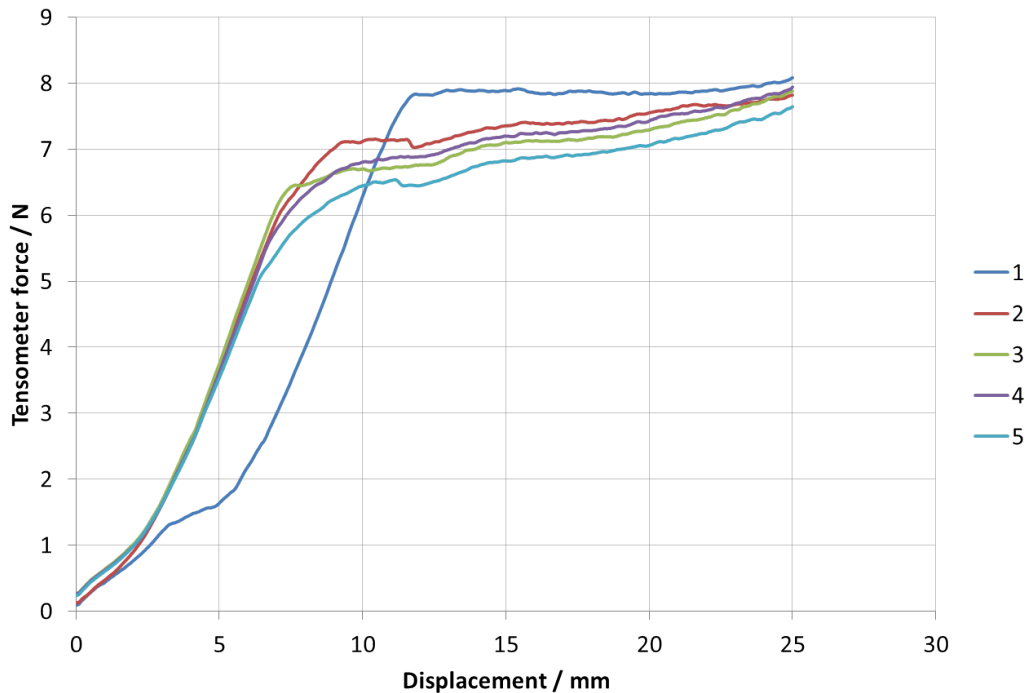


Figure G.7: Friction forces between nonwoven fabric DC6 and excised breast skin under 8.1N

G.1.3.3 Discussion

None of these graphs have a noticeable peak, clearly identifying static friction force, as was seen with all measurements on the skin surrogate and most on volar forearm skin. The behaviours are evidently different, but it is still unknown if the same mechanism(s) were operating for both the surrogate and excised skin. It may be that the differences observed so far are irrelevant to the onset of skin damage, in which case Lorica Soft might remain an appropriate surrogate for extensive friction testing. Alternatively, they may be direct indications that Lorica Soft is of little use for predicting frictional behaviour of skin and that Amontons' law does not always hold. Before any such inferences can be made, more data must be collected and the coefficients of friction corrected for applied load.

G.2 Compression tests

The compressive moduli of excised breast skin was measured under a range of loads to ensure that the anvils used in friction experiments with the skin surrogate were appropriate for friction measurements on the skin. This was important to know because the manufacturing process of the anvils involved the use of a base similar in compression to that of the surface against which the nonwoven fabrics would be pulled. If the manufacturing base/surface is too different from the test surface, the anvils may not have the same contact area, therefore altering applied pressure. These compression tests were performed in an attempt to quickly, but fairly accurately, estimate the compressive moduli of the excised skin within the force range used for friction measurements.

It is, of course, noted that each person's skin is different, not only visually, but mechanically, and, to an extent, structurally. Furthermore, the samples used for these compression experiments were not then used for friction tests due to the insufficient quantity of skin (smaller dimensions and only one piece).

Nevertheless, it was assumed that the moduli of the skin would have small enough variation between samples so that the few measurements made could be considered representative of all excised breast skin. It could be argued that measuring the compressive moduli of each sample to be used in a friction experiment would be more reliable and more accurate, but the main issue with carrying this out is that the aim of these experiments is to assess the suitability of the current anvils for use on skin. All friction experiments may have been completed before discovering that the anvils had applied a broad range of different pressures to each sample of skin. Other issues include timing, dehydration of the skin before commencing friction measurements, sample size, potential damage to the skin (during compression) and experimental setup (apparatus).

G.2.1 Materials & methods

For all compression measurements, a digital indicator [Mahr Millitast 1075 Digital Indicator, Mahr GmbH, Göttingen, Germany], depicted in figure G.8, was used. It applied a starting known load of 0.79N and dead weights were added to increase normal load accordingly. This piece of apparatus was chosen for these measurements because it is simple to use and incremental load application can be easily controlled.

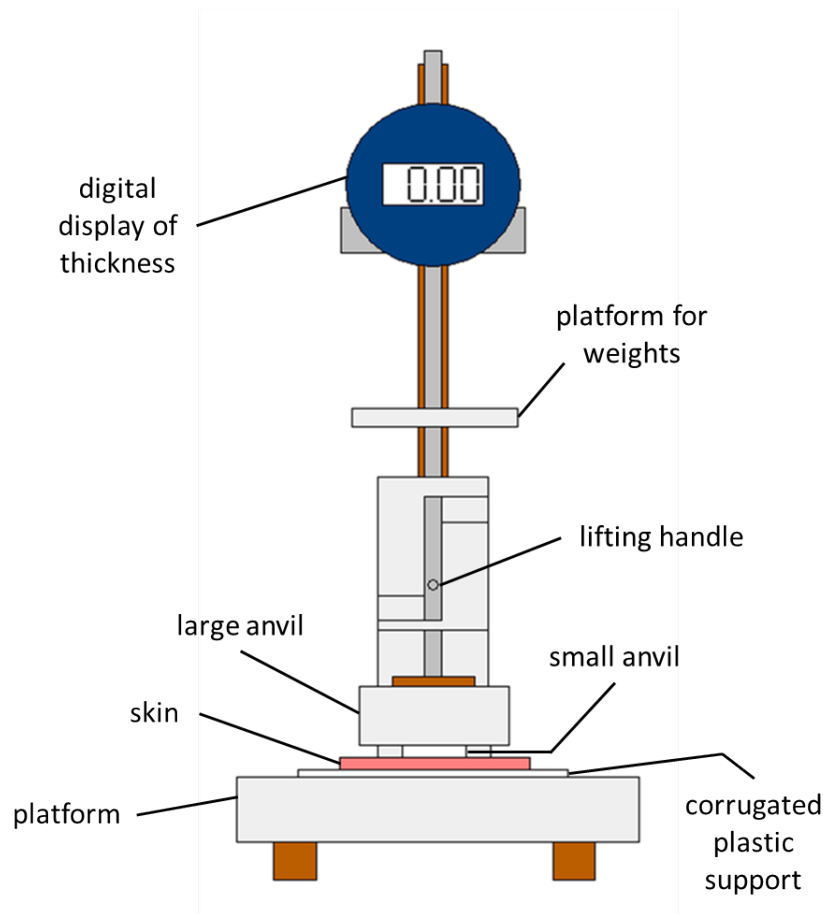


Figure G.8: Diagram of Millitast equipment (extra loads are applied to the skin through the anvil(s) by adding dead weights to the upper platform; thickness is measured by the apparatus and displayed digitally)

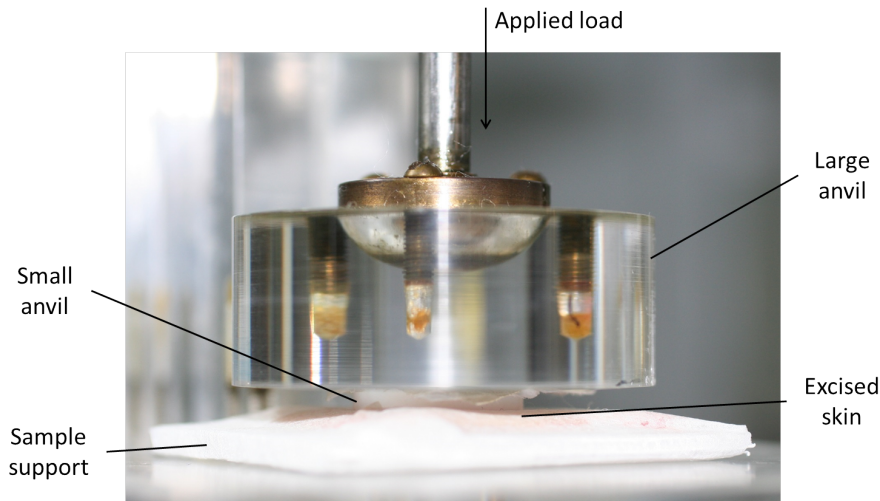


Figure G.9: Sample of excised skin in compression apparatus

1. A photograph of the skin was taken after cleaning, before and during (see figure G.9) the compression test. The skin was distended to its original size ($\approx 30 \text{ mm} \times 30 \text{ mm}$).
2. The smaller anvil was attached with double-sided tape to the larger anvil of the Millitast apparatus and the thickness of the smaller anvil was measured. The thickness of the skin was also measured with this apparatus.
3. The skin was attached to the flat surface of a piece of corrugated plastic – the same material used to make frames on which to fasten excised skin for the experiments described in §G.1.3. This was so that the skin may be compressed while the skin was more or less, under the appropriate natural tension.
4. A “zero” thickness was set by switching on the digital screen when the bottom anvil was touching the platform. This was checked by raising the anvils by the lifting handle and lowering them back onto the platform.
5. The skin was securely placed – with its “support” – on the platform under the anvils, as shown in figure G.8.
6. The full weight of the anvils were applied to the skin and the new thickness of the skin was measured, having allowed 5 minutes for the reading to stabilize. The pressure applied via the smaller anvil on the skin surface was $\approx 2.5 \text{ kPa}$.
7. Seven weights, each 10g, were added to the platform for weights individually at 5-minute intervals, between which, the new skin thickness was recorded. One final weight of 11g was also added before the apparatus was unloaded, again, at 5-minute intervals. The maximum total pressure applied reached approximately 5kPa.
8. The previous two steps were repeated for a total applied load of 490g ($\approx 15 \text{ kPa}$) added all at once; the load was then completely removed (minus the weight of the apparatus anvil).

G.2.2 Results

Figure G.10 shows the relationship between compressive stress and strain for a sample of excised breast skin. As expected, the relationship is non-linear and the rate of change in sample thickness slows as the applied stress increases. However, these data are not particularly enlightening without

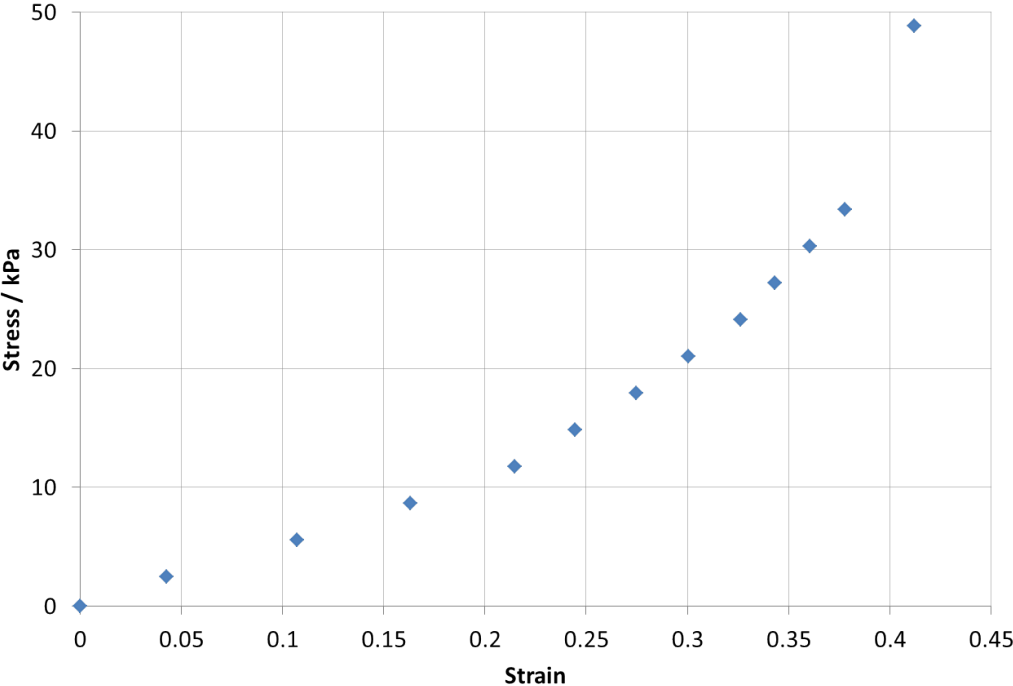


Figure G.10: Stress-strain curve for excised skin sample

the equivalent data for the skin surrogate. Compression measurements were not carried out on Lorica Soft due to the study ending prematurely, but would be useful to carry out in future before continuing with friction measurements on excised skin, for reasons explained in the introduction of this section.

APPENDIX H

RESEARCH ETHICS COMMITTEE APPLICATION: EXCISED SKIN FRICTION STUDY PROTOCOL

BEFORE THE WORK IN THIS THESIS BEGAN, David Cottenden – a former PhD student in the Continence and Skin Technology Group – applied for ethics approval for a study to measure friction between nonwoven fabrics and excised breast skin, using the equipment described in §3.2.1. This apparatus was, in fact, originally designed for measurements on human skin in a flat configuration. Despite obtaining REC approval and due to factors beyond his control, the study did not go ahead. After this, the intention was to continue the work on excised skin to bridge the gap between friction measurements made on flat Lorica Soft and those on (curved) volar forearm skin performed in *this* project. The REC application was amended to accommodate a new researcher/investigator and extend the study end date; the updated protocol, written by David Cottenden, has been included in this chapter to summarise the planned work. The actual experimental procedures attempted were described in appendix G.

Protocol for a study of friction between human skin and nonwoven fabrics

Alan Cottenden¹, Sabrina Falloon¹, James Malone-Lee², Jayant Vaidya², Alan Wilson²

¹Department of Medical Physics & Bioengineering, University College London UK

²Department of Medicine, University College London, UK

August 31, 2011, Version 2.3

Full title of study: An experimental study of the friction between excised, healthy, blemish-free human skin and nonwoven coverstock fabrics, preparatory to theoretical modelling of this interaction.

Short title: A study of friction between human skin and nonwoven fabrics

Chief investigator: Dr. Alan Cottenden

Co-investigators: Miss Sabrina Falloon, Prof. James Malone-Lee, Mr. Jayant Vaidya, Mr. Alan Wilson

Sponsor: University College London

Summary

Wearers of incontinence pads and sanitary towels frequently experience skin abrasion due to friction. The Continence and Skin Technology Group has worked for some years to develop techniques for measuring this friction *in vivo*. In order to deepen our understanding of how this friction works, we now need to conduct a study on excised skin.

The study will involve taking residual skin from routine mastectomy operations and performing microscopy and some mechanical tests on it. There will be no interaction between the investigators and the participants; all interaction will be via the participants' surgeons, who will make the initial approach to their patients, and obtain informed consent.

Contents

1	Introduction	2
1.1	Background	2
1.2	Preliminary experiments	3
1.3	Aims and objectives	3

<i>Introduction</i>	2
2 Methodology	4
2.1 Identification of subjects, consent, and tissue sourcing	4
2.2 Transport, preparation, storage, and disposal of tissue	6
2.3 Experiment methodology	6
2.3.1 Simple microscopy (objective 1)	6
2.3.2 Simultaneous friction measurement and simple microscopy (objective 2)	7
2.4 Health and safety	8
2.5 Projected timing	9
3 Ethics	9
4 Expertise	11
Appendices	12
A Participant information sheet	12
B Participant consent form	17
C Sample information form	19

1 Introduction

The work described in this document follows a series of *in vivo* experimental studies of friction between skin and nonwoven coverstock fabrics (similar to teabag material, and commonly used as topsheets in incontinence pads and feminine hygiene products) which have provided the immediate motivation for this study (§1.1). The eventual aim of the project of which this study forms a part is to develop a mathematical model that can predict (at least semi-quantitatively) the friction between a particular person's skin and a certain nonwoven fabric on the basis of their material properties.

The procedures proposed (§2.3.1 and §2.3.2) have been trialled as far as possible using an unverified skin surrogate (§1.2), and so it has been established that it is very likely that the study described here will meet its stated objectives (§1.3).

1.1 Background

Three million people in the UK are incontinent of urine, and the prevalence is anticipated to increase further as the population ages [1]. Whilst many sufferers can be at least partially cured, the significant minority who cannot be fully cured require products to manage their condition. The most common product type is absorbent pads. When pad materials and skin are wet the coefficient of friction between the wearer and their pad increases [2], increasing the vulnerability of the skin to abrasion damage [3].

Introduction

3

An improved understanding of the mechanisms of friction between skin and typical nonwoven pad coverstocks is needed in order to design products that are less damaging to the skin.

The Contenance and Skin Technology Group (CSTG) have been researching friction between human skin and nonwoven fabrics (such as those commonly used in incontinence pads and other hygiene products) for a number of years. In the course of this research we have developed and published methods for repeatably measuring this friction, and using these methods have discovered that under the same nominal conditions the friction between a given fabric and equivalent sites on different people can be quite different [4]. Further, a set of subjects ordered by increasing friction against fabric A will not generally be in the same order for fabric B. This represents a significant advance in the study of the skin / nonwoven system.

We now wish to understand why this is, and to model it mathematically in terms of the material properties of skin and nonwovens, and so in the long term to understand how to design fabrics that are kinder to the skin. This requires that we gain a microscopic understanding of the interface between the two surfaces and the nature of sliding. This is not possible using *in vivo* skin (as in previous work) due to subject movement and the requirements of microscopy: excised skin is needed for the research to progress.

1.2 Preliminary experiments

In preparation for the acquisition of human skin, experimental methodologies for investigating the interface between nonwovens and thin (~ 1 mm) silicone rubber have been preliminarily developed. These have included methods for (a) examining the nonwoven-silicone interface under a microscope; and (b) determining the force required to drive the interface at a constant speed, whilst simultaneously observing the interface under a microscope. It is hoped that as silicone rubber has many comparable mechanical properties to skin its behaviour will be similar enough that experiments developed using silicone will be readily adaptable to use skin.

The experiments are described in detail in §2.3.1 and §2.3.2.

1.3 Aims and objectives

The role of this study is to elucidate the mechanism by which friction arises. To this end, the immediate objectives are as follows.

1. **To establish the nature of the skin-nonwoven interface across an anatomically representative pressure range.** This will require a small number (roughly five) of varied skin samples to be observed using the method described in §2.3.1.

2. **To establish the relationship between intersurface intimate contact and friction across the speed and pressure ranges specified.** This constitutes the most substantial and quantitative objective of this study, and will require ten or fifteen skin samples. The method for obtaining these data is described in §2.3.2, where the reason for the adequacy of a relatively small sample is further explained.

Experiments relating to each of these objectives must give an indication of the extent to which the mechanisms and rules identified are common to all people. Consequently, the individuals from whom the skin is taken should vary in ethnicity and age if possible so that any important features that are identified can be established as likely universal, or not. However, though this would be desirable, it is not of primary importance for the present project.

2 Methodology

This section describes all procedures and methods that will be employed in the execution of this work, including the identification of subjects, obtaining consent, and the sourcing of skin (§2.1); the transport, storage, and disposal of skin (§2.2); and the experimental methodologies that will make use of the excised skin (§2.3).

The timing of different stages in the skin acquisition and storage, and the experiments are given in §2.5.

2.1 Identification of subjects, consent, and tissue sourcing

This study will involve working with two surgeons based at the Whittington Hospital: Mr Jayant Vaidya (JSV), and Mr Alan Wilson (AJW). Both surgeons routinely perform mastectomy operations, the skin from which is generally smooth and free from hair. This makes it well suited to our experiments: in this exploratory work it is more important that skin is uniform and simple than that it is from the diaper area.

Criteria for *inclusion* in this study are as follows.

- The patient is on the operating list of JSV or AJW for a mastectomy: less major breast surgery will not yield skin samples of sufficient size to be usable in the study's experiments. A minimum size for a sample to be used in this study is 2 cm × 2 cm.
- The patient is 18 years old or above.
- The patient is capable of understanding the information given them about the study, and is fit to give informed consent themselves.

Materials

5

It is possible that patients who have consented to participate in this study will not yield any suitable samples in consequence of the details of their surgery. This is unavoidable, and necessary so that normal surgical procedures are not interrupted.

Criteria for *exclusion* from this study are as follows:

- The patient is under 18 years old.
- The patient is incapable of understanding the information about the study or giving informed consent themselves.

All interaction with the patient will be via JSV and AJW, from first identification of patients scheduled for mastectomy on the operating list, through initial approach and information, to consenting. The researchers will never meet any of the patients, and will have access to no personal information pertaining to them.

The procedure from first identification to the skin being handed to the researchers is as follows.

1. Operating lists are provisionally decided on a Monday morning. JSV and AJW identify any mastectomy patients, and contact Sabrina Falloon (SSF) if any suitable patients are scheduled, for organisational purposes. The identity of any such patient is not passed on.
2. JSV and AJW conduct clinics on Monday and Wednesday mornings, during which they will see patients on their forthcoming lists. During these sessions they will make the initial approach to the patient, and provide them with all the information that they will need to make an informed decision as to whether or not to participate (see appendix A).
3. Surgery is conducted on Tuesday mornings (AJW), Tuesday afternoons (JSV, AJW), and Monday afternoons (JSV or AJW). Normal practice is for the patient to consent to the operation immediately before it; at the same time they will be asked whether they consent to take part in this study also (see appendix B). This will give each patient at least 24 hours (Monday clinic) or five days (Wednesday clinic) to consider the information given them. **However, there are some cases where it may be necessary to get consent less than 24 hours before the operation, such as a patient having a pre-clerking appointment several weeks before their mastectomy.**
4. JSV and AJW will contact SSF immediately prior to the relevant operation so that he can be waiting outside the theatre. When the operation is complete, skin from an unaffected part of the breast will be taken by the surgeon and given to SSF, who will begin experiments as soon as possible. The Whittington Hospital Pathology laboratory have consented to this sample bypassing them. All samples will be anonymous, though the hospital notes will carry the study number.

This will be continued until sufficient samples have been gathered: as discussed in §1.3, the number of samples needed is expected to be about 20, and will not exceed 30. No more precise figure is possible due to the exploratory nature of this work.

Appropriate training and experience: Procedures which incur a heightened risk are carried out by people fitted by training to do them. The principal example in this study is deferring to SB and his surgical training for the preparation of skin.

No other significant health and safety issues are raised by this study.

2.5 Projected timing

The purposes of this section are to clarify the rather complex train of events which follows the surgeons' receipt of their operating lists, and to give an approximate guide to the start and end dates of the work.

The sequence and timing of events following the surgeons' receipt of a week's operating list early on Monday is laid out in table 1. It is important to note that in all cases the patient will have at least 24 hours to consider whether or not they wish to take part, and in most cases several days. The relatively small number of mastectomies on any given list means that most of sessions during which the surgeons operate will not result in any skin, and so no action will be needed. For this reason, it will be possible for one person (DJC) to conduct all of the experiments.

As stated in §2.2, no samples will be retained beyond 24 hours after their removal; there are therefore no issues pertaining to tissue storage.

Mr Jayant Vaidya estimates that he and Mr Alan Wilson perform a total of three or four mastectomies per month, so it is to be expected that 20 samples will take in the region of five to ten months, depending upon the uptake rate. The PhD project that this work forms part of currently has well in excess of a year to run, so it is very likely that the study will be completed in good time for the end of the project.

3 Ethics

This study involves very little interaction with the participants that would not otherwise take place, and none on the part of the investigators. All samples and the data generated from them are anonymised prior to supply, with no links remaining to the participant other than the record of the study number in the hospital notes. Samples will not be retained for substantial periods of time; all will have been destroyed by the end of the study; indeed, they will not be kept beyond the period that experiments take, which will be no more than 24 hours (§2.5). Samples will be obtained from residual material from normal, scheduled operations that would be undertaken without reference to this study; no additional procedures or alterations to existing ones are required. The skin would otherwise be disposed of by the Whittington Hospital.

In consequence of this, the primary ethical requirement is to obtain informed consent from participants. As described in §2.1, this will be managed by the prospective participant's surgeon using

	Monday	Tuesday	Wednesday	Thursday	Friday
< 09:30 AM	JSV, AJW receive operating list JSV, AJW clinic: initial approach made and information given	— AJW surgery	— JSV, AJW clinic: initial approach made and information given DJC completes experiments and disposes of skin	—	—
PM	—	JSV, AJW surgery SB prepares skin; DJC experiments	SB prepares skin; DJC experiments disposes of skin	—	—
AM	—	AJW surgery SB prepares skin; DJC experiments	DJC completes experiments and disposes of skin	—	—
PM	JSV or AJW surgery	DJC completes experiments and disposes of skin SB prepares skin; DJC experiments JSV, AJW surgery	SB prepares skin; DJC experiments DJC completes experiments and disposes of skin	—	—

Table 1: A guide to the timing of the study, taking the surgeons' receipt of an operating list as the starting point. As explained in §2.1, patients on the operating list received on a Monday are seen in clinic on either Monday or Wednesday AM, when JSV or AJW will introduce the study to them and provide information. Patients at the Monday AM clinic will come back in for surgery on either Tuesday AM or later; patients at the Wednesday clinic will come back for the following Monday PM, or later: in either case they will have at least 24 hours to consider the information. For each of the possible surgery slots, the timing of sample preparation and experiments is shown in the same colour; the low frequency of mastectomies makes it unlikely that the substantial overlap of tasks relating to each possible surgery slot will be a problem.

materials prepared by us (see appendices A and B). At least 24 hours will be given, **where appropriate**, to the prospective participants in which to consider the information, before they are given the opportunity to take part or not when consent is sought for their surgery (§2.1). **In cases where the surgeons believe that information would best be given less than 24 hours before surgery, they will deal with this pragmatically.** Consent forms for this study will be kept with the patients' notes.

Though the samples will be anonymised, they will be kept in a keypad secured laboratory. The data obtained by experiment will be entirely untraceable to the participant, but will be kept on password secured computers; our practice with experimental data of this type is to keep them indefinitely. Samples will be coded with a single number, and linked to the gender, ethnicity, and age of the participant, as well as a general description of other skin conditions and medical interventions which may significantly alter the skin.

4 Expertise

Dr Alan Cottenden is a Medical Physicist with 25 years' experience working on incontinence technology. He has managed, directed, or participated in around 25 clinical trials of incontinence products and clinical studies involving *in vivo* measurements on skin.

Sabrina Falloon is a PhD student in the Continence and Skin Technology Group, a joint venture of the departments of Medical Physics and Medicine. Her previous training is in Medical Engineering. Her direct supervisor is Alan Cottenden.

Prof. James Malone-Lee is Professor of Medicine at University College London, and has been working on incontinence for about 25 years. In this time he has overseen 15 clinical trials, and has considerable experience in this respect. He is head of the centre within which this work will be undertaken.

Mr Jayant Vaidya is a Fellow of the Royal College of Surgeons, and is presently a Consultant Surgeon and Senior Lecturer at UCL, based in the Whittington Hospital. He has recently taken up this post, having previously practised in the University of Dundee for five years.

Mr Alan Wilson is also a Fellow of the Royal College of Surgeons, and is a Senior Consultant Surgeon based at the Whittington Hospital.

Mr Samuel Bishara is a Member of the Royal College of Surgeons, and works with Prof. James Malone-Lee in his research group. He has worked on a number of clinical trials in this context.

REFERENCES

- [1] Thomas, S., Billington, A., & Getliffe, K. (2004) Improving continence services a case study in policy influence. *Journal of Nursing Management* **12**, 252–257.
- [2] Cottenden, A., Bliss, D. Z., Buckley, B., Fader, M., Getliffe, K., Paterson, J., Pieters, R., & Wilde, M. (2009) *Incontinence* Chap. *Management Using Continence Products*, eds. Abrams, P., Cardozo, L., Khoury, S., & Wein, A. (Health Publication Ltd.), 4th edition, pp. 1538–1540, 1618–1619.
- [3] Wong, W. K. R. (2008) *A Study of Evaporation and Friction on Hydrated Forearm Skin*. Ph.D. thesis (University College London).
- [4] Cottenden, D. (2011) *A Multiscale Analysis of Friction Interaction Between Human Skin and Non-woven Fabrics*. Ph.D. thesis (University College London).
- [5] Nevéus, T., von Gontard, A., Hoebeke, P., s, K. H., Bauer, S., Bower, W., rgensen, T. M. J., ren Rittig, S., Vande Walle, J., Yeung, C.-K., & Djurhuus, J. C. (2006) The standardization of terminology of lower urinary tract function in children and adolescents: Report from the standardisation committee of the international children’s continence society. *Journal of Urology* **176**, 314–324.
- [6] Sand, P. K. & Dmochowski, R. (2002) Analysis of the standardisation of terminology of lower urinary tract dysfunction: Report from the standardisation sub-committee of the international continence society. *Journal of Neurological Urodynamics* **21**, 167–178.
- [7] NHS Choices. (2012) Incontinence, urinary (<http://www.nhs.uk/conditions/Incontinence-urinary/Pages/Introduction.aspx>). Accessed: March 2012.
- [8] Staskin, D., Kelleher, C., Bosch, R., Coyne, K., Cotterhill, N., Yoshida, E. M., & Kopp, Z. (2009) *Incontinence* Chap. *Initial Assessment of Urinary and Faecal Incontinence in Adult Male and Female Patients*, eds. Abrams, P., Cardozo, L., Khoury, S., & Wein, A. (Health Publication Ltd.), 4th edition, p. 334.
- [9] NHS Choices. (2012) Incontinence, urinary - causes (<http://www.nhs.uk/Conditions/Incontinence-urinary/Pages/Causes.aspx>). Accessed: March 2012.
- [10] NHS Choices. (2012) Incontinence, urinary - symptoms (<http://www.nhs.uk/Conditions/Incontinence-urinary/Pages/Symptoms.aspx>). Accessed: March 2012.
- [11] The Cystitis and Overactive Bladder Foundation. (2014) Continence support (<http://www.cobfoundation.org/continence-support>). Accessed: 15 May 2014.
- [12] Hunskar, S., Lose, G., & Voss, S. (2004) The prevalence of urinary incontinence in women in four european countries. *BJU International* **93**, 324–330.

- [13] Milsom, I., Altman, D., Lapitan, M. C., Nelson, R., Sillén, U., & Thom, D. (2009) *Incontinence Chap. Epidemiology of Urinary (UI) and Faecal (FI) Incontinence and Pelvic Organ Prolapse (POP)*, eds. Abrams, P., Cardozo, L., Khoury, S., & Wein, A. (Health Publication Ltd.), 4th edition, p. 91.
- [14] Gray, M. (2010) Optimal management of incontinence-associated dermatitis in the elderly. *American Journal of Clinical Dermatology* **11**, 201–210.
- [15] Gray, M. (2004) Preventing and managing perineal dermatitis: a shared goal for wound and continence care. *Journal of Wound, Ostomy and Continence Nursing* **31**, S2–S9.
- [16] Zulkowski, K. (2008) Perineal dermatitis versus pressure ulcer: Distinguishing characteristics. *Advances in Skin and Wound Care* **21**, 382–388.
- [17] Getliffe, K., Fader, M., Cottenden, A., Jamieson, K., & Green, N. (2007) Absorbent products for incontinence: 'treatment effects' and impact on quality of life. *Journal of Clinical Nursing* **16**, 1936–1945.
- [18] Weller, R. P. J. B., Hunter, J. A. A., Savin, J. A., & Dahl, M. V. (2008) *Clinical Dermatology*. (John Wiley & Sons), 4th edition. DOI: 10.1002/9781444300086.ch2.
- [19] Saladin, K. (2007) *Human Anatomy*. (McGraw-Hill), International edition.
- [20] Geerligs, M. (2009) *Skin layer mechanics*. Ph.D. thesis (Eindhoven University of Technology).
- [21] Martino, F., Silvestri, E., & Grassi, W. (2007) *Musculoskeletal sonography: technique, anatomy, semeiotics & pathological findings in rheumatic diseases*. (Springer-Verlag Italia).
- [22] Martini, F. (2007) *Anatomy and Physiology*. (Pearson Education, Inc.).
- [23] Forslind, B. (2000) *Handbook of Occupational Dermatology Chap. The Structure of the Human Skin Barrier*. (Springer-Verlag), pp. 56–63.
- [24] Kottner, J., Schario, M., Bartels, N. G., Pantchechnikova, E., Hillmann, K., & Blume-Peytavi, U. (2012) Comparison of two in vivo measurements for skin surface topography. *Skin Research and Technology* **19**, 84–90.
- [25] van der Valk, P. G. M., Kucharekova, M., & Tupker, R. A. (2005) Transepidermal water loss and its relation to barrier function and skin irritation In *Bioengineering of the Skin: Water and the Stratum Corneum*, eds. Fluhr, J., Elsner, P., Berardesca, E., & Maibach, H. I. (Boca Raton, USA : CRC Press LLC), 2nd edition, pp. 97–104.
- [26] Fader, M., Clark-O'Neill, S. R., Wong, W. K. R., Runeman, B., Farbrot, A., & Cottenden, A. M. (2011) Development and preliminary testing of a standardized method for quantifying excess water in over-hydrated skin using evaporimetry. *Physiological Measurement* **32**, 305–317.
- [27] Xiao, P., Ou, X., Ciortea, L. I., Berg, E. P., & Imhof, R. E. (2012) In vivo skin solvent penetration measurements using opto-thermal radiometry and fingerprint sensor. *International Journal of Thermophysics* **33**, 1787–1794.

- [28] Clarys, P., Clijsen, R., Taeymans, J., & Barel, A. O. (2012) Hydration measurements of the stratum corneum: comparison between the capacitance method (digital version of the corneometer cm 825 (r)) and the impedance method (skicon-200ex (r)). *Skin Research And Technology* **18**, 316–323.
- [29] Dowson, D. (1997) Tribology and the skin surface In *Bioengineering of the Skin: Skin Surface Imaging and Analysis*, eds. Wilhelm, K.-P., Elsner, P., Berardesca, E., & Maibach, H. I. (Boca Raton, USA : CRC Press), pp. 159–179.
- [30] Comaish, J. S. (1973) Epidermal fatigue as a cause of friction blisters. *The Lancet* **301**, 81–83.
- [31] Bronneberg, D., Bouten, C. V. C., Oomens, C. W. J., v Kemenade, P. M., & Baaijens, F. P. T. (2006) A model system to study the damaging effects of prolonged mechanical loading of the epidermis. *Annals of Biomedical Engineering* **34**, 506–514.
- [32] Nacht, S., Close, J.-A., Yeung, D., & Gans, E. H. (1981) Skin friction coefficient: changes induced by skin hydration and emollient application and correlation with perceived skin feel. *Journal of the Society of Cosmetic Chemists* **32**, 55–65.
- [33] Zimmerer, R. E., Lawson, K. D., & Calvert, C. J. (1986) The effects of wearing diapers on skin. *Pediatric Dermatology* **3**, 95–101.
- [34] Marks, R. (1991) *Physiology, Biochemistry, and Molecular Biology of the Skin*. (Oxford, UK : Oxford University Press).
- [35] Xu, F. & Lu, T. (2011) *Introduction to Skin Biothermomechanics and Thermal Pain*. (London, UK : Springer).
- [36] Langer, K. (1978) On the anatomy and physiology of the skin: I. the cleavability of the cutis. *British Journal of Plastic Surgery* **31**, 3–8.
- [37] Thacker, J. G., Iachetta, F. A., Allaire, P. E., Edgerton, M. T., Rodeheaver, G. T., & Edlich, R. F. (1977) In vivo extensometer for measurement of the biomechanical properties of human skin. *Review of Scientific Instruments* **48**, 181–185.
- [38] Khatyr, F., Imberdis, C., Vescovo, P., Varchon, D., & Lagarde, J.-M. (2004) Model of the viscoelastic behaviour of skin *in vivo* and study of anisotropy. *Skin Research and Technology* **10**, 96–103.
- [39] Delalleau, A., Josse, G., Lagarde, J.-M., Zahouani, H., & Bergheau, J.-M. (2006) Characterization of the mechanical properties of skin by inverse analysis combined with the indentation test. *Journal of Biomechanics* **39**, 1603–1610.
- [40] Khaothong, K. (2010) *In Vivo Measurements of the Mechanical Properties of Human Skin and Muscle by Inverse Finite Element Method Combined with the Indentation Test* In *6th World Congress of Biomechanics (WCB 2010). August 1-6, 2010 Singapore*. Vol. 31, pp. 1467–1470.
- [41] Abellan, M.-A., Zahouani, H., & Bergheau, J.-M. (2013) Contribution to the determination of in vivo mechanical characteristics of human skin by indentation test. *Computational and Mathematical Methods in Medicine* **2013**, 1–11.

- [42] Dikstein, S. & Hartzshtark, A. (1981) In vivo measurement of some elastic properties of human skin In *Bioengineering and the Skin*, eds. Marks, R. & Payne, P. A. (Lancaster : MTP Press), pp. 45–53.
- [43] Boyer, G., Laquieze, L., Le Bot, A., Laquieze, S., & Zahouani, H. (2009) Dynamic indentation on human skin in vivo: ageing effects. *Skin Research and Technology* **15**, 55–67.
- [44] Pailler-Mattei, C., Bec, S., & Zahouani, H. (2008) In vivo measurements of the elastic mechanical properties of human skin by indentation tests. *Medical Engineering & Physics* **30**, 599–606.
- [45] Craves, C. J. & Edwards, C. (2002) Hardware and measuring principles: The microindentometer In *Bioengineering of the Skin: Skin Biomechanics*, eds. Elsner, P., Berardesca, E., Wilhelm, K.-P., & Maibach, H. I. (Boca Raton, USA : CRC Press LLC), pp. 161–178.
- [46] Crichton, M. L., Chen, X. F., Huang, H., & Kendall, M. A. F. (2013) Elastic modulus and viscoelastic properties of full thickness skin characterised at micro scales. *Biomaterials* **34**, 2087–2097.
- [47] Dunn, M. & Silver, F. (1983) Viscoelastic behaviour of human connective tissues: relative contribution of viscous and elastic components. *Connective Tissue Research* **12**, 59–70.
- [48] Sanjeevi, R. (1982) A viscoelastic model for the mechanical properties of biological materials. *Journal of Biomechanics* **15**, 107–109.
- [49] Manschot, J. F. M. & Brakkee, A. J. M. (1986) The measurement and modelling of the mechanical properties of human skin in vivo—ii. the model. *Journal of Biomechanics* **19**, 517–521.
- [50] Silver, F. H., Freeman, J. W., & DeVore, D. (2001) Viscoelastic properties of human skin and processed dermis. *Skin Research and Technology* **7**, 18–23.
- [51] Leyden, J. J. (1990) Clinical features of ageing skin. *British Journal of Dermatology* **122**, 1–3.
- [52] Cerimele, D., Celleno, L., & Serri, F. (1990) Physiological changes in ageing skin. *British Journal of Dermatology* **122**, 13–20.
- [53] Rona, C. & Berardesca, E. (2002) Skin biomechanics: Antiaging products In *Bioengineering of the Skin: Skin Biomechanics*, eds. Elsner, P., Berardesca, E., Wilhelm, K.-P., & Maibach, H. I. (Boca Raton, USA : CRC Press LLC), pp. 231–239.
- [54] Schulze, C., Wetzels, F., Kueper, T., Malsen, A., Muhr, G., Jaspers, S., Blatt, T., Wittern, K.-P., Wenck, H., & Käs, J. A. (2010) Stiffening of human skin fibroblasts with age. *Biophysical Journal* **99**, 2434–2442.
- [55] Alexander, C. H. & Cook, T. H. (1977) Accounting for the natural tension in the mechanical testing of human skin. *Journal of Investigative Dermatology* **69**, 310–314.
- [56] Grahame, R. (1970) A method for measuring human skin elasticity in vivo with observations on the effects of age, sex and pregnancy. *Clinical Science* **39**, 223–238.
- [57] Jost, H. P. (1966) *Lubrication (tribology) – A Report on the Present Position and Industry's Needs*. (London : Department of Education and Science, HM Stationary Office).

- [58] Stachowiak, G. W. & Batchelor, A. W. (2001) *Engineering Tribology*. (MA, USA : Butterworth-Heinemann), 2nd edition.
- [59] Bhushan, B. (1999) *Principles and Applications of Tribology*. (USA : John Wiley and Sons).
- [60] Bhushan, B., ed. (2004) *Springer Handbook of Nanotechnology* Chap. *Surface Forces and Nanorheology of Molecularly Thin Films*. (Berlin and Heidelberg, Germany : Springer-Verlag).
- [61] Mang, T. (2007) *Lubricants and Lubrication* Chap. *Lubricants in the Tribological System*. (Weinheim, Germany : Wiley-VCH GmbH), 2nd edition.
- [62] Bowden, F. P. & Tabor, D. (2001) *The Friction and Lubrication of Solids*. (New York, USA : Oxford University Press Inc.).
- [63] Basu, B. & Kalin, M. (2011) *Tribology of Ceramics and Composites: A Materials Science Perspective*. (John Wiley & Sons, Inc.).
- [64] Berman, A. D. & Israelachvili, J. N. (2001) Microtribology and microrheology of molecularly thin liquid films In *Modern Tribology Handbook*, ed. Bhushan, B. (Boca Raton, USA : CRC Press LLC) Vol. 1, pp. 573–574, 582–583.
- [65] Johnson, K. L., Kendall, K., & Roberts, A. D. (1971) *Surface energy and the contact of elastic solids*, Series A, Mathematical and Physical Sciences In *Proceedings of the Royal Society of London*, Series A, Mathematical and Physical Sciences. Vol. 324, pp. 301–313.
- [66] Müser, M. H. (2006) *Lecture Notes in Physics* Chap. *Theory and simulation of friction and lubrication*, eds. Ferrario, M., Ciccotti, G., & Binder, K. (Springer-Verlag Berlin Heidelberg) Vol. 704, pp. 65–104.
- [67] Nakajima, K. & Narasaka, H. (1993) Evaluation of skin surface associated with morphology and coefficient of friction. *International Journal of Cosmetic Science* **15**, 135–151.
- [68] El-Shimi, A. (1977) In vivo skin friction measurements. *Journal of the Society of Cosmetic Chemists* **28**, 37–51.
- [69] Derler, S. & Rotaru, G.-M. (2013) Stick–slip phenomena in the friction of human skin. *Wear* **301**, 324–329.
- [70] Derler, S., Gerhardt, L.-C., Lenz, A., Bertaux, E., & Hadad, M. (2009) Friction of human skin against smooth and rough glass as a function of the contact pressure. *Tribology International* **42**, 1565–1574.
- [71] Veijgen, N. K., Masen, M. A., & van der Heide, E. (2012) A novel approach to measuring the frictional behaviour of human skin in vivo. *Tribology International* **54**, 38–41.
- [72] Veijgen, N. K., Masen, M. A., & van der Heide, E. (2013) Relating friction on the human skin to the hydration and temperature of the skin. *Tribology Letters* **49**, 251–262.
- [73] Derler, S. & Gerhardt, L.-C. (2012) Tribology of skin: Review and analysis of experimental results for the friction coefficient of human skin. *Tribology Letters* **45**, 1–27.

- [74] Tomlinson, S. E., Lewis, R., Liu, X., Texier, C., & Carré, M. J. (2011) Understanding the friction mechanisms between the human finger and flat contacting surfaces in moist conditions. *Tribology Letters* **41**, 283–294.
- [75] Tomlinson, S. E., Lewis, R., & Carré, M. J. (2009) Understanding the effect of finger-ball friction on the handling performance of rugby balls. *Sports Engineering* **11**, 109–118.
- [76] André, T., Lefevre, P., & Thonnard, J.-L. (2009) A continuous measure of fingertip friction during precision grip. *Journal of Neuroscience Methods* **179**, 224–229.
- [77] Nonomura, Y., Fujii, T., Arashi, Y., Miura, T., Maeno, T., Tashiro, K., Kamikawa, Y., & Monchi, R. (2009) Tactile impression and friction of water on human skin. *Colloids and Surfaces B: Biointerfaces* **69**, 264–267.
- [78] Hendriks, C. P. & Franklin, S. E. (2010) Influence of surface roughness, material and climate conditions on the friction of human skin. *Tribology Letters* **37**, 361–373.
- [79] Kwiatkowska, M., Franklin, S. E., Hendriks, C. P., & Kwiatkowski, K. (2009) Friction and deformation behaviour of human skin. *Wear* **267**, 1264–1273.
- [80] Gerhardt, L.-C., Strassle, V., Lenz, A., Spencer, N. D., & Derler, S. (2008) Influence of epidermal hydration on the friction of human skin against textiles. *Journal of the Royal Society Interface* **5**, 1317–1328.
- [81] Zhu, Y. H., Song, S. P., Luo, W., Elias, P. M., & Man, M. Q. (2011) Characterization of skin friction coefficient, and relationship to stratum corneum hydration in a normal chinese population. *Skin Pharmacology and Physiology* **24**, 81–86.
- [82] CK Electronic. (2014) Scientific devices: Frictiometer fr 700 (<http://www.courage-khazaka.de/index.php/en/products/scientific/268-frictiometer-e>).
- [83] Man, M. Q., Xin, S. J., Song, S. P., Cho, S. Y., Zhang, X. J., Tu, C. X., Feingold, K. R., & Elias, P. M. (2009) Variation of skin surface ph, sebum content and stratum corneum hydration with age and gender in a large chinese population. *Skin Pharmacology and Physiology* **22**, 190–199.
- [84] Marrakchi, S. & Maibach, H. I. (2007) Biophysical parameters of skin: map of human face, regional, and age-related differences. *Contact Dermatitis* **57**, 28–34.
- [85] Diridollou, S., de Rigal, J., Querleux, B., Leroy, F., & Barbosa, V. H. (2007) Comparative study of the hydration of the stratum corneum between 4 ethnic groups: influence of age. *International Journal of Dermatology* **46**, 11–1.
- [86] Kompaore, F. & Tsuruta, H. (1993) In vivo differences between asian, black and white in the stratum corneum barrier function. *International archives of occupational and environmental health* **65**, S223–S225.
- [87] Elkhyat, A. & Humbert, P. (2010) Wettability and friction coefficient hydrophobic/hydrophilic balance influence. *Skin Research and Technology* **16**, 482.
- [88] Derler, S., Huber, R., Feuz, H.-P., & Hadad, M. (2009) Influence of surface microstructure on the sliding friction of plantar skin against hard substrates. *Wear* **267**, 1281–1288.

- [89] Gerhardt, L.-C., Lenz, A., Spencer, N. D., Münzer, T., & Derler, S. (2009) Skin–textile friction and skin elasticity in young and aged persons. *Skin Research and Technology* **15**, 288–298.
- [90] Darden, M. A. & Schwartz, C. J. (2009) Investigation of skin tribology and its effects on the tactile attributes of polymer fabrics. *Wear* **267**, 1289–1294.
- [91] Derler, S., Schrade, U., & Gerhardt, L.-C. (2007) Tribology of human skin and mechanical skin equivalents in contact with textiles. *Wear* **263**, 1112–1116.
- [92] Adams, M. J., Briscoe, B. J., & Johnson, S. A. (2007) Friction and lubrication of human skin. *Tribology Letters* **26**, 239–253.
- [93] Sivamani, R. K., Goodman, J., Gitis, N. V., & Maibach, H. I. (2003) Friction coefficient of skin in real-time. *Skin Research and Technology* **9**, 235–239.
- [94] Egawa, M., Oguri, M., Hirao, T., Takahashi, M., & Miyakawa, M. (2002) The evaluation of skin friction using a frictional feel analyzer. *Skin Research and Technology* **8**, 41–51.
- [95] Koudine, A. A., Barquins, M., Anthoine, P. H., Aubert, L., & Lévêque, J. L. (2000) Frictional properties of skin: proposal of a new approach. *International Journal of Cosmetic Science* **22**, 11–20.
- [96] Asserin, J., Zahouani, H., Humbert, P., Couturaud, V., & Mougín, D. (2000) Measurement of the friction coefficient of the human skin in vivo – quantification of the cutaneous smoothness. *Colloids and Surfaces B* **19**, 1–12.
- [97] Zhang, M. & Mak, A. F. T. (1999) In vivo friction properties of human skin. *Prosthetics and Orthotics International* **23**, 135–141.
- [98] Kenins, P. (1994) Influence of fiber type and moisture on measured fabric-to-skin friction. *Textile Research Journal* **64**, 722–728.
- [99] Elsner, P., Wilhelm, D., & Maibach, H. I. (1990) Frictional properties of human forearm and vulvar skin: influence of age and correlation with transepidermal water loss and capacitance. *Dermatologica* **181**, 88–91.
- [100] Cua, A. B., Wilhelm, K. P., & Maibach, H. I. (1990) Frictional properties of human skin: relation to age, sex and anatomical region, stratum corneum hydration and transepidermal water loss. *British Journal of Dermatology* **123**, 473–479.
- [101] Highley, D. R., Coomey, M., DenBeste, M., & Wolfram, L. J. (1977) Frictional properties of skin. *The Journal of Investigative Dermatology* **69**, 303–305.
- [102] Naylor, P. F. D. (1955) The skin surface and friction. *British Journal of Dermatology* **67**, 239–248.
- [103] Cottenden, A. M., Wong, W. K. R., Cottenden, D. J., & Farbrot, A. (2008) Development and validation of a new method for measuring friction between skin and nonwoven materials. *Journal of Engineering in Medicine* **222**, 791–803.
- [104] Kondo, S. (2002) The frictional properties between fabrics and the human skin. part 1: Factors of human skin characteristics affecting the frictional properties between fabrics and the human skin. *Journal of the Japan Research Association for Textile End-Uses* **43**, 264–275.

- [105] Comaish, S. & Bottoms, E. (1971) The skin and friction: Deviations from amonton's laws, and the effects of hydration and lubrication. *British Journal of Dermatology* **84**, 37–43.
- [106] Berman, A. D., Ducker, W. A., & Israelachvili, J. N. (1996) Origin and characterization of different stick-slip friction mechanisms. *Langmuir* **12**, 4559–4563.
- [107] Rice, J. R. & Ruina, A. L. (1983) Stability of steady frictional slipping. *Journal of Applied Mechanics* **50**, 343–349.
- [108] Nonomura, Y., Arashi, Y., & Maeno, T. (2009) How do we recognize water and oil through our tactile sense? *Colloids and Surfaces B: Biointerfaces* **73**, 80–83.
- [109] Pasumarty, S. M., Johnson, S. A., Watson, S. A., & Adams, M. J. (2011) Friction of the human finger pad: Influence of moisture, occlusion and velocity. *Tribology Letters* **44**, 117–137.
- [110] Tang, W., Ge, S., Zhu, H., Cao, X., & Li, N. (2008) The influence of normal load and sliding speed on frictional properties of skin. *Journal of Bionic Engineering* **5**, 33–38.
- [111] Wilson, A. (2007) *Handbook of nonwovens* Chap. *Development of the nonwovens industry*, ed. Russell, S. J. (Cambridge, England : Woodhead Publishing Limited), pp. 1–15.
- [112] EDANA. (2008) What are nonwovens? (<http://www.edana.org/discover-nonwovens/what-are-nonwovens->). Accessed: February 2012.
- [113] Rosato, D. V., Rosato, M. G., & Rosato, D. V. (2000) *Concise encyclopedia of plastics*. (USA : Kluwer Academic Publishers), p. 272.
- [114] EDANA. (2008) Formation (<http://www.edana.org/discover-nonwovens/how-they%27re-made/formation>). Accessed: February 2012.
- [115] Kuo, C.-F. J., Chou, Y.-C., & Lin, T.-Y. (2012) Automatic control of roller carding machine. part i: Modeling and validation of roller carding machine. *Textile Research Journal* **82**, 3–10.
- [116] Ahmed, A. I. (2007) *Handbook of nonwovens* Chap. *Nonwoven fabric finishing*, ed. Russell, S. J. (Cambridge, England : Woodhead Publishing Limited), pp. 368–400.
- [117] EDANA. (2008) Bonding (<http://www.edana.org/discover-nonwovens/how-they%27re-made/bonding>). Accessed: February 2012.
- [118] Petrulis, D. (2012) The influence of fabric construction and fibre type on textile durability: woven, knitted and nonwoven fabrics In *Understanding and Improving the Durability of Textiles*, ed. Annis, P. A. (Cambridge, UK : Woodhead Publishing), pp. 3–30.
- [119] Mao, N., Russell, S. J., & Pourdeyhimi, B. (2007) *Handbook of nonwovens* Chap. *Characterisation, testing and modelling of nonwoven fabrics*, ed. Russell, S. J. (Cambridge, England : Woodhead Publishing Limited), pp. 401–502.
- [120] Amirbayat, J. & Cooke, W. D. (1989) Change in surface properties of fabrics during wear. *Textile Research Journal* **59**, 469–477.
- [121] Ozdil, N., Marmarali, A., & Oglakcioglu, N. (2009) The abrasion resistance of socks. *International Journal of Clothing Science and Technology* **21**, 56–63.

- [122] Bais-Singh, S. & Goswami, B. C. (1998) Predicting the biaxial tensile deformation behavior of spunbonded nonwovens. *Textile Research Journal* **68**, 219–227.
- [123] Schaff, A. J. & Ogale, A. A. (1991) Tensile viscoelastic properties of spunbonded nonwoven polypropylene backing. *Textile Research Journal* **61**, 386–392.
- [124] Watanabe, A., Miwa, M., Yokoi, T., & Nakayama, A. (1998) Fatigue behavior of aramid nonwoven fabrics under hot-press conditions part v: Effect of punching density on mechanical properties. *Textile Research Journal* **68**, 171–178.
- [125] Patel, P. C. & Kothari, V. K. (2001) Relationship between tensile properties of fibres and nonwoven fabrics. *Indian Journal of Fibre & Textile Research* **26**, 398–402.
- [126] Kothari, V. K. & Das, A. (1993) The compressional behaviour of spunbonded nonwoven fabrics. *The Journal of The Textile Institute* **84**, 16–30.
- [127] Watanabe, A., Miwa, M., Yokoi, T., & Nakayama, A. (1998) Fatigue behavior of aramid nonwoven fabrics under hot-press conditions part iv: Effect of fiber fineness on mechanical properties. *Textile Research Journal* **68**, 77–86.
- [128] MacNeil, S. (2007) Progress and opportunities for tissue-engineered skin. *Nature* **445**, 874–880.
- [129] Rolin, G., Placet, V., Jacquet, E., Tauzin, H., Robin, S., Pazart, L., Viennet, C., Saas, P., Muret, P., Binda, D., & Humbert, P. (2012) Development and characterization of a human dermal equivalent with physiological mechanical properties. *Skin Research and Technology* **18**, 251–258.
- [130] Shevchenko, R. V., James, S. L., & James, S. E. (2010) A review of tissue-engineered skin bioconstructs available for skin reconstruction. *Journal of the Royal Society Interface* **7**, 229–258.
- [131] Harleya, B. A., Leungb, J. H., Silvaca, E. C. C. M., & Gibson, L. J. (2007) Mechanical characterization of collagen–glycosaminoglycan scaffolds. *Acta Biomaterialia* **3**, 463–474.
- [132] Powell, H. M. & Boyce, S. T. (2006) Edc cross-linking improves skin substitute strength and stability. *Biomaterials* **27**, 5821–5827.
- [133] Garcia, Y., Wilkins, B., Collighan, R. J., Griffin, M., & Pandit, A. (2008) Towards development of a dermal rudiment for enhanced wound healing response. *Biomaterials* **29**, 857–868.
- [134] Saddiq, Z. A., Barbenel, J. C., & Grant, M. H. (2009) The mechanical strength of collagen gels containing glycosaminoglycans and populated with fibroblasts. *Journal of Biomedical Materials Research Part A* **89**, 697–706.
- [135] Hong, K. H., Kim, S. C., & Kang, T. J. (2005) Effect of abrasion and absorbed water on the handle of nonwovens for disposable diapers. *Textile Research Journal* **75**, 544–550.
- [136] Gerhardt, L.-C., Mattle, N., Schrade, G. U., Spencer, N. D., & Derler, S. (2008) Study of skin-fabric interactions of relevance to decubitus: friction and contact-pressure measurements. *Skin Research and Technology* **14**, 77–88.
- [137] Gilchrist, M. D., Keenan, S., Curtis, M., Cassidy, M., Byrne, G., & Destrade, M. (2008) Measuring knife stab penetration into skin simulant using a novel biaxial tension device. *Forensic Science International* **177**, 52–65.

- [138] Gerhardt, L. C., Schiller, A., Mueller, B., Spencer, N. D., & Derler, S. (2009) Fabrication, characterisation and tribological investigation of artificial skin surface lipid films. *Tribol Lett* **34**, 81–93.
- [139] Shao, F., Childs, T. H. C., & Henson, B. (2009) Developing an artificial fingertip with human friction properties. *Tribology International* **42**, 1575–1581.
- [140] Guerra, C. & Schwartz, C. J. (2011) Development of a synthetic skin simulant platform for the investigation of dermal blistering mechanics. *Tribol Lett* **44**, 223–228.
- [141] Cottenden, D. J. & Cottenden, A. M. (2013) A study of friction mechanisms between a surrogate skin (lorica soft) and nonwoven fabrics. *Journal of the Mechanical Behavior of Biomedical Materials* **28**, 410–426.
- [142] Greenwood, J. & Tabor, D. (1958) The friction of hard sliders on lubricated rubber: the importance of deformation losses. *Proceedings of the Physics Society* **71**, 989–1001.
- [143] Moore, D. & Geyer, W. (1974) A review of hysteresis theories for elastomers. *Wear* **30**, 1–34.
- [144] Flom, D. G. & Bueche, A. M. (1959) Theory of rolling friction for spheres. *Journal of Applied Physics* **30**, 1725–1730.
- [145] Norman, R. H. (1962) The rolling friction of cylinders on planes. *British Journal of Applied Physics* **13**, 358–361.
- [146] Persson, B. N. J. (2001) Theory of rubber friction and contact mechanics. *Journal of Chemical Physics* **115**, 3840–3861.
- [147] Müser, M. H. (2008) Rigorous field-theoretical approach to the contact mechanics of rough elastic solids. *Phys. Rev. Lett.* **100**, 055504–1–4.
- [148] Hanson, M. T. & Keer, L. M. (1990) A simplified analysis for an elastic quarter-space. *Quarterly Journal Of Mechanics And Applied Mathematics* **43**, 561–586.
- [149] Keer, L. M., Lee, J. C., & Mura, T. (1983) Hetényi's elastic quarter space problem revisited. *International Journal of Solids Structures* **19**, 497–506.
- [150] Keer, L. M., Lee, J. C., & Mura, T. (1984) A contact problem for the elastic quarter space. *International Journal of Solids Structures* **20**, 513–524.
- [151] Hanson, M. T. & Keer, L. M. (1990) Stress analysis and contact problems for an elastic quarter-plane. *Quarterly Journal Of Mechanics And Applied Mathematics* **42**, 363–383.
- [152] Cottenden, A. M., Cottenden, D. J., Karavokiros, S., & Wong, W. K. R. (2008) Development and experimental validation of a mathematical model for friction between fabrics and a volar forearm phantom. *Journal of Engineering in Medicine* **222**, 1097–1106.
- [153] Gwosdow, A. R., Stevens, J. C., Berglund, L. G., & Stolwijk, J. A. J. (1986) Skin friction and fabric sensations in neutral and warm environments. *Textile Research Journal* **56**, 574–580.
- [154] Asimakopoulos, V. (2013) *An experimental study of friction between skin and nonwoven fabrics*. Ph.D. thesis (University College London).

- [155] Nonwovens Industry. (2001) A new spin on spunlace (<http://www.nonwovens-industry.com/articles/2001/04/a-new-spin-on-spunlace>). Accessed: April 2012.
- [156] Karavokyros, S. (2007) *Skin friction: validating a mathematical model with a simple laboratory model*. Master's thesis (University College London).
- [157] Bogatu, C. (2014) *An experimental study of friction between nonwoven fabrics and model arms*. Master's thesis (University College London).